

**Mechanisms of retention on
porous graphitic carbon:
Chromatographic and
computational chemistry
studies**

by

David Anthony Simpson, BSc (Hons)

**Submitted in accordance with the requirements for the degree
of
Doctor of Philosophy**



**University of Nottingham
School of Pharmaceutical Sciences**

September 2000

The candidate confirms that the work submitted is his own and that appropriate credit has been given where reference has been made to the work of others.

Abstract

Porous graphitic carbon has been developed as a high-performance liquid chromatography stationary phase over the past 30 years. The evolution of PGC as a stationary phase was motivated by the desire to find a substitute for reversed-phase silica gel based materials in areas where these materials are inadequate (e.g. extremes of pH). However, PGC possesses a number of chromatographic properties which are thus far largely unexplained and differ from traditional silica-based reversed-phase supports.

The retention mechanisms of *mono*-substituted benzenes and biphenyls on porous graphitic carbon stationary phase were investigated using chromatographic and computational methods.

The studies on a range of *n*-alkylbenzene analytes demonstrated that retention on PGC was found to be greatly influenced by hydrophobic parameters such as Hansch-Fujita and $\log P$ and that PGC has superior selectivity for isomers of amylbenzene in terms of its chromatographic retention properties when compared to octadecyl-silica (ODS). Molecular modelling of the alkylbenzene analytes indicated that the interaction between toluene and ethylbenzene and PGC was in a cofacial geometry whereas that between the longer chain alkylbenzene was of a face-edge (perpendicular) nature. This was confirmed by the relatively poor retention of highly branched amylbenzenes.

Benzene derivatives demonstrated retention properties on PGC such that the logarithm of the retention factor ($\log k_w$) was found to be closely correlated with a combination of the Hansch-Fujita parameter and Lowest Unoccupied Molecular Orbital Energy (E_{lumo}) of the analytes. This was augmented by similar correlations between $\log k_w$

and Hansch-Fujita, E_{lum} and mean polarisability. Chromatographic studies of the benzene derivatives on PGC gave enhanced retention for polar and charged analytes and reduced retention for the alkyl substituted benzenes used in this study when compared with ODS. Preliminary semi-empirical calculations of the interaction between the analyte and the PGC stationary phase for benzene derivatives showed qualitative relationships between the energy of interaction and $\log k_w$ for closely related benzene derivatives.

The retention of mono-substituted biphenyl compounds was found to be greater on PGC than on ODS stationary phase, with the strongest retention found for highly conjugated species (such as 4-phenylcinnamic acid and 4-vinylbiphenyl). This observation supports the hypothesis that the presence of a planar moiety in a molecule imparts an increased retention when using PGC as the stationary phase. PGC was found to be more retentive for the separation of both polar and non-polar biphenyl derivatives. Semi-empirical calculations suggested that the ease with which an analyte could attain a planar geometry was an important factor influencing the retention of biphenyl derivatives on PGC.

My grandfather once told me that there are two kinds of people: those who work and those who take the credit. He told me to try to be in the first group; there was less competition there.

Indira Gandhi

Acknowledgements

Many thanks to my supervisors Dave Barrett, Nick Shaw and Cristina De Matteis for continued support and giving me enough harassment to make sure that this thesis was completed. I would also like to thank Astra Charnwood, now AstraZeneca for funding and particularly Andy Teasdale and Mel Euerby for support and advice during my time at Loughborough.

I'd like to thank my molecular modelling consultants, Sarah Harris and Charlie Laughton for discussions and advice on my model chromatographic system (go look at chapters 3 & 4). Also thanks for allowing me to use valuable computational time.

A big thank you to Mike Baynham for general encouragement and fathering me in times of hopelessness and perhaps more importantly for giving me his computer for the duration of writing up my thesis - I suppose you want it back now. Debbie Baynham for chauffeuring me for 3 months. Adele Patterson for the all her help with trying to get the Beckman HPLC working. Thanks also to the ex-Beckman representative who told me that our model of Beckman equipment was the worst the company had ever produced. I would also like to thank the following people for their support, advice and friendship during my time at Nottingham University: Snow Stolnik, Alan McKeown, Mohammed Al-Jafari, Adam Watkins, Jon Gillham (junglist), Stuart Procter, Cath Ortori and Lee Hibbert.

I want to thank my family, for their support and faith in me, who will no doubt see me slightly more often now.

Lastly a big thank you to the person who of late has become my typist, proof reader, chef and much more. Thanks for all the support, Jo.

Table of Contents

Abstract	ii
Acknowledgements	iv
Table of contents	vi
List of abbreviations	x
List of figures	xi
List of tables	xvi
Chapter 1 - Introduction	1-1
1.1 Development of carbon-based HPLC packing materials	1-1
1.1.1 Manufacture of PGC	1-3
1.1.2 Structure of PGC	1-4
1.1.3 Performance of PGC	1-5
1.1.4 Retention studies on PGC	1-6
1.1.5 Theories of retention and their application to PGC	1-8
1.2 Background on silica-based HPLC packing materials	1-16
1.3 Correlation of retention on PGC with physical properties of analytes	1-17
1.3.1 Quantitative-structure retention relationships	1-18
1.3.1.1 Introduction	1-18
1.3.2 Molecular descriptors in QSRR	1-22
Structural descriptor parameters	1-22
Electronic effects	1-22
Hydrophobic effects	1-26
Steric effects	1-27
Topological Indices	1-29
1.3.3 Analysis techniques	1-31
Statistical Approaches to QSRR	1-31
Pattern Recognition techniques	1-31
Hierarchical cluster analysis	1-31
Principal Component Analysis	1-32
Correlation analysis techniques	1-34
Linear regression	1-34
Multiple linear regression	1-34
Principal component regression	1-36
1.4 Molecular modelling of chromatographic systems	1-36
1.4.1 Introduction & background	1-36
1.4.2 Previous modelling studies of chromatographic systems	1-37
1.5 Aims	1-38
1.6 References	1-39

Chapter 2 - Experimental methods	2-1
2.1 Chromatographic methods	2-1
2.1.1 Alkylbenzenes	2-1
Chemicals and reagents	2-1
Instrumentation	2-1
Chromatographic conditions	2-2
Mobile phase preparation	2-2
Sample preparation	2-2
Data treatment	2-2
2.1.2 Benzene derivatives	2-3
Chemicals and reagents	2-3
Instrumentation	2-3
Chromatographic conditions	2-3
Mobile phase preparation	2-3
Sample preparation	2-4
Data treatment	2-4
2.1.3 Biphenyl compounds	2-4
Chemicals and reagents	2-4
Instrumentation	2-4
Chromatographic conditions	2-5
Mobile phase preparation	2-5
Sample preparation	2-5
Data treatment	2-5
2.2 Molecular modelling of interactions between an analyte and a model graphite surface by semi-empirical molecular orbital methods	2-5
2.2.1 MOPAC	2-6
Geometry specification and optimisation	2-6
Self-consistent field (SCF) criterion	2-7
Output of SCF calculations	2-7
2.2.2 Building the molecules	2-8
Analyte molecules and graphite surface model	2-8
The model chromatographic system	2-8
2.2.3 MOPAC geometry optimisation	2-9
2.3 Conformational analysis of biphenyl derivatives by molecular modelling methods	2-13
2.3.1 Building the molecules	2-13
2.3.2 Semi-empirical molecular orbital method	2-13
2.4 Quantitative structure- retention relationship methods	2-15
2.4.1 Regression analysis	2-15
2.4.2 Principal component analysis	2-16
2.5 References	2-17
Appendix 2.1 - Example PDB file	2-18

Chapter 3 - The retention mechanisms of alkylbenzenes on PGC	3-1
3.1 Introduction	3-1
3.2 Chromatographic results on ODS and PGC	3-2
3.2.1 n-Alkylbenzenes	3-4
3.2.2 Amylbenzene structural isomers	3-6
3.3 Quantitative structure- retention relationship analysis of alkylbenzenes	3-8
3.3.1 Bivariate analysis of n-alkylbenzenes	3-8
3.3.2 Bivariate analysis of amylbenzenes	3-13
3.4 Molecular modelling of analyte interactions with PGC surface	3-19
3.4.1 n-alkylbenzenes	3-21
3.4.2 Amylbenzene structural isomers	3-25
3.4.3 Molecular modelling studies - Conclusions	3-27
3.5 Application of QSRR methods to literature data – Polymethylbenzenes and comparisons with n-alkylbenzenes and amylbenzene structural isomers	3-28
3.6 Conclusions	3-31
3.7 References	3-32
Chapter 4 - The retention mechanisms of benzene derivatives on PGC	4-1
4.1 Introduction	4-1
4.2 Chromatographic results on ODS and PGC	4-3
4.2.1 Hydrocarbon compounds	4-3
4.2.2 Halogenated compounds	4-6
4.2.3 Alcohols, aldehydes, ketones, esters	4-8
4.2.4 Carboxylic acids	4-14
4.2.5 Neutral nitrogen containing compounds	4-15
4.2.6 Charged analytes	4-17
4.3 Discussion of chromatographic results on ODS and PGC	4-20
4.4 Molecular modelling of the interaction between analyte and PGC surface	4-25
4.4.1 Hydrocarbon compounds	4-27
4.4.2 Halogenated compounds	4-30
4.4.3 Alcohols, aldehydes, ketones, esters	4-31
4.4.4 Carboxylic acids	4-33
4.4.5 Neutral nitrogen containing compounds	4-34
4.4.6 Charged analytes	4-35
4.4.7 Molecular modelling conclusions	4-36
4.5 Quantitative structure- retention relationship analysis of benzene derivatives	4-38
4.5.1 Bivariate analysis	4-38
4.5.2 Multiple linear regression analysis	4-43
PGC pH 2.5	4-44

PGC pH 7.0	4-45
ODS pH 2.5	4-46
ODS pH 7.0	4-46
4.5.3 Principal component analysis	4-47
4.6 Conclusions	4-49
4.6.1 Chromatographic studies	4-49
4.6.2 QSRR studies	4-50
4.6.3 Molecular modelling studies	4-51
4.7 References	4-53
Appendix 4.1 - Chromatography data for benzene derivatives	4-54

Chapter 5 - The retention mechanisms of biphenyl derivatives on PGC

	5-1
5.1 Introduction	5-1
5.2 Results and discussion of chromatographic studies on ODS and PGC	5-6
5.2.1 Hydrocarbon substituted biphenyls	5-6
5.2.2 Halogenated compounds	5-9
5.2.3 Alcohols, aldehydes & ketones	5-10
5.2.4 Carboxylic acid derivatives	5-13
5.2.5 Acids 15	
5.2.6 General results and discussion	5-17
5.3 Quantitative structure- retention relationship analysis of para-substituted biphenyl derivatives	5-24
5.3.1 Bivariate analysis	5-24
5.3.2 Conformational analysis studies by semi-empirical molecular modelling methods.	5-30
5.3.3 Multi-variate analysis	5-35
Multiple linear regression	5-35
Principal component analysis	5-36
5.3.3 Summary of QSRR analysis	5-37
5.4 Conclusions	5-37
5.4.1 Chromatographic studies	5-37
5.4.2 Conformational analysis studies	5-38
5.4.3 QSRR studies	5-39
5.5 References	5-40
Appendix 5.1 - Chromatography data for biphenyl derivatives	5-42
Appendix 5.2 - The charge program	5-43

Chapter 6 - Concluding remarks

6-1

List of abbreviations

AM	Adjacency matrix
C_n	Coquart's excess charge parameter
CPK	Corey, Pauling and Kolton
Δ	Kaliszan's submolecular polarity parameter
ΔH_f	The change in the total heat of formation of an analyte species and a model surface when the separation between the molecules is changed from approximately 3.8 Å to infinite separation.
DAD	Diode-array detector
DM	Distance matrix
E_{homo}	Energy of the highest occupied molecular orbital
E_{lumo}	Energy of the lowest unoccupied molecular orbital
HOMO	Highest occupied molecular orbital
HPLC	High-performance liquid chromatography
k	Retention factor
k_w	Retention factor extrapolated to 100 % aqueous mobile phase composition
Δk_w	Change in k_w from ODS to PGC
LC	Liquid chromatography
$\log k_w$	The logarithm of the retention factor extrapolated to 100 % aqueous mobile phase composition
LUMO	Lowest unoccupied molecular orbital
MOPAC	Molecular orbital package
MLR	Multiple linear regression
ODS	Octadecyl silica
PAH	Polycyclic aromatic hydrocarbon
PC	Principal component
PCA	Principal component analysis
PCB	Polychlorinated biphenyl
PCR	Principle component regression
PGC	Porous graphitic carbon
PTMA	Phenyl trimethyl ammonium
PTMAC	Phenyl trimethyl ammonium chloride
PREG	Polar retention effect on graphite
QSAR	Quantitative structure- activity relationships
QSRR	Quantitative structure- retention relationships
r	Correlation coefficient
RPLC	Reversed-phase liquid chromatography
RSD	Relative standard deviation
t_0	Retention time of an unretained peak
TEI	Topological electronic index
t_R	Retention time
UV	Ultra violet

List of Figures

Chapter 1

Fig. 1.1	Diagrams of the surface of bonded silica and porous graphitic carbon stationary phases.	1–4
Fig. 1.2	Structural diagrams of true 3 dimensional graphite and porous graphitic carbon, a two-dimensional graphite.	1–5
Fig. 1.3	A diagrammatical representation of Snyder's theory for adsorption chromatography.	1–10
Fig. 1.4	Transfer of analyte, A, from solution to association with ligand, L, via evaporation into the gas phase	1–12
Fig. 1.5	A simplified diagram of the equilibrium process between an analyte molecule in the mobile phase and adsorbed onto the PGC stationary phase	1–15
Fig. 1.6	Structure of chloramphenicols used by Hansch <i>et al.</i>	1–18
Fig. 1.7	The relationship between $\log P$ and retention ($\log k$) for <i>n</i> -alkylbenzenes on ODS stationary phase.	1–19
Fig. 1.8	Methodology and goals in QSRR studies	1–20
Fig. 1.9	Rate of base-catalysed hydrolysis of benzoic esters	1–22
Fig. 1.10	Interaction of a three charge body with its oppositely charged image	1–24
Fig. 1.11	Transition state	1–26
Fig. 1.12	Verloop box that surrounds the substituent is defined by the values of the calculated Verloop parameters.	1–27
Fig. 1.13	Hierarchical cluster analysis	1–31
Fig. 1.14	3D graph showing $\log P$, molecular volume and molar refractivity and their summary variable, PC1.	1–32

Chapter 2

Fig. 2.1	An example PDB format file for the model surface and benzoic acid.	2–8
Fig. 2.2	CPK model of the $C_{78}H_{22}$ hydrocarbon model surface	2–9
Fig. 2.3	The model surface. Cofacial geometry with no offset.	2–10
Fig. 2.4	The model surface. Cofacial geometry with offset.	2–11
Fig. 2.5	The model surface. Face-edge geometry with substituent directed away from the surface.	2–11
Fig. 2.6	The model surface. Face-edge geometry with substituent directed parallel to the surface	2–11
Fig. 2.7	The model surface. Face-edge geometry with substituent directed towards the surface.	2–12

Fig. 2.8	The calculation of ΔH_f by subtracting heat of formation of analyte and model surface at a large separation from the heat of formation of analyte and model surface at close separation.	2–12
Fig. 2.10	The inter-phenyl torsion angle measured.	2–13
Fig. 2.11	Calculation of the energy barrier to rotation of biphenyl derivatives.	2–14

Chapter 3

Fig. 3. 1	The structure of alkylbenzenes.	3–2
Fig. 3. 2	Amylbenzene structural isomers.	3–3
Fig. 3. 3	The relationship between alkyl chain length and retention for <i>n</i> -alkylbenzenes on PGC and ODS stationary phases.	3–5
Fig. 3. 4	Separation of amylbenzene structural isomers on ODS and PGC.	3–6
Fig. 3. 5	Two possible orientations of interaction between the analyte molecule and the flat PGC surface.	3–7
Fig. 3. 6	The relationship between $\log k$ and (a) $\log P$, (b) molecular surface area, (c) Randic index and (d) molecular volume for <i>n</i> -alkylbenzenes on PGC and ODS.	3–9
Fig. 3. 7	The relationship between $\log k$ and Balaban index for <i>n</i> -alkylbenzenes on PGC and ODS.	3–10
Fig. 3. 8	The relationship between $\log k$ and Wiener index for <i>n</i> -alkylbenzenes on PGC and ODS.	3–11
Fig. 3. 9	The relationship between $\log k$ and dipole moment for <i>n</i> -alkylbenzenes on PGC and ODS.	3–12
Fig. 3. 10	The relationship between $\log k$ and Wiener index for amylbenzenes on PGC and ODS.	3–14
Fig. 3. 11	The relationship between $\log k$ and Balaban index for amylbenzenes on PGC and ODS.	3–15
Fig. 3. 12	The relationship between $\log k$ and Randic index for amylbenzenes on PGC and ODS.	3–16
Fig. 3. 13	The relationship between $\log k$ and $\log P_{calc}$ for amylbenzenes on PGC and ODS.	3–17
Fig. 3. 14	The relationship between $\log k$ and molecular surface area for amylbenzenes on PGC and ODS.	3–18
Fig. 3. 15	The five geometries for the alignment of an analyte and part of the model graphite surface considered in molecular modelling studies.	3–19
Fig. 3. 16	The calculation of ΔH_f by subtracting heat of formation of analyte and model surface at large separation from the heat of formation of analyte and model surface at a	

	close separation.	3-20
Fig. 3. 17	The relationship between alkyl chain length and the heat of formation of the lowest energy geometry of a complex between <i>n</i> -alkylbenzenes and a model graphite 'surface' molecule.	3-22
Fig. 3. 18	A model of π - π interactions which considers the the σ -framework and the π -electrons separately.	3-24
Fig. 3. 19	The relationship between $\log k_w$ and ΔHf_{min} retention on PGC.	3-25
Fig. 3.20	The relationship between retention on PGC and ΔHf_{min} .	3-26
Fig. 3. 21	The structures of polymethylbenzenes.	3-28
Fig. 3. 22	The relationship between $\log k$ and Wiener index for amylbenzenes and polymethylbenzenes.	3-29
Fig. 3. 24	The relationship between $\log k$ and Balaban index for polymethylbenzenes and <i>n</i> -alkylbenzenes.	3-30

Chapter 4

Fig. 4.1	The structure of the benzene derivatives used.	4-2
Fig. 4.2	The relationship between retention ($\log k$) and mobile phase composition on ODS and PGC at different pH values.	4-4
Fig. 4.3	The relationship between retention ($\log k$) and mobile phase composition on ODS and PGC at different pH values.	4-6
Fig. 4.4	The relationship between retention ($\log k$) and mobile phase composition on ODS and PGC at different pH values.	4-9
Fig. 4.5	Canonical forms of anisole.	4-10
Fig. 4.6	Canonical forms of acetophenone.	4-11
Fig. 4.7	The relationship between retention ($\log k$) and mobile phase composition on ODS and PGC at different pH values.	4-12
Fig. 4. 8	Canonical forms of methylbenzoate	4-13
Fig. 4.9	The relationship between retention ($\log k$) and mobile phase composition on ODS and PGC at different pH values.	4-14
Fig. 4.10	The relationship between retention ($\log k$) and mobile phase composition on ODS and PGC at different pH values.	4-16
Fig. 4.11	The relationship between retention ($\log k$) and mobile phase composition on ODS and PGC at different pH values.	4-17
Fig. 4. 12	Δk_w for each analyte in this study.	4-22
Fig. 4. 13	The five geometries for the alignment of the analyte	

	with part of the model graphite surface.	4-25
Fig. 4. 14	The aromatic hydrocarbon compound ($C_{78}H_{22}$) chosen to represent the PGC surface.	4-25
Fig. 4. 15	The calculation of ΔH_f by subtracting heat of formation of analyte and model surface at a large separation from the heat of formation of analyte and model surface at close separation.	4-27
Fig. 4. 16	Staggered and coplanar conformations of biphenyl. The hydrogen atoms shown have the steric effect of driving the conformation away from coplanarity.	4-29
Fig. 4. 17	Analytes with resonance structures which result in a more rigid and planar molecule.	4-33
Fig. 4.18	The relationship between $\log k_w$ and $\Delta H_{f_{min}}$ at pH 7.0 (a & b) and pH 2.5 (c & d).	4-37
Fig. 4. 19	The relationship between $\log k_w$ and $\log P$ on ODS at (a) pH 2.5 and (b) pH 7.0 and on PGC at (c) pH 2.5 and (d) pH 7.0.	4-41
Fig. 4.20	The relationship between retention and the Hansch-Fujita hydrophobicity constant on ODS at (a) pH 2.5 and (b) pH 7.0 and on PGC at (c) pH 2.5 and (d) pH 7.0	4-42
Fig. 4.21	The relationship between $\log k_w$ at pH 7.0 on PGC and $\log k_w$ at pH 2.5 on PGC.	4-43
Fig. 4.22	The relationship between $\log k_w$ and mean polarisability on PGC at pH 2.5 and pH 7.0.	
Fig. 4. 23	MLR analysis of $\log k_w$ on PGC at pH 7.0. Variables used are π , mean polarisability (P_E) and E_{lumo}	4-45
Fig. 4.24	MLR analysis of $\log k_w$ on PGC at pH 7.0. Variables used are π and E_{lumo} .	4-46
Fig.4.26	MLR analysis of $\log k_w$ on ODS at pH 7.0. Variables used are $\log P$ and π . (a) Complete dataset and (b) with PTMAC removed.	4-47

Chapter 5

Fig. 5. 1	The lowest energy conformation of the biphenyl molecule. The four central hydrogen atom which force the twisted conformation are highlighted in yellow.	5-1
Fig. 5.2	Inter-phenyl torsion angle, ϑ	5-2
Fig. 5.3	General structure of the <i>para</i> -substituted biphenyl derivatives.	5-5
Fig. 5.4	The relationship between retention ($\log k$) and mobile phase composition for the hydrocarbons compounds studied.	5-8
Fig. 5.5	The relationship between retention ($\log k$) and mobile phase composition for the halogenated compounds	

	studied.	5-9
Fig. 5. 6	The relationship between retention ($\log k$) and mobile phase composition for the alcohols, aldehydes & ketones studied.	5-11
Fig. 5.7	Resonance structures of 4-biphenylcarboxaldehyde and 4-acetylbiphenyl showing the inter-phenyl double bond.	5-12
Fig. 5.8	The relationship between retention ($\log k$) and mobile phase composition for the carboxylic acid derivatives studied.	5-14
Fig. 5.9	The relationship between retention ($\log k$) and mobile phase composition for the acids.	5-15
Fig. 5.10	Δk_w for <i>para</i> -substituted biphenyl derivatives at pH 2.5 and pH 7.0.	5-19
Fig. 5.11	The relationship between $\log k_w$ and $\log P$ on ODS at (a) pH 2.5 & (b) pH 7.0, and on PGC at (c) pH 2.5 & (d) pH 7.0.	5-25
Fig. 5.12	The relationship between $\log k_w$ and the Hansch parameter on ODS at (a) pH 2.5 & (b) pH 7.0, and on PGC at (c) pH 2.5 & (d) pH 7.0.	5-27
Fig. 5. 13	The relationship between $\log k_w$ and Coquart's excess charge parameter, C_n on PGC at pH 2.5 and pH 7.0.	5-28
Fig. 5.14	The relationship between $\log k_w$ and C_n on PGC for polar analytes at (a) pH 2.5 and (b) pH 7.0.	5-29
Fig. 5.15	The relationship between $\log k_w$ and the torsion angle on the inter-phenyl bond on PGC at pH 2.5 and pH 7.0.	5-32
Fig. 5.16	The relationship between $\log k_w$ and the energy barrier to coplanarity of the biphenyl rings on PGC at pH 2.5 and pH 7.0.	5-33

List of Tables

Chapter 1

Table 1.1	The structural descriptors that are most commonly used in QSRR studies	1–22
Table 1.2	Energy matrix for the interaction of a charged analyte with its image in the graphite surface	1–25
Table 1.3	Statistical approaches to QSRR	1–31

Chapter 3

Table 3.1	Retention data for alkylbenzenes on PGC and ODS stationary phases eluted with 90:10 methanol/water.	3–4
Table 3.2	Correlation between structural descriptors and log <i>k</i> for <i>n</i> -alkylbenzenes, where <i>r</i> is the correlation coefficient.	3–8
Table 3.3	Linear regression correlation between structural descriptors and log <i>k</i> for amylbenzene isomers, where <i>r</i> is the correlation coefficient.	3–13
Table 3.4	Heats of formation (in kcal) of a complex between a series of alkylbenzenes and a model graphite 'surface' molecule.	3–21

Chapter 4

Table 4.1	The benzene derivatives studied	4–3
Table 4.2	Retention data for hydrocarbons	4–5
Table 4.3	Retention data for halogenated analytes	4–8
Table 4.4	Retention data for alcohols, aldehydes, ketones and esters	4–9
Table 4.5	Retention data for carboxylic acids	4–15
Table 4.6	Retention data for neutral nitrogen containing analytes	4–17
Table 4.7	Retention data for charged analytes	4–19
Table 4.8	The difference in <i>k_w</i> from ODS to PGC at pH 2.5 and pH 7.0	4–22
Table 4.9	Values of ΔH_f calculated by semi-empirical molecular modelling methods for hydrocarbon compounds.	4–28
Table 4.10	Values of ΔH_f calculated by semi-empirical molecular modelling methods for halogenated compounds.	4–32
Table 4.11	Values of ΔH_f calculated by semi-empirical molecular modelling methods for alcohols, aldehydes, ketones, esters.	4–33

Table 4.12	Values of ΔH_f calculated by semi-empirical molecular modelling methods for carboxylic acid analytes.	4-35
Table 4.13	Values of ΔH_f calculated by semi-empirical molecular modelling methods for neutral nitrogen containing compounds.	4-36
Table 4.14	Values of ΔH_f calculated by semi-empirical molecular modelling methods for charged compounds.	4-37
Table 4.15	Linear regression correlation between structural descriptors and $\log k_w$ for benzene derivatives	4-41
Table 4.16	Principal component analysis of the structural descriptors used for statistical analysis of benzene derivatives.	4-48
Table 4.17	Bivariate analysis of principal components with $\log k_w$.	4-48
Table 4.18	Highest values of Δk_w for benzene derivatives	4-51

Chapter 5

Table 5.1	The biphenyl derivatives studied	5-5
Table 5.2	Retention data for hydrocarbons	5-7
Table 5.3	Retention data for halogenated compounds.	5-9
Table 5.4	Retention data for alcohols, aldehydes & ketones.	5-10
Table 5.5	Retention data for carboxylic acid derivatives.	5-13
Table 5.6	Retention data for acids.	5-16
Table 5.7	Values of Δk_w for biphenyl derivatives.	5-20
Table 5.8	Linear regression correlation between structural descriptors and $\log k_w$ for <i>para</i> substituted biphenyl derivatives.	5-24
Table 5.9	Rotation barrier and torsion angles for the biphenyl compounds studied.	5-31
Table 5.10	Principal component analysis of the structural descriptors used for statistical analysis of benzene derivatives.	5-32
Table 5.11	The variance explained by principal component analysis of the structural descriptors used for the statistical analysis of biphenyl derivatives.	5-36
Table 5.12	Bivariate analysis of principal components with $\log k_w$.	5-37

Chapter One

Introduction

1.1 Development of carbon-based HPLC packing materials

The development of carbon-based stationary phases for HPLC stems from attempts to alleviate the problems associated with the more traditional silica gel based packing materials. Since their development in the early 1970s, bonded silica phases have always had the following associated problems.

- (i) Manufacturing reproducibility. Difficult to control variability of the starting materials used to manufacture the silica gel results in unpredictability in composition between batches. Variability in the reagents used in the subsequent bonding process also has a partial effect.
- (ii) Supposedly equivalent bonded silica stationary phases from different manufacturers possess different retention properties.
- (iii) Silica based packing materials possess a limited hydrolytic stability. This means that for long-term usage, the pH range of eluents is restricted to 2-8.

- (iv) The type and number of surface silanol groups on the silica surface results in differences in chromatographic performance between ostensibly similar phases.
- (v) Variable metallic concentrations of the support.

The development of PGC was motivated by a desire to alleviate at least some of the problems associated with reversed-phase silica gels as given above. Graphite is a crystalline material and there are, in principle, no functional groups on the surface because the aromatic carbons have all their valencies satisfied within the graphite sheets. Graphite therefore should be free of many of the disadvantages exhibited by silica-based materials. Differences in manufacturing reproducibility should be reduced as this is a crystalline material. Reversed-phase interactions should not be undermined by superfluous surface functionality as is the case for silica-based stationary phases. A crystalline graphite material is far more robust than silica-based materials to extremes of pH, enabling chromatography to be carried out under a more diverse variety of conditions.

Knox and Kaur [1] outlined the properties required by the ideal support for HPLC. The following points were regarded as essential.

The support should:

- be mechanically strong enough to withstand pressures up to 300 bar
- be manufactured as spherical particles with a narrow particle-size distribution.
- have a mean particle size in the range of 3-10 μm .
- have a uniform pore structure with no micropores less than 60Å in diameter
- have a surface area in the range of 50-400 m^2g^{-1}
- have an energetically homogeneous internal surface

- be inert to all reasonable eluents
- be geometrically stable and free from any swelling or shrinkage.
- have the capacity for surface modification
- offer batch-to-batch reproducibility

In spite of a staggering variety of carbons available in bulk form (from activated charcoals and glassy carbons to industrial graphites) it has not been until quite recently that carbon-based materials, which are robust enough to withstand the strong demands that HPLC exerts, have become commercially available. A detailed review of these carbons, their structure and performance was recently given by Knox and Ross [2] and so the detail of these materials, their methods of manufacture, structure and chromatographic performance is omitted here.

1.1.1 Manufacture of PGC

In 1978 Knox and Gilbert [3] patented a method of making a porous carbon, which could be easily scaled up to manufacturing proportions. A highly porous 5 μ m silica material was used as the template for the carbon-based material and impregnated with a phenol-formaldehyde mixture. This mixture was then polymerised to produce a phenol-formaldehyde resin. This material was then carbonised by heating to approximately 1000°C in nitrogen to yield solid particles consisting of a silica backbone with carbon filled pores. The silica backbone was then removed by dissolution in 5M sodium hydroxide solution. The material was termed “porous glassy carbon” by its makers and its HPLC performance was found to be poor.

By heating the material to above 2000°C, a complete rearrangement of the carbon structure results, changing the material from a microporous amorphous structure to a crystalline material with a planar surface. The resulting material was now called “porous graphitised carbon”, leaving the original acronym (PGC) intact. This material was

originally manufactured in the Chemistry Department at the University of Edinburgh and subsequent manufacture was transferred to Shandon HPLC (now Hypersil, part of ThermoQuest). A diagram of the surfaces of ODS and PGC stationary phases is given in figure 1.1.

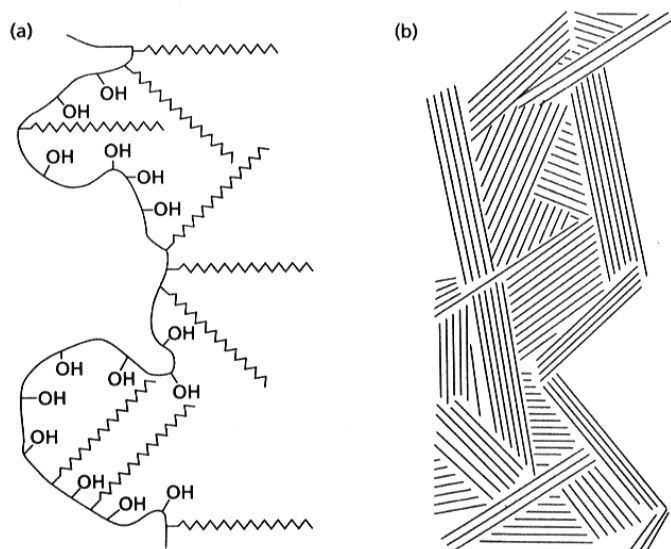


Figure 1.1 Diagrams of the surface of (a) bonded silica and (b) porous graphitic carbon stationary phases. From ref [4]

1.1.2 Structure of PGC

PGC is made up of intertwined ribbons of carbon, consisting of approximately 30 discrete sheets with a separation of about 3.35 Å between layers, as observed by high-resolution transmission electron microscopy [5]. The surface comprises flat sheets of crystalline hexagonally arranged carbon atoms [6] showing sp^2 hybridisation.

Neighbouring carbon atoms along the same plane have a separation of 1.42 Å which is very close to that of large polycyclic aromatic molecules. These sheets could indeed be regarded as large polycyclic aromatic carbon molecules. X-ray diffraction studies have shown that the spacing between the layers is typical for that of a three-dimensional graphite at 3.35 Å. In three-dimensional graphite there is a distinct registration of carbon atoms between layers (stacked in an ABABAB sequence), as proposed by Hull [7]. However there is no

registration of one layer relative to those above or below in PGC and therefore PGC can only be thought of as a two-dimensional graphite (see figure 1.2).

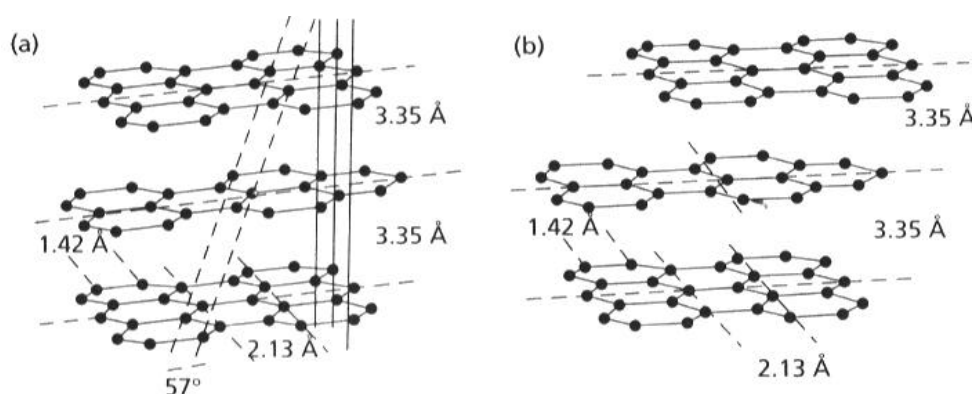


Figure 1.2 Structural diagrams of (a) true 3 dimensional graphite and (b) porous graphitic carbon, a two-dimensional graphite. From ref [4]

PGC is a template material and the pore size and pore volume can therefore be adjusted by choosing an appropriate pore-size and porosity for the silica gel template material. As the porosity of the particles will govern the quantity of material in each particle, the mechanical strength of the material will be greatly affected by the porosity. PGC is currently manufactured with a porosity of approximately 70% and a surface area around $120\text{m}^2\text{g}^{-1}$ [6]. This results in a material which is almost as mechanically robust as silica gel and can withstand pressures of 500 bar.

1.1.3 Performance of PGC

Initial tests on the performance of PGC as a HPLC stationary phase proved to be disappointing, due to poor peak shapes that exhibited significant tailing [8]. These early problems were regarded as difficulties in obtaining a reliable and consistent graphitisation of the porous glassy carbon base material. The quality of the material had significantly improved by 1986 [5] when the first high-quality material was produced. Knox demonstrated that excellent peak shapes and symmetry could finally be obtained from PGC. This improvement

resulted from continued research and development with an improvement to the graphitisation process, resulting in efficiencies which are comparable to that of bonded phase silicas.

1.1.4 Retention studies on PGC

Since the introduction of commercially available PGC columns in 1988 (marketed as Hypercarb[®]) there has been considerable application of PGC to the analysis of a wide variety of analytes. Initially, it was assumed that retention would be based upon dispersive forces of interaction between the analyte and the PGC surface. It was therefore assumed that retention behaviour on graphite would be similar to that on ODS. The difference was that pH ranges could be extended and selectivity for closely related compounds would be improved.

Initial studies by Kaur [9] supported this view, however, as the number of analysts employing PGC in liquid chromatography increased it became apparent that other, as yet unknown, interactions were occurring. Reviews of these observations relating to the areas of application of PGC and the suspected retention mechanism were recently carried out by Knox and Ross [2].

When compared to other stationary phases, some key observations regarding retention on graphite were highlighted:

- (a) An increased selectivity to structurally similar analytes such as geometric/structural isomers [10].
- (b) An increased retention of non-polar analytes compared with reversed phase silica based supports [11].
- (c) The absence of eluotropic series. These are present for oxide supports and are based on the ability of the solvent to hydrogen bond to the surface. As the graphite surface has no functionality (e.g. polar groups) no such interactions are present for graphite [9].
- (d) A notable polar retention effect giving increased retention of polar

analytes compared with reversed phase silica based supports, indicating an unexpected affinity between the polar analytes and the graphite surface [12-14].

The retention behaviour of a series of alkanols was investigated by Tanaka *et al.* [12]. They observed that when changing from alkanes to their corresponding alkanols, on ODS, the retention was substantially reduced. However, on PGC the retention increased.

Kaliszan and co-workers [15] studied the retention on PGC of a wide variety of small aromatic compounds, where one hydrogen was substituted by a polar functional group. Using heptane as the mobile phase, they observed that retention was stronger for the polar substituted analytes on PGC. On ODS, the retention in general was seen to be reduced for the polar analytes. Kaliszan went on to correlate his results with a submolecular polarity parameter [16] (see section 1.2.2) and put forward the hypothesis that a localised polar segment of the analyte was responsible for retention. He further stated that graphite has metal like characteristics and that this was not completely unexpected because of the two-dimensional delocalisation of electrons in the layers of graphite.

Coquart and Hennion highlighted the polar retention effect in their study of polar substituted benzenes [13, 17]. They determined the value of $\log k_w$ for ODS and PGC for a range of mono, di- and tri-substituted benzenes. Their results showed that, on ODS, by increasing the substitution on the benzene ring, the retention would decrease substantially, often leading to the analytes being unretained. Conversely, on PGC, increasing the number of polar functionalities on the ring, retention was significantly increased.

These and other studies provided strong evidence that retention on PGC was in many cases quite unlike that for any other reversed phase

support. They suggested that a different, perhaps additional mechanism, which does not rely on dispersive interactions may be present. They also meant that existing theories of retention (detailed in section 1.1.5) could not explain the analyte-support interactions which must have occurred.

1.1.5 Theories of retention and their application to PGC

Retention in reversed-phase HPLC can be separated into four main categories:

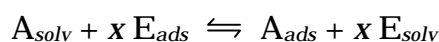
- Analyte-mobile phase attractions - London forces (dispersive interactions), dipole-dipole and hydrogen bonding interactions. Any or all of these may reduce retention.
- Analyte-mobile phase repulsion - these arise from resistance to disruption of hydrogen-bonded solvents by non-hydrogen-bonded analytes. This is likely to occur between a hydrophilic mobile phase and non-polar analytes or non-polar segments of analytes. These interactions encourage strong retention on graphite.
- London forces between the stationary phase surface and the analyte. These are balanced by similar interactions between the stationary phase surface and the mobile phase, which is displaced by the analyte. This is a net interaction, so depending on the analyte, may increase or reduce retention.
- Charge-induced interactions of the analyte and the stationary phase surface. On bonded phase silica gels, such as ODS, these weak largely secondary interactions generally occur between polar analytes and any unshielded surface silanol groups. Similar interactions are thought to promote the retention of polar molecules due to a polar retention effect on graphite (PREG). However, they are compensated to some extent by the polar interactions between the analyte and the mobile phases. The increased interaction with the PGC stationary phase in many cases outweighs the polar analyte-eluent interactions.

This study is aimed at further determining retention mechanisms on PGC and highlighting differences between these and the mechanisms of retention on ODS. As a consequence, a consideration of charge-induced interactions between the analyte and PGC is important. The first two of the retention mechanism categories, described above, characterise analyte-mobile phase interaction and show that different molecular attractions or repulsions can result in either increased or decreased retention. The balance between these two categories can be accurately estimated by considering the hydrophobicity parameter, $\log P$ and its value for an analyte. Reversed-phase HPLC gives strong correlations between $\log P$ and $\log k_w$ when ODS is employed as the stationary phase. One objective of the work presented in this thesis is to establish analogous descriptors which similarly describe the relationship between retention on PGC and physicochemical properties of the analyte.

Many retention models of partitioning and adsorption mechanisms have been proposed in the past [18-24]; however the main theories of chromatography which will be discussed here are Snyder's theory for adsorption chromatography, the solvophobic theory of Horváth *et al.*, and the unified retention theory of Martire and Boehm for reversed-phase liquid chromatography.

Snyder's theory

Snyder's theory for adsorption chromatography [23] was originally developed to explain the idea of an elutropic series for oxide adsorbents. If the specific assumptions made for oxide adsorbents are revised, the theory can then be applied to retention on PGC. The adsorption process can be regarded as the displacement of x eluent molecules (E) by an analyte molecule (A):



The resulting free energy change can thus be transcribed:

$$\Delta F = x F(E_{solv}) + F(A_{ads}) - x F(E_{ads}) - F(A_{solv})$$

The free energies of the adsorbed species can be broken down into two parts which are also given in figure 1.3.

- (a) A contribution due to one face of the molecule and its contact with the stationary phase.
- (b) A contribution due to the rest of the molecular surface and its contact with the eluent.

Part (b) will cancel with part of the free energies of the solvated species. This leads us to assume that the most important free energies to consider are given in part (a) i.e. the parts of A and E that become desolvated upon adsorption.

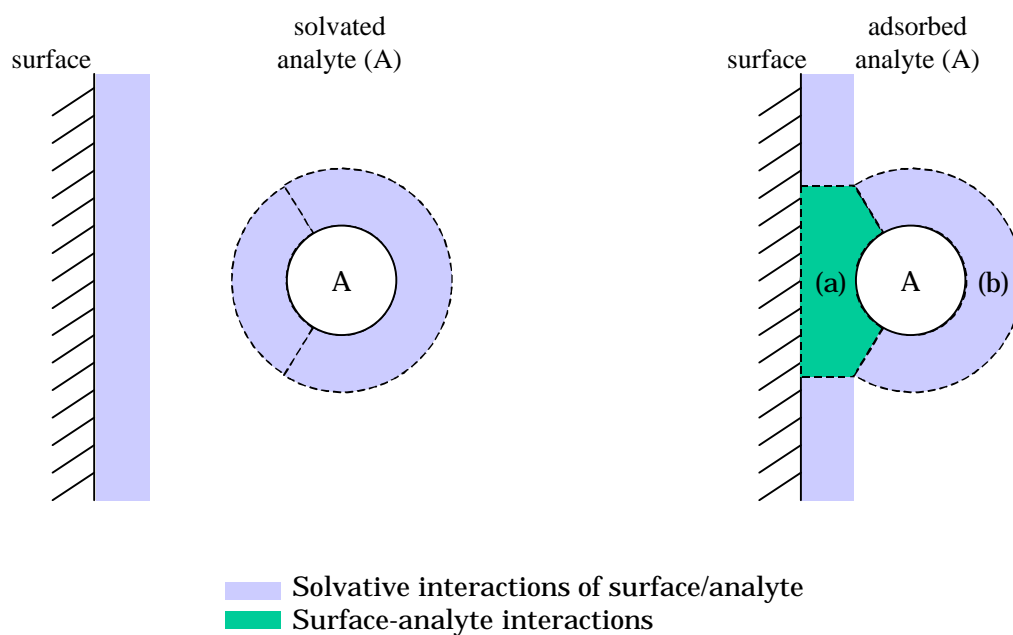


Figure 1.3 A diagrammatical representation of Snyder's theory for adsorption chromatography. (a) The contribution due to one face of the molecule and its contact with the stationary phase. (b) The contribution due to the rest of the molecular surface and its contact with the eluent. (The free energy for (b) cancels with part of the free energies of the solvated species.)

When Snyder first applied this theory, he assumed that the free energies of the solvated species would cancel. This greatly simplifies

the overall picture and was the key assumption in the theory. Snyder felt that he could justify this assumption because, as he was working with oxide stationary phases (adsorbents), the dominant intermolecular interactions between adsorbent and eluent, with typical solvents, were likely to be hydrogen bonding between the surface hydroxyl groups and electronegative atoms in the eluent (e.g. O, N, Cl etc). This meant that solvents could easily be ranked in order of their polarity and thus the eluting strength of the eluents/solvents could be measured by averaging the retention of a wide range of analytes. With this in mind, Snyder derived an expression to describe the retention factor, $\log k$:

$$\log k = \log (V_a / V_m) + \beta(S^\circ A_a E^\circ)$$

Where V_a/V_m is the ratio of the volume of solvent adsorbed (onto the adsorbent), to the volume in the mobile phase. β is the surface activity coefficient ($\beta \leq 1$), $S^\circ (= \Delta G^\circ / 2.303.RT)$ is a dimensionless free energy of adsorption of solute onto the stationary phase surface. A_a is the contact area of the adsorbed analyte with the stationary phase surface and E° is the eluotropic strength of the mobile phase/solvent. If this theory is applied to non-polar adsorbents such as PGC or ODS, the solvents can no longer be ranked in a series based on polarity, as hydrogen bonding cannot occur with the stationary phase. The cancellation of free energies of solvation is no longer possible as this factor has become one of the major contributors to the analyte's retention, and as such is no longer appropriate for the adsorption of an analyte onto the surface of PGC [25].

Horváth and co-worker's solvophobic theory:

In 1976 Horváth *et al.* published their solvophobic theory of retention [21]. This theory was based upon a general theory developed by Simanoglu and coworkers [26, 27] to describe the effect of the solvent on chemical events.

Horváth's model presented the interaction between the solute and the stationary phase as a reversible association of isolated

solvated analyte molecules, A, with the solvated hydrocarbonaceous ligands at the stationary phase surface. Accordingly, solute retention is governed by the equilibrium



Where the complex LA is assumed to be formed by solvophobic interactions. Horváth's model is restricted to unionised solutes i.e. ionic interactions are neglected.

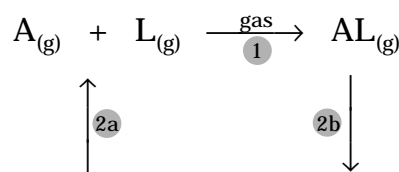
The molecular interactions in the analyte were conceptually broken down into two processes:

1. The interaction of the molecules, A and L, to yield LA in a hypothetical gas phase without any intervention by the solvent.
2. A more involved process consisting of the interactions of the associated species and the complex individually with the solvent.

The association in the gas phase is assumed to occur by London forces only. The second process can be split into two further stages - (a) desolvation of the individual species A and L into the gas phase and (b) the solvation of LA. This is summarised in figure 1.4.

If we consider stage (b), the solvation of LA. In order to solvate LA, the creation of a cavity of sufficient size to accommodate the complex LA is required.

Gas Phase



Solution/Stationary Phase

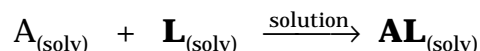


Figure 1.4 Transfer of analyte, A, from solution to association with ligand, L, via evaporation into the gas phase. The stationary phase and associated species are highlighted in **bold**.

LA is then placed in the cavity and solvative bonds between the complex and solvent molecules at the wall of the cavity are formed.

Sinanoglu [28] expressed the free energy change of the cavity formation as

$$\Delta F_{cavity} = C A_{cavity} \gamma$$

where A_{cavity} is the molecular surface area of the species LA, γ is the surface tension of the solvent and C is a complex correction factor for the cavity size, reorganisation energy and entropy.

Stage (a) can therefore be calculated in an identical manner for A and L individually, but will have an opposite sign.

When applied to retention on PGC, L would be represented by a small part of the graphite surface.

- The desolvation step (a) would be represented by complete removal of the solvent from the graphite surface.
- The formation of LA in the gas phase would be represented by adsorption of the hydrophobic part of the analyte, A onto this small area of the graphite surface in the gas phase.
- Solvation of the solvent LA would be represented by wetting the surface of the graphite which the analyte A has adsorbed onto.

This theory assumes that the bond formed between L and A is the result of dispersive interactions. This assumption is incorrect on PGC, where a large part of retention can be assigned to the so called polar retention effect on graphite (PREG). This/these interaction(s) are not allowed for by the solvophobic theory and therefore this theory cannot be applied to explain PREG and thus retention on graphite.

Unified retention theory of Martire and Boehm

Horváth's theory is modelled by invoking "solvophobic" interactions i.e. exclusion of the less polar solute molecule from the polar mobile phase with subsequent adsorption onto the non-polar stationary phase. The mobile phase "drives" the solute towards the stationary phase, rather than any inherently strong attraction between the solute and the stationary phase. This description is therefore incomplete as it does not provide a sufficiently detailed explanation of the dependence of the

solute retention and selectivity on the stationary phase structure. For this reason, Martire and Boehm attempted to address the shortcomings of the theory proposed by Horváth *et al.* Their model consisted of a lattice constructed from cubic cells with atomic dimensions. The stationary phase is represented as a semi-flexible chain (e.g. C₁₈) that occupies a number of adjacent cells, a number denoted by γ Ligand. Eluent molecules occupy γ cells and the solute/analyte occupies γ solute cells.

Martire and Boehm considered this for both pure solvents and solvent mixtures, analysing the structure and composition of the stationary phase as a function of the alkyl chain length, chain stiffness, surface coverage and nature of the mobile-phase solvent. Subsequently, solute distribution constants were determined and their dependence on the aforementioned variables assessed. The treatment is statistical and mathematically complex, providing treatments for entropy and enthalpy changes for the processes considered. It also provides the ability to predict a variety of the properties of the system, including the degree of solvation of the flexible alkyl chain on the stationary phase and the differential positioning of solvent components into the hydrocarbon layer.

However, the theory lacks any insight into how to determine the key energetic parameters i.e. the interactions between the segments of the different species. For this reason, Martire and Boehm's theory does not assist in the interpretation of the molecular processes that influence the polar retention effect on graphite.

As previously stated above, the three theories explain the forces of attraction between the solute and the stationary phase as consisting of only London forces. However when retention on PGC is examined, it becomes apparent that further additional interactions are present which are responsible for the increased retention of polar solutes (PREG). Each theory stresses the significance of a thorough

understanding of the forces that bind the solute and indeed the solvent to the stationary phase and the importance of changes in solvation enthalpy for the adsorption of the solute onto the stationary phase. Each of the theories can be summarised pictorially by the schematic given in figure 1.5 below.

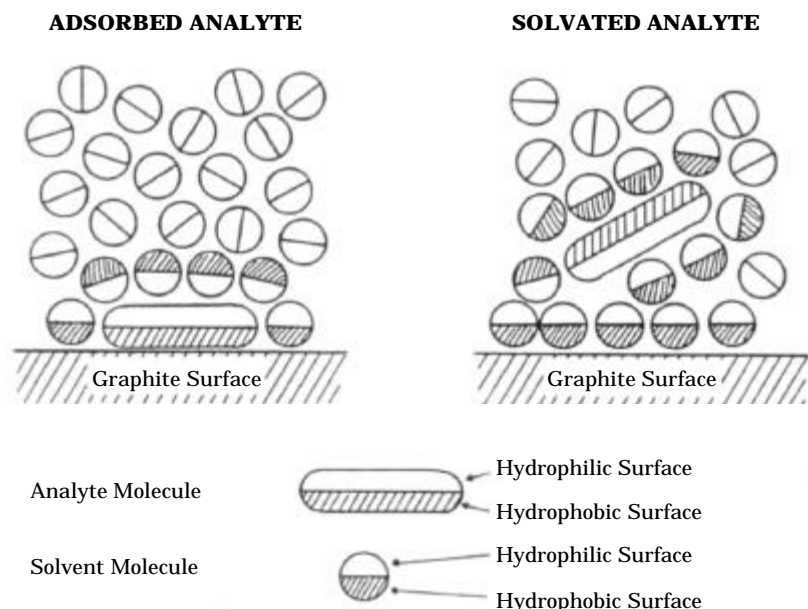


Figure 1.5 A simplified diagram of the equilibrium process between an analyte molecule in the mobile phase and adsorbed onto the PGC stationary phase. Unshaded solvent molecules have random orientation. The diagram can easily be redrawn for a two-component mobile phase system with hydrophilic and hydrophobic components.

From ref [4]

The key consideration when trying to apply each of these models to the retention on PGC is that London forces alone do not sufficiently describe the intermolecular interactions between the analyte and the stationary phase on adsorption, therefore they cannot be used to investigate how the increased retention of polar analytes on PGC occurs.

1.2 Background on silica-based HPLC packing materials

The prominence of silica as a material for chromatographic supports is based on its low compressibility, a pore structure which can be controlled, a particle size which can be controlled, and the reactivity of surface silanol groups (SiOH) which allows the attachment of any of many functional groups to form a coating useful for the separation of a variety of classes of compounds [29]. HPLC users are familiar with the concept of ODS (figure 1.1a) and octyl monolayers covalently attached to silica spheres and these two are by far the most popular stationary phases in HPLC [30, 31].

Selectivity is based predominantly on dispersive interactions between the stationary phase and the analyte [32], with control of separation and retention achieved by variation of the solvent strength. Water is used as the base solvent, with a volume percentage of an organic solvent used to increase or decrease solvent strength. The solvent strength is related to the dispersive interactions between the analyte and the stationary phase [33, 34]. The selectivity of a given ODS phase depends on the type of silane used and the conditions under which the synthesis has taken place [35, 36], since both of these factors will affect the density of the bonded phase ligands on the surface. This density of bonded phase coverage is important since the greater the access of the analyte to the underlying silica support, the greater the opportunity for secondary interactions [33]. Theories of retention on reversed-phase supports such as ODS were studied in section 1.1.5.

The main disadvantage of the porous silica bonded phases is the left-over silanol groups which interfere with the separation of polar compounds [1]. Manufacturers have struggled for years to cover the silica surface completely but have always been limited by the steric

hindrance of the large ODS chains. Classical bonding chemistry typically reacts less than half of the total silanol groups [37] and the residual surface silanols remain accessible to the mobile phase and therefore the compounds of interest in the sample. These surface silanols are often negatively-charged and can interfere with the separation of drugs, peptides, and proteins (which are frequently positively-charged) [33]. Electrostatic interaction of some of the sample molecules with the silanols slows their transfer back to the mobile phase, peak-tailing occurs, and complete separation of similar compounds may not be possible.

The problem of the residual silanols was partly solved by the introduction of an "end-capping" reaction [38]. A small reactive silane is introduced which can find its way to unreacted silanols which otherwise would be accessible to the sample molecules. "Exhaustive" and "double-endcapping" describes multiple reactions with small silanes in an attempt to eliminate more of the remaining silanols. Larger difunctional silanes have also been used. Alternative approaches are to extend the chain length of the alkylsilane to 22 carbons and even 30 carbons and protect the surface by making it more hydrophobic or to use polymeric rather than monomeric coatings in order to cover the silica surface more completely [32].

1.3 Correlation of retention on PGC with physical properties of analytes

Extensive work has been carried out to try and explain the retentive properties of PGC and relating these retentive properties to independent physical or physicochemical properties of the analytes studied by using quantitative structure- retention relationships (QSRRs). In this way it is believed that retention on PGC may correlate with one or more key descriptor parameters [14].

Two basic approaches have been predominant in past work - the single parameter approach and the multivariate approach. In the former, correlation is desired between retention and a single physical parameter. In the latter, a group of descriptor parameters is sought which will give an optimum correlation of chromatographic data with independent physical properties. Before drawing conclusions from previous QSRR analysis work, it is important to outline the basis upon which these studies were performed. This background into the methodology of QSRR analysis is given in the section that follows.

1.3.1 Quantitative-structure retention relationships

1.3.1.1 Introduction

Since the common availability of computer hardware in the late 1960s, there has been an unquestionable trend in chemistry towards quantitation of chemical, physicochemical and biological activity of various compounds. Pioneering work by Hansch [39] and others on quantitative structure-activity relationships (QSARs) has led to a means of characterising solute molecular structure numerically, and the statistical procedures developed for QSAR purposes have been successfully employed for quantitative structure-retention relationship (QSRR) studies.

Hansch *et al.* used multiple linear regression analysis to obtain an insight into the activity of chloramphenicol (figure 1.6), an inhibitor of protein synthesis by bacterial ribosomes, and 37 derivatives [40]. Two QSARs were studied, one for side chain modification at R, and one for ring substitution in the 4 position (X).

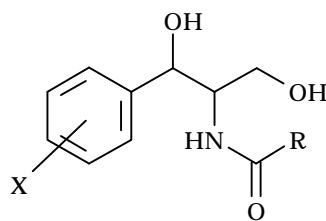


Figure 1.6 Structure of chloramphenicols used by Hansch *et al.* [40]

They found that for substitution in the 4 position on the ring, hydrophobic properties have the greatest effect on activity. For substitution at R, the inductive effect of the acyl group on the side-chain became important.

Chromatography may be used in the study of structure-activity relationships involving intermolecular interactions. The great advantage that chromatography has over other systems, is that all conditions can be kept constant or controlled, and thus the solute structure is the single independent variable in the system. Contrary to biological determinations, chromatography is readily able to yield precise and reproducible data. It is therefore quite possible that through QSRR studies, more precise methods of solute structure parameterisation will be established which will be applied to derive reliable QSAR equations allowing the rational design of new drugs.

The goal of QSRR studies is to predict retention behaviour based on structural properties of the analytes. The simplest example of this is the linear relationship often found between $\log k$ and $\log P$ [41] (figure 1.7).

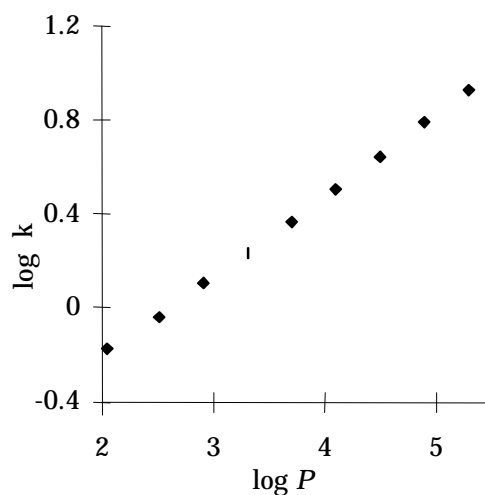


Figure 1.7 The relationship between $\log P$ and retention ($\log k$) for *n*-alkylbenzenes on ODS stationary phase. From chapter 3.

however it is more normal to use multi-parameter equations to describe retention of groups of compounds. The main aims of QSRR are as follows :

1. Prediction of retention for a new analyte.
2. Identification of the most informative structural descriptors.
3. Elucidation of the mechanism of separation for a particular chromatographic system.

The methodology and goals in QSRR studies are shown in Figure 1.8 [14].

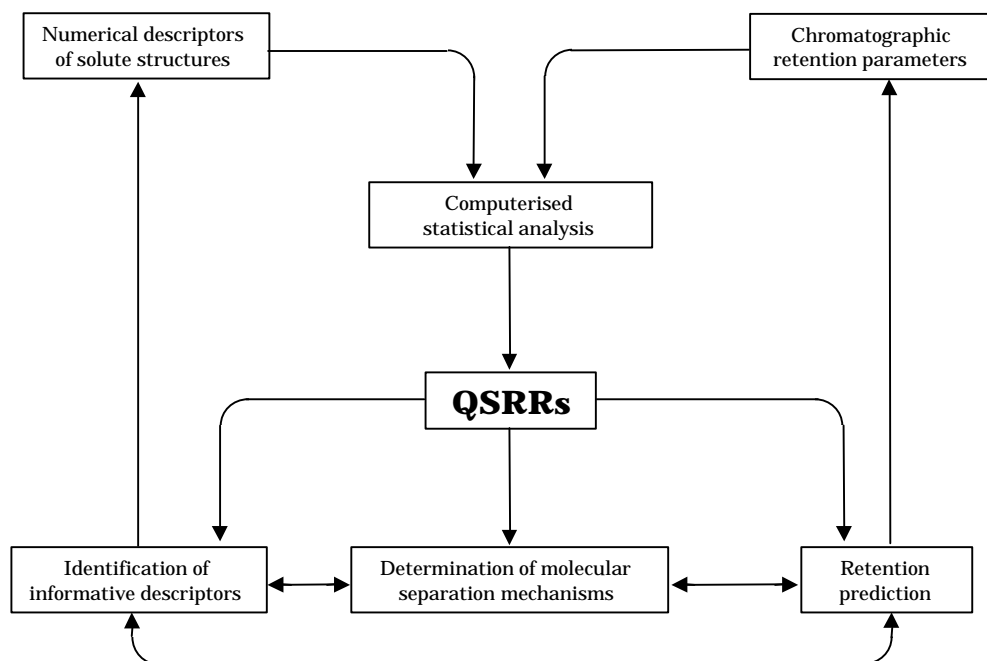


Figure 1.8 Methodology and goals in QSRR studies

The basic principles of QSRR studies are adapted from the quantitative structure-(biological) activity relationship (QSAR) approach to drug design. Two kinds of input data are vital to undertake a QSRR study (see figure 1.8): dependent variables (i.e. quantitatively comparable chromatographic retention data) for a sufficiently large group of analytes, and a set of descriptor parameters assumed to reflect the structural features of the analytes under investigation.

It is possible to attempt to derive QSRRs without reference to any existing chromatographic theories. Such a strategy would involve considering a wide variety of analyte descriptors and correlating them with retention data. The next stage is to select the minimum number of descriptors to produce a statistically significant equation which can calculate the retention data in satisfactory agreement with the observed retention values. Table 1.1 gives the structural descriptors that are most commonly used in QSRR studies [14].

Table 1.1

Structural descriptors of analytes used in QSRR analysis

<i>Size related parameters</i>	<i>Electronic parameters</i>
Molecular mass	Hammett constants
Refractivity	Dipole moments
Molecular volume	Orbital energies
Total energy	Quadrupole moments
Solvent-accessible surface area	Atomic excess charges
	Superdelocalisabilities
<i>Geometry related parameters</i>	Partially charged surfaces
Moments of inertia	
Length to breadth ratio	<i>Physico-chemical properties</i>
Angle strain energy	Hydrophobic constants
	Solubility parameters
<i>Topological parameters</i>	Melting/Boiling Points
Adjacency matrix indices	Solvatochromic parameters
Distance matrix indices	
Information content indices	

1.3.2 Molecular descriptors in QSRR**Structural descriptor parameters***Electronic effects*

The polar retention effect on graphite may be viewed as a chromatographic manifestation of an electronic effect. Such effects are key to an understanding of the retention behaviour of graphite [25]. Therefore, it is important to have good descriptors of these effects for QSRR studies.

The electronic substituent constant (Hammett Parameter) was first introduced by Hammett in 1935 [42] in order to quantify and hence predict the effect of substituents on the rate and equilibrium constants of groups of reactions which involve a reactive centre that can be influenced by a substituent. The example used by Hammett was the hydrolysis of phenyl esters (see figure 1.9).

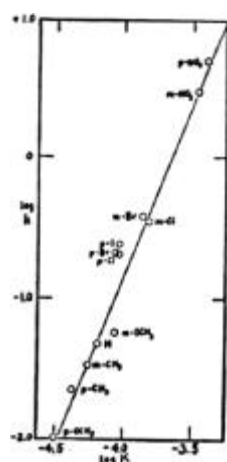


Figure 1.9 Base-catalysed hydrolysis of *meta* and *para* ethyl benzoate esters. From reference [42].

The *meta* and *para* groups form a good linear correlation however the *ortho* groups deviate substantially. This is because the *meta* and *para* groups are a sufficient distance the centre of reaction so that only electronic effects are present. However at the *ortho* position steric effects also play a major role in the reaction. The Hammett Parameter for any substituent was determined from equation 1.1.

$$s_x = \log K_x - \log K_H \quad (1.1)$$

where K_H and K_x are the ionisation constants of benzoic acid and benzoic acid substituted with X respectively. s has a range of values between -1 and +1. A positive value denotes that X is an electron-withdrawing group, and a negative value implies an electron-donating group. The value of s is dependent on the position of the substituent X, i.e. different for *meta* and *para* positions. The Hammett equation is defined as

$$\log k_x = r s_x + \log k_H \quad (1.2)$$

where k_H and k_x are the equilibrium or rate constants for the test molecule and the molecules with the substituent X, respectively and r is the reaction constant.

Kaliskan's polarity parameter D was developed as an alternative to dipole moment [16]. Overall, dipole moment performs poorly when

describing polar, but symmetrical molecules such as 1,4-disubstituted compounds. D is a submolecular measure of polarity and reflects the largest local dipole in the molecule. It is calculated by the largest difference in the individual excess charges in the molecule. It requires the determination of the electron densities on all the atoms and then locating the atom with the highest electron excess ($q_i (max)$) and the atom with the highest electron deficiency ($q_j (min)$).

$$D = q_i (max) - q_j (min) \quad (1.3)$$

Another similar parameter is the excess charge parameter C_n , of Coquart, defined by:

$$C_n = \frac{1}{2} \sum |q_i| \quad (1.4)$$

where q_i are the excess charges on each atom [13]. Coquart correlated this parameter with the retention of mono-substituted benzenes on PGC. She found a strong correlation between C_n and $\log k_w$ on PGC for polar analytes. However for hydrophobic analytes such as alkylbenzenes, retention had little or no correlation with C_n . Forces between charges and the associated energies, however, depend on the product of charges [2], not the sums of charges. As there is little theoretical basis for C_n , Knox suggested that the sum of the squares of the charges on each atom, S , [2] would make a better descriptor.

$$S = \sum (q_i^2) \quad (1.5)$$

Graphite is a two-dimensional conductor and therefore has certain properties which are analogous to those of a metal. Such metallic properties are attributed to the extended delocalisation of π -electrons. When a charged molecule interacts with a conductor, the energy of interaction is equal to the energy of interaction between the molecule and an imaginary oppositely charged self image reflected in the surface [2]. This is illustrated in figure 1.10 for a molecule carrying three charges. The energy of interaction, U_{ij} , for each atom in the molecule with each atom in its image is given by:

$$U_{ij} = \frac{1}{4\pi\epsilon_0} \frac{q_i q_j}{r_{ij}} \quad (1.6)$$

where r_{ij} is the separation between the real and imaginary atoms. The total energy of interaction, U , is given by the sum of all the energy terms in the matrix in Table 1.2; which is:

$$U = \frac{1}{4\pi\epsilon_0} \sum \frac{q_i q_j}{r_{ij}} \quad (1.7)$$

The sum of the energies of interaction between an atom and its image (U') is given by the sum of the diagonal elements of the matrix:

$$U' = \frac{1}{4\pi\epsilon_0} \sum \frac{q_i^2}{r_{ij}} \quad (1.8)$$

which is closely approximated by $U' = S / (4\pi\epsilon_0 r)$ [2].

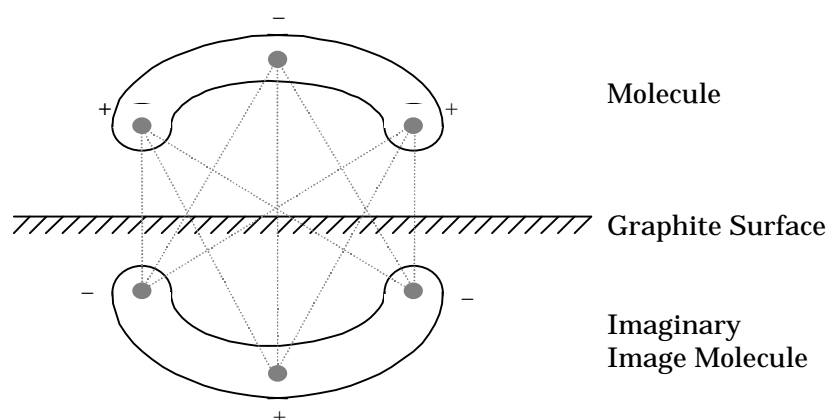


Figure 1.10 Interaction of a three charge body with its oppositely charged image. Redrawn from ref [4]

Table 1.2 Energy matrix for the interaction of a charged analyte with its image in the graphite surface

Image atom				1	2	3
Analyte atom	Co-ordinate of analyte atom			Inter-atom energies		
1	x_1	y_1	z_1	U_{11}	U_{12}	U_{13}
2	x_2	y_2	z_2	U_{21}	U_{22}	U_{23}
3	x_3	y_3	z_3	U_{31}	U_{32}	U_{33}

Hydrophobic effects

Meyer [43] observed that the narcotic activity of simple organic compounds was reflected in their oil-water partition coefficients (P). However, it was not until the 1950s when Collinder considered the octanol-water partition coefficient that there became adopted a standard system for the measurement of hydrophobicity [44]. The logarithm of the octanol-water partition coefficient has since become the standard measure for hydrophobicity. The advantage of $\log P$ is that it is useful both as a measure of hydrophobicity and as a predictor of potential interactions with biological lipid phases [45].

For ionisable compounds, $\log P$ is clearly insufficient to describe hydrophobicity. This is because these compounds will have differing hydrophobicities at different pH values. For such compounds, the apparent hydrophobicity parameter D has been used [46]. $\log D$ can be related to $\log P$ by the following simple equations:

$$\text{For acids} \quad \log D = \log P + \log \left[\frac{1}{1 + 10^{pH - pK_a}} \right] \quad (1.9)$$

$$\text{For bases} \quad \log D = \log P + \log \left[\frac{1}{1 + 10^{pK_a - pH}} \right] \quad (1.10)$$

These equations give rise to a $\log D$ profile instead of a single numerical value as in $\log P$.

$\log P$ is a measure of the hydrophobicity of a whole molecule. It is therefore often important to describe the effect that individual substituents have on the hydrophobicity of their parent molecule. A need to work with the relative hydrophobicity of substituents led to the introduction of the hydrophobicity substituent constant, ρ [45, 47]. The parameter ρ has been defined in an analogous manner to the electronic substituent constant (Hammett parameter):

$$\rho_x = \log P_x - \log P_H \quad (1.11)$$

where P_X and P_H are the partition coefficients of the substituted and H substituted compounds respectively. A positive value of ρ means that the substituent has a greater affinity for the octanol phase, whereas a negative value indicates a hydrophilic nature relative to the unsubstituted molecule.

Steric effects

The importance of molecular shape in influencing retention on PGC is universally conceded [2]. However, whereas size or bulk is a scalar quantity for which several measurements are conceivable and accessible, the distribution of bulk (i.e. shape) is a vectorial quantity. The problem of finding mathematical means to express differences in such a geometric feature in an adequate manner has been a continued challenge.

Quantification of the steric effect of substituents on organic reaction rates began as early as 1895 when Meyer postulated that the atomic weight of the ortho substituents determined the ease of esterification of ortho substituted aryl acids [48]. However it was Taft who first developed a successful numerical definition of steric effects in organic reactions [49, 50]. Taft's steric constant was defined as

$$E_s = \log \left(\frac{k_X}{k_H} \right)_A \quad (1.12)$$

where k_X and k_H are the rate constants of the acid-catalysed hydrolysis (denoted by A) of aliphatic esters of the formula $X\text{-CO}_2\text{R}$ and $\text{H-CO}_2\text{R}$ respectively, where R is typically ethyl. The size of X affects the attainment of the transition state (figure 1.11).

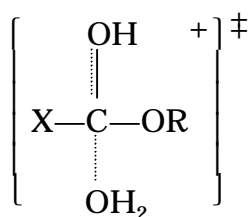


Figure 1.11 Transition state

The definition assumes that the electronic effects of X can be neglected.

Taft only used a single value to describe steric effects, however substituents are three dimensional moieties. This led Verloop *et al.* to propose a vector solution for steric effects[51, 52] . Verloop *et al.* proposed to treat the problem of directionality of steric effects by modelling a substituent and calculating its extension in five orthogonal directions, and developed a computer program using Van der Waals radii, standard bond lengths and angles to define the shape of the substituent. The five parameters are labelled L , B_1 , B_2 , B_3 and B_4 (figure 1.12) [51].

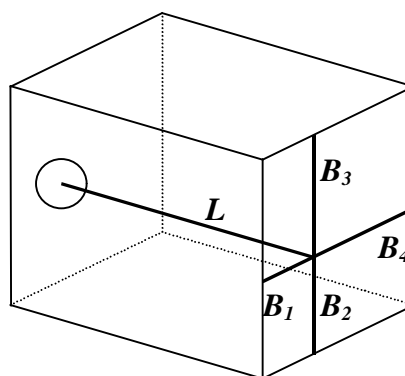


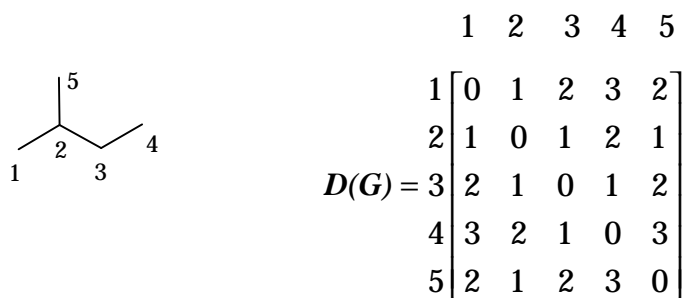
Figure 1.12 Verloop box that surrounds the substituent is defined by the values of the calculated Verloop parameters. L lies on the axis defined by the bond joining the substituent to the remainder of the molecule

The length parameter L is defined by the length of a substituent in the direction in which it is attached to the parent molecule (i.e. along the bond axis from the parent molecule). $B_1 - B_4$ are the four width parameters, perpendicular to the length parameter L .

Topological Indices

Topological indices are a convenient method of translating chemical constitution into numerical values that can be used for correlations with physical properties or indeed for QSAR or QSRR studies. The constitution of the molecular skeleton (hydrogen excluded molecular graph) can be converted into either (i) the adjacency matrix (AM) whose entries are 1 for adjacent non-hydrogen atoms and zero otherwise, or (ii) into the distance matrix (DM). The topological distance in a graph is the number of bonds in the shortest path between two non-hydrogen atoms.

The Wiener index is a method of defining how compact a molecule is [16]. A distance matrix $\mathbf{D}(\mathbf{G})$ shows how many bonds there are between atoms in the molecule. e.g.



The Wiener index (w) is defined by the half sum of the off-diagonal elements of the distance matrix $\mathbf{D}(\mathbf{G})$. It corresponds to the total number of distances between all pairs of atoms (vertices) in acyclic and cyclic molecules and is given by

$$w = \frac{1}{2} \sum_{i,j} d_{ij} \quad (1.14)$$

where d_{ij} is the number of bonds between atom i and atom j .

The Molecular Connectivity (Randic) Index (c) was introduced by Randic for characterisation of molecular branching [53]. It is based on the concept of the degree D_i of the vertex i in the hydrogen-suppressed molecular graph. The D_i is equal to the number of bonds from the

atom (vertex) i to non-hydrogen atoms. The term *valency of vertex* is often used.

The Randic index was originally calculated by the following equation

$${}^1C = \sum_{s=1}^t (D_i D_j)_s^{-1/2} \quad i \neq j \quad (1.15)$$

where s refers to an edge in the graph; t is the total number of edges; D_i and D_j represent values attributed to adjacent atoms i and j ; the superscript 1 on the χ denotes first-order connectivity index.

The connectivity index concept has been elaborated to give a general formula for connectivity indices ${}^h\chi$, which may be extended over all possible paths of length h :

$${}^hC = \sum_{s=1}^t (D_i D_j \cdots D_{h+1})^{-1/2} \quad (1.16)$$

where s refers to a single path of length h , and t is the total number of paths of length h in the graph.

The zero-order connectivity index is thus defined as:

$${}^0C = \sum_{s=1}^t (D_i)_N^{-1/2} \quad (1.17)$$

where N is the total number of vertices and s is just a vertex. The second order index is

$${}^2C = \sum_{s=1}^t (D_i D_j D_k)_s^{-1/2} \quad (1.18)$$

where s is a single path of length 2 and t is the number of paths of length 2 in the graph.

The Balaban index, J , is the average-distance sum connectivity [54, 55]. For a connected molecular graph G ,

$$J = \frac{M}{m+1} \sum_{\substack{\text{all} \\ \text{edges}}} (d_i d_j)^{-1/2} \quad (1.19)$$

where M is the number of edges in G , m is the cyclomatic number of G (on a polycyclic molecular graph, m is the number of edges that must be removed for G to become acyclic).

$$d_i = \sum_{j=1} d_{ij} \text{ and } d_{ij} \text{ is as defined for the Wiener index}$$

1.3.3 Analysis techniques

Statistical Approaches to QSRR

There are several methods for correlating analyte structural descriptors to retention. The most common approaches are given in table 1.3 [56] and are summarised below. These statistical tools can be divided into two classes; *pattern recognition techniques*, which are used to find how compounds group in 'property space', and *correlation methods*, which identify quantitative relationships between the structure descriptors and retention.

Table 1.3 Statistical approaches to QSRR

<i>Pattern recognition</i>	<i>Correlation analysis</i>
Cluster Analysis	Multiple Linear Regression
Principal Component Analysis	Principal Components Regression
Non-linear Mapping	Partial Least Squares Regression
Neural Networks	Neural Networks

The most important aspect of choosing a statistical method is not to choose the method that achieves the best correlation, but to give confidence that the correlation has not arisen by chance, i.e. that there is a real relationship between the descriptors and retention.

Pattern Recognition techniques

Hierarchical cluster analysis

This type of analysis looks for natural groups within datasets and suggests that each species within a cluster is more similar to other species within that cluster than to any species belonging to different clusters[56]. Hierarchical cluster analysis initially assumes that all compounds are in the same group (i.e. are all similar, as measured by a

similarity criterion) and in a stepwise manner makes its similarity cut-off more and more stringent thus splitting the compounds into smaller and smaller groups until eventually each compound is in its own group (figure 1.13).

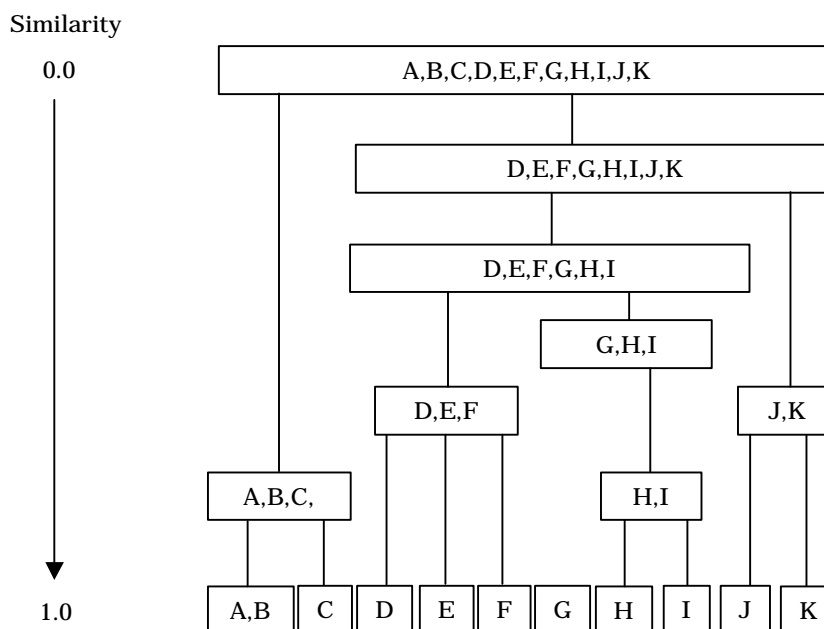


Figure 1.13 Hierarchical cluster analysis

Principal Component Analysis

In multiple linear regression analysis, all descriptors are assumed to be independent. However, in a chemical environment this is normally not possible because for example electronic parameters affect hydrophobic parameters and vice-versa. When many descriptors are used, chance correlations can result. A number of approaches can be used to identify intercorrelations in a descriptor set and as a result create new variables which summarise this information into a smaller set of descriptors. Principal component analysis (PCA) is one such technique.

For example, $\log P$, molecular volume and molar refractivity are strongly related. Figure 1.14 shows this graphically:

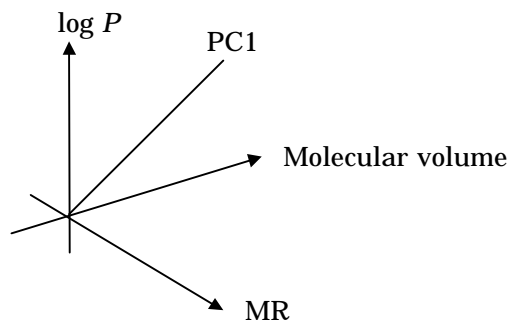


Figure 1.14 3D graph showing $\log P$, molecular volume and molar refractivity and their summary variable, PC1.

The principal component is a vector on the graph which passes through as much of the data as possible and is denoted PC1. Other principal components are identified as orthogonal to PC1 and so they represent data which are truly independent of PC1. PC1 can now be used to replace $\log P$, molecular volume and molar refractivity, and thus can be used instead of the original 3 in any subsequent correlation analysis. PCA generates 2 new pieces of information; PC scores (or *eigenvector*) and PC loading (or *eigenvalues*). The PC score is the PC value for that compound. The PC loading tells how much of the new extracted descriptor (PC) is described by each original descriptor. The cross-correlation between independent variables can be assessed by inspecting the correlation matrix of the parameters. If the dependent variable is included, the variance-covariance matrix is constructed. Such matrices can be transformed by prescribed methods of linear algebra into new matrices containing non-zero elements only on the diagonal^[57]. These are the eigenvalues of the matrix. With each eigenvalue obtained, an eigenvector is associated which is a linear combination of the original set of variables. The correlation coefficient between eigenvectors is zero (They are orthogonal). This is a characteristic feature of PCA. If there is significant covariance between the original variables, most of the variance will be described by a number of eigenvectors which is a fraction of the number of variables in the original data set. Principal component analysis has frequently been used for the evaluation of large data matrices in

chromatography [58]. The retention mechanisms of benzene derivative on PGC, using *n*-hexane as the mobile phase were evaluated by PCA [59, 60]. PCA was further employed for the determination of the origin of cinnamon [61], the identification of white wines according to chromatographic retention data [62] and the retention behaviour of environmental pollutants on PGC [63].

Correlation analysis techniques

Linear regression

Linear regression routines calculate a 'line of best fit' through a set of data points for an *x* and *y* parameter. This ensures that there is equal residual variance above and below the line. The linear regression calculates an equation of the form

$$y = m x + c \quad (1.20)$$

where the constants *m* (the gradient) and *c* (the intercept) are chosen to give the smallest sum of least squares difference between the true *y* values and the *y* values predicted from the equation.

Multiple linear regression

In multiple linear regression additional variables are included to describe some of the residual variance about the correlation between *x* and *y*. The analysis gives rise to an equation of the form:

$$y = a_1 x_1 + a_2 x_2 + \dots + a_n x_n + c \quad (1.21)$$

If the number of variables is increased, the correlation will be improved. For 50 molecules, 50 descriptors would give a perfect match to the data. However in practice no more than 1 descriptor is used per 4-5 compounds. This is because extra descriptors may simply be describing noise or the standard error in the retention data [56]. MLR assumes that all descriptors are independent of each other and that they are all important to retention. A good guide to statistical integrity

is given by Goodford [64] who states that the number of degrees of freedom in multiple linear regression should always be greater than ten:

$$\text{No. of degrees of freedom in MLR} = (n - k - 1) \geq 10 \quad (1.22)$$

where n is the number of data points for the dependent variable and k is the number of independent variables.

The multiple linear regression coefficient r^2 describes how closely the equation fits the data. A value of $r^2=1$ means that the data perfectly fits the equation.

$$r^2 = \frac{ESS}{TSS} \quad (1.23)$$

where ESS is the explained sum of squares of y and TSS is the total sum of squares of y .

The total sum of squares of y is the sum of the difference between the observed y values and their mean, squared.

$$TSS = \sum_{i=1}^n (y_i - \bar{y})^2 \quad (1.24)$$

The explained sum of squares of y is the sum of the difference between the predicted y values (y') and the mean, squared.

$$ESS = \sum_{i=1}^n (y'_i - \bar{y})^2 \quad (1.25)$$

The standard error of the model is given by the s -value. For a model with good predictive power, this is an example of how accurately the model will predict unknown y -values. For example, a regression with an s -value of 0.4 should be able to predict y -values with a standard error of 0.4 units.

The F -value is derived from the sum of squares values and degrees of freedom. Under certain assumptions about the data, it can be shown that this value should have a specific distribution [65].; This

distribution can be used to test the hypothesis that the regression is statistically significant, leading to a derived F -probability. The smaller this F -probability, the more significant the regression. i.e. if F -probability is 0.05, then the regression is significant at a 95% level.

MLR is only valid when the structural descriptors are orthogonal - i.e. independent variables (independent variables). Two data vectors are truly orthogonal if their intercorrelation coefficient, r is zero. Taking the square of this value (r^2) and multiplying by 100 gives the percentage of the dependent variable which is mutually described by the 2 structural descriptors. So if $r^2 = 0.42$, then 42 % of the dependent variable is mutually described by the 2 structural descriptors.

Principal component regression

Principal component regression (PCR) can be simply described as the application of the multiple linear regression technique to the results of principle component analysis. The main advantage of PCR over MLR is that the variables used to describe structure are truly orthogonal independent variables. With MLR analysis of a chemical system, there can never be true orthogonality of the descriptor variables, because hydrophobic descriptors are correlated with electronic parameters and so forth. PCR uses truly orthogonal eigenvectors as the starting point for analysis and so is seen as more accurate.

1.4 Molecular modelling of chromatographic systems

1.4.1 Introduction & background

Computational chemistry has undergone considerable change since its inception approximately thirty years ago. Initially there was a myriad of untested computational methods of questionable accuracy and limited applicability [66]. However, today there are three main branches which are widely used: molecular mechanics, semi-empirical

and *ab initio* or Gaussian methods. Introductions to these techniques are given in references [67] and [68]. Each branch has its own niche, therefore the conformations of macromolecules are most effectively studied using molecular mechanics, while the electronic properties of small molecules are most accurately calculated using *ab initio* methods. Semi-empirical calculations can be found in the middle ground between these two methods. They are computationally time consuming in comparison to molecular mechanics and far less rigorous than *ab initio* methods. Semi-empirical methods are not particularly good at any one thing. However as a result of this, semi-empirical methods are extremely versatile and so have numerous applications. Further background on semi-empirical calculations can be found in section 2.2 of this thesis.

1.4.2 Previous modelling studies of chromatographic systems

Previous studies involving molecular modelling and chromatography on PGC have concentrated mainly on computational calculations of analyte compounds in isolation. Most studies have ignored the interactions between the analyte and the stationary phase, the analyte and the mobile phase and the interactions between the stationary phase and the mobile phase. These calculation have generally been carried out in order to obtain properties of the analyte molecule such as dipole moment and other electronic parameters

Kaliszan *et al.* used a semi-empirical method (using the CNDO/2 Hamiltonian) to calculate the submolecular polarity parameter, Δ [69] defined in section 1.3.2 for correlation analysis with chromatographic data. Hennion *et al.* [70] used a semi-empirical method (using the MNDO Hamiltonian) to calculate Coquart's excess charge parameter. This parameter was found to correlate with retention on PGC ($\log k_w$) for polar benzene derivatives. Jackson *et al.* [71] used the MOPAC program [66] to perform semi-empirical calculations (using the AM1

Hamiltonian) to determine molecular geometry and thus calculate solute surface area for their investigation of reversed phase HPLC on carbon media. They found that polarisability was an important factor in retention on PGC. Each of these studies have used molecular modelling calculations to determine electronic parameters which cannot be experimentally measured.

1.5 Aims

The aim of this research is to investigate the retention mechanisms on porous graphitic carbon using both chromatographic and computational chemistry methodologies to predict the retention of compounds of interest to the pharmaceutical industry. Quantitative structure – retention relationships have been used to compare the retention on PGC and ODS stationary phases. Semi-empirical molecular modelling studies have been used to predict the geometry and strength of interaction between the analyte and the PGC stationary phase. This approach should lead to a better understanding of the underlying mechanisms of retention on PGC.

1.6 References

- [1] J. H. Knox, B. Kaur, *Eur. Chromatogr. News* 1 (1987) 12.
- [2] J. H. Knox, P. Ross, *Adv. Chromatogr.* 37 (1997) 73.
- [3] J. H. Knox, M. T. Gilbert, 1978.
- [4] J. H. Knox, Q. H. Wan, *Chromatographia* 42 (1996) 83.
- [5] J. H. Knox, B. Kaur, G. R. Millward, *J. Chromatogr.* 352 (1986) 3.
- [6] *Shandon Hypercarb Guide*, Life Sciences International, Runcorn, UK 1993.
- [7] A. W. Hull, *Phys. Rev.* 10 (1917) 66.
- [8] J. H. Knox, K. K. Unger, H. Mueller, *J. Chromatogr* 6 (1983) 1.
- [9] B. Kaur, *LC-GC Int.* (1989) 41.
- [10] Q. H. Wan, P. N. Shaw, M. C. Davies, D. A. Barrett, *J. Chromatogr A* 697 (1995) 219.
- [11] J. Kriz, E. Adamcova, J. H. Knox, J. Hora, *J. Chromatogr A* 663 (1994) 151.
- [12] M. Tanaka, T. Tanigawa, K. Kimata, K. Hosaya, T. Araki, *J. Liq. Chromatogr.* 549 (1991) 29.
- [13] V. Coquart, *PhD Thesis*, University of Paris, Paris 1993.
- [14] R. Kaliszan, *J. Chromatogr. A* 656 (1993) 417.
- [15] R. Kaliszan, K. Osmialowski, B. J. Bassler, R. A. Hartwick, *J. Chromatogr.* 461 (1989) 139.
- [16] R. Kaliszan, *Quantitative Structure- Chromatographic Retention Relationships*, John Wiley & Sons, New York 1987.
- [17] V. Coquart, M. C. Hennion, *Journal Of Chromatography* 600 (1992) 195.
- [18] J. G. Dorsey, K. A. Dill, *Chem. Rev.* 89 (1989) 331.
- [19] M. Jaroniec, D. E. Martire, *J. Chromatogr.* (1986) 1.
- [20] W. Melander, C. Horváth , in C. Horváth (Ed.): *High Performance Liquid Chromatography; Advances and Perspectives, Vol. 2*, Academic Press, New York 1980.

- [21] C. Horváth, W. Melander, I. Molnár, *J. Chromatogr.* **125** (1976) 125.
- [22] D. E. Martire, R. E. Boehm, *J. Phys. Chem.* **87** (1983) 1045.
- [23] L. R. Snyder, *Principles of Adsorption Chromatography*, Marcel Dekker Inc., New York 1968.
- [24] D. H. Everett, R. H. Ottewill, C. H. Rochester, A. L. Smith, (Editors), *Adsorption from Solution*, Academic Press, New York 1983.
- [25] P. Ross, PhD Thesis, Univeristy of Edinburgh 1999.
- [26] O. Simanoglu, S. Abdunur, *Adv. Chem. Phys.* **24** (1965) 12.
- [27] O. Simanoglu, *Molecular Associations in Biology*, Academic Press, New York 1968.
- [28] O. Sinanoglu, in B. Pullman (Ed.): *Molecular Associations in Biology*, Academic Press, New York 1968, p. 425.
- [29] K. K. Unger, *Porous Silica - Its Properties and Use as Support in Column Liquid Chromatography.*, Elsevier, Amsterdam 1980.
- [30] L. R. Snyder, J. J. Kirkland, *Introduction to Modern Liquid Chromatography*, Wiley, New York 1979.
- [31] R. E. Majors, *LC-GC* **9** (1991) .
- [32] R. E. Majors, *Current Issues in HPLC Technology. A supplement to LC-GC* 1997.
- [33] V. R. Meyer, *Practical High-Performance liquid Chromatography*, Wiley, New York 1994.
- [34] L. R. Snyder, *J. Chromatogr. Sci.* **16** (1978) 223.
- [35] J. Nawrocki, *Chromatographia* **31** (1991) 193.
- [36] J. Nawrocki, *Chromatographia* **31** (1991) 177.
- [37] L. C. Sanders, M. Pursch, S. A. Wise, *Anal. Chem.* **71** (1999) 4821.
- [38] C. H. Lochmüller, D. B. Marshall, *Anal. Chem. Acta* **142** (1982) 63.
- [39] C. Hansch, in E. J. Ariens (Ed.): *Drug Design, Vol. 1*, Academic Press, New York 1971, p. 271.

- [40] C. Hansch, K. Nakamoto, M. Gorin, P. Denisevich, E. R. Garrett, S. M. Heman-Ackah, C. H. Won, *J. Med. Chem.* **16** (1973) 917.
- [41] D. A. Simpson, , University of Nottingham 2000.
- [42] L. P. Hammett, *Chem. Rev.* **17** (1935) 125.
- [43] H. Meyer, *Arch. Exp. Path. Pharmacol.* **42** (1889) 110.
- [44] R. Collinder, *Physiol. Plant.* **7** (1954) 420.
- [45] A. Leo, C. Hansch, D. Elkins, *Chem. Rev.* **71** (1971) 525.
- [46] A. T. Florence, D. Attwood, *Physicochemical principles of pharmacy*, MacMillan, London 1991.
- [47] T. Fujita, J. Iwasa, C. Hansch, *J. Amer. Chem. Soc.* **86** (1964) 5175.
- [48] V. Meyer, *Chem. Ber.* **28** (1895) 1254.
- [49] R. W. Taft, *J. Amer. Chem. Soc.* **74** (1952) 3120.
- [50] R. W. Taft, *Steric effects in organic chemistry*, John Wiley, New York 1956.
- [51] V. Verloop, W. Hoogenstraaten, J. Tipker, in E. J. Ariens (Ed.): *Drug Design*, Academic Press, New York 1976, p. 165.
- [52] V. Verloop, J. Tipker, *Pestic. Sci.* **7** (1976) 379.
- [53] M. J. Randic, *J. Amer. Chem. Soc.* **97** (1975) 6609.
- [54] A. T. Balaban, *Chem. Phys. Lett.* **89** (1982) 399.
- [55] A. T. Balaban, I. Motoc, D. Bonchev, O. Mekenyan, in M. Charlton, I. Motoc (Eds.): *Steric Effects in Drug Design*, Springer-Verlag, Berlin 1983, p. 21.
- [56] A. Davis, *Medicinal Chemistry : Principles and Practice*, Royal Society of Chemistry, Cambridge, UK 1994.
- [57] R. D. Cramer, *J. Amer. Chem. Soc.* **102** (1980) 1837.
- [58] R. Kaliszan, *Structure and Retention in Chromatography. A Chemometric Approach*, Harwood Academic Publishers, Australia 1997.
- [59] B. J. Bassler, R. Kaliszan, J. Hartwick, *J. Chromatogr.* **461** (1989) 139.
- [60] R. Kaliszan, K. Osmialowski, B. J. Bassler, R. A. Hartwock, *J. Chromatogr.* **499** (1990) 333.

- [61] K. G. Miller, C. F. Poole, T. M. P. Pawloski, *Chromatographia* 42 (1996) 639.
- [62] C. M. Garcia-Jares, M. S. Garcia-Martin, N. Carro-Marino, R. Cela-Torrijos, *J. Sci. Food Agric.* 69 (1995) 175.
- [63] T. Cserhati, E. Forgacs, *J. Chromatogr. A* 869 (2000) 41.
- [64] P. J. Goodford, *Adv. Pharmacol. Chemother.* 11 (1973) 51.
- [65] *TSAR 3.0 User Guide*, Oxford Molecular Group, Oxford 1997.
- [66] J. J. P. Stewart, *Journal of Computer-Aided Molecular Design* 4 (1990) 1.
- [67] F. Jenson, *Introduction to Computational Chemistry*, Wiley, New York 1999.
- [68] A. R. Leach, *Molecular Modelling. Principles and Applications*, Longman, Harlow 1995.
- [69] K. Osmialowski, J. Halkiewicz, A. Radecki, R. Kaliszan, *J. Chromatogr.* 346 (1985) 53.
- [70] M. C. Hennion, V. Coquart, S. Guenu, C. Sella, *J. Chromatogr. A* 712 (1995) 287.
- [71] P. T. Jackson, M. R. Schure, T. P. Weber, P. W. Carr, *Anal. Chem.* 69 (1997) 416.

Chapter Two

Experimental methods

2.1 Chromatographic methods

2.1.1 Alkylbenzenes

Chemicals and reagents

Methanol (HPLC grade) was supplied by Fisher Chemicals (Loughborough, U.K.). All water used was supplied by an Elgastat very high purity unit (Elga Ltd., High Wycombe, U.K.). All analyte compounds were purchased from Sigma-Aldrich (Poole, U.K.) unless stated otherwise. *t*-Amylbenzene was purchased from Lancaster (Morcombe, U.K.).

Instrumentation

HPLC analysis was performed on an Integral Micro-Analytical 100Q Workstation (PerSeptive Biosystems, now part of Applied Biosystems, Foster City, U.S.A.) with a variable wavelength UV detector set at 220 nm.

Chromatographic conditions

HPLC was performed using a 5 μm Hypersil ODS column (150 mm \times 4.6 mm i.d.) and 5 μm Hypercarb PGC column (100 mm \times 3.0 mm i.d.), from Hypersil, Runcorn (now part of ThermoQuest). Conditions used were 90:10 (unbuffered) methanol:water (v/v) mobile phase, detection wavelength 220 nm and flow rates of 1.0 ml min⁻¹ and 0.42 ml min⁻¹ for ODS and PGC systems respectively. The flow rates were different to maintain comparable linear flow velocities. Chromatography was performed at ambient temperature.

Mobile phase preparation

All mobile phases were prepared fresh at the beginning of the week and stored for that week at 4°C. On the day of use, the required solutions were filtered through a 0.45 μm nylon filter under vacuum, then degassed by helium sparge for 20 minutes.

Sample preparation

Samples were dissolved in methanol to 100 $\mu\text{g ml}^{-1}$ concentration and were injected in triplicate. Sample injections were 10 μl volumes.

Data treatment

Chromatographic retention factors, k , were calculated from the computerised integration software within the Integral Workstation according to equation 2.1

$$k = (t_{\text{R}} - t_0) / t_0 \quad (2.1)$$

where t_{R} is the retention time for the analyte peak, and t_0 is the retention time of the unretained analyte peak. The retention time of the unretained analyte peak was taken as the time interval from the moment of injection to the time when the trace for the solvent disturbance crossed the baseline. The solvent disturbance peak was generated by the methanol in which the samples were dissolved.

2.1.2 Benzene derivatives

Chemicals and reagents

Methanol (HPLC grade) was supplied by Fisher Chemicals (Loughborough, U.K.). All water used was supplied by an Elgastat very high purity unit (Elga Ltd., High Wycombe, U.K.). All analyte compounds were purchased from Sigma-Aldrich (Poole, U.K.).

Instrumentation

Instrumentation was as given in section 2.1.1

Chromatographic conditions

HPLC was performed using a 5 μm Hypersil ODS column (150 mm \times 4.6 mm i.d.) and 5 μm Hypercarb PGC column (100 mm \times 3.0 mm i.d.), from Hypersil, Runcorn (now part of ThermoQuest). Conditions used were methanol:water (v/v) mobile phase with 5mM tris(hydroxymethyl)aminomethane buffer at pH 7.0 and pH 2.5, detection wavelength 220 nm and flow rates of 1.0 ml min⁻¹ and 0.42 ml min⁻¹ for ODS and PGC systems respectively. The flow rates were different to maintain comparable linear flow velocities. Chromatography was performed at ambient temperature.

Mobile phase preparation

All running buffers were prepared fresh from solid salts and then stored at 4°C until used. Buffer solution pH was produced by adjusting the solution with hydrochloric acid as necessary. The pH meter was calibrated using the slope standards (Mettler Ltd) which encompassed the desired pH range. Buffers were filtered through a 0.45 μm nylon filter under vacuum, then degassed by helium sparge for 20 minutes. All methanol used was filtered through a 0.45 μm nylon filter under vacuum, then degassed by helium sparge for 20 minutes. The mobile phase was then prepared by adding the appropriate volume quantity of buffer solution to the appropriate

volume quantity of methanol.

Sample preparation

20 mg amounts of each analyte were weighed into 10 ml volumetric flasks and methanol added. These solutions were then sonicated for 20 minutes and made up to volume. These solutions were then diluted, 1 in 20 with mobile phase to produce a 100 $\mu\text{g ml}^{-1}$ sample and injected in triplicate. Sample injections were 10 μl volumes.

Data treatment

Data treatment was as given in section 2.1.1

2.1.3 Biphenyl compounds

Chemicals and reagents

Methanol (HPLC grade) was supplied by Fisher Chemicals (Loughborough, U.K.). All water used was supplied by an Elgastat very high purity unit (Elga Ltd., High Wycombe, U.K.). All analyte compounds were purchased from Sigma-Aldrich (Poole, U.K.) unless stated otherwise. 4-Biphenyl sulfonic acid, 4-biphenyl methanol, and 4-biphenyl carboxamide were purchased from Avocado (Heysham, U.K.). Methyl 4-phenylbenzoate and 1-(4-biphenyl)ethanol were purchased from Lancaster (Morcombe, U.K.).

Instrumentation

The HPLC system consisted of Hewlett-Packard 1090 HPLC system (Hewlett-Packard, Stockport, U.K.) with a diode array wavelength detector measuring wavelengths at 220 nm and 260 nm. Integration was performed using ChemStation software (Hewlett-Packard, Stockport, U.K.) on a Hewlett-Packard Vectra personal computer.

Chromatographic conditions

HPLC was performed using a 5 μm Hypersil ODS column (150 mm \times 4.6 mm i.d.) and 5 μm Hypercarb PGC column (30 mm \times 2.1 mm i.d.), from Hypersil, Runcorn (now part of ThermaQuest). Conditions used were $x:(100-x)$ methanol:water (v/v) mobile phase with 5mM tris(hydroxymethyl)aminomethane buffer at pH 7.0 and pH 2.5, where x was changed in increments of 10%. The detection wavelength was 220 nm and flow rates of 1.0 ml min⁻¹ and 0.42 ml min⁻¹ for ODS and PGC systems respectively. The flow rates were different to maintain comparable linear flow velocities. Chromatography was performed at ambient temperature.

Mobile phase preparation

Mobile phase preparation was as given in section 2.1.1

Sample preparation

Sample preparation was as given in section 2.2.1

Data treatment

Data treatment was as given in section 2.1.1

2.2 Molecular modelling of interactions between an analyte and a model graphite surface by semi-empirical molecular orbital methods

Adsorption of analytes onto the surface of porous graphitic carbon stationary phase was simulated using the public domain MOPAC program within the Insight II molecular modelling software package (Molecular Simulations Inc.) on a Silicon Graphics Indigo² Workstation.

An extended aromatic molecule (chemical formula C₇₈H₂₂) was used to represent the PGC stationary phase (figure 2.1).

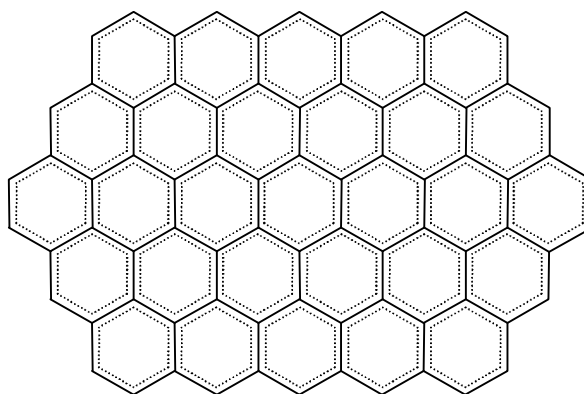


Figure 2.1 Structure of the model surface

Energy-minimised molecules were generated as described in subsequent sections.

2.2.1 MOPAC

MOPAC is a general purpose semi-empirical molecular orbital package for the study of chemical structures and reactions. The semi-empirical Hamiltonian AM1 [1] was used and a geometry optimization calculation was performed. There are four distinct methods available within MOPAC [2]: MINDO/3, MNDO, PM3 and the method used here, AM1. All are semi-empirical methods and have similar structure. A comprehensive review of the MOPAC program is given by Stewart [2].

Geometry specification and optimisation

Three Cartesian co-ordinates define the position of each atom. These are the x , y , and z values of the atom's position from an arbitrary origin. The MOPAC program systematically changes the geometry of the molecules so as to lower the heat of formation. When no further change in geometry can significantly lower the heat of formation, the optimisation is halted. This geometry will correspond to a stationary point on the potential energy surface.

The geometry is considered to be optimised if one or more of the following calculated quantities is sufficiently small:

- (a) the predicted change in geometry
- (b) the predicted change in heat of formation

The degree with which these are termed to be “sufficiently” small is set within the program and can be specified by the user.

Self-consistent field (SCF) criterion

The heat of formation and charge densities are the principal results of an SCF calculation. The precision with which these properties are calculated is determined by the SCF calculation. For routine use, this criterion will ensure a heat of formation (or energy convergence) within 0.1 calories of the semi-empirical answer. Decreasing the value of this energy convergence will increase the precision but this is at the expense of computational time.

Output of SCF calculations

The MOPAC SCF calculations generate two kinds of results that are of interest in this study.

- (a) Results which can be measured by experiment.
- (b) Quantum mechanical predictions which cannot be measured by experiment.

The former set is observable properties such as heat of formation, ionisation potential and dipole moment. When fully optimised geometries are used, these can be compared with experimental values. The heat of formation is used in this study when calculating the association between the model surface and the analyte. The ionisation potential and dipole moment can be used in subsequent QSRR analyses.

The latter set allows molecular orbital energies, charges, bond orders and valencies to be calculated. These quantities cannot be measured by experiment. The atomic point charges produced from MOPAC geometry optimisations can be transformed into useful molecular

descriptors such as Kaliszan's submolecular polarity parameter, Δ [3] and Coquart's excess charge parameter, C_n [4], which are used in the QSRR analyses of subsequent chapters.

2.2.2 Building the molecules

Analyte molecules and graphite surface model

Molecules were built individually using the Builder module within the Insight II molecular modelling package (Molecular Simulations Inc.) and saved in the Brookhaven protein databank (PDB) file format on a Silicon Graphics Indigo² workstation.

Once built, the individual molecules were then geometry optimised using molecular mechanics (MM) calculations. The CVFF force field was employed for the MM calculations and default atom centred charges were used.

Following MM minimisation, the geometry of the molecule was optimised using the AM1 Hamiltonian in MOPAC module within the MSI Insight II molecular modelling package, according to section 2.2.2.

The model chromatographic system

The minimised structure of the analyte molecule was placed at a specific distance from the surface of the $C_{78}H_{22}$ aromatic molecule. The analyte molecule was saved with co-ordinates relative to the $C_{78}H_{22}$ molecule. The PDB files for the $C_{78}H_{22}$ molecule and the analyte molecule were then concatenated to produce a single PDB file containing two molecules. An example file is given in Appendix 2.1. This procedure is performed as Insight II cannot perform MOPAC calculations on two files.

2.2.3 MOPAC geometry optimisation

Firstly, a geometry optimisation was carried out using the molecular mechanics technique (CVFF force field), within Insight II. The CVFF force field was used and the default atom centred charges used.

The resulting geometry was then fully optimised with MOPAC (AM1 Hamiltonian [1]). Default settings within MOPAC were used, but with the following exceptions. The PRECISE keyword was used in order to increase the geometric and electronic convergency criteria. The XYZ keyword was also used in order to use Cartesian coordinates in preference to internal coordinates. This is because the use of internal co-ordinates often results in premature program termination for planar molecules.

The model surface and each of the analytes were geometry optimised (as two isolated molecules in a vacuum) in an identical manner for consistency. These low energy conformations of analyte and model surface were used as the starting point for further energy minimisations to measure the heat of association of the model surface with the analytes under investigation.

The model analyte and surface were geometry optimised in a cofacial geometry at an initial separation of 50Å (measured between alternate carbon atoms on the benzene ring of the analyte and the central aromatic ring on the model surface), to find an initial heat of formation for a model surface and analyte. The separation and geometry were measured after energy minimisation to check for any surface-analyte interactions. If the separation altered, analyte-surface interaction would be assumed to have taken place. Separation and geometry were found to remain constant indicating no interaction.

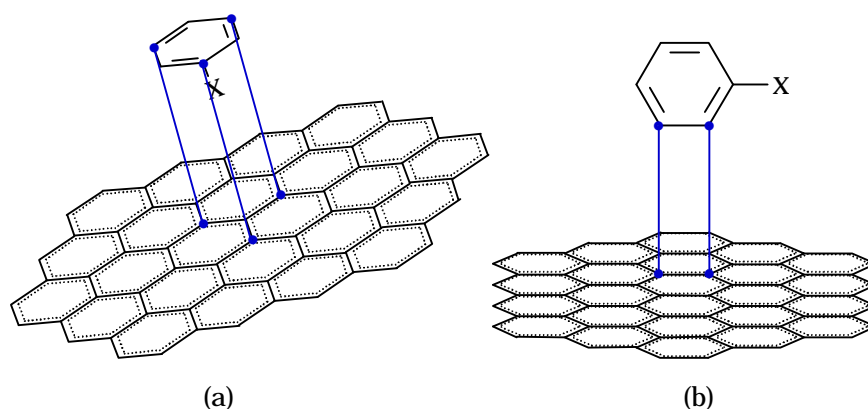


Figure 2. 2 Two example geometries, showing the positioning of the analyte molecules on (part of) the model graphite surface. (a) The offset cofacial geometry and (b) the face-edge geometry with the C–X bond parallel to the surface.

The model surface and analyte were placed at a separation of 3.6 Å and geometry optimised using the five initial geometries given in figures 2.3 – 2.7. Two example separations of the analyte and model surface are given in figure 2.2. Separation was calculated by measuring the distance between an atom in the analyte and an atom in the model surface as seen in figure 2.2 (distances are shown in blue). For cofacial geometries, three measurements were taken to ensure coplanarity. For perpendicular geometries, two separation distances were measured. All measurements were taken in a direction perpendicular to the plane of the model surface.

For each geometry optimisation, the following procedure was undertaken:

- (i) Analyte and surface positioned.
- (ii) MOPAC geometry optimisation.
- (iii) Geometry re-examined to check for repositioning of the analyte relative to the model surface.

The five geometries investigated are given below.

- (i) Cofacial geometry with no offset.

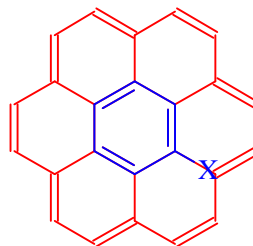


Figure 2.3 Cofacial geometry with no offset. Part of the model surface (red) with the analyte (blue).

- (ii) Offset cofacial geometry.

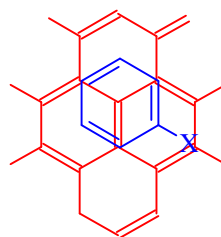


Figure 2.4 Cofacial geometry with offset, the model surface (part of) is in Blue with the analyte in red.

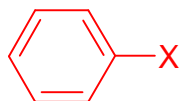
- (iii) Face-edge geometry with substituent directed away from the model surface



surface _____

Figure 2.5 Face-edge geometry with substituent directed away from the surface.

- (iv) Face-edge geometry with substituent directed parallel to the plane of the model surface



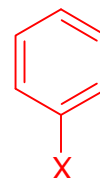
surface _____

Figure 2.6 Face-edge geometry with substituent directed parallel to the surface

- (iv) Face-edge geometry with substituent directed towards the model surface



or



surface _____

Figure 2.7 Face-edge geometry with substituent directed towards the surface.

The energy of interaction between the analyte molecule and the model graphite surface molecule, termed ΔH_f (in kcal, defined in figure 2.8) was calculated by subtracting the heat of formation of the analyte and the surface at small separation (approx. 3.6Å) from the heat of formation of the analyte and surface at a separation of 50 Å, as in figure 2.8. The stronger the attractive interaction between the analyte and the model surface, the more negative the value of ΔH_f . The more positive the value, the weaker the attraction between the analyte and the model surface becomes.

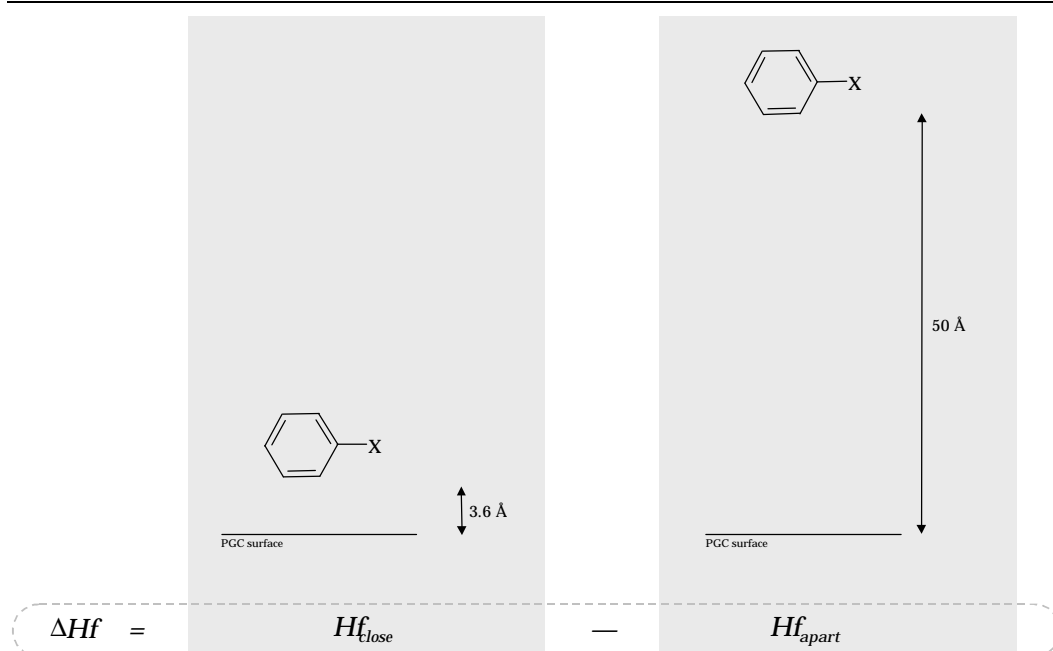


Figure 2.8 The calculation of ΔHf by subtracting heat of formation of analyte and model surface at a large separation from the heat of formation of analyte and model surface at close separation.

2.3 Conformational analysis of biphenyl derivatives by molecular modelling methods

2.3.1 Building the molecules

Three-dimensional models of the compounds of interest were built using the software and methods given in section 2.2.2.

2.3.2 Semi-empirical molecular orbital method

Three-dimensional models of the compounds of interest were built using the software and methods given in section 2.2.1. A geometry optimisation was then carried out using the molecular mechanics technique (CVFF force field), within Insight II. The CVFF force field was used and the default atom centred charges used.

The resulting geometry was then fully optimised with MOPAC (AM1 Hamiltonian [1]). Default settings within MOPAC were used, but with the following exceptions. The PRECISE keyword was used in order to

increase the geometric and electronic convergence criteria. The XYZ keyword was also used in order to use Cartesian coordinates in preference to internal coordinates. This is because the use of internal co-ordinates often results in premature program termination for planar molecules.

After geometry optimisation, the inter-phenyl torsion angle was measured (figure 2.9). For biphenyl this is a geometry with the phenyl rings out-of-co-planar by approximately 44° , as determined by experimental methods [5].

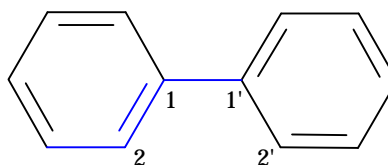


Figure 2.9 The inter-phenyl torsion angle measured (atoms & bonds highlighted in blue).

The inter-phenyl torsion angle ($C(2)-C(1)-C(1')-C(2')$) was then constrained at an angle of 0° to force the biphenyl derivative molecule into a conformation with coplanar phenyl rings. The biphenyl derivative molecule was then geometry optimisation with the inter-phenyl torsion angle constrained at 0° to find the minimum energy geometry for the planar molecule.

Heats of formation for the minimum energy conformations obtained (as described above) were used to calculate the energy barrier to coplanarity (ΔE). ΔE was calculated by subtraction of the heat of formation of the lowest energy conformation (E_{θ}) from the heat of formation for the co-planar conformation (E_0) according to figure 2.10.

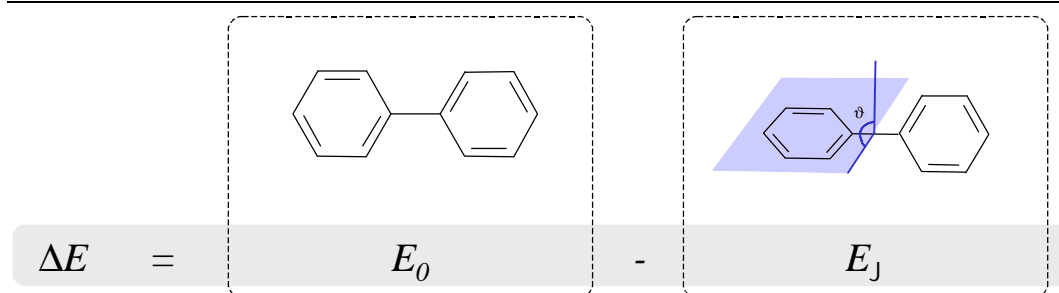


Figure 2.10 Calculation of the energy barrier to rotation of biphenyl derivatives, where E_0 & E_ϕ are the heats of formation for the flat molecule and the lowest energy conformation respectively.

2.4 QSRR methods

2.4.1 Regression analysis

Logarithms of retention factors were mutually related by means of bivariate and multivariate regression analysis using the TSAR 3.0 software (Oxford Molecular Ltd., Oxford, U.K.) on a Silicon Graphics Indigo² Workstation. The equations were derived by a stepwise regression analysis and then refined by a standard regression method (using the default settings within the software) taking into consideration the significance of individual descriptors, the intercorrelations among them, the number of data points and the variable data range and distribution. The relationships derived were tested according to the requirements of a meaningful correlation analysis [6].

2.4.2 Principal component analysis

Principal component analysis (PCA) is a technique to reduce a large number of variables into a smaller number without losing useful information. It is a useful technique with which to remove any cross-correlation between different descriptors and also to prepare for further multiple linear regression (MLR) analysis.

PCA was used in this thesis, primarily as a method for producing orthogonal descriptors for MLR analysis with retention data. PCA was performed using the TSAR 3.0 software (Oxford Molecular Ltd., Oxford, U.K.) on a Silicon Graphic Indigo² Workstation.

Structural descriptor parameters were chosen to describe properties such as hydrophobicity, polarity, topology, size and physicochemical properties. PCA was performed using the default conditions within the TSAR software and results were outputted. The first few principal components (PCs, as described in section 1.3.3) usually describe the majority of the variance within the dataset. These PCs were then used in a multiple linear regression analysis with retention (in the form of $\log k$ or $\log k_w$) as the dependant variable.

2.5 References

- [1] M. J. S. Dewar, E. G. Zoebisch, E. F. Healy, J. J. P. Stewart, *J. Amer. Chem. Soc.* 107 (1985) 3902.
- [2] J. J. P. Stewart, *Journal of Computer-Aided Molecular Design* 4 (1990) 1.
- [3] R. Kaliszan, *J. Chromatogr. A* 656 (1993) 417.
- [4] V. Coquart, *PhD Thesis*, University of Paris, Paris 1993.
- [5] A. Almenningen, O. Bastiansen, L. Fernholt, B. N. Cyvin, S. J. Cyvin, S. Samdal, *J. Mol. Struct.* 128 (1985) 59.
- [6] M. Charlton, S. Clementi, S. Ehrenson, O. Exner, J. Shorter, S. Wold, *Quant. Struct.-Act. Relat.* 4 (1985) 29.

Appendix 2.1 - Example PDB file

The model graphite surface with a biphenyl molecule placed at 50 Å separation. The biphenyl molecule is highlighted in a blue font at the end of the file.

```
REMARK THE MODEL GRAPHITE SURFACE WITH BIPHENYL PLACED AT 50 ANGSTROM SEPARATION
REMARK 4 1PGC COMPLIES WITH FORMAT V. 2.0, 30-NOV-1999
ATOM 1 C1 MON 1 24.133 -10.193 0.002 1.00 0.00 C
ATOM 2 C2 MON 1 24.136 -11.557 0.003 1.00 0.00 C
ATOM 3 C3 MON 1 25.354 -12.292 0.003 1.00 0.00 C
ATOM 4 C4 MON 1 26.566 -11.571 0.003 1.00 0.00 C
ATOM 5 C5 MON 1 26.561 -10.141 0.005 1.00 0.00 C
ATOM 6 C6 MON 1 25.339 -9.435 0.003 1.00 0.00 C
ATOM 7 C7 MON 1 27.799 -12.280 0.000 1.00 0.00 C
ATOM 8 C8 MON 1 27.802 -13.692 -0.006 1.00 0.00 C
ATOM 9 C9 MON 1 29.035 -14.400 -0.004 1.00 0.00 C
ATOM 10 C10 MON 1 30.246 -13.690 0.001 1.00 0.00 C
ATOM 11 C11 MON 1 30.241 -12.260 0.000 1.00 0.00 C
ATOM 12 C12 MON 1 29.027 -11.560 0.002 1.00 0.00 C
ATOM 13 C13 MON 1 29.022 -10.127 0.003 1.00 0.00 C
ATOM 14 C14 MON 1 30.229 -9.414 0.003 1.00 0.00 C
ATOM 15 C15 MON 1 30.225 -7.985 0.004 1.00 0.00 C
ATOM 16 C16 MON 1 29.006 -7.288 0.003 1.00 0.00 C
ATOM 17 C17 MON 1 27.779 -8.009 0.002 1.00 0.00 C
ATOM 18 C18 MON 1 27.786 -9.420 0.004 1.00 0.00 C
ATOM 19 C19 MON 1 31.475 -11.541 -0.002 1.00 0.00 C
ATOM 20 C20 MON 1 33.913 -11.532 -0.005 1.00 0.00 C
ATOM 21 C21 MON 1 33.910 -10.112 -0.005 1.00 0.00 C
ATOM 22 C22 MON 1 32.687 -9.406 -0.001 1.00 0.00 C
ATOM 23 C23 MON 1 31.470 -10.121 0.000 1.00 0.00 C
ATOM 24 C24 MON 1 31.485 -14.398 0.007 1.00 0.00 C
ATOM 25 C25 MON 1 31.493 -15.824 0.013 1.00 0.00 C
ATOM 26 C26 MON 1 32.713 -16.510 0.019 1.00 0.00 C
ATOM 27 C27 MON 1 33.931 -15.817 0.014 1.00 0.00 C
ATOM 28 C28 MON 1 33.925 -14.391 0.005 1.00 0.00 C
ATOM 29 C29 MON 1 32.703 -13.686 0.004 1.00 0.00 C
ATOM 30 C30 MON 1 35.153 -12.241 -0.008 1.00 0.00 C
ATOM 31 C31 MON 1 36.374 -14.374 -0.001 1.00 0.00 C
ATOM 32 C32 MON 1 37.596 -12.241 -0.013 1.00 0.00 C
ATOM 33 C33 MON 1 36.360 -11.528 -0.012 1.00 0.00 C
ATOM 34 C34 MON 1 25.370 -13.708 -0.006 1.00 0.00 C
ATOM 35 C35 MON 1 26.562 -14.406 -0.011 1.00 0.00 C
ATOM 36 C36 MON 1 29.053 -15.839 -0.005 1.00 0.00 C
ATOM 37 C37 MON 1 27.780 -16.527 -0.019 1.00 0.00 C
ATOM 38 C38 MON 1 30.246 -16.518 0.007 1.00 0.00 C
ATOM 39 C39 MON 1 26.611 -15.852 -0.022 1.00 0.00 C
ATOM 40 C40 MON 1 32.696 -12.246 -0.001 1.00 0.00 C
ATOM 41 C41 MON 1 35.158 -13.672 -0.001 1.00 0.00 C
ATOM 42 C42 MON 1 35.181 -16.503 0.018 1.00 0.00 C
ATOM 43 C43 MON 1 36.372 -15.814 0.009 1.00 0.00 C
ATOM 44 C44 MON 1 35.146 -9.392 -0.006 1.00 0.00 C
ATOM 45 C45 MON 1 36.359 -10.094 -0.008 1.00 0.00 C
ATOM 46 C46 MON 1 35.143 -7.962 -0.003 1.00 0.00 C
ATOM 47 C47 MON 1 37.591 -9.375 -0.009 1.00 0.00 C
ATOM 48 C48 MON 1 38.822 -10.090 -0.009 1.00 0.00 C
ATOM 49 C49 MON 1 37.591 -7.963 -0.003 1.00 0.00 C
ATOM 50 C50 MON 1 38.824 -11.521 -0.013 1.00 0.00 C
ATOM 51 C51 MON 1 36.357 -7.253 -0.002 1.00 0.00 C
ATOM 52 C52 MON 1 33.903 -7.255 -0.002 1.00 0.00 C
ATOM 53 C53 MON 1 33.895 -5.829 0.001 1.00 0.00 C
ATOM 54 C54 MON 1 32.684 -7.968 0.001 1.00 0.00 C
ATOM 55 C55 MON 1 31.459 -7.268 0.003 1.00 0.00 C
ATOM 56 C56 MON 1 25.345 -8.017 0.002 1.00 0.00 C
ATOM 57 C57 MON 1 26.532 -7.308 0.001 1.00 0.00 C
ATOM 58 C58 MON 1 26.574 -5.862 -0.002 1.00 0.00 C
ATOM 59 C59 MON 1 29.014 -5.849 0.000 1.00 0.00 C
ATOM 60 C60 MON 1 31.455 -5.842 0.003 1.00 0.00 C
ATOM 61 C61 MON 1 27.736 -5.173 -0.002 1.00 0.00 C
ATOM 62 C62 MON 1 30.202 -5.159 -0.001 1.00 0.00 C
ATOM 63 C63 MON 1 32.672 -5.147 0.002 1.00 0.00 C
ATOM 64 C64 MON 1 35.142 -5.132 0.004 1.00 0.00 C
ATOM 65 C65 MON 1 36.338 -5.812 0.003 1.00 0.00 C
ATOM 66 C66 MON 1 37.654 -16.488 0.012 1.00 0.00 C
```

Chapter 2 – Experimental methods

ATOM	67	C67	MON	1	38.815	-15.800	0.002	1.00	0.00	C
ATOM	68	C68	MON	1	38.849	-14.354	-0.005	1.00	0.00	C
ATOM	69	C69	MON	1	40.035	-13.642	-0.007	1.00	0.00	C
ATOM	70	C70	MON	1	40.046	-12.226	-0.011	1.00	0.00	C
ATOM	71	C71	MON	1	41.264	-11.484	-0.010	1.00	0.00	C
ATOM	72	C72	MON	1	41.263	-10.117	-0.008	1.00	0.00	C
ATOM	73	C73	MON	1	40.041	-9.378	-0.007	1.00	0.00	C
ATOM	74	C74	MON	1	40.026	-7.960	-0.002	1.00	0.00	C
ATOM	75	C75	MON	1	38.835	-7.253	0.001	1.00	0.00	C
ATOM	76	C76	MON	1	38.785	-5.806	0.012	1.00	0.00	C
ATOM	77	C77	MON	1	37.615	-5.131	0.006	1.00	0.00	C
ATOM	78	C78	MON	1	37.602	-13.653	-0.009	1.00	0.00	C
ATOM	79	H1	MON	1	23.177	-9.644	0.012	1.00	0.00	H
ATOM	80	H2	MON	1	23.190	-12.120	0.004	1.00	0.00	H
ATOM	81	H26	MON	1	32.717	-17.611	0.028	1.00	0.00	H
ATOM	82	H34	MON	1	24.411	-14.249	-0.008	1.00	0.00	H
ATOM	83	H37	MON	1	27.805	-17.627	-0.027	1.00	0.00	H
ATOM	84	H38	MON	1	30.262	-17.619	0.010	1.00	0.00	H
ATOM	85	H39	MON	1	25.647	-16.386	-0.030	1.00	0.00	H
ATOM	86	H42	MON	1	35.173	-17.604	0.028	1.00	0.00	H
ATOM	87	H56	MON	1	24.381	-7.485	-0.003	1.00	0.00	H
ATOM	88	H58	MON	1	25.606	-5.334	-0.002	1.00	0.00	H
ATOM	89	H61	MON	1	27.747	-4.072	-0.004	1.00	0.00	H
ATOM	90	H62	MON	1	30.209	-4.059	0.005	1.00	0.00	H
ATOM	91	H63	MON	1	32.668	-4.047	0.004	1.00	0.00	H
ATOM	92	H64	MON	1	35.125	-4.031	0.006	1.00	0.00	H
ATOM	93	H66	MON	1	37.642	-17.589	0.019	1.00	0.00	H
ATOM	94	H67	MON	1	39.781	-16.328	0.002	1.00	0.00	H
ATOM	95	H69	MON	1	41.001	-14.173	-0.005	1.00	0.00	H
ATOM	96	H71	MON	1	42.213	-12.042	-0.013	1.00	0.00	H
ATOM	97	H72	MON	1	42.211	-9.554	-0.007	1.00	0.00	H
ATOM	98	H74	MON	1	40.985	-7.424	0.003	1.00	0.00	H
ATOM	99	H76	MON	1	39.748	-5.268	0.012	1.00	0.00	H
ATOM	100	H77	MON	1	37.595	-4.030	0.013	1.00	0.00	H
ATOM	1	C1	BENZ	1	32.547	-16.070	-49.991	1.00	0.00	C
ATOM	2	C2	BENZ	1	31.492	-15.403	-49.381	1.00	0.00	C
ATOM	3	C3	BENZ	1	31.458	-14.012	-49.381	1.00	0.00	C
ATOM	4	C4	BENZ	1	32.492	-13.254	-49.976	1.00	0.00	C
ATOM	5	C5	BENZ	1	33.558	-13.965	-50.573	1.00	0.00	C
ATOM	6	C6	BENZ	1	33.577	-15.355	-50.589	1.00	0.00	C
ATOM	7	H1	BENZ	1	32.566	-17.150	-50.001	1.00	0.00	H
ATOM	8	H2	BENZ	1	30.701	-15.964	-48.904	1.00	0.00	H
ATOM	9	H3	BENZ	1	30.632	-13.523	-48.882	1.00	0.00	H
ATOM	10	H5	BENZ	1	34.363	-13.439	-51.069	1.00	0.00	H
ATOM	11	H6	BENZ	1	34.387	-15.880	-51.077	1.00	0.00	H
ATOM	12	C1	BENZ	1B	32.393	-9.048	-50.044	1.00	0.00	C
ATOM	13	C2	BENZ	1B	31.245	-9.772	-50.340	1.00	0.00	C
ATOM	14	C3	BENZ	1B	31.271	-11.163	-50.301	1.00	0.00	C
ATOM	15	C4	BENZ	1B	32.457	-11.863	-49.985	1.00	0.00	C
ATOM	16	C5	BENZ	1B	33.609	-11.097	-49.695	1.00	0.00	C
ATOM	17	C6	BENZ	1B	33.572	-9.706	-49.715	1.00	0.00	C
ATOM	18	H1	BENZ	1B	32.370	-7.969	-50.071	1.00	0.00	H
ATOM	19	H2	BENZ	1B	30.335	-9.256	-50.611	1.00	0.00	H
ATOM	20	H3	BENZ	1B	30.366	-11.696	-50.560	1.00	0.00	H
ATOM	21	H5	BENZ	1B	34.537	-11.578	-49.417	1.00	0.00	H
ATOM	22	H6	BENZ	1B	34.458	-9.138	-49.471	1.00	0.00	H
TER										

Chapter Three

The retention mechanisms of alkylbenzenes on PGC

3.1 Introduction

In chapter 1, we have seen that the chemistry of the graphite surface plays a significant role in analyte retention. This role is much greater than had originally been expected by those who developed PGC [1] and predicted a near perfect reversed phase mechanism [2, 3]. However this has proved to be an over simplification of the retention on PGC which appears to be a combination of mechanisms based on hydrophobicity, polarity, size, topology and planarity [4-6].

One key aspect of retention on PGC is the rigid planar graphite surface which results in very strong retention of large planar molecules [5]. By investigating the retention of a series of structurally similar analytes which possess a common aromatic backbone, it is possible to investigate how the shape of a molecule affects its retention. By choosing hydrophobic analytes the polar retention effect on graphite (PREG) described by Knox and Ross [7, 8] can be minimised.

It has been shown that PGC has far greater resolution of structurally similar hydrocarbons such as alkylbenzenes and polymethylbenzenes than ODS [5, 9, 10]. ODS is unable to resolve instances of these two

groups of molecules which are structural isomers (e.g. ethylbenzene and 2-methyltoluene), whereas PGC gives complete resolution. Although these studies have shown the greater selectivity of PGC compared with ODS for these hydrocarbons, the way in which the analyte interacts with the PGC surface has not been fully investigated.

The aim of this chapter was to investigate a series of *n*-alkylbenzenes and amylbenzene structural isomers by chromatographic and computational chemistry techniques to determine the mechanisms of retention on PGC. Quantitative structure-retention relationship (QSRR) methods were used to assess which structural descriptors are important to retention. Molecular modelling of analyte-surface interactions was used to find the relative orientation of the analyte and PGC demonstrating the strongest attraction.

3.2 Chromatographic results on ODS and PGC

The retention characteristics of 16 alkylbenzenes were measured on PGC and ODS using 90:10 methanol/water. The general structure of the analytes is given in figure 3.1

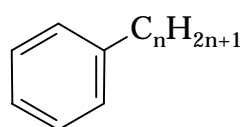


Figure 3. 1 Structure of alkylbenzenes; $n = 0$ to 8.

The individual structures of the amylbenzene isomers are given in figure 3.2.

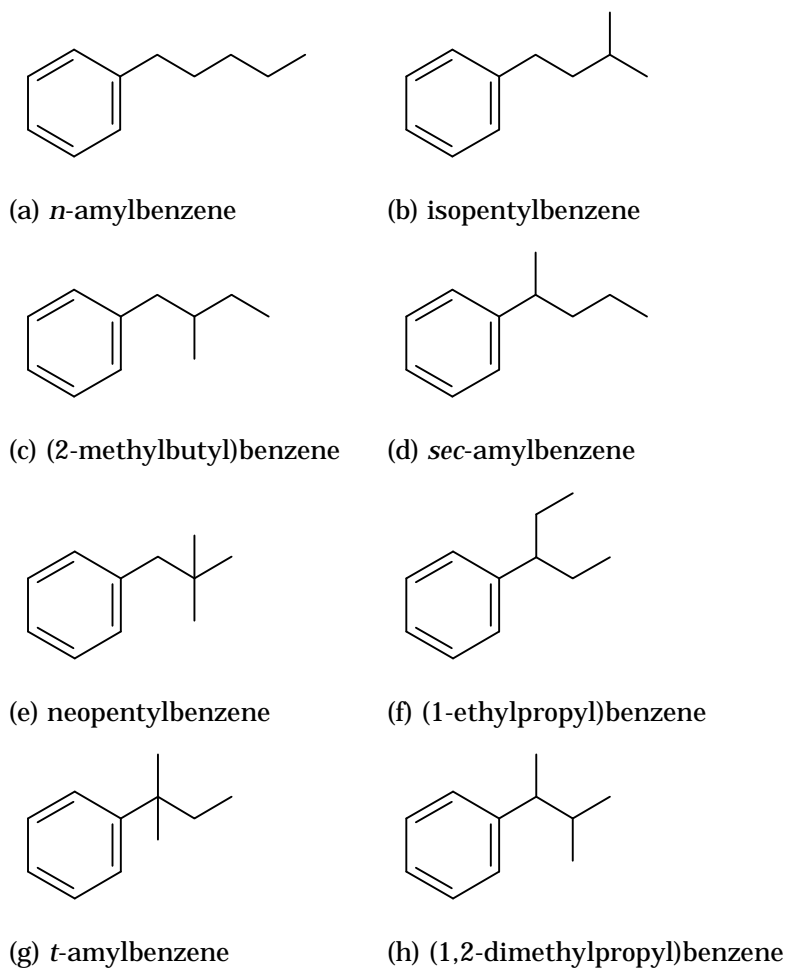


Figure 3. 2 Amylbenzene structural isomers.

Table 3.1 outlines the values of log capacity factor for the 16 alkylbenzenes under investigation. Each value represents the mean of three measurements. Retention data were reproducible to better than 1% from run to run. The experimental methods used are discussed in section 2.1.1.

Table 3.1 Retention data for alkylbenzenes on PGC and ODS stationary phases eluted with 90:10 methanol/water.

Analyte	PGC		ODS	
	log <i>k</i>	RSD*	log <i>k</i>	RSD*
benzene	-0.680	0.159	-0.180	0.562
toluene	-0.350	0.421	-0.045	0.072
ethylbenzene	-0.270	0.644	0.100	0.768
<i>n</i> -propylbenzene	-0.078	0.490	0.227	0.963
<i>n</i> -butylbenzene	0.119	0.351	0.358	0.228
<i>n</i> -amylbenzene	0.392	0.392	0.499	0.050
isopentylbenzene	0.216	0.255	0.476	0.451
<i>t</i> -amylbenzene	-0.203	0.812	0.466	0.514
neopentylbenzene	-0.021	0.278	0.469	0.815
<i>sec</i> -amylbenzene	0.046	0.856	0.477	0.634
(1-ethylpropyl)benzene	-0.067	0.457	0.478	0.642
(2-methylbutyl)benzene	0.112	0.654	0.479	0.329
(1,2-dimethylpropyl)benzene	-0.101	0.889	0.452	0.547
phenyl hexane	0.627	0.534	0.639	0.137
phenyl heptane	0.898	0.169	0.784	0.203
phenyl octane	1.166	0.560	0.922	0.212

*RSD is the relative standard deviation

$$(RSD = 100 \times (\text{standard deviation} / \text{mean}))$$

3.2.1 *n*-Alkylbenzenes

On octadecyl silica, there was a linear relationship between alkyl chain length and log *k* for *n*-alkylbenzenes (figure 3.3), this result was also observed by Kriz and co-workers [5]. The average selectivity, *a* (where $a = \log k_2 / \log k_1$) for a CH₂ addition on ODS was 1.373. ODS showed increased retention of smaller *n*-alkylbenzenes compared with PGC.

On porous graphitic carbon, the dependence of $\log k$ on alkyl chain length only becomes linear above *n*-butylbenzene (figure 3.3).

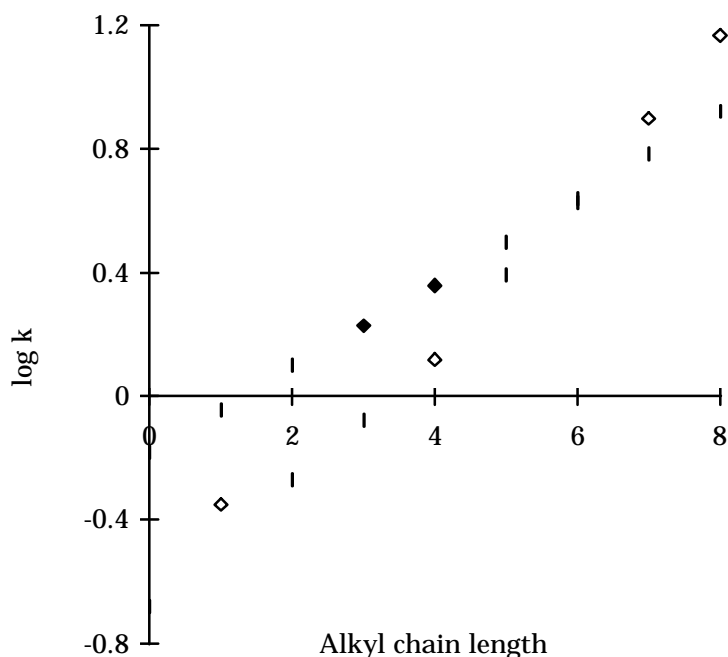


Figure 3. 3 The relationship between alkyl chain length and retention for *n*-alkylbenzenes on PGC (solid diamonds) and ODS (empty diamonds) stationary phases.

Below *n*-butylbenzene there was a positive deviation from linearity which may indicate a different or additional mode of interaction between the analyte and the stationary phase. This may also indicate a different geometry of interaction for lower alkylbenzenes compared with their larger relatives. The position of benzene was anomalous for PGC when compared to the lower *n*-alkylbenzenes. However, it was approximately in line with the retention of the higher *n*-alkylbenzenes. It is therefore possible that the retention of benzene has more in common with the higher *n*-alkylbenzenes rather than the smaller ones such as toluene and ethylbenzene. Although the retention of *n*-alkylbenzenes was weaker on PGC, for analytes below phenyl hexane compared with ODS, there was an improved selectivity ($\alpha = 1.723$).

3.2.2 Amylbenzene structural isomers

Chromatographs of a mixture of 8 amylbenzene structural isomers show that on ODS, the analytes remained largely unresolved (figure 3.4a), whereas on PGC there was almost complete separation for all peaks (figure 3.4b) and thus superior selectivity. A possible explanation for the poor resolution of analytes on ODS is the small differences in hydrophobicity between the analytes. The mechanism of retention on ODS is based largely on partitioning between the polar mobile phase and the hydrophobic stationary phase. The separation on PGC, while partly based on hydrophobic interactions, as seen in the *n*-alkylbenzenes, is also based on other factors. The aim of this study was to identify/investigate these additional /alternative mechanisms of interaction.

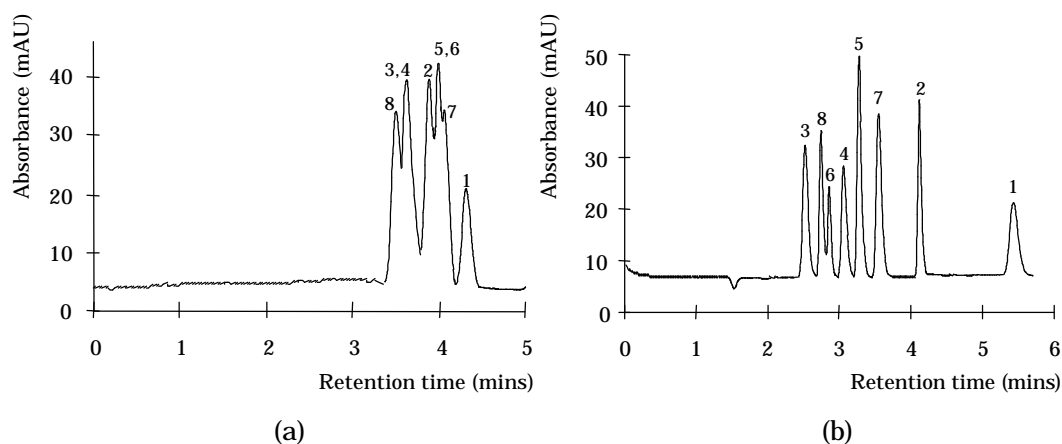


Figure 3. 4 Separation of amylbenzene structural isomers on (a) ODS and (b) PGC. (Analytes: 1. *n*-amylbenzene, 2. isopentylbenzene, 3. *t*-amylbenzene, 4. neopentylbenzene, 5. *sec*-amylbenzene, 6. (1-ethylpropyl)benzene, 7. (2-methylbutyl)benzene, 8. (1,2-dimethylpropyl)benzene.)

For uncharged non-polar analytes, such as alkylbenzenes, there can only be a limited number of factors influencing retention on PGC and these will include size (which incurs hydrophobicity in non polar molecules) and topology. In the case of the amylbenzene structural isomers, the size is constant. The separation should thus be based on

Chapter 3 - The retention mechanisms of alkylbenzenes on PGC topology. Branching of the alkyl group in alkylbenzenes decreased the retention on PGC in comparison to the straight chain isomer. It is therefore possible that branching of the amyl group reduces the interaction of the analyte molecule with the surface. The orientation of this interaction may be cofacial with the amyl group spread along the surface and π - π stacking of the aromatic ring with the graphite surface, or it may be face-edge with the amyl group spread along the surface and the 'end-on' interaction of the aromatic ring with the graphite surface (figure 3.5).



Figure 3. 5 Two possible orientations of interaction between the analyte molecule and the flat PGC surface. (a) The perpendicular face-edge geometry & (b) the coplanar (or cofacial) geometry.

The geometry of approach of the amylbenzene to the graphite surface can be envisaged to occur in a number of ways, and in each case with an increasingly branched amyl group, there would be less contact between the amyl group and the surface, and thus retention would be lessened. The observations reported here support this hypothesis.

QSRR analysis of alkylbenzenes

3.3.1 Bivariate analysis of n-alkylbenzenes

Linear regression analysis was performed on the experimentally obtained retention data for the benzene derivatives on both PGC and ODS stationary phases according to the methodology given in section 2.4.1. The resulting correlations between structural descriptors and retention are given in table 3.2.

Table 3.2 Correlation between structural descriptors and log *k* for *n*-alkylbenzenes, where *r* is the correlation coefficient.

Descriptor	<i>r</i> ²	
	PGC	ODS
Heat of Formation ^a	0.992	0.999
Mean Polarisability ^a	0.990	1.000
Molecular Surface Area ^a	0.990	1.000
Total Energy ^a	0.989	1.000
Alkyl chain length	0.989	1.000
Molar Refractivity ^b	0.989	1.000
log <i>P</i> _{calc} ^b	0.989	0.999
Randic Index ^b	0.988	0.999
π ^d	0.984	0.998
Wiener Index ^b	0.968	0.946
log <i>P</i> _{expt} ^d	0.964	0.980
Ellipsoidal Volume ^b	0.910	0.880
van der Waals Energy ^c	0.726	0.761
S^* ^d	0.568	0.675
Taft <i>E</i> _s ^d	0.451	0.481
<i>E</i> _{lumo} ^a	0.409	0.399
H-bond basicity ^e	0.339	0.296
Total Dipole Moment ^a	0.321	0.320
Total Dipole Moment ^b	0.212	0.224
Ionisation Potential ^a	0.255	0.253
<i>E</i> _{homo} ^a	0.255	0.253
Balaban Index ^b	0.007	0.016
Electrostatic Energy ^c	0.001	0.000

^a Calculated using VAMP software (Oxford Molecular Ltd).

^b Calculated using TSAR software (Oxford Molecular Ltd).

^c Calculated using COSMIC software. ^d From [11]. ^e From [12]

A strong linear relationship between $\log P$ and $\log k$ was observed for ODS (figure 3.5a). This result was in agreement with chromatography on PGC by Kriz and co-workers [5]. For PGC however, the linear relationship was only observed for *n*-alkylbenzenes above *n*-butylbenzene (figure 3.5a). For analytes below *n*-butylbenzene this dependence was non linear indicating a different or additional interaction between the analyte and the stationary phase. The position of benzene was anomalous.

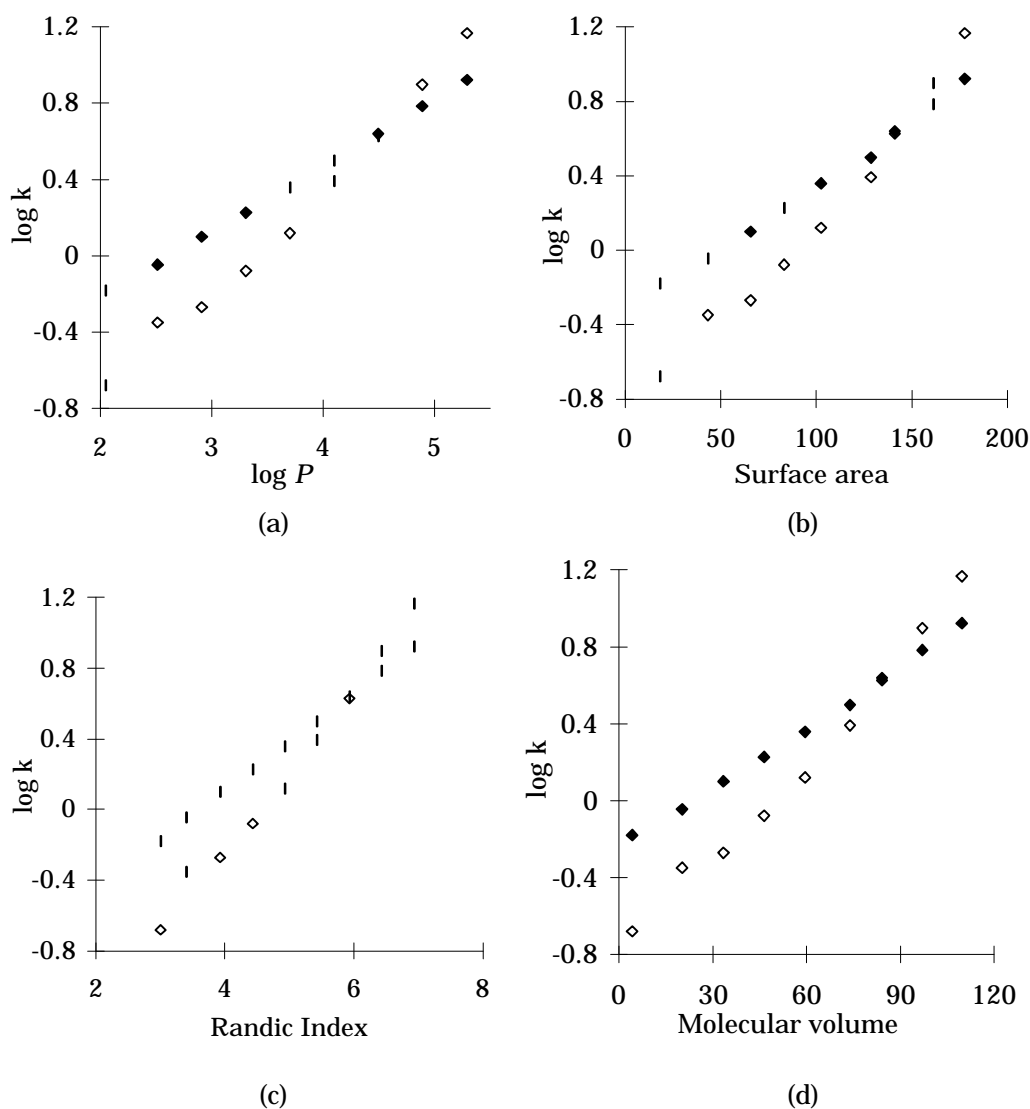


Figure 3. 6 The relationship between $\log k$ and (a) $\log P$, (b) molecular surface area, (c) Randic index and (d) molecular volume for *n*-alkylbenzenes on PGC (open diamonds) and ODS (solid diamonds).

Several other parameters describe the retention on ODS and PGC in

an almost identical manner. Graphical results for the relationships between $\log k$ and descriptor parameters (molecular surface area, Randic index [13, 14] and molecular volume) can also be seen in figure 3.5. This suggests that these descriptors are cross-correlated. The reason for the strong cross-correlation of many descriptors in this dataset is that these are very simple non-polar hydrocarbons and so in this case hydrophobicity can be described using the many different descriptors that are linked to hydrophobicity, such as $\log P$, molecular volume, molecular surface area, molecular refractivity, etc., and since this is a homologous series, heat of formation and total energy can also describe hydrophobicity (addition of a CH_2 to the chain merely increments the value of these descriptors).

However, there are exceptions to this rule. The Balaban index [15, 16] shows a linear relationship with $\log k$ for both PGC and ODS, but only for *n*-alkylbenzenes above *n*-butylbenzene (figure 3.7). Below *n*-butylbenzene extreme non-linearity was observed.

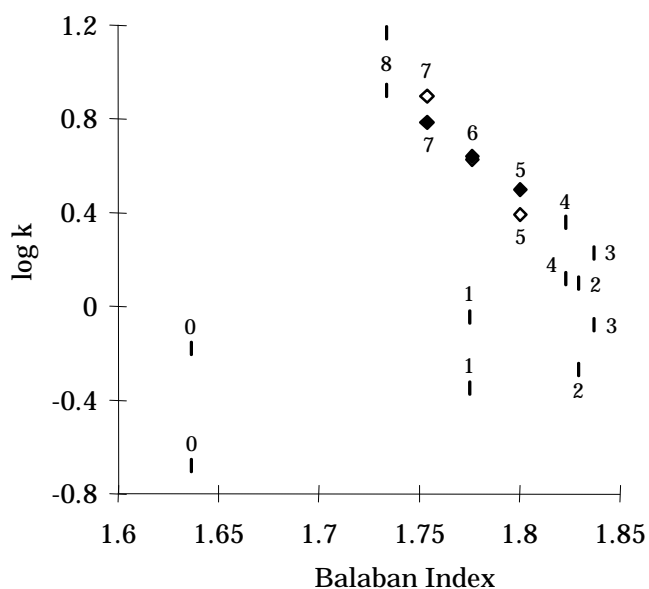


Figure 3. 7 The relationship between $\log k$ and Balaban index for *n*-alkylbenzenes on PGC (open diamonds) and ODS (solid diamonds).

The labels (0-8) indicate the length of the alkyl chain
e.g. 0 is benzene and 3 is *n*-butylbenzene.

The Wiener index was non linear with $\log k$ for both PGC and ODS (figure 3.8). There are distinct trends for both curves, however the curve for PGC is disrupted by toluene, ethylbenzene and *n*-propylbenzene.

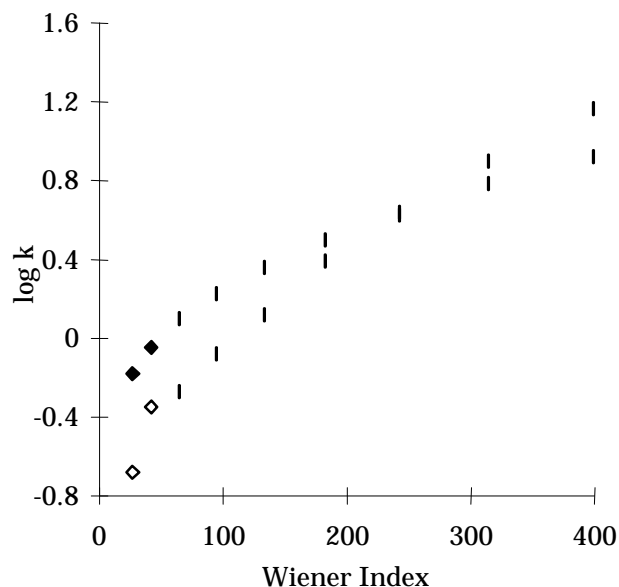


Figure 3. 8 The relationship between $\log k$ and Wiener index for *n*-alkylbenzenes on PGC (open diamonds) and ODS (solid diamonds).

There was poor correlation between dipole moment and $\log k$ for PGC or ODS (figure 3.9). This is because there is little variation in dipole moment along the series. Benzene ($\mu = 0.0$ D) is the only outlier because of its symmetry. Other electrostatic parameters are also poor at describing the retention of *n*-alkylbenzenes (e.g. electrostatic energy, ionisation potential, energy of the highest occupied molecular orbital, E_{homo} and energy of the lowest unoccupied molecular orbital E_{lumo}).

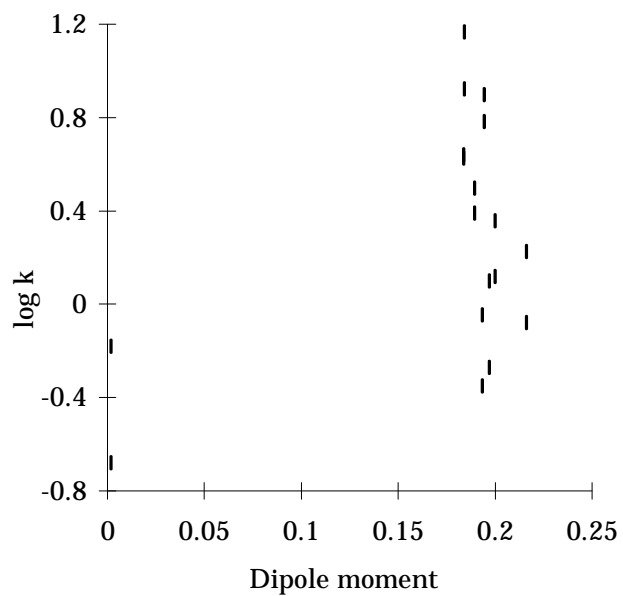


Figure 3. 9 The relationship between $\log k$ and dipole moment for n -alkylbenzenes on PGC (open diamonds) and ODS (solid diamonds).

3.3.2 Bivariate analysis of amylbenzenes

Quantitative structure-retention relationship analysis was performed on the amylbenzenes. The resulting linear regression correlation between descriptor and retention data are given in table 3.3.

Descriptors were selected to assess topology, geometry, polarity, size, hydrophobicity and were calculated using the TSAR software. For more information about the structural descriptor chosen, refer to section 1.3.2.

Table 3.3 Linear regression correlation between $\log k$ and structural descriptors for amylbenzene isomers, where r is the correlation coefficient.

Descriptor	r^2	
	PGC	ODS
<i>Topology</i>		
Wiener index	0.998	0.637
Balaban index	0.984	0.589
Randic index	0.381	0.525
<i>Geometry</i>		
Ellipsoidal Volume	0.231	0.248
<i>Polarity</i>		
Total Dipole Moment	0.729	0.617
<i>Size</i>		
Molecular Surface Area	0.718	0.575
Molecular Refractivity	0.583	0.488
Molecular Volume	0.062	0.046
<i>Hydrophobicity</i>		
$\log P_{calc}$	0.158	0.496

^a Calculated using TSAR software (Oxford Molecular Ltd).

A strong linear relationship was observed on PGC between $\log k$ and Wiener index (figure 3.10). The Wiener index [17] is a global molecular descriptor (i.e. its terms cannot be associated with a molecular fragment) in which the distance between each pair of atoms

make a contribution. Amylbenzenes with high Wiener index are more flexible molecules with minimal branching of the amyl group. Low values of Wiener index indicate amylbenzenes with poorer flexibility, due to the increased branching of the amyl group. The strong linear relationship was thought to indicate that decreased branching of the amyl chain and the resultant increase in flexibility would increase the contact area between the analyte and the PGC surface and therefore increase retention.

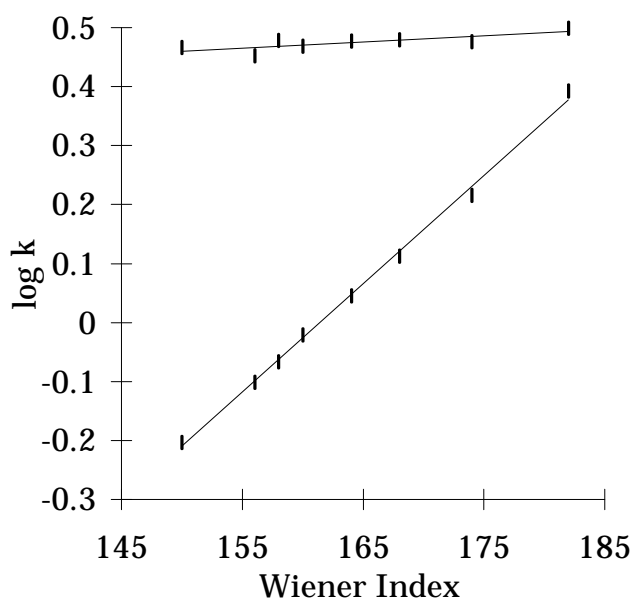


Figure 3. 10 The relationship between $\log k$ and Wiener index for amylbenzenes on PGC (open diamonds) and ODS (solid diamonds).

The strong relationship between Wiener index and $\log k$ was not observed on ODS, indicating a different mechanism of retention. On ODS the stationary phase is made up of flexible alkyl chains which analyte molecules can freely move between. This 'spongy' more liquid like phase discriminates far less between the shapes of the structural isomers.

A strong linear relationship was observed on PGC between $\log k$ and Balaban index (figure 3.11). The Balaban index, J is the average distance sum connectivity [15, 16]. Amylbenzenes with high Balaban

index are highly branched and therefore have difficulty adapting to the flat graphite surface (i.e. the contact area between the analyte and the surface is small). Low Balaban index denotes less branching of the amyl chain in amylbenzenes and thus incurs greater retention. The strong relationship between Balaban index and $\log k$ was not observed on ODS. Wiener and Balaban indices are strongly related with a high cross-correlation coefficient ($r^2 = 0.992$)

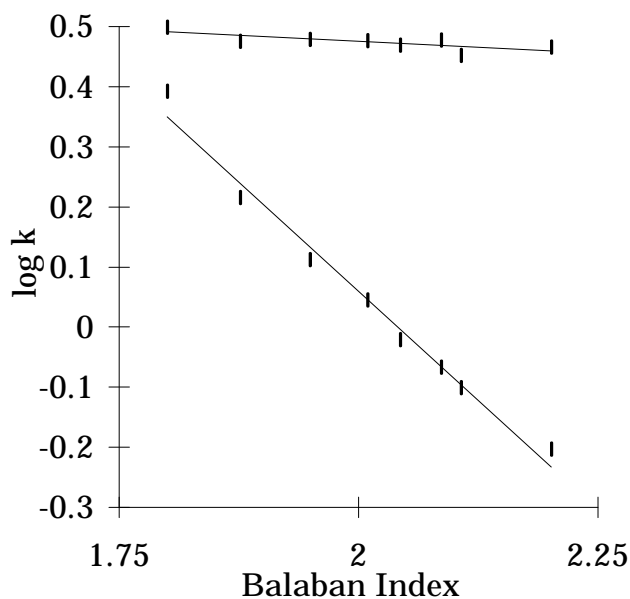


Figure 3. 11 The relationship between $\log k$ and Balaban index for amylbenzenes on PGC (open diamonds) and ODS (solid diamonds).

The relationship between Randic index and $\log k$ for amylbenzenes on both PGC and ODS is shown in figure 3.12. The correlation is poor for both stationary phases. This result was not as expected from the correlations of other topological indices with $\log k$ for PGC and may show that the Randic index examines another aspect of molecular topology.

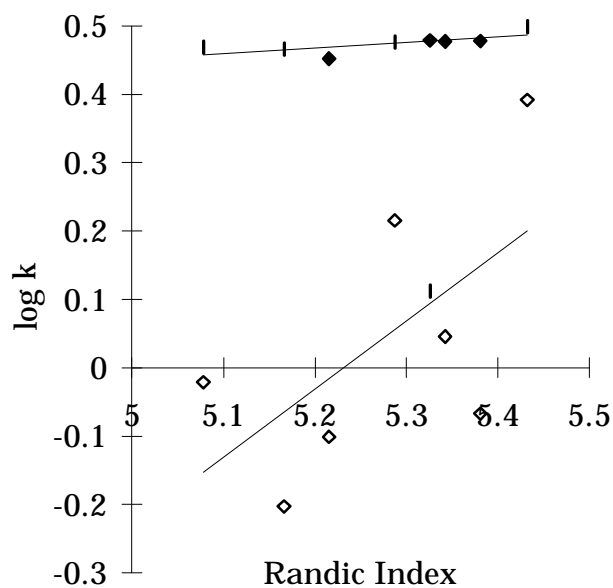


Figure 3. 12 The relationship between $\log k$ and Randic index for amylbenzenes on PGC (open diamonds) and ODS (solid diamonds).

The correlation between $\log P$ and $\log k$ was poor for amylbenzenes on PGC (figure 3.13) due to the method of calculating $\log P$ [18] and the closely related structures of the analytes. Isopentylbenzene, (2-methylbutyl)benzene, *sec*-amylbenzene and (1-ethylpropyl)benzene are all constructed of the same types of atoms.

2 x	CH ₃ (aliphatic carbon)	0.5473	=	1.0946
2 x	CH ₂ (aliphatic carbon)	0.4911	=	0.9822
1 x	CH (aliphatic carbon)	0.3614	=	0.3614
6 x	Aromatic carbon	0.2940	=	1.7640
		<hr/>		
		$\log P$	=	4.4312

As a result, each of these four analytes had the same calculated value of $\log P$. The same problem arises for neopentylbenzene and *t*-amylbenzene. This invalidates the analysis. In order to probe the relationship between hydrophobicity and retention of amylbenzenes on PGC more thoroughly, the experimental values of $\log P$ for these analytes would have to be measured. This remit has not been

The separation of the amylbenzene structural isomers on ODS is driven by the differences in hydrophobicity between the analytes. As there are only slight differences in $\log P$, the selectivity of amylbenzenes on ODS was poor (figure 3.13).

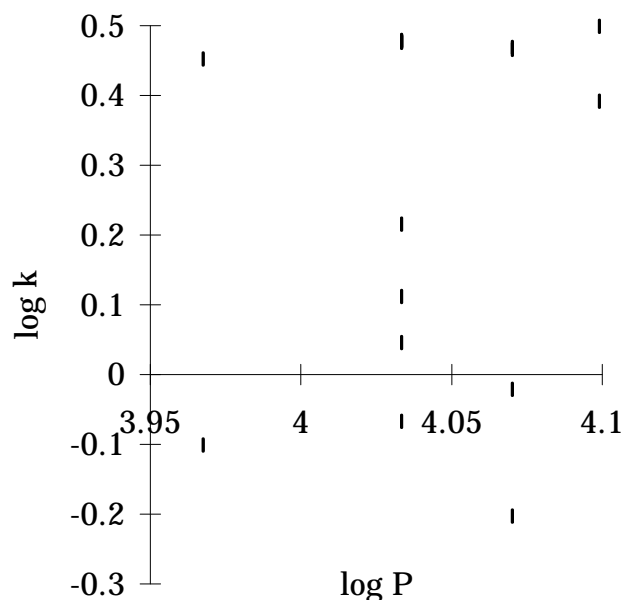


Figure 3. 13 The relationship between $\log k$ and $\log P_{calc}$ for amylbenzenes on PGC (open diamonds) and ODS (solid diamonds).

The linear relationship between molecular surface area and retention on PGC (correlation coefficient, $r^2 = 0.718$) appears to break down for *t*-amylbenzene, *sec*-amylbenzene and isopentylbenzene. The correlation between molecular surface area and $\log k$ was poor on ODS (figure 3.14).

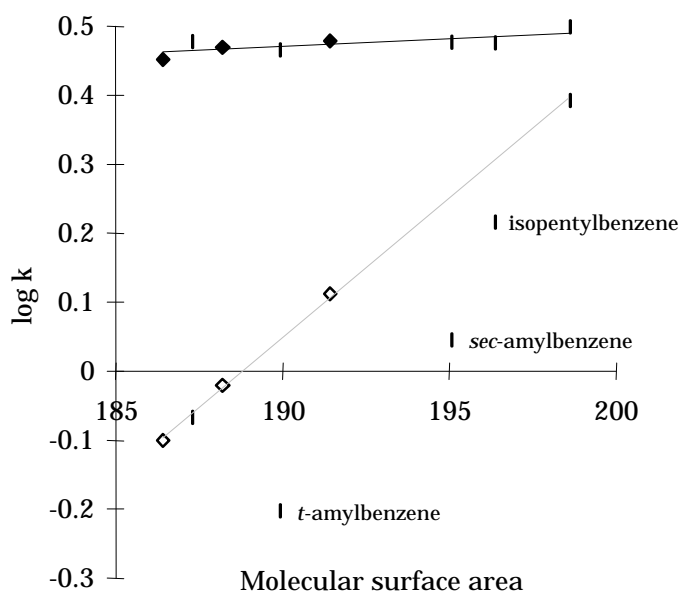


Figure 3. 14 The relationship between $\log k$ and molecular surface area for amylbenzenes on PGC (open diamonds) and ODS (solid diamonds).

3.4 Molecular modelling of analyte interactions with PGC surface

The energy of interaction between alkylbenzene analytes and a model graphite surface was considered using the semi-empirical molecular orbital methods described in section 2.2.3. Five alternative geometries for alignment of the analyte with the model graphite surface were considered, and are shown in figure 3.15.

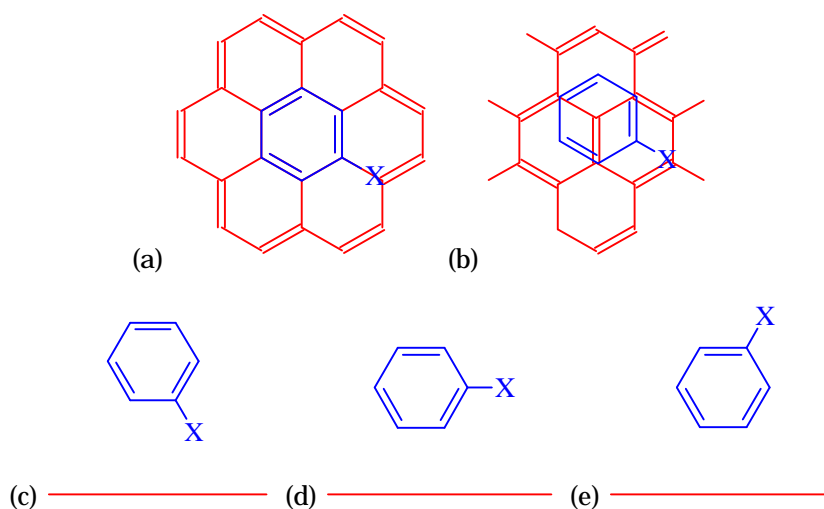


Figure 3. 15 The five geometries for the alignment of an analyte and part of the model graphite surface considered in molecular modelling studies. (a) Cofacial with no offset, (b) cofacial with offset, (c) face-edge with substituent X 'down' towards the model surface, (d) face-edge with substituent X parallel the model surface, (e) face-edge with substituent X 'up' away from the model surface. Red indicates the model surface. Blue indicates the analyte molecule

The energy of interaction between the analyte molecule and the model graphite surface molecule was calculated by subtracting the heat of formation of the analyte and the surface at a separation of 50 Å from the heat of formation of the analyte and the surface at small separation (approx. 3.6 Å), as in figure 3.16. The resulting difference in heat of formation values, termed ΔH_f (in kcal) are tabulated for the alkylbenzenes in table 3.4. The stronger the attractive interaction

between the analyte and the model surface, the more negative the value of ΔH_f . The more positive the value, the weaker the attraction between the analyte and the model surface becomes.

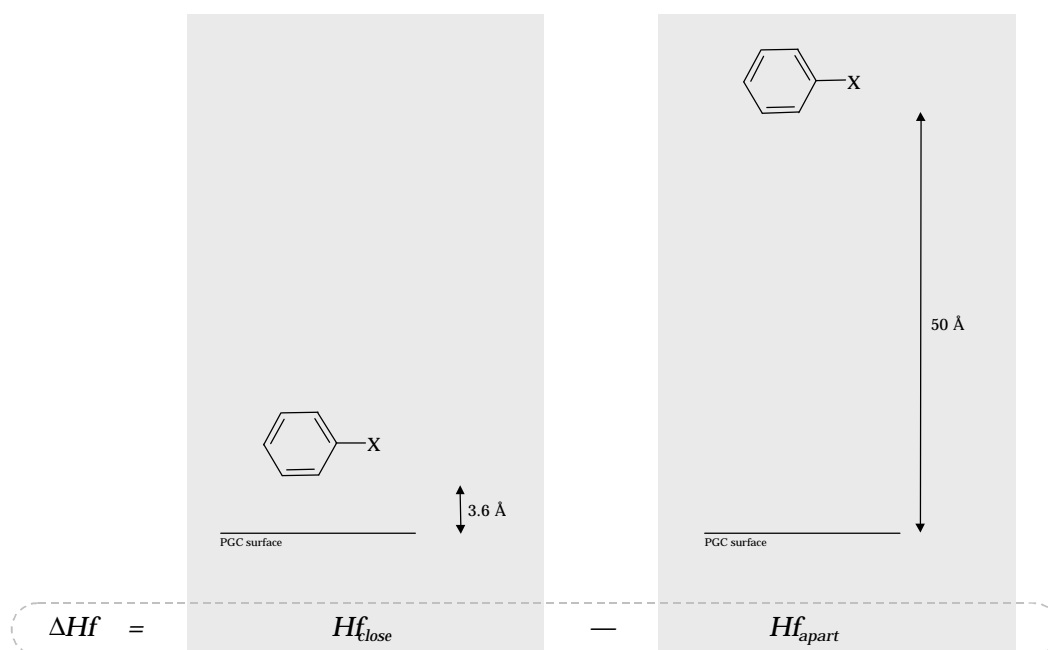


Figure 3. 16 The calculation of ΔH_f by subtracting heat of formation of analyte and model surface at large separation from the heat of formation of analyte and model surface at a close separation.

The important feature to note is the differences between the values for analytes, not their absolute value. This is because the calculations are based on a series of assumptions [19]. It is important to stress that the model used is a simplistic version of the retention on PGC with no solvent presence included.

Table 3.4 Heats of formation (in kcal) of a complex between a series of alkylbenzenes and a model graphite 'surface' molecule. The heat of formation which represents the strongest adsorption of the given analyte onto the surface, Hf_{min} is highlighted in **bold**.

Analyte	Cofacial		Face-edge			ΔHf_{min} (kcal)
	no offset ^a	offset ^b	x down ^c	x side ^d	x up ^e	
benzene	0.068	-0.038	-0.119	-0.119	-0.119	-0.119
toluene	0.226	-0.246	0.532	-0.109	0.682	-0.246
ethylbenzene	-0.262	-0.216	-0.259	-0.121	0.175	-0.262
<i>n</i> -propylbenzene	0.152	-0.119	-0.301	0.497	1.032	-0.301
<i>n</i> -butylbenzene	-0.153	-0.006	-0.376	-0.350	0.475	-0.376
<i>n</i> -amylbenzene	-0.050	0.021	-0.421	-0.440	-0.356	-0.440
isopentylbenzene	0.349	0.187	-0.197	0.513	0.402	-0.197
(2-methylbutyl)benzene	0.709	0.777	0.165	0.068	0.631	0.068
<i>sec</i> -amylbenzene	0.628	0.292	0.523	0.824	0.208	0.208
neopentylbenzene	0.094	-0.047	0.835	2.357	0.371	-0.047
(1-ethylpropyl)benzene	1.210	0.756	0.041	1.295	0.426	0.041
(1,2-dimethylpropyl)benzene	0.342	0.352	1.012	0.327	0.411	0.327
<i>t</i> -amylbenzene	0.312	0.328	2.133	0.934	0.251	0.251
phenyl hexane	-0.134	-0.023	-0.478	-0.487	-0.366	-0.487
phenyl heptane	-0.201	-0.009	-0.567	-0.506	-0.136	-0.567
phenyl octane	-0.328	-0.098	-0.548	-0.576	-0.116	-0.576

a,b,c,d & *e* Correspond to the geometries shown in figure 3.6

3.4.1 *n*-alkylbenzenes

As stated previously, the retention of *n*-alkylbenzenes on PGC ($\log k$) gave a linear relationship with alkyl chain length for *n*-alkylbenzenes larger than *n*-butylbenzene (figure 3.3). Below *n*-butylbenzene the relationship was non-linear with stronger retention than would be expected when compared with the higher *n*-alkylbenzenes. The behaviour of benzene was anomalous within this series. Figure 3.17

shows the relationship between alkyl chain length and Hf_{min} . The graph describes a similar trend to that in figure 3.3, however in this case the gradient is negative.

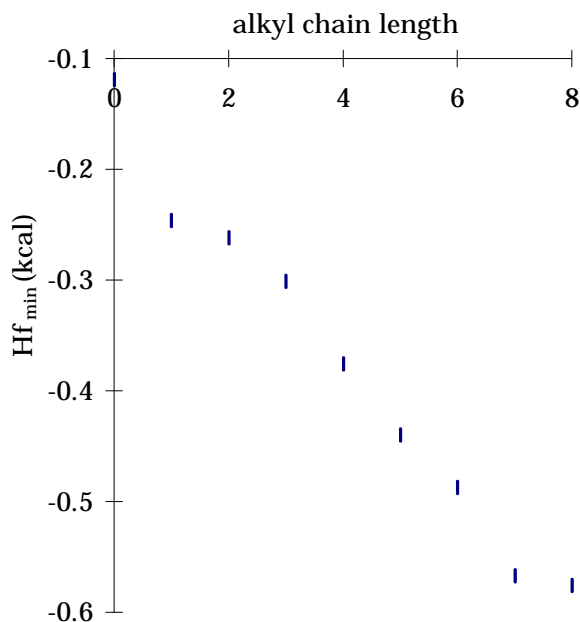


Figure 3. 17 The relationship between alkyl chain length and the heat of formation of the lowest energy geometry of a complex between *n*-alkylbenzenes and a model graphite 'surface' molecule.

The geometry of strongest interaction between the analyte and the model surface given in table 3.4 shows some interesting trends.

Benzene gave its strongest interaction with the surface with a face-edge geometry ($\Delta Hf = -0.119$ kcal). As $X = H$, all face-edge values were identical. This interaction was significantly stronger than either cofacial geometries (no offset: $\Delta Hf = 0.068$ kcal; offset: $\Delta Hf = -0.038$ kcal). Toluene gave its strongest interaction with the surface ($\Delta Hf = -0.246$ kcal) for an offset cofacial geometry (figure 3.14b). Face-edge geometries gave much weaker values of attraction ($\Delta Hf = 0.532$ kcal, 0.487 kcal & 0.682 kcal). Ethylbenzene gave its strongest interaction with the surface ($\Delta Hf = -0.262$ kcal) for a cofacial geometry with no offset (figure 3.15a), however cofacial with offset

($\Delta = -0.216$) and face-edge x-down ($Hf =$ comparable interactions.

The strongest interaction with the surface for n -propylbenzene was in face-edge x-side geometry. All higher n interactions with the model surface for either face-edge x-down (figure 3.15c) or face-edge x-side (figure 3.15d) geometries. The interactions

These results show a trend for face-edge interactions between the analyte and the model surface for benzene and n -alkylbenzenes above n propylbenzene, with the alkyl chain directed towards the surface or parallel to the surface. Toluene and ethylbenzene have strongest geometry of interaction may explain their stronger retention on PGC seen in chromatographic studies.

n -alkylbenzenes lie in the nature of the π interactions which control the cofacial adsorption of these analytes onto the model surface. A

interaction between aromatic molecules is given in reference [20] key feature of this model is that it considers the σ π -electrons separately and demonstrates that net favourable interactions are actually the result of π - σ π

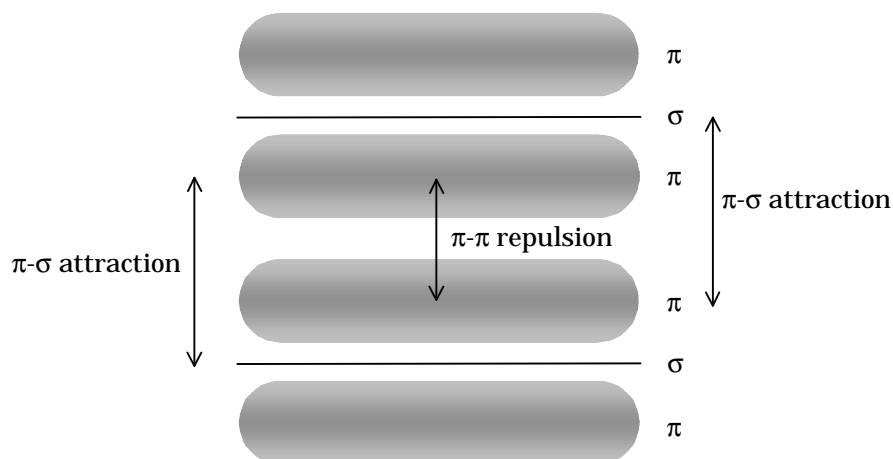


Figure 3. 18 A model of π - π interactions which considers the σ -framework and the π -electrons separately. This figure represents π - π interactions as the result of π - σ attractions that overcome π - π repulsions.

Benzene, toluene and ethylbenzene have face-edge x-side interactions with the model surface of comparable magnitude. For benzene, this face-edge geometry is more strongly attractive than any cofacial interaction, however for toluene and ethylbenzene this is not so. It is possible that in a cofacial geometry, toluene and ethylbenzene both have strong π - σ attractions that overcome π - π repulsions, whilst in benzene a face-edge interaction is needed to increase the π -electrons attraction. With the extension of the σ -framework outside of the benzene ring there may be an increased π - σ attraction which would explain the increased retention for these analytes. At *n*-propylbenzene the cofacial interaction becomes weaker than the face-edge interaction and so the relationship between alkyl chain length and $\log k$ begins to return to linearity.

The relationship between adsorption onto the model surface (ΔHf_{min}) and $\log k$ is explored in figure 3.19. There is a strong correlation with a value of 0.979 for the correlation coefficient, r^2 . The most noticeable outliers being benzene and phenyloctane.

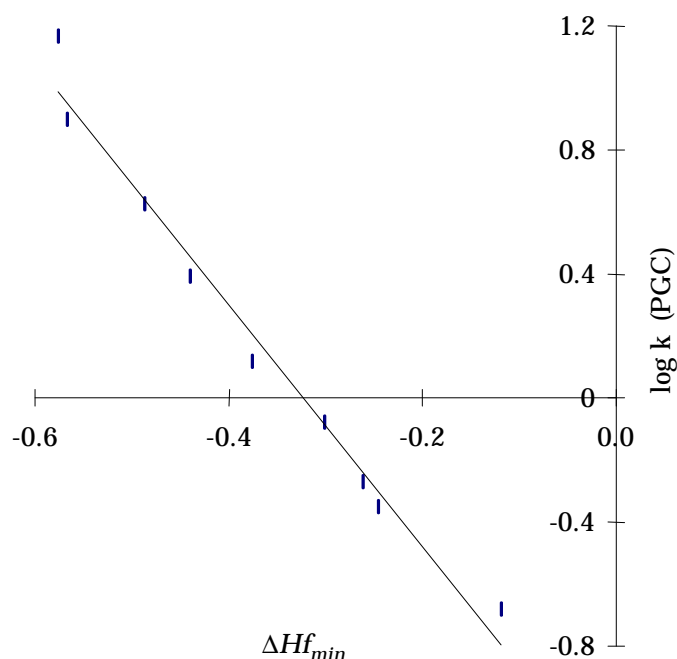


Figure 3. The relationship between $\log k$ and ΔHf_{min} retention on

This result provides evidence that a molecular modelling approach can yield information of chromatographic relevance which can help in

simple alkylbenzene series. This is significant because it suggests that although the molecular modelling technique used is rather crude,

considerations, the results it produces could be chromatographically

3.4.2 Amylbenzene structural isomers

k
 amylbenzenes. This relationship was thought to be based on the flexibility and branching of the amyl group and its unbranched chain would have more surface coverage than a more branched amyl group. Semi-empirical methods agree with this hypothesis, however in this data set,

the correlation between ΔHf_{min} and $\log k$ (figure 3.20) is substantially weaker ($r^2 = 0.756$) than for *n*-alkylbenzenes.

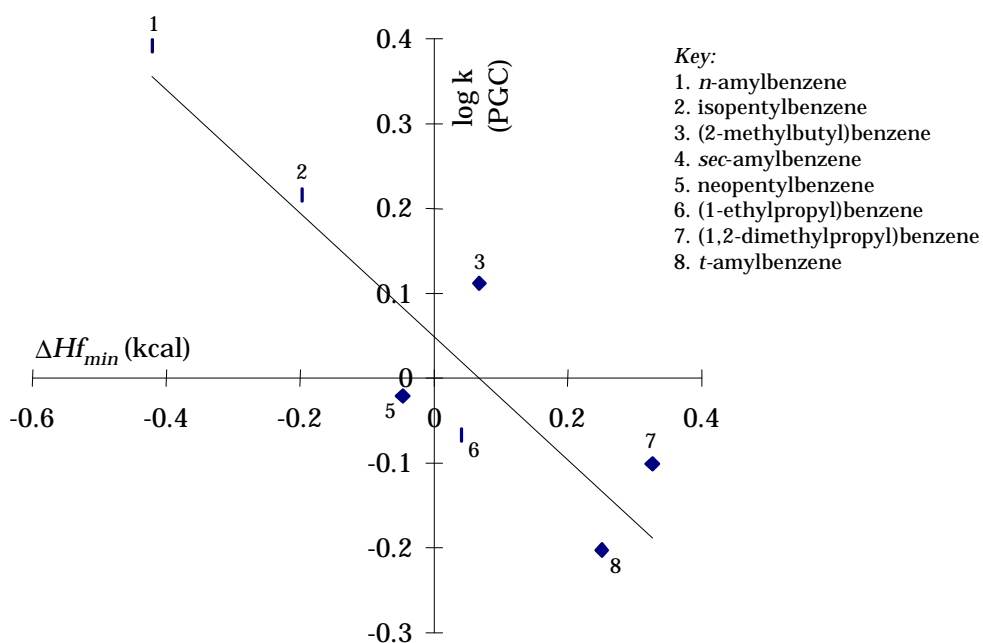


Figure 3.20 The relationship between retention on PGC and ΔHf_{min}

All amylylbenzene isomers, with the exception of neopentylylbenzene, have strongest interaction with the model surface in a face-edge configuration. For *t*-amylylbenzene (the most weakly retained species), the strongest interaction with the surface occurs when the amylyl group is pointed up, away from the surface. This is also seen for *sec*-amylylbenzene.

The straight chain *n*-amylylbenzene ($\Delta Hf_{min} = -0.440$ kcal) and isopentylylbenzene ($\Delta Hf_{min} = -0.197$ kcal) have substantially larger interactions with the model surface than the other amylylbenzenes and as such are outliers in the correlation between ΔHf_{min} and $\log k$. As outliers, they significantly improve the correlation. It may be that these results are qualitative rather than quantitative. This may be because the calculations are based on a series of assumptions^[19] which in this particular case are inappropriate. It may also be due to the lack of solvent in the semiempirical model used

3.4.3 Molecular modelling studies - Conclusions

The molecular modelling studies have proved invaluable to determine the geometries of interaction between the analytes and the PGC stationary phase. This rather simplistic molecular modelling approach has yielded a strong correlation between retention of *n*-alkylbenzenes and ΔH_{min} on PGC. It has also shown that lower *n*-alkylbenzenes have a different geometry of interaction with the PGC surface than higher *n*-alkylbenzenes and so given a reason for the increased retention of the lower *n*-alkylbenzenes. Molecular modelling of the amylbenzene structural isomers gave a lower correlation between $\log k$ and ΔH_{min} but a linear trend could be seen.

3.5 Application of QSRR methods to literature data — Polymethylbenzenes and comparisons with *n*-alkylbenzenes and amylbenzene structural isomers

After considering the retention of *n*-alkylbenzenes and amylbenzenes, it was of interest to extend our observations to polymethylbenzenes (figure 3.21). Kriz and co-workers [5] found that while ODS could not distinguish between polymethylbenzenes and *n*-alkylbenzenes which were structural isomers, PGC offered complete resolution of these hydrocarbons.

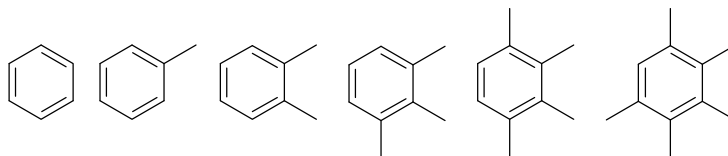


Figure 3. 21 The structures of polymethylbenzenes

The molecular modelling studies of *n*-alkylbenzenes highlighted some interesting points concerned with the geometry of adsorption onto the graphite surface. Higher *n*-alkylbenzenes appear to interact with the model surface in a face-edge manner providing end-on interactions for the π -systems of the surface and the analyte, placing the two π -systems perpendicular to each other.

Lower *n*-alkylbenzenes, toluene and ethylbenzene interact with the surface in a cofacial manner, therefore stacking of the π -systems occurs. This different mode of interaction was explained by regarding the net π - π attractions as strong π - σ attractions that overcome π - π repulsions. With the extension of the σ -framework outside of the benzene ring there may be an increasingly strong π - σ attraction which may explain the increased retention for these analytes.

Taking this one stage further, and considering polymethylbenzenes, this suggests that polymethylbenzenes may interact with the surface

in a cofacial manner. The extension of the σ benzene ring in this manner would provide increasingly strong π - σ extension of the σ effect, making end-on interactions increasingly unlikely along the series.

polymethylbenzenes is their strong correlation with topological indices (figure 3.22). For Wiener index k $r^2 = 0.989$) with a similar gradient ($m = 0.0184$). amylbenzenes, Wiener index explains the differences in the ability of the amyl chain to adapt to the flat surface (the shape polymethylbenzenes, Wiener index describes the ability of the whole molecule to adapt to the surface.

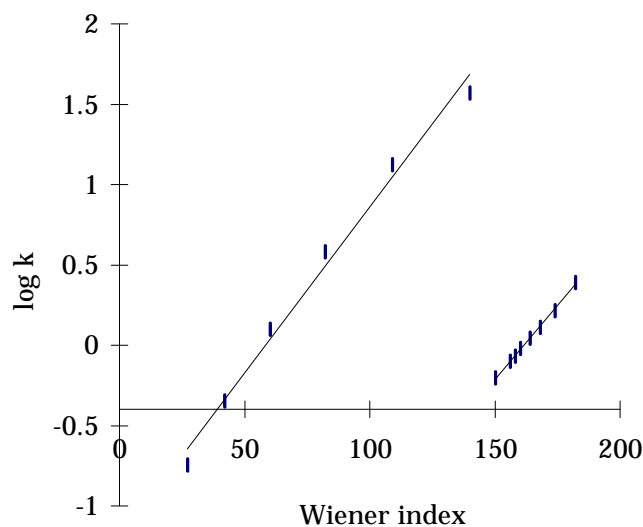


Figure 3. 22 The relationship between Wiener index and $\log k$ for amylbenzenes (open diamonds) and polymethylbenzenes (solid diamonds).

The relationship between Balaban index and $\log k$ is particularly interesting when comparing polymethylbenzenes and n -alkylbenzenes (figure 3.23). While there is a strong linear relationship between

Balaban index and $\log k$ for polymethylbenzenes, the relationship for *n*-alkylbenzenes involves a non-linear positive gradient between benzene and ethylbenzene, then a turning point and a negative gradient for higher *n*-alkylbenzenes with a linear relationship above *n*-butylbenzene. These relationships may be interpreted to be indicative of the geometry of interaction between the analyte and the surface of the PGC. The turning point indicating a departure from one orientation of interaction to another orientation of interaction. A negative gradient indicates a face-edge interaction and a positive gradient indicating a cofacial orientation.

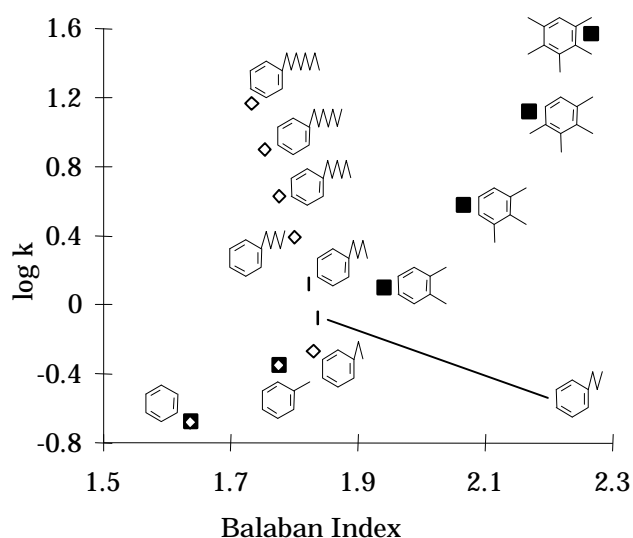


Figure 3. 23 The relationship between Balaban index and $\log k$ for polymethylbenzenes (solid squares) and *n*-alkylbenzenes (open diamonds).

3.6 Conclusions

Retention studies on ODS and PGC have show that PGC has superior selectivity for alkylbenzenes when compared to PGC. PGC is especially useful for the separation of alkylbenzene structural isomers.

Molecular modelling studies have suggested that the most energetically favoured orientation for interaction between analytes and the PGC surface is cofacial for toluene and ethylbenzene whereas higher *n*-alkylbenzenes this interaction is in a face-edge orientation. These results would suggest a cofacial orientation of interaction for polymethylbenzenes with the PGC surface.

The orientation of interaction of amylbenzene structural isomers with the PGC surface is largely in a face-edge geometry. The retention being based on the ability of the amyl group to unfold onto the PGC surface and maximise its interaction. As a result of this highly branched amylbenzenes are poorly retained in comparison with straight chain *n*-amylbenzene.

3.7 References

- [1] J. H. Knox, M. T. Gilbert, U.K. Patent 1978.
- [2] M. T. Gilbert, J. H. Knox, B. Kaur, *Chromatographia* 16 (1982) 138.
- [3] J. H. Knox, B. Kaur, G. R. Millward, *J. Chromatogr.* 352 (1986) 3.
- [4] V. Coquart, *PhD Thesis*, University of Paris, Paris 1993.
- [5] J. Kriz, E. Adamcova, J. H. Knox, J. Hora, *J. Chromatogr. A* 663 (1994) 151.
- [6] M. C. Hennion, V. Coquart, S. Guenu, C. Sella, *J. Chromatogr. A* 712 (1995) 287.
- [7] P. Ross, J. H. Knox, *Adv. Chromatogr.* 37 (1997) 121.
- [8] J. H. Knox, P. Ross, *Adv. Chromatogr.* 37 (1997) 73.
- [9] J. Kriz, L. Vodicka, J. Puncochárová, M. Kuras, *J. Chromatogr.* 219 (1981) 3.
- [10] J. H. Knox, J. Kriz, E. Adamcova, *J. Chromatogr.* 447 (1988) 13.
- [11] C. Hansch, Leo, *Substituent constants for correlation analysis in chemistry and biology*, John Wiley & Son, New York 1979.
- [12] P. T. Jackson, M. R. Schure, T. P. Weber, P. W. Carr, *Anal. Chem.* 69 (1997) 416.
- [13] M. J. Randic, *J. Amer. Chem. Soc.* 97 (1975) 6609.
- [14] M. Randic, N. Trinajstic, *Theochem-Journal Of Molecular Structure* 103 (1993) 209.
- [15] A. T. Balaban, *Chem. Phys. Lett.* 89 (1982) 399.
- [16] A. T. Balaban, I. Motoc, D. Bonchev, O. Mekenyan, in M. Charlton, I. Motoc (Eds.): *Steric Effects in Drug Design*, Springer-Verlag, Berlin 1983, p. 21.
- [17] H. Wiener, *J. Amer. Chem. Soc.* 69 (1947) 2636.
- [18] SRC, Environmental Science Center, Syracuse Research Corporation 1997-1999.

- [19] J. J. P. Stewart, *J. Computer-Aided Molecular Design* 4 (1990) 1.
- [20] C. A. Hunter, J. K. M. Sanders, *J. Amer. Chem. Soc.* 112 (1990) 5525.

Chapter Four

The retention mechanisms of benzene derivatives on PGC

4.1 Introduction

The aim of this chapter was to investigate a series of *mono*-substituted benzene derivatives by chromatographic and computational chemistry techniques to determine the mechanisms of retention on PGC.

The retention characteristics of 28 *mono*-substituted benzene derivatives were measured on PGC and ODS using a variety of methanol-water mobile phase compositions. The geometry of interaction between the analytes and the PGC stationary phase was investigated using semi-empirical molecular orbital methods. QSRR analysis was performed on the chromatographic and molecular modelling data produced.

The analytes studied in Chapter 3 were a series of non-polar analytes, and as such, retention was found to be based mainly upon hydrophobic and shape effects. Chapter 3 did not expose any evidence of the polar retention effect on graphite (PREG), a theory of retention on graphite which was introduced by Ross and Knox [1].

The 28 *mono*-substituted benzene derivatives investigated in Chapter 4 represent a more diverse range of analytes than those seen in Chapter 3, enabling us to study additional characteristics (such as

Chapter 4 - The retention mechanisms of benzene derivatives on PGC polarity, ionisation, topology) and their effect on retention for PGC supports. These analytes can be categorised in a number of different ways, but for the purpose of this study, were grouped into the six sections given in table 4.1.

Table 4.1 The mono substituted benzene derivatives studied

Analyte name	X
<i>Hydrocarbons (C_xH_y):</i>	
benzene	H
toluene	CH ₃
ethylbenzene	CH ₂ CH ₃
<i>t</i> -butylbenzene	CH(CH ₃) ₃
styrene	CH=CH ₂
biphenyl	C ₆ H ₆
<i>Halogenated compounds (C_xH_yX):</i>	
chlorobenzene	Cl
bromobenzene	Br
iodobenzene	I
benzylchloride	CH ₂ Cl
benzylbromide	CH ₂ Br
<i>Alcohols, aldehydes, ketones, esters (C_xH_yO_z):</i>	
phenol	OH
anisole	OCH ₃
benzyl alcohol	CH ₂ OH
benzaldehyde	CHO
acetophenone	COCH ₃
methylbenzoate	CO ₂ CH ₃
phenylacetate	OCOCH ₃
cinnamaldehyde	CH=CHCHO
<i>Carboxylic acids (C_xH_yCO₂H):</i>	
benzoic acid	CO ₂ H
phenylacetic acid	CH ₂ CO ₂ H
<i>trans</i> -cinnamic acid	CH=CHCO ₂ H
<i>Neutral nitrogen containing compounds (C_xH_yNO_z):</i>	
nitrobenzene	NO ₂
aniline	NH ₂
benzonitrile	CN
benzamide	CONH ₂
<i>Charged analytes (under aqueous conditions):</i>	
phenyltrimethyl ammonium chloride	N(CH ₃) ₃ Cl
benzenesulfonic acid	SO ₃ H

The structures of these analytes are given in figure 4.1, their chemical names are given in table 4.1.

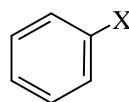


Figure 4.1 The structure of the analytes studied,
where X is defined in table 4.1

4.2 Chromatographic results on ODS and PGC

The values of the logarithm of the chromatographic retention factor extrapolated to 100% water ($\log k_w$) for all the analytes under investigation according to equation 4.1 are given in appendix 4.1.

$$\log k = \log k_w + a C \quad (4.1)$$

where C is the percentage of organic modifier in the mobile phase and a is the slope of the graph produced. Each $\log k_w$ value was extrapolated using $\log k$ measurements from six different mobile phase compositions. Each $\log k$ value represents the mean of three measurements. Retention times were reproducible to better than 1% from run to run. The experimental methods used in this work are discussed in section 2.x.

4.2.1 Hydrocarbons

The hydrocarbon compounds in this study represent non-polar analytes, and as such, the retention of these compounds is expected to be based largely on hydrophobic interactions in reversed-phase systems. The retention behaviour of these analytes on PGC and ODS over a range of mobile phase compositions at pH 2.5 and pH 7.0 is given in figure 4.2. Values of $\log k_w$ and a for these analytes are given in table 4.2. These analytes exhibited linear relationships between percentage of organic modifier (C) and $\log k$ over the mobile phase compositions studied. Benzene, toluene, ethylbenzene and *t*-butylbenzene were more strongly retained on ODS than PGC over the entire range considered as seen in table 4.2. These molecules also gave

a retention order in accordance with their size and hydrophobicity on both PGC and ODS (i.e. benzene first, then toluene, ethylbenzene, and finally *t*-butylbenzene). This result was in agreement with the results of chapter 3 and those of Kriz *et al.* [2].

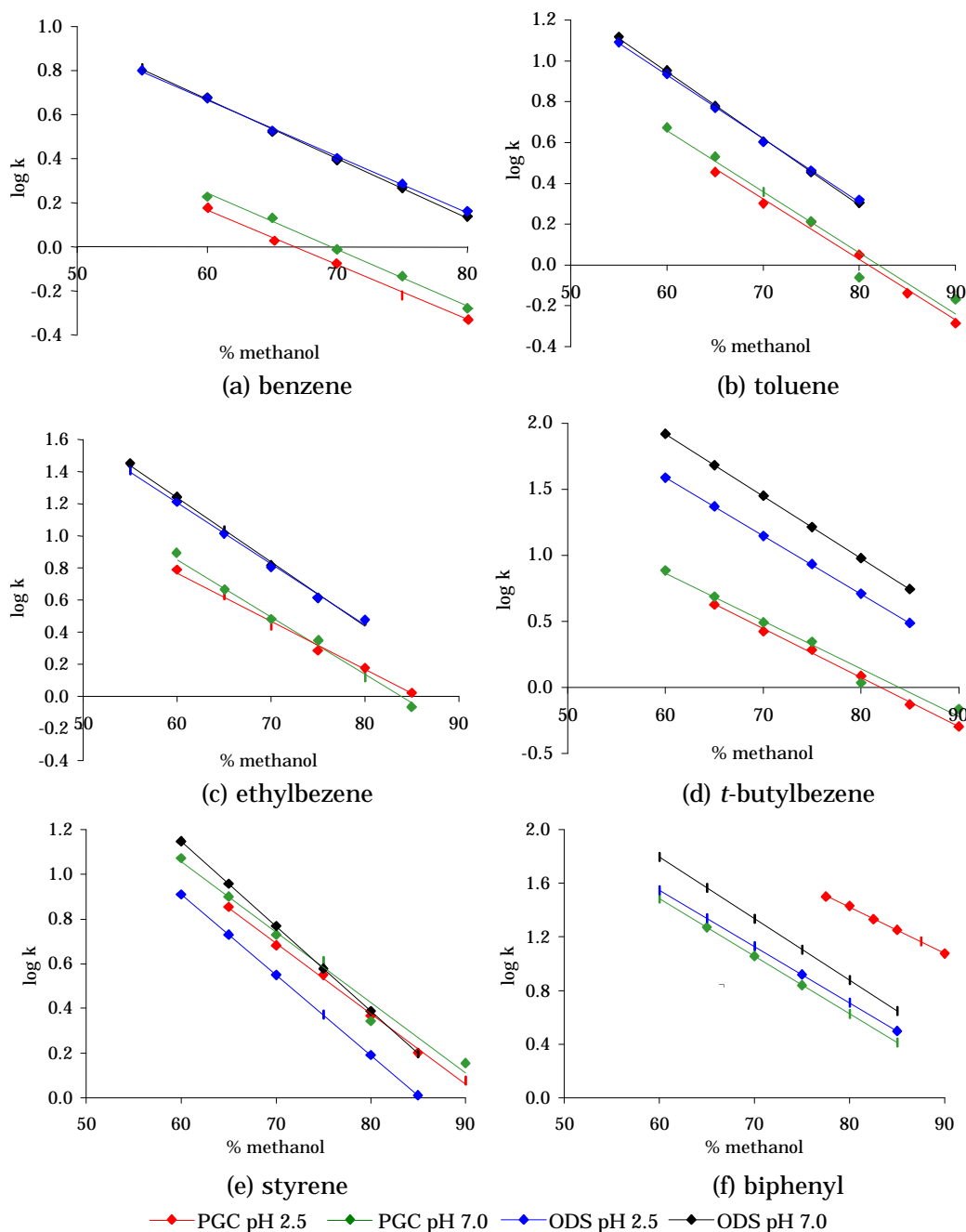


Figure 4.2 The relationship between retention ($\log k$) and mobile phase composition on ODS and PGC at different pH values

Benzene, toluene and ethylbenzene had similar a values (where a is

Chapter 4 - The retention mechanisms of benzene derivatives on PGC
 the slope in equation 4.1) when comparing ODS and PGC, whereas *t*-butylbenzene had lower *a* values for PGC than for ODS. On ODS the value of *a* increased with the size of the alkylbenzene. On PGC this was only true for *n*-alkylbenzenes.

Table 4.2 Retention data for hydrocarbons

Analyte	ODS				PGC			
	pH 2.5		pH 7.0		pH 2.5		pH 7.0	
	log k_w	<i>a</i>						
benzene	2.058	-0.025	2.289	-0.027	1.945	-0.025	1.778	-0.026
toluene	2.627	-0.031	2.917	-0.033	2.396	-0.030	2.454	-0.030
ethylbenzene	3.254	-0.037	3.641	-0.040	2.946	-0.036	3.102	-0.037
<i>t</i> -butylbenzene	4.230	-0.044	4.739	-0.047	3.032	-0.037	3.030	-0.036
styrene	3.071	-0.036	3.429	-0.038	2.896	-0.031	2.945	-0.031
biphenyl	4.070	-0.042	4.557	-0.046	4.172	-0.034	4.066	-0.035

One possible explanation for this is the orientation of interaction for *t*-butylbenzene with PGC and ODS. On ODS, orientation is probably less important because the stationary phase is made up of flexible alkyl chains, whereas on PGC the steric effect of the bulky *t*-butyl group may reduce the interaction between the phenyl ring and the PGC surface therefore reducing the retention. This effect was seen in Chapter 3.

The values of log k_w for styrene were lower on PGC than on ODS. The value of *a* was also smaller on PGC compared with ODS. When the retention of styrene is compared with ethylbenzene, it was seen to be more weakly retained on both ODS and PGC. Although these analytes have the same number of carbon atoms, ethylbenzene is more hydrophobic than styrene, because the polarisable nature of the CH=CH₂ π-π bond on the styrene molecule reduces hydrophobicity (from log *P* calculations in the TSAR software package). The difference between retention on PGC and ODS for styrene was less pronounced than for ethylbenzene as seen in figure 4.2 (c & e). This may be a result of increased interaction between the π-system of aromatic styrene and the PGC surface. This point is expanded upon in section

4.4.1.

Retention of biphenyl on PGC at pH 2.5 was strong in comparison to the other conditions at high mobile phase composition as seen in figure 4.2(f), however the low value of a led to a low $\log k_w$ value.

Retention of biphenyl at pH 2.5 was greater on PGC than on ODS, however the reverse was true at pH 7.0.

4.2.2 Halogenated compounds

Retention of the halogenated analytes on PGC and ODS over a range of mobile phase compositions at pH 2.5 and pH 7.0 is given in figure 4.3. Values of $\log k_w$ for the halogenated compounds are listed in table 4.3.

Table 4.3 Retention data for halogenated analytes

Analyte	ODS				PGC			
	pH 2.5		pH 7.0		pH 2.5		pH 7.0	
	$\log k_w$	a						
chlorobenzene	2.602	-0.031	2.924	-0.033	2.520	-0.030	2.430	-0.028
bromobenzene	2.773	-0.033	3.074	-0.035	2.777	-0.032	2.568	-0.028
iodobenzene	2.975	-0.034	3.358	-0.037	3.026	-0.032	2.786	-0.028
benzylchloride	1.853	-0.024	2.071	-0.026	1.264	-0.015	2.284	-0.028
benzylbromide	2.495	-0.031	2.788	-0.033	2.684	-0.033	2.336	-0.028

The retention of chlorobenzene, bromobenzene and iodobenzene showed the following trends:

- An increase in $\log k_w$ on both ODS and PGC was observed on increasing the size of the halogen atom.
- The values of $\log k_w$ for ODS and PGC were similar at pH 2.5.
- An increase in $\log k_w$ on ODS was observed with increased pH.
- A decrease in $\log k_w$ on PGC was observed with increased pH.
- Increased values of a with increased size of the halogen atom on ODS.
- Higher values of a on ODS with higher pH.
- Lower values of a on PGC with higher pH

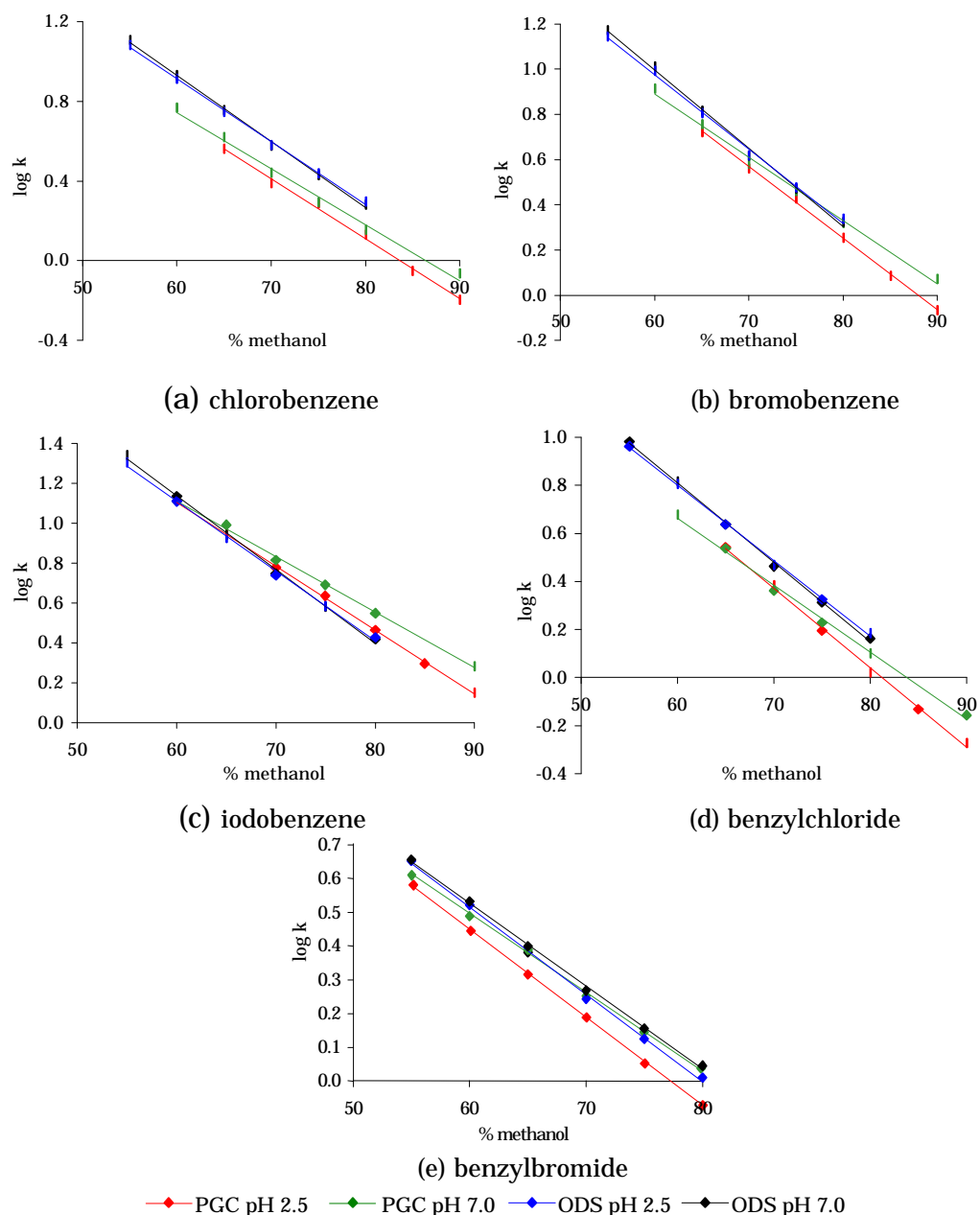


Figure 4.3 The relationship between retention ($\log k$) and mobile phase composition on ODS and PGC at different pH values

The values of $\log k_w$ for benzylhalides were lower than that of halobenzenes on ODS and PGC. Retention of benzyl chloride was weaker than chlorobenzene because of the larger dipole moment on benzyl chloride (calculated in the TSAR software package). The electronegative chlorine atom on benzyl chloride results in a polar analyte, whereas for chlorobenzene, the adjacent aromatic ring reduces the polarity. There are two explanations for this observation:

- (i) The carbon-chlorine bond in benzyl chloride may be represented approximately as $C_{sp^3} - Cl_p$. The bond in chlorobenzene is approximately $C_{sp^2} - Cl_p$. The higher *s*-character of the benzene orbital makes it more electronegative than an sp^3 orbital, hence the electronegativity difference with the more electronegative chlorine atom is reduced.
- (ii) The second contribution to the reduced dipole moment in chlorobenzene results from conjugation of one of the chlorine lone pairs with the benzene π -system.

Retention of benzyl bromide was weaker than bromobenzene for the same reason.

4.2.3 Alcohols, aldehydes, ketones, esters

These polar analytes were used in the data-set to investigate the polar retention effect on graphite (PREG) proposed by Knox and Ross[1]. By studying the relationship between mobile phase composition and retention for these polar analytes (figures 4.4) it is clear that the retention on PGC was greater than on ODS. This can also be seen numerically in table 4.4 which lists values of $\log k_w$ for these analytes.

Table 4.4 Retention data for alcohols, aldehydes, ketones and esters

Analyte	ODS				PGC			
	pH 2.5		pH 7.0		pH 2.5		pH 7.0	
	$\log k_w$	<i>a</i>						
phenol	1.118	-0.020	1.364	-0.022	1.705	-0.024	1.889	-0.026
anisole	1.947	-0.025	2.209	-0.027	2.295	-0.027	2.661	-0.032
benzyl alcohol	1.142	-0.042	1.388	-0.022	2.087	-0.028	1.789	-0.024
benzaldehyde	1.324	-0.020	1.620	-0.024	2.406	-0.028	2.099	-0.023
acetophenone	1.441	-0.022	1.657	-0.023	2.434	-0.026	2.434	-0.025
methylbenzoate	1.999	-0.026	2.241	-0.028	2.794	-0.027	3.179	-0.032
phenylacetate	1.637	-0.024	1.830	-0.026	1.720	-0.024	1.588	-0.022
cinnamaldehyde	1.720	-0.025	1.926	-0.026	2.971	-0.024	2.548	-0.033

Retention on both ODS and PGC was greater at pH 7.0 than at pH 2.5 for phenol. A possible explanation of this is in the polar nature of the

Conjugation of one of the lone pairs on oxygen with the aromatic ring gives a very electron rich benzene ring. ODS consists of a silica support with hydrophobic alkyl groups chemically bonded onto the silica support to create a largely hydrophobic interface with the mobile phase. Any surface silanol groups that have not been capped with a C₁₈ hydrocarbon can also interact with the analyte. In acidic conditions the effect of this will be minimal, however at higher pH values, the silanol group will ionise and the effect of their interaction with analytes will become more apparent.

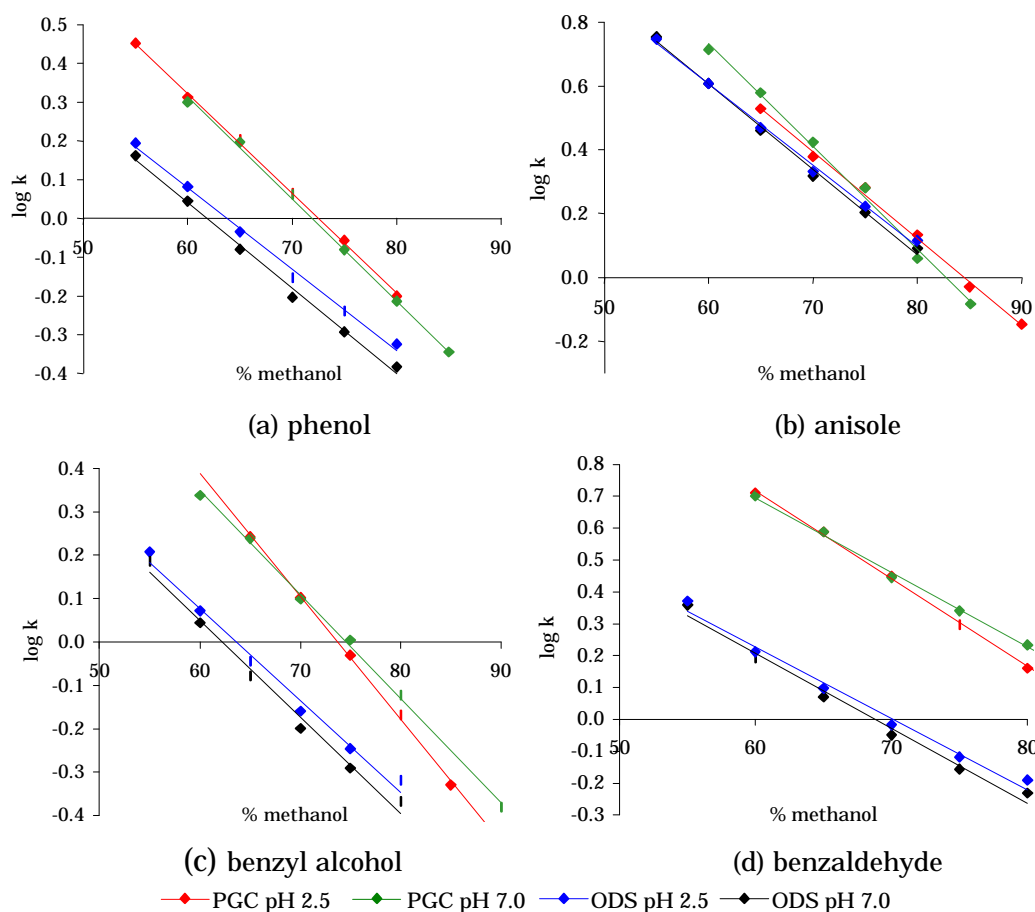


Figure 4.4 The relationship between retention ($\log k$) and mobile phase composition on ODS and PGC at different pH values

On ODS at pH 7.0, there would be attractive electronic interaction between any exposed ionised silanol (SiO^-) groups on the ODS stationary phase and the polar analyte, resulting in an increase in retention. On PGC, the increase in retention with increased pH would support the argument for the presence of weakly acidic functionality on the PGC surface. As PGC is manufactured by a template process

[3], the presence of any residual silica on the PGC surface would account for the observations.

A similar effect was seen for the structurally similar anisole molecule with increased retention at higher pH on both ODS and PGC. This polarity stems from an inductive and mesomeric effect. The canonical forms of anisole (figure 4.5) show how electron density from the lone pair can be moved into the aromatic ring.

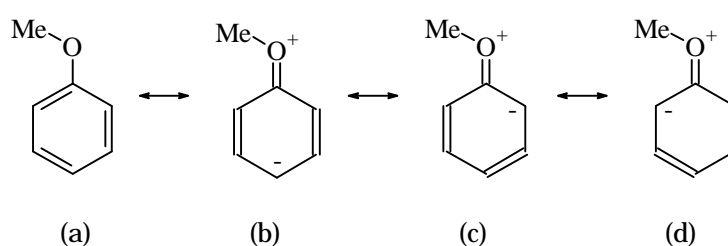


Figure 4.5 Canonical forms of anisole. Forms (b)–(d) are relatively unstable when compared to form (a).

The methyl group will also be electron donating and thus increase the dipole present. Retention of anisole was greater for PGC than for ODS, giving further weight to the occurrence of a polar retention effect on graphite. Benzylalcohol (a structural isomer of anisole) also exhibited greater retentive properties for PGC than for ODS as seen in figure 4.4(c). However, in this case, the value of $\log k_w$ on PGC was reduced with increased pH.

The value of $\log k_w$ for acetophenone was considerably greater on PGC than on ODS at both pH values. This observation may be further evidence for a polar retention effect on graphite, introduced by Ross and Knox [1]. This increased retention on PGC may be attributed to the conjugated nature of the acetophenone molecule and its ability to adopt a planar geometry. Conjugation of the carbonyl group with the benzene ring results in two effects that are beneficial to retention on PGC.

- (a) An increased tendency towards planarity, because of the partial double bond character of the C₆H₅—COMe (figure 4.6).
- (b) An electron-withdrawing mesomeric effect, removing electron density away from the ring onto the carbonyl oxygen.

This ability of a neutral molecule to have local “excesses” of charge was thought by Kaliszan to be a key factor in retention on PGC [4].

The value of $\log k_w$ on PGC for acetophenone was identical regardless of pH, with very little difference in slope, however on ODS, there was an increase in $\log k_w$ with increased pH.

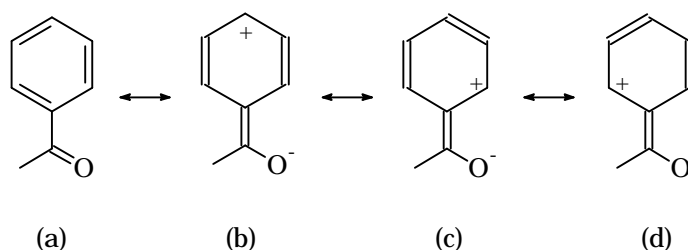


Figure 4.6 Canonical forms of acetophenone. Forms (b)–(d) are relatively unstable when compared to form (a).

The behaviour of *trans*-cinnamaldehyde and benzaldehyde on ODS and PGC followed similar trends (table 4.4). On ODS, $\log k_w$ was greater at pH 7.0 than at pH 2.5 with similar slopes. On PGC, retention (and $\log k_w$) was much greater at pH 2.5 than at pH 7.0. However, the value of a was greater for the neutral pH conditions than in acidic conditions. The difference in a for the two pH conditions could imply a difference in the retention mechanisms. The presence of acidic groups on the surface of the PGC could explain some of these observations. As *trans*-cinnamaldehyde is a large highly conjugated molecule, any local excesses of charge due to relatively the unstable canonical forms of *trans*-cinnamaldehyde are minimised by the ability to spread the charge over the large π -system present. This means that at pH 7.0 the presence of any ionised acidic functionality on the PGC surface would have a negative effect on retention of *trans*-

Chapter 4 - The retention mechanisms of benzene derivatives on PGC cinnamaldehyde and thus benzaldehyde. Although this explanation is useful for understanding differences in retention, it cannot explain the low value of a for *trans*-cinnamaldehyde on PGC at pH 2.5 when compared with a at pH 7.0 (figure 4.7). This difference in a on PGC at different pH values was absent from the retention of benzaldehyde (figure 4.4d).

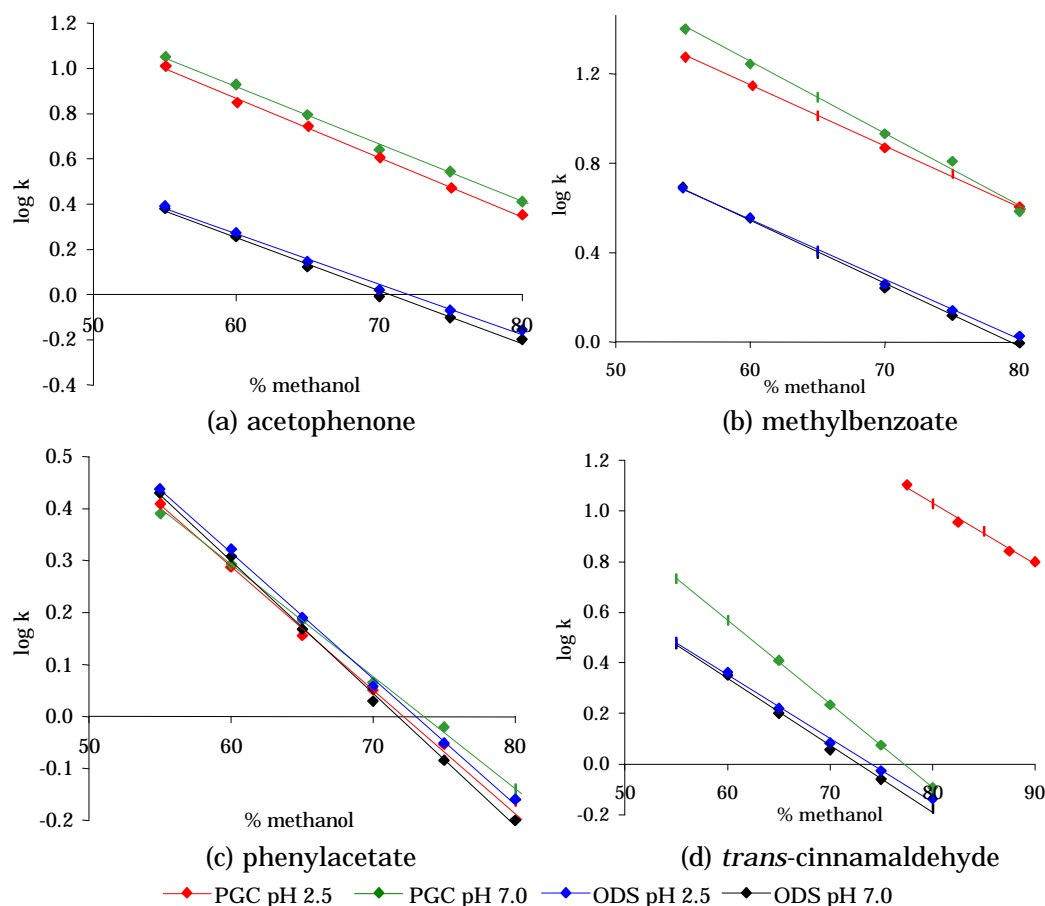


Figure 4.7 The relationship between retention ($\log k$) and mobile phase composition on ODS and PGC at different pH values

Methylbenzoate and phenylacetate are structural isomers with striking differences in retention. The retention exhibited by phenylacetate was very similar for all conditions studied. As such, there was little in the way of a PREG present. However the inverse was true for methylbenzoate which showed increased retention on PGC compared with ODS (figure 4.7(b)).

The value of $\log k_w$ for methyl benzoate on both ODS and PGC was

larger at pH 7.0 than at pH 2.5. This may be because of the ability of the carbonyl oxygen to accept protons at low pH values. At moderate acid concentration, a small proportion of the ester will be protonated [5]. A direct result of this, which can be seen in figure 4.7(b), was a decrease in retention at low pH and a shallower slope.

Retention of methyl benzoate on PGC was substantially stronger than on ODS. This observation may indicate the presence of a polar retention effect on graphite, but may also be connected with the planar nature of the molecule and its ability to interact with the planar PGC surface. The conjugated nature of the molecule gives it the ability to exist in several canonical forms (see figure 4.8).

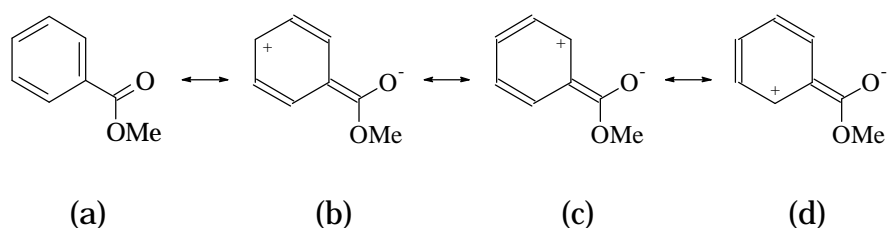


Figure 4. 8 Canonical forms of methylbenzoate

Although form (a) is the predominant and most stable form, the presence of forms (b) to (d) will impart some double bond nature to the $C_6H_5 - CO_2Me$ bond. This results in a more rigid and thus more planar analyte.

The retention of these polar, oxygen containing, analytes is much stronger on PGC than on ODS and as such does not conform to the established mechanisms of retention [6-8] explained in Chapter 1.

4.2.4 Carboxylic acids

Retention of the carboxylic acid analytes on PGC and ODS over a range of mobile phase compositions at pH 2.5 and pH 7.0 is given in figure 4.9. Values of $\log k_w$ and a are given in table 4.5. The most striking feature of the retention of the carboxylic acids on PGC and ODS was the differences in retention ($\log k_w$) and gradient (a) for benzoic acid and also *trans*-cinnamic acid at different pH values. On ODS, where retention is expected to be based mainly on analyte hydrophobicity and so at pH 2.5 these analytes will be mainly unionised, resulting in strong retention. At neutral pH, however, these analytes are negatively charged and so a drop in retention is expected and is observed. The reduction in retention on PGC at higher pH was greatest for benzoic acid. A possible explanation for this lies in the conjugation of the two analytes.

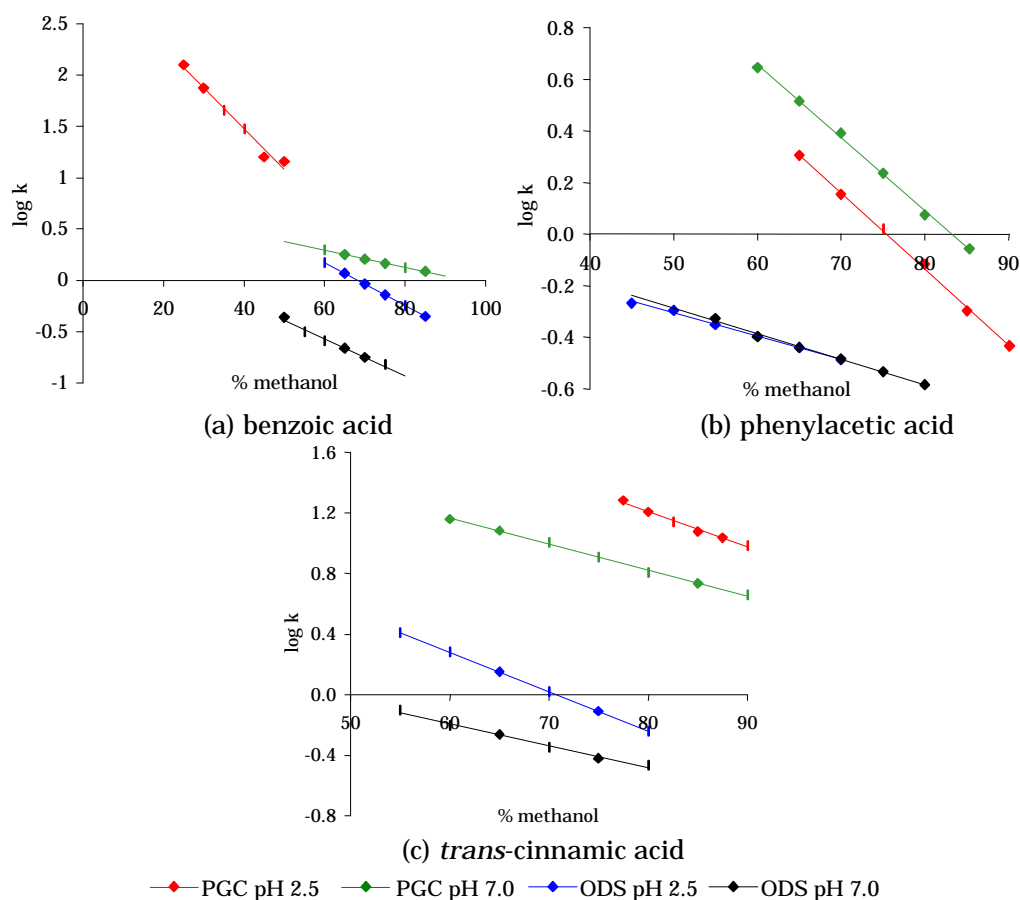


Figure 4.9 The relationship between retention ($\log k$) and mobile phase composition on ODS and PGC at different pH values

Table 4.5 Retention data for carboxylic acids

Analyte	ODS				PGC			
	pH 2.5		pH 7.0		pH 2.5		pH 7.0	
	log k_w	a						
benzoic acid	1.435	-0.021	0.387	-0.016	3.058	-0.039	0.803	-0.010
phenylacetic acid	0.144	-0.009	0.210	-0.010	2.223	-0.029	2.360	-0.028
<i>trans</i> -cinnamic acid	1.841	-0.026	0.684	-0.015	3.089	-0.023	2.193	-0.017

trans-Cinnamic acid is a highly conjugated molecule and so can distribute the negative charge throughout its structure with a lower quantity of charge per atom than benzoic acid. This may result in a smaller decrease in retention for *trans*-cinnamic acid on PGC. On ODS both analytes showed a similar reduction in retention at neutral pH compared with pH 2.5. Another explanation for the relatively strong retention of *trans*-cinnamic acid at pH 7.0 may be the highly planar nature of the molecule and the possibility of strong π - π interactions between the conjugated π -system of the *trans*-cinnamic acid and the electron cloud on the PGC surface.

Retention of phenylacetic acid was larger at higher pH. This result was unexpected, as retention of weak acids was predicted to be lower for the ionised species at neutral pH than under acidic conditions where these analytes are likely to be in the neutral form and so reversed-phase interactions will be stronger at lower pH.

Retention on PGC was much greater than on ODS for all carboxylic acids. This was seen as yet further evidence for a polar retention effect on graphite.

4.2.5 Neutral nitrogen containing compounds

Retention of the neutral nitrogen containing analytes on PGC and ODS over a range of mobile phase compositions at pH 2.5 and pH 7.0 is given in figure 4.10. Values of log k_w and a are given in table 4.6.

Table 4.6 Retention data for neutral nitrogen containing analytes

Analyte	ODS				PGC			
	pH 2.5		pH 7.0		pH 2.5		pH 7.0	
	log k_w	a						
nitrobenzene	1.760	-0.025	1.952	-0.026	2.545	-0.027	2.807	-0.030
aniline	0.478	-0.028	1.048	-0.019	0.443	-0.005	1.186	-0.018
benzonitrile	1.435	-0.023	1.538	-0.023	2.332	-0.029	2.124	-0.025
benzamide	0.640	-0.016	0.796	-0.018	1.881	-0.023	1.506	-0.019

Retention of these analytes followed similar trends with the exception of aniline (figure 4.10). Nitrobenzene, benzonitrile and benzamide are all polar molecules and exhibited stronger retention on PGC when compared with ODS. This can be seen as further evidence for a polar retention effect on graphite.

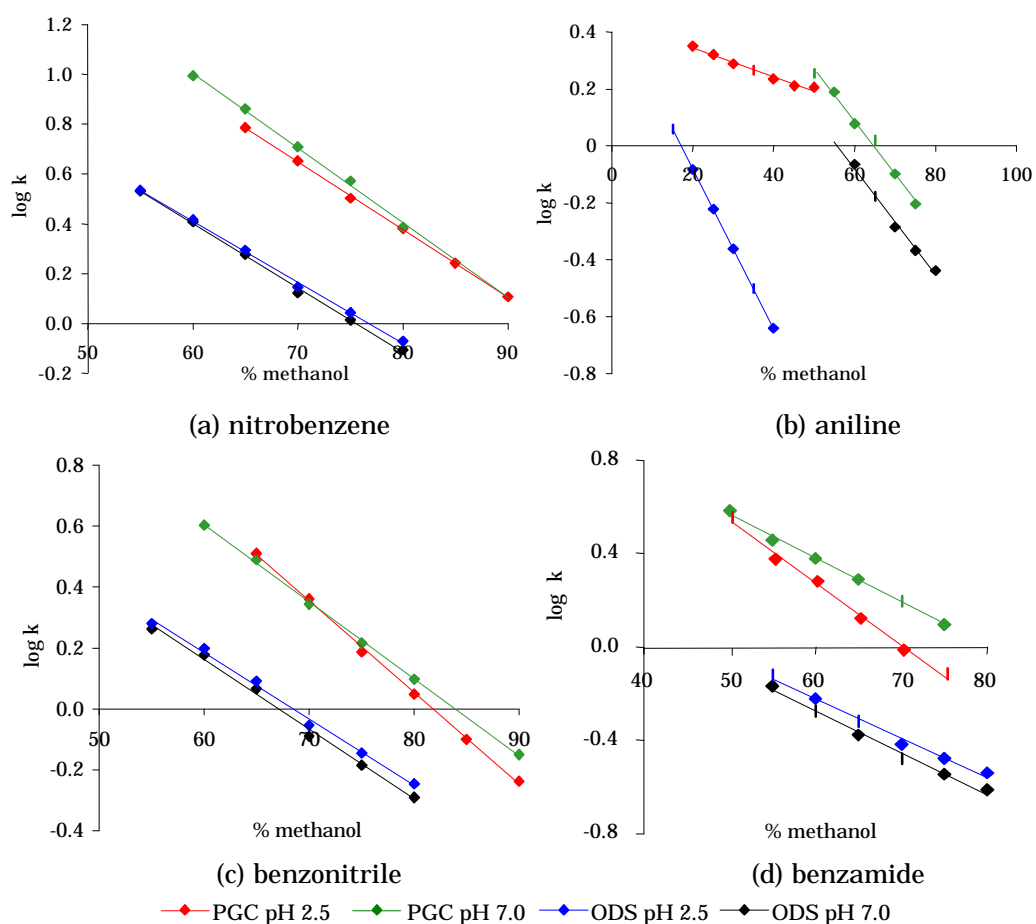


Figure 4.10 The relationship between retention ($\log k$) and mobile phase composition on ODS and PGC at different pH values.

However, retention of aniline on PGC was different at pH 2.5 than at all other conditions investigated. The value of $\log k_w$ was smaller at pH 2.5 on PGC than for the other conditions investigated, with a smaller value of a . On ODS retention of nitrobenzene, benzonitrile and benzamide increased with pH suggesting the presence of interactions between the analyte and any uncapped ionised silanol groups present on the ODS surface.

On PGC at pH 2.5, the value of a was far smaller than at pH 7.0 for aniline. This difference in a suggested a change in retention mechanism between the pH values studied. This may be explained by the nature of aniline, which has a pK_a value of 4.6 and therefore it will be almost fully ionised at pH 2.5, and almost completely unionised at pH 7.0. Stronger retention was seen for the neutral species at pH 7.0 on both supports, as expected from reversed-phase theory. However the value of a on ODS was higher for the charged anilinium species at lower pH. This result was unexpected as a steeper slope is normally associated with stronger reversed-phase interactions between the support and the analyte.

4.2.6 Charged analytes

The retention of the charged analytes on PGC and ODS over a range of mobile phase compositions at pH 2.5 and pH 7.0 is given in figure 4.11. Values of $\log k_w$ and a are given in table 4.7.

Table 4.7 Retention data for charged analytes

Analyte	ODS				PGC			
	pH 2.5		pH 7.0		pH 2.5		pH 7.0	
	$\log k_w$	a						
PTMAC	-0.271	-0.008	-0.140	-0.009	-0.203	-0.006	-0.114	-0.011
benzene sulfonic acid	0.228	-0.021	0.243	-0.021	1.604	-0.024	1.494	-0.027

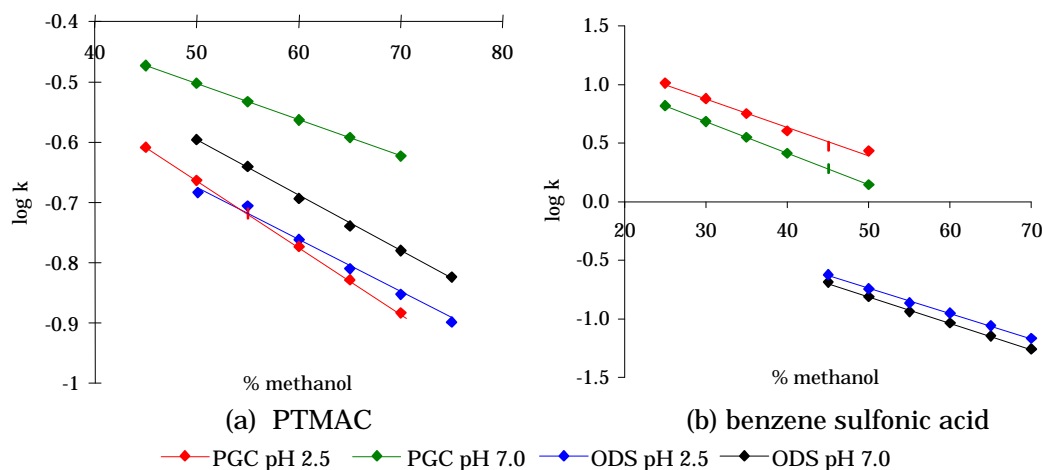


Figure 4.11 The relationship between retention ($\log k$) and mobile phase composition on ODS and PGC at different pH values

The phenyl trimethyl ammonium (PTMA) ion is a positively charged species in aqueous solution which exhibited very weak retention on both ODS and PGC stationary phases. As there was no change in the ionisation of the PTMA ion at different pH values, any difference in retention when examining a chromatographic system would depend on either the mobile phase composition or a change in functionality on the surface of the stationary phase.

On PGC, there were differences in the values of the slope and the intercept ($\log k_w$) between the two pH values suggesting differences in the analyte-stationary phase interactions. This change in retention could be explained by the presence of acidic groups on the surface of the PGC stationary phase. At pH 2.5 the acidic groups would be unionised and at higher pH values the degree of ionisation would increase. For a positively charged analyte, such as the PTMA cation, a negatively charged stationary phase would substantially increase the retention observed (figure 4.11).

On ODS there was little increase in the value of a when pH was changed from 2.5 to 7.0, but an increase in retention was observed.

This finding is probably due to changes in the stationary phase with pH. As ODS is based on silica, any exposed silanol groups will become ionised at higher pH values and so increase the retention of oppositely charged cationic species. At lower pH values the number of exposed silanol groups is reduced and this ionic retention effect is diminished.

Benzene sulfonic acid, is negatively charged under the aqueous conditions used in this study. It was therefore weakly retained on most reversed-phase support materials. Due to its ionisation state, any differences in retention at different pH values may be explained by the change in stationary phase surface functionality with pH. On ODS support material, benzene sulfonic acid was poorly retained at both pH 2.5 and 7.0.

There was stronger retention on PGC than on ODS for benzene sulfonic acid suggesting yet again the presence of a polar retention effect on graphite. An increase in retention was observed as the mobile phase pH was reduced from pH 7.0 to pH 2.5. This may be explained by the presence of a weakly acidic group on the PGC surface, which may be ionised at pH 7.0 and therefore produce an electrostatic repulsive effect. There may be an additional effect on retention resulting from the presence of residual silica remaining from the template manufacturing process. This silica may have negatively charged ionised functionality's at pH 7.0 producing a similar electrostatic effect to that described above.

4.3 Discussion of chromatographic results on ODS and PGC

It has previously been reported that the retention mechanism on PGC is based on a combination of different types of interactions including reversed-phase interactions, shape and size factors as well as polar interactions [1]. The retention of analytes on ODS is based, for the most part, on reversed-phase interactions [9]. It is possible to identify those analytes whose retention is significantly greater on PGC than on ODS by calculating the Δk_w term shown in equation 4.2.

$$\Delta k_w = 100 \left(\frac{k_w(\text{PGC})}{k_w(\text{ODS})} - 1 \right) \quad (4.2)$$

The values of this change in k_w between ODS and PGC, termed “ Δk_w ” are given in table 4.8 below and in figure 4.12.

For the hydrocarbon group of compounds (except biphenyl) there was, at pH 2.5, a decreased retention on PGC compared with ODS. This observation was particularly notable for *t*-butylbenzene where the value was substantially more negative than the other hydrocarbons. This may be due to the presence of the bulky *t*-butyl group that prevented the benzene ring from interacting with the PGC in cofacial geometry and thus reduced retention. This explanation is less compatible with the data for the other hydrocarbons.

Another possible explanation for the diminished retention of hydrocarbons on graphite when compared with ODS is the possible role of the PREG combined with a clear absence of molecular polarity in this group of compounds. Non-polar compounds would be expected to have an enhanced retention on ODS due to interaction with the non-polar alkyl bonded phase. On PGC their molecular structure will mitigate against any polar retention effect on graphite.

Table 4.8 The difference in k_w from ODS to PGC at pH 2.5 and pH 7.0

Analyte	Δk_w	
	pH 2.5	pH 7.0
benzene	-22.8	-69.1
toluene	-41.3	-65.6
ethylbenzene	-50.9	-71.1
<i>t</i> -butylbenzene	-93.7	-98.0
styrene	-33.2	-67.2
biphenyl	26.4	-67.7
chlorobenzene	-17.2	-67.9
bromobenzene	0.92	-68.8
iodobenzene	12.3	-73.2
benzyl chloride	-74.2	63.4
benzyl bromide	54.5	-64.7
benzyl alcohol	782	152
benzaldehyde	1110	202
benzoic acid	4100	161
methyl benzoate	525	765
anisole	123	183
nitrobenzene	509	617
<i>trans</i> -cinnamaldehyde	1680	319
cinnamic acid	1670	3130
phenyl acetate	21.2	-42.8
acetophenone	884	499
benzonitrile	690	286
phenol	229	235
aniline	-7.71	37.3
benzamide	1640	413.0
benzene sulfonic acid	2270	1680
phenyl acetic acid	11900	14000
PTMAC	6.20	16.9

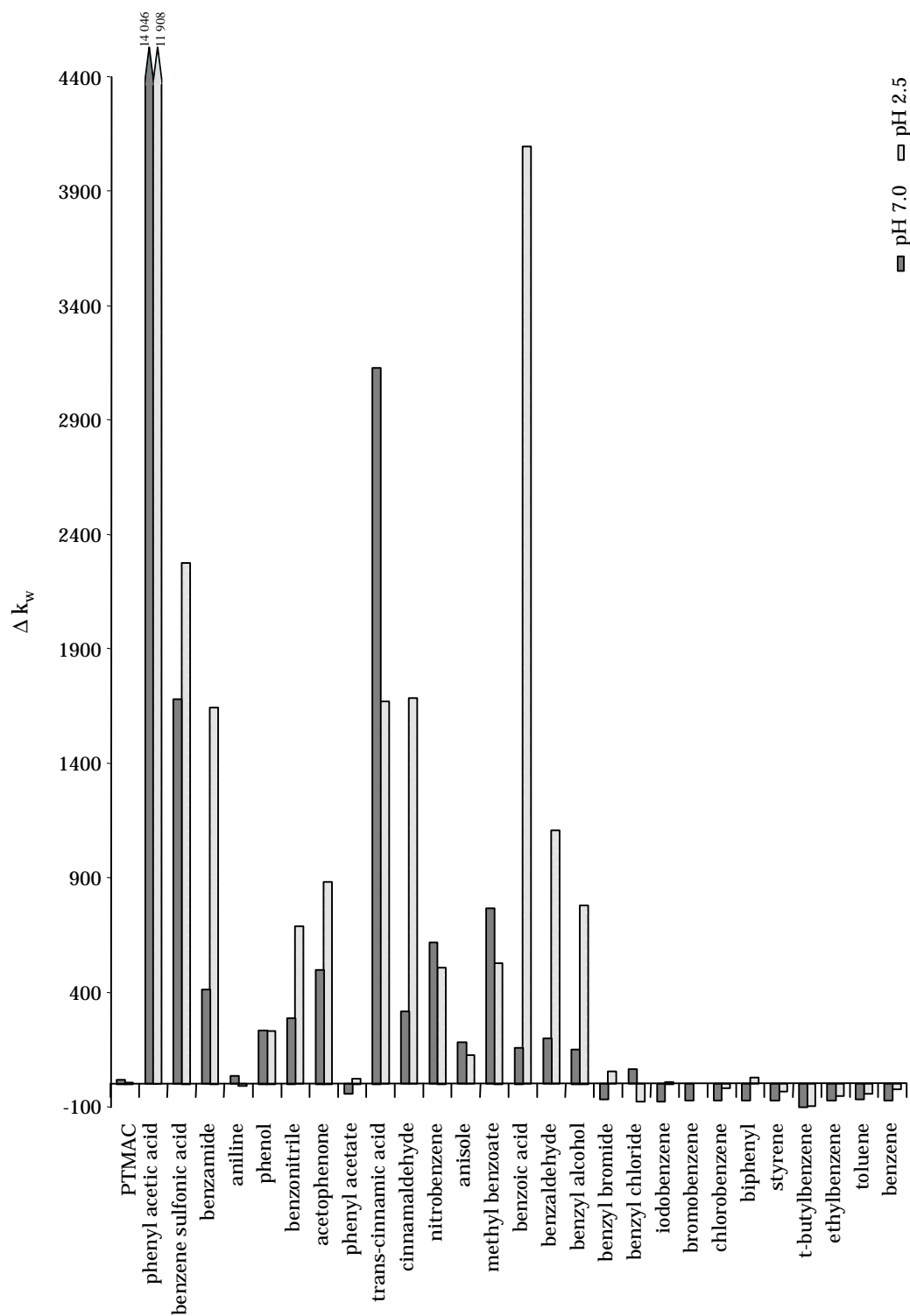


Figure 4. 12 Δk_w for each analyte in this study.

Moving to neutral pH, there was a larger decrease in retention of the hydrocarbon analytes. This observation may be explained by the presence of weakly acidic functionality on the graphite surface. This will have the effect of further diminishing the possible interaction with the graphite surface at neutral pH. Studies by Patterson [10] confirm the presence of acidic groups on the PGC surface by potentiometric titration of PGC stationary phase material. The high organic mobile phase used for these analyses will ensure that any residual silanol functionalities which may be present (and ionised) on the ODS will be effectively shielded by the alkyl chains thereby permitting a reversed-phase interaction to take place.

For the halogenated benzenes, the change in retention from ODS to PGC was relatively small at pH 2.5. However at pH 7.0, there was a marked decrease in retention on PGC compared with ODS. This observation may be explained in a similar manner to that of the hydrocarbon compounds above. The structure of these analytes will be largely unaffected by changes in pH, and therefore the diminished retention of the halogenated benzenes on PGC suggested a change in the nature of the stationary phase. The presence of a weakly acidic group on the PGC surface may account for these observations. The benzyl halides used in this study do not fit in with this pattern of observation.

All compounds which contain oxygen (with the exception of phenyl acetate) showed a positive value for Δk_w . This observation provides further evidences for the presence of a polar retention effect on graphite. Phenyl acetate does not fit in with this pattern of observation.

Benzoic acid and benzene sulfonic acid had substantially higher Δk_w values at pH 2.5 than at pH 7.0. This may be explained by the reduction in reversed-phase/hydrophobic interactions for the charged

species at pH 7.0 on the ODS support. It may also be due to electrostatic repulsion between the negatively charged acid analytes and any weakly acidic functionality on the surface of the PGC. The weakly acidic functionality would be negatively charged at this pH. On ODS, this effect will be minimised, because any residual silanol functionality's which may be present (and ionised) on the ODS would be partially shielded by the alkyl chains thereby permitting a reversed-phase interaction to take place.

The most intriguing observation to be drawn from this study was the value of Δk_w for phenyl acetic acid at both pH values (11900 at pH 2.5 and 14000 at pH 7.0). This could be interpreted as further evidence of a polar retention effect on graphite, however the magnitude of these Δk_w values was considerably larger than for any other compound under investigation in this study, and as such is unexplained.

The polar analytes used in this study, which do not contain oxygen (i.e. PTMAC and aniline), do not appear to exhibit a noticeable polar retention effect on graphite as seen in figure 4.12. This observation may be of major importance for determining the basis of PREG.

PTMAC had a larger Δk_w value at pH 7.0 than at pH 2.5. This observation may be due to electrostatic attractive interactions between the cationic PTMAC species and any (anionic) weakly acidic which may be present on the PGC surface. The negative value of Δk_w at pH 2.5 may be explained by the reduced hydrophobicity of the charged anilinium cationic species at pH 2.5. This positive charge on the analyte will lead to a reduction in reversed-phase interactions.

4.4 Molecular modelling of the interaction between analyte and PGC surface

The energy of interaction between benzene derivatives and a model graphite surface was considered using the semi-empirical molecular orbital methods described in Chapter 2 (section 2.2). Five alternative geometries for alignment of the analyte with the model graphite surface were considered, and are shown in figure 4.13. The molecule used to represent the stationary phase is given in figure 4.14.

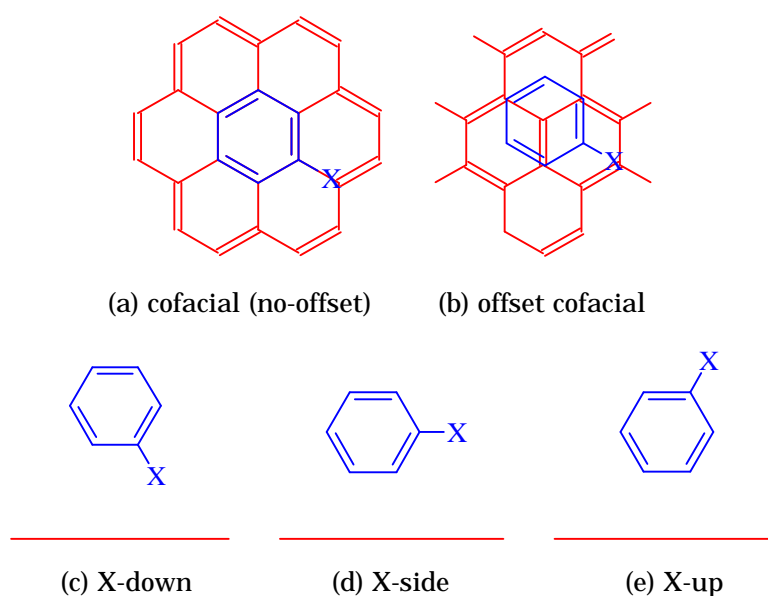


Figure 4. 13 The five geometries for the alignment of the analyte with part of the model graphite surface. (a) and (b) are cofacial geometries, (c)–(e) are face-edge geometries. Blue indicates the analyte molecule.

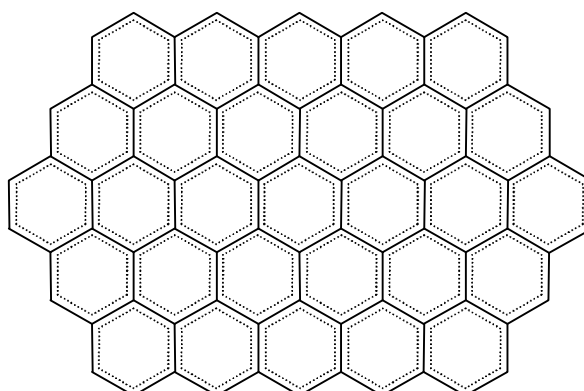


Figure 4. 14 The aromatic hydrocarbon compound ($C_{78}H_{22}$) chosen to represent the PGC surface.

The energy of interaction between the analyte molecule and the model graphite surface molecule was calculated by subtracting the heat of formation of the analyte and the surface at small separation (approx. 3.6 Å) from the heat of formation of the analyte and surface at a separation of 50 Å, as seen in figure 4.15. The stronger the attractive interaction between the analyte and the model surface, the smaller the value of ΔHf . The more positive the value the weaker the attraction between the analyte and the model surface becomes.

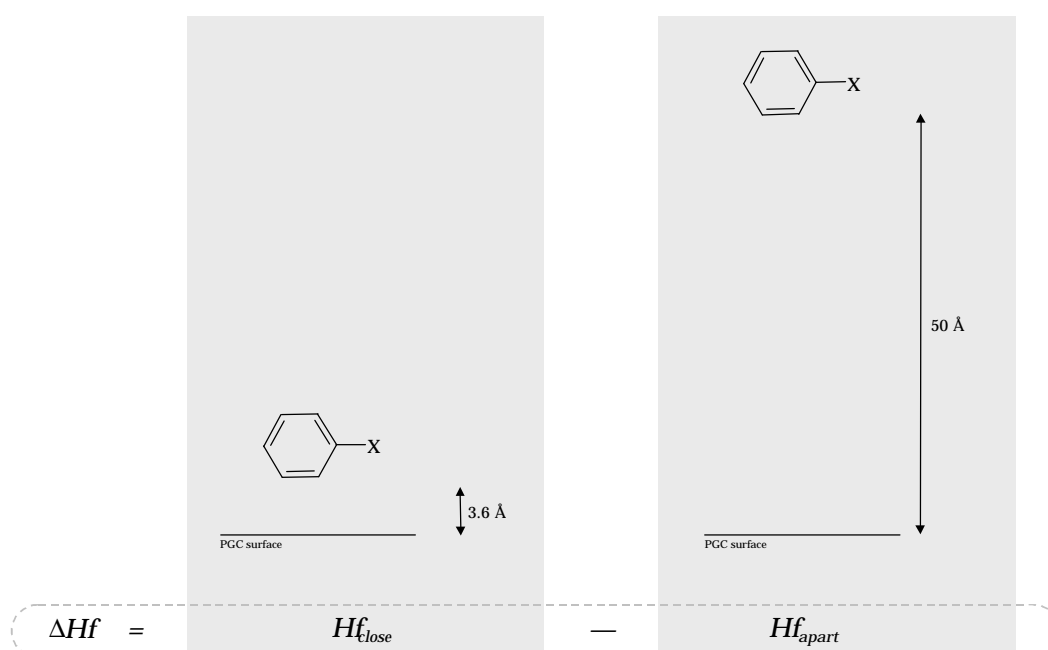


Figure 4. 15 The calculation of ΔHf by subtracting heat of formation of analyte and model surface at a large separation from the heat of formation of analyte and model surface at close separation.

The important feature to note is the differences between the values for analytes, not their absolute value. This is because these results are from theoretical calculations based on a series of approximations and assumptions [11]. It is important to stress that the model used is a simplistic version of the retention on PGC with no solvent presence included.

4.4.1 Hydrocarbon compounds

The molecular modelling results for benzene, toluene and ethylbenzene, shown in table 4.9, are also described in section 3.4.1, as these compounds represent the main overlap between Chapters 3 and 4.

Table 4.9 Values of ΔH_f calculated by semi-empirical molecular modelling methods for hydrocarbon compounds. The strongest adsorption of the analyte onto the surface, $\Delta H_{f_{min}}$ is highlighted in **bold**.

Analyte	Cofacial		Face-edge			$\Delta H_{f_{min}}$ (kcal)
	no offset	offset	x down	x side	x up	
benzene	0.068	-0.038	-0.119	-0.119	-0.119	-0.119
toluene	0.226	-0.246	1.153	-0.109	0.682	-0.246
ethylbenzene	-0.262	-0.216	-0.259	-0.121	0.175	-0.262
<i>t</i> -butylbenzene	0.081	1.268	0.843	-0.108	1.032	-0.108
styrene	-0.005	-0.120	-0.216	0.371	1.356	-0.216
biphenyl	-0.385	-0.277	0.790	0.341	0.790	-0.385

As previously stated, benzene was found to show the strongest associative interaction with the model surface when orientated in a face-edge geometry. Each of the face-edge geometries was identical for benzene as $X = H$. However, toluene and ethylbenzene were found to show the most negative ΔH_f in cofacial geometries, toluene adapting an offset cofacial geometry with ΔH_f at -0.246kcal. Ethylbenzene adopted a cofacial geometry with ΔH_f at -0.262kcal, however a face-edge (x-down) geometry gave a ΔH_f value of -0.259kcal, indicating that these two geometries had very similar association with the model surface.

$\Delta H_{f_{min}}$ was found to become increasingly negative for the benzene, toluene and ethylbenzene series as expected from the values of $\log k_w$. Styrene was found to have a less negative $\Delta H_{f_{min}}$ than ethylbenzene, as

was expected when considering $\log k_w$ on PGC for both compounds. The most negative value for ΔHf was found to be in the face-edge (x-down) geometry for styrene.

t-Butylbenzene was found to have the strongest association with the model surface for a face-edge (x-side) geometry with a ΔHf_{min} value of -0.108kcal. The presence of the bulky *t*-butylbenzene group may have prevented any cofacial association between the analyte and the model surface. This result is therefore analogous to that seen for the molecular modelling of amylbenzene structural isomers (section 3.4.2) where the value of ΔHf_{min} was found to become less negative as branching of the amyl group increased. As the branching was increased, the association between the analyte and the model surface decreased, as did the value of $\log k$. Kriz *et al.* [2] found that the retention of *t*-butylbenzene was weaker than the straight chain *n*-butylbenzene, indicating a weaker association with the stationary phase. The decreased retention was thought by Kriz *et al.* to be the steric effect of the bulky *t*-butyl group preventing coplanarity of the aromatic ring in the analyte molecule and the stationary phase. This result was paralleled in our molecular modelling study.

The modelling of biphenyl was undertaken in a different manner to the rest of the compounds. This was because biphenyl is a large conjugated molecule with the ability to adopt a flat geometry. When considered in isolation, the biphenyl molecule adopts a familiar staggered conformation where steric hindrance of the hydrogen atoms in 2, 6, 2' and 6' positions is minimised as seen in figure 4.16. This is as expected from previously published experimental and theoretical studies [12, 13].

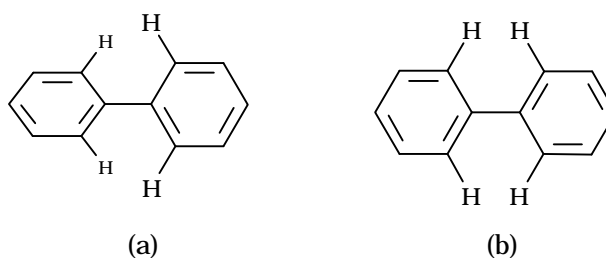


Figure 4. 16 (a) Staggered and (b) coplanar conformations of biphenyl.

The hydrogen atoms shown have the steric effect of driving the conformation away from coplanarity.

If however biphenyl is placed on a flat surface, such as PGC, the unfavourable steric interaction of the hydrogen atoms may be overcome by stronger associative interactions with the model surface. If this is indeed the case it is important that when minimising the structures in close proximity we investigate both scenarios:

- (1) Planar biphenyl interacting with the model surface,
- (2) Staggered biphenyl interacting with the model surface.

For biphenyl, each of the geometries given in figure 4.13 was studied for both the flat and the staggered conformation. The resulting Hf value was then subtracted from the value of Hf for a staggered biphenyl with 50Å separation from the model surface. With one exception, the lowest value of ΔHf in each case was found for the flat biphenyl molecule. In the face edge x-side geometry, the staggered biphenyl had stronger association with the model surface than the flat biphenyl molecule.

Biphenyl was found to have the strongest associative interaction with the model surface when both rings were coplanar with the surface. This meant that the energy of interaction with the surface was greater than the energy barrier to molecular planarity and so the phenyl rings on biphenyl became coplanar to facilitate increased interaction with the model surface. The cofacial geometry with no offset was found to be more strongly favoured than the offset cofacial geometry. ΔHf for

Chapter 4 - The retention mechanisms of benzene derivatives on PGC biphenyl in the perpendicular (face-edge) geometries was much higher (more positive) and therefore less favoured than the cofacial geometries.

Biphenyl was found to be more strongly associative towards the model surface than any of the other hydrocarbons, an observation that is paralleled in its strong retention on PGC when compared with the other hydrocarbons in the study. This result is very significant as it shows the strong association of a planar molecule with the model graphite surface.

4.4.2 Halogenated compounds

The molecular modelling results (given in table 4.10) for the halobenzenes clearly showed that the most favoured geometry for associative interaction was cofacial geometry with no offset. This was found to be true for chloro, bromo and iodo substituted benzenes with a similar increase in association from chlorobenzene to bromobenzene as there was for bromobenzene to iodobenzene. Although this is not a statistically significant linear relationship, with only three halobenzene analytes considered, a qualitative relationship is present.

Table 4.10 Values of ΔH_f calculated by semi-empirical molecular modelling methods for halogenated compounds. The strongest adsorption of the analyte onto the surface, $\Delta H_{f_{min}}$ is highlighted in **bold**.

Analyte	Cofacial		Face-edge			$\Delta H_{f_{min}}$ (kcal)
	no offset	offset	x down	x side	x up	
chlorobenzene	-0.229	-0.201	0.454	-0.107	-0.067	-0.229
bromobenzene	-0.535	-0.504	0.344	-0.003	0.088	-0.535
iodobenzene	-0.780	-0.581	0.210	0.665	0.294	-0.780
benzyl chloride	-0.003	0.129	-1.148	0.259	-1.260	-1.260
benzyl bromide	-1.520	-1.424	-1.371	-0.219	0.178	-1.520

With the halobenzenes in a face-edge geometry with a C-X (where X = halogen) bond parallel to the surface, there was a decrease in associative interactions as the size of the halo atom increased. This may be a result of the halo atom increasing and thus sterically pushing the benzene ring away from the surface. A similar effect was also present in the cofacial geometry. However, in the cofacial geometry, there was more coverage of the model surface by the benzene ring than in the face-edge geometry (X-side).

The benzylhalide analytes also showed an increase in associative interaction with the model surface with increased size. For benzylbromide, as with the halobenzenes, the greatest associative interaction was in the cofacial geometry with no offset. However, benzylchloride favoured face-edge geometry with the chloromethyl group directed away from the model surface ($H_f = -1.260$ kcal for x-up). Face-edge x-down is also a favoured geometry for benzylchloride ($H_f = -1.148$ kcal), where the chloromethyl group aligns down and along the model surface.

4.4.3 Alcohols, aldehydes, ketones, esters

The values of ΔH_f for each of the five geometries investigated are given in Table 4.11 for this group of compounds. With the exception of anisole, a cofacial geometry was most favoured for association between these compound and the model surface. In the case of anisole, the perpendicular face-edge x-side geometry was the most favoured associative interaction with the model surface.

Analytes which have resonance structures in which planarity occurs are more likely to adopt a planar geometry, as seen in figure 4.17. These analytes had the most favoured geometry in the offset cofacial position.

Table 4.11 Values of ΔH_f calculated by semi-empirical molecular modelling methods for alcohols, aldehydes, ketones, esters. The strongest adsorption of the analyte onto the surface, $\Delta H_{f_{min}}$ is highlighted in **bold**.

Analyte	Cofacial		Face-edge			$\Delta H_{f_{min}}$ (kcal)
	no offset	offset	x down	x side	x up	
phenol	-0.275	-0.023	0.581	0.027	0.823	-0.275
anisole	0.241	0.217	2.385	0.016	0.016	0.016
benzyl alcohol	0.283	0.215	0.948	0.872	0.605	0.215
benzaldehyde	-0.412	-0.605	1.216	-0.168	1.162	-0.605
acetophenone	-0.583	-0.863	1.742	-0.673	0.042	-0.863
methylbenzoate	-0.141	-0.980	0.188	0.312	0.144	-0.980
phenyl acetate	-0.177	-0.150	0.301	0.635	0.668	-0.177
cinnamaldehyde	-1.439	-1.659	-0.356	-1.499	-1.259	-1.659

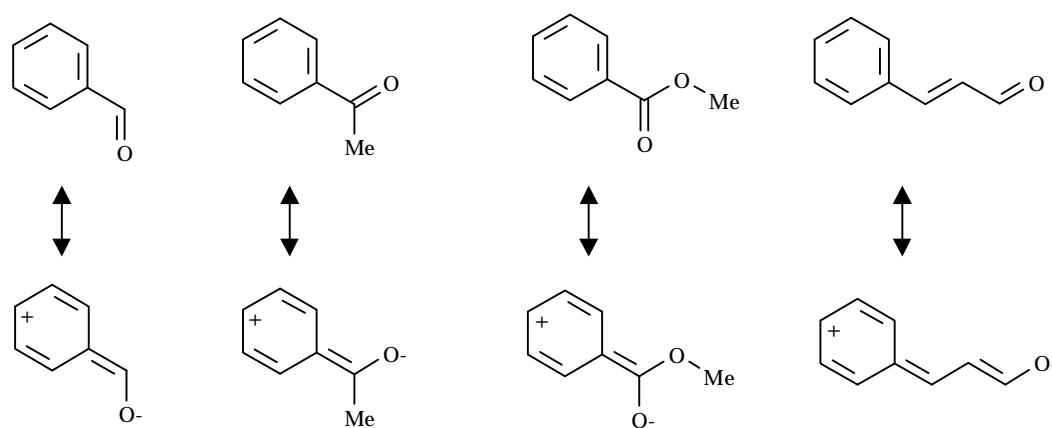


Figure 4.17 Analytes with resonance structures which result in a more rigid and planar molecule. Only two canonical forms are shown here for simplicity.

These analytes had a more negative $\Delta H_{f_{min}}$ than the other compounds in this section, suggesting that there may be increased retention on graphite for molecules with the ability to attain a planar conformation. This observation was in agreement with the $\log k_w$ values for these compounds on PGC.

Benzyl alcohol and anisole had high values for ΔHf_{min} in comparison with the other compounds in this section. This result was not expected and is not easily explained.

4.4.4 Carboxylic acids

The carboxylic acid compounds were modelled as both ionised and unionised species. The resulting ΔHf_{min} values, given in table 4.12, can be considered to represent the different pH conditions.

When considering the uncharged species that represent the low pH (2.5), the order of strength of association with the model surface was the same order as $\log k_w$ at pH 2.5 (i.e. *trans*-cinnamic acid > benzoic acid > pyhenylacetic acid). However, *trans*-cinnamic acid had a far greater association with the model surface than either benzoic acid or phenyl acetic acid. Each of the compounds had the strongest association with the model surface in the cofacial (coplanar) geometry, benzoic acid and phenylacetic acid adopting the cofacial geometry with no offset and *trans*-cinnamic acid adopting the offset cofacial geometry.

Table 4.12 Values of ΔHf calculated by semi-empirical molecular modelling methods for carboxylic acid analytes. The strongest adsorption of the analyte onto the surface, ΔHf_{min} is highlighted in **bold**.

Analyte	Cofacial		Face-edge			ΔHf_{min} (kcal)
	no offset	offset	x down	x side	x up	
benzoic acid ^u	-0.519	0.153	1.329	1.399	0.271	-0.519
benzoic acid ⁱ	4.732	4.496	5.232	5.264	4.414	4.414
phenylacetic acid ^u	-0.295	0.100	1.421	1.622	0.847	-0.295
phenylacetic acid ⁱ	3.778	4.454	5.129	5.854	4.911	3.778
<i>trans</i> -cinnamic acid ^u	-1.514	-1.705	-0.498	-0.525	1.209	-1.705
<i>trans</i> -cinnamic acid ⁱ	-0.282	-0.372	2.441	0.039	2.309	-0.372

^u unionised ⁱ ionised

The anionic species, which represented the chromatographic system at neutral pH, had noticeably less negative (or positive) values of ΔHf_{min} suggesting a weaker association with the model surface. In the case of the benzoate anion and the phenylacetic acid anion, ΔHf_{min} was strongly positive. This would appear to represent a repulsive interaction between the compounds and the model stationary phase surface.

The comparatively large values of ΔHf_{min} for the charged analytes may be explained by the lack of solvent in the model used. $\log k_w$ represents retention at 100% water mobile phase composition, so any charged species will be highly solvated. This result suggests that the presence of solvent in our model is less important for hydrophobic, but for charged (and possibly neutral hydrophilic compounds) the presence of solvation effects are more important. This highlights the weakness of the model.

This observation was also true for the *trans*-cinnamic acid anion, but the effect was significantly decreased because of the ability of this large conjugated molecule to distribute its charge throughout the π -system.

4.4.5 Neutral nitrogen containing compounds

The compounds within this group all had the most associative interaction with the model surface for the cofacial geometry, as seen in table 4.14. Modelling was undertaken on aniline in the neutral and cationic forms. Values of ΔHf for the anilinium cation were assumed to represent retention of aniline at pH 2.5, as aniline is protonated under these conditions (table 4.13).

The difference in ΔHf_{min} for the cationic and neutral aniline species was far smaller than for the different carboxylic acid species studied.

This may suggest that solvation effects are less important for these compounds.

Table 4.13 Values of ΔH_f calculated by semi-empirical molecular modelling methods for neutral nitrogen containing compounds. The strongest adsorption of the analyte onto the surface, $\Delta H_{f_{min}}$ is highlighted in **bold**.

Analyte	Cofacial		Face-edge			$\Delta H_{f_{min}}$ (kcal)
	no offset	offset	x down	x side	x up	
nitrobenzene	-0.494	-0.268	2.052	0.452	-0.386	-0.494
aniline ^u	0.636	0.257	0.425	0.770	0.579	0.257
aniline ⁱ	0.842	0.684	0.711	0.894	0.725	0.684
benzonitrile	-0.536	-0.374	0.805	-0.280	-0.515	-0.536
benzamide	-0.877	-1.375	2.265	1.919	0.403	-1.375

The values of $\Delta H_{f_{min}}$ for nitrogen containing compounds did not appear to relate the $\log k_w$ values for these analytes. This may reflect the absence of solvent and thus solvation effects in our model which may be important for retention of these polar analytes on PGC.

4.4.6 Charged analytes

The values of ΔH_f can be seen in table 4.14. The charged analytes both had the strongest associative interaction with the model surface in the perpendicular face-edge geometry. The values of $\Delta H_{f_{min}}$ were positive, indicating that the major contribution comes from electrostatic repulsive interactions between the charged analytes and the model surface. This observation may be explained by the lack of solvent in our model, as these charged analytes will be highly solvated in aqueous conditions. It also suggests that solvation may be an important factor in retention of polar and charged species on PGC. This suggests that the observations of Knox and Ross [19] (who proposed that solvent effects on PGC will not be a major influence on retention) may only apply to more hydrophobic analytes

Table 4.14 Values of ΔH_f calculated by semi-empirical molecular modelling methods for charged compounds. The strongest adsorption of the analyte onto the surface, $\Delta H_{f_{min}}$ is highlighted in **bold**.

Analyte	Cofacial		Face-edge			$\Delta H_{f_{min}}$ (kcal)
	no offset	offset	x down	x side	x up	
benzene sulfonic acid ⁱ	4.681	5.453	6.713	4.583	4.755	4.583
PTMAC ⁱ	10.532	10.868	11.348	9.523	6.958	6.958

ⁱ ionised

4.4.7 Molecular modelling conclusions

In Chapter 3, there was very strong correlation for the retention on PGC with the molecular modelling of the analytes interactions with a model a surface. For the mono-substituted benzene derivatives no overall correlation was found. This may be because of a number of factors, which are discussed below. The compounds studied in Chapter 3 were a homogeneous series of *n*-alkylbenzenes and also amylbenzene structural isomers. For those molecules, a rather simplistic model of analyte retention on PGC proved to be an adequate model. However, important factors in the retention were ignored for simplicity.

Chromatography depends on varying degrees of analyte association between a mobile and stationary phase. Our model ignored the presence of solvent and only considered an analyte and model surface in isolation in the gas phase. The idea of modelling retention whilst neglecting the presence of solvent was first proposed by Knox and Ross [19], who suggested that the analyte-solvent interaction was of little importance when compared with the analyte-stationary phase interactions. This may not however be the case. The entropy considerations for the chromatographic system were also ignored.

The relationship between ΔHf_{min} and $\log k_w$ on PGC at pH 2.5 and pH 7.0 is given in figure 4.18.

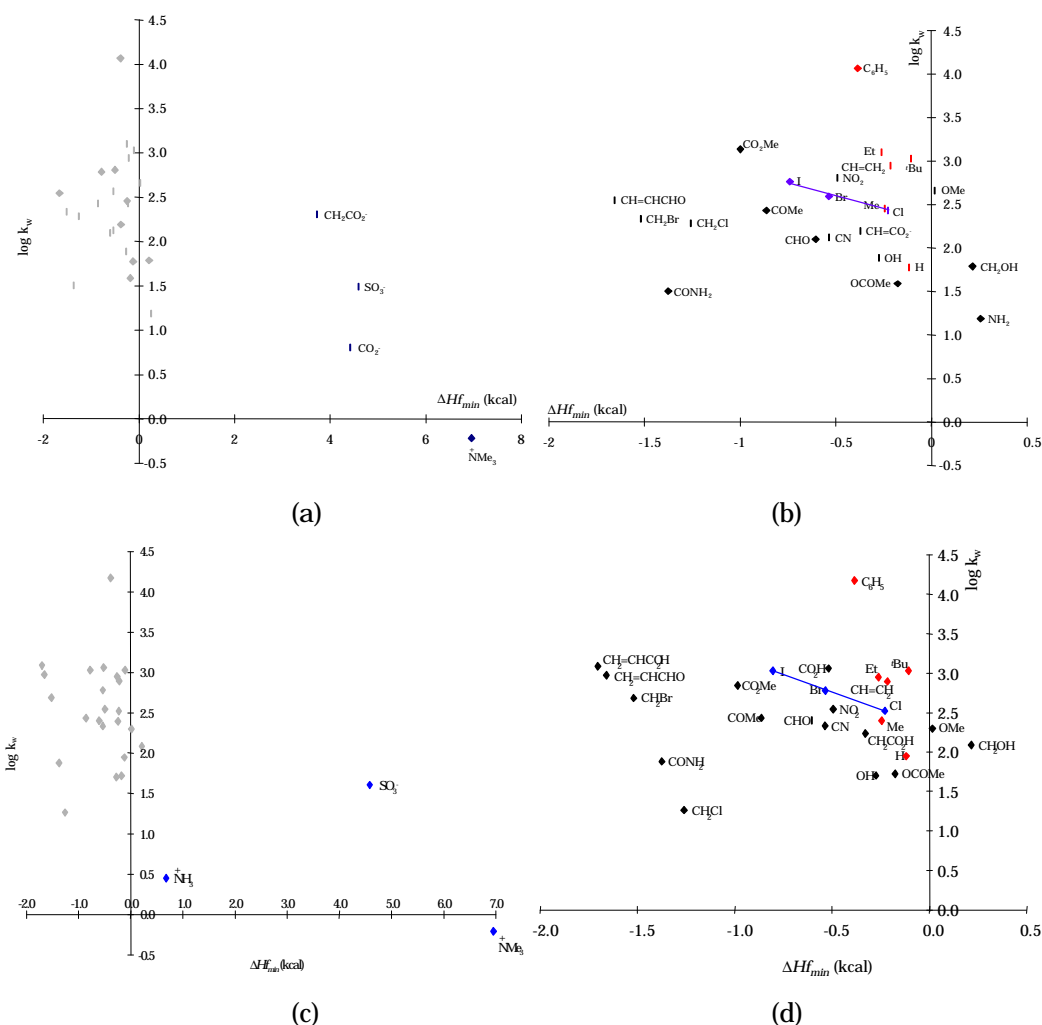


Figure 4.18 The relationship between ΔHf_{min} and $\log k_w$ at pH 7.0 (a & b) and pH 2.5 (c & d). (b) and (d) are expansion of the grey data points from (a) and (c).

Another major factor lacking in the model used was that in chromatography there is a dynamic system. The solvent is pumped through the column thus pushing the analyte along the stationary phase surface. This dynamic aspect was missing in the model.

The results shown here are useful to explain which geometry of interaction is most likely and also for the study the retention of closely related analytes.

4.5 Quantitative structure- retention relationship analysis of benzene derivatives

In Chapter 3, the analytes considered were a series of alkylbenzenes and so the retention was found to be based largely on hydrophobic interactions between the analytes and the stationary phase. In this chapter however, the series of analytes under investigation had a variety of different electronic, steric and lipophilic characteristics. There are both charged and neutral analytes and so the basis of retention on PGC for these analytes is more complicated.

4.5.1 Bivariate analysis

Linear regression analysis was performed on the experimentally obtained retention data for the benzene derivatives on both PGC and ODS stationary phases. The resulting correlations between structural descriptors and retention are given in table 4.15.

With a more diverse selection of analytes including non-polar, polar and charged species, the results of bivariate linear regression analysis are likely to have limited success for describing the mechanisms underpinning retention for the complete data-set of compounds on PGC. The strongest linear correlations will, however, be discussed below.

Table 4.15 Linear regression correlation between structural descriptors and $\log k_w$ for benzene derivatives, where r^2 is the index of determination.

Independent variable	r^2			
	pH 7.0		pH 2.5	
	PGC	ODS	PGC	ODS
ΔHf_{min}	0.383	0.332	0.372	0.194
Sum of squares of charges	0.040	0.149	0.054	0.156
Coquart excess charge	0.079	0.245	0.078	0.256
Topological Electronic Index	0.034	0.000	0.002	0.000
Molecular Mass	0.022	0.011	0.085	0.031
Molecular Surface Area	0.025	0.003	0.063	0.020
Molecular Volume	0.002	0.004	0.003	0.003
Verloop L (Subst. X)	0.099	0.018	0.209	0.041
Verloop B4 (Subst. X)	0.006	0.015	0.020	0.001
Ellipsoidal Volume	0.037	0.001	0.107	0.016
Total Dipole Moment	0.012	0.219	0.007	0.203
Total Dipole Moment (Subst. X)	0.026	0.216	0.030	0.184
$\log P$	0.435	0.786	0.333	0.755
Total Lipole	0.197	0.443	0.108	0.356
Molecular Refractivity	0.077	0.062	0.106	0.091
VAMP Total Energy	0.005	0.152	0.012	0.076
VAMP Electronic Energy	0.001	0.043	0.008	0.019
VAMP Mean Polarizability	0.457	0.194	0.604	0.407
VAMP Heat of Formation	0.068	0.000	0.238	0.004
VAMP Ionizational Potential	0.003	0.045	0.360	0.148
VAMP LUMO	0.154	0.144	0.361	0.261
VAMP HOMO	0.003	0.045	0.360	0.148
VAMP Total Dipole	0.044	0.212	0.212	0.398
π (Subst. X)*	0.714	0.775	0.785	0.804
MR (Subst. X)*	0.023	0.106	0.042	0.110
Swain and Lupton F (Subst. X)*	0.185	0.316	0.148	0.254
Swain and Lupton R (Subst. X)*	0.001	0.053	0.008	0.002
σ_{meta} (Subst. X)*	0.157	0.336	0.108	0.223
σ_{para} (Subst. X)*	0.078	0.283	0.033	0.120
Taft E_s (Subst. X)*	0.196	0.261	0.398	0.301

* These linear correlation values are from a reduced data set which excludes benzene sulfonic acid, phenyl acetic acid, *trans*-cinnamic acid and cinnamaldehyde (because of limited availability of molecular descriptors).

Figure 4.19 shows the relationship between $\log P$ and $\log k_w$ for the four sets of chromatographic conditions considered. On ODS (figure 4.19 a & b) the linear relationship between $\log P$ and $\log k_w$ gave correlation coefficients of 0.755 and 0.786 at pH 2.5 and pH 7.0 respectively. Although these were not strong linear correlations, they suggest that there is a correlation between retention on ODS and

Chapter 4 - The retention mechanisms of benzene derivatives on PGC hydrophobicity. On PGC however, there was little correlation between $\log P$ and $\log k_w$ at either pH value (r^2 is 0.435 at pH 7.0 and 0.333 at pH 2.5). This observation was mirrored by Hennion *et al.* [14] whilst studying the retention behaviour of polar compounds on PGC. Hennion concluded that hydrophobic interactions were not the most important interactions that govern the retention mechanism. Only if more compounds containing hydrophobic moieties were studied, would a trend be obtained. This observation was illustrated by the results of QSRR analysis of *n*-alkylbenzenes in Chapter 3.

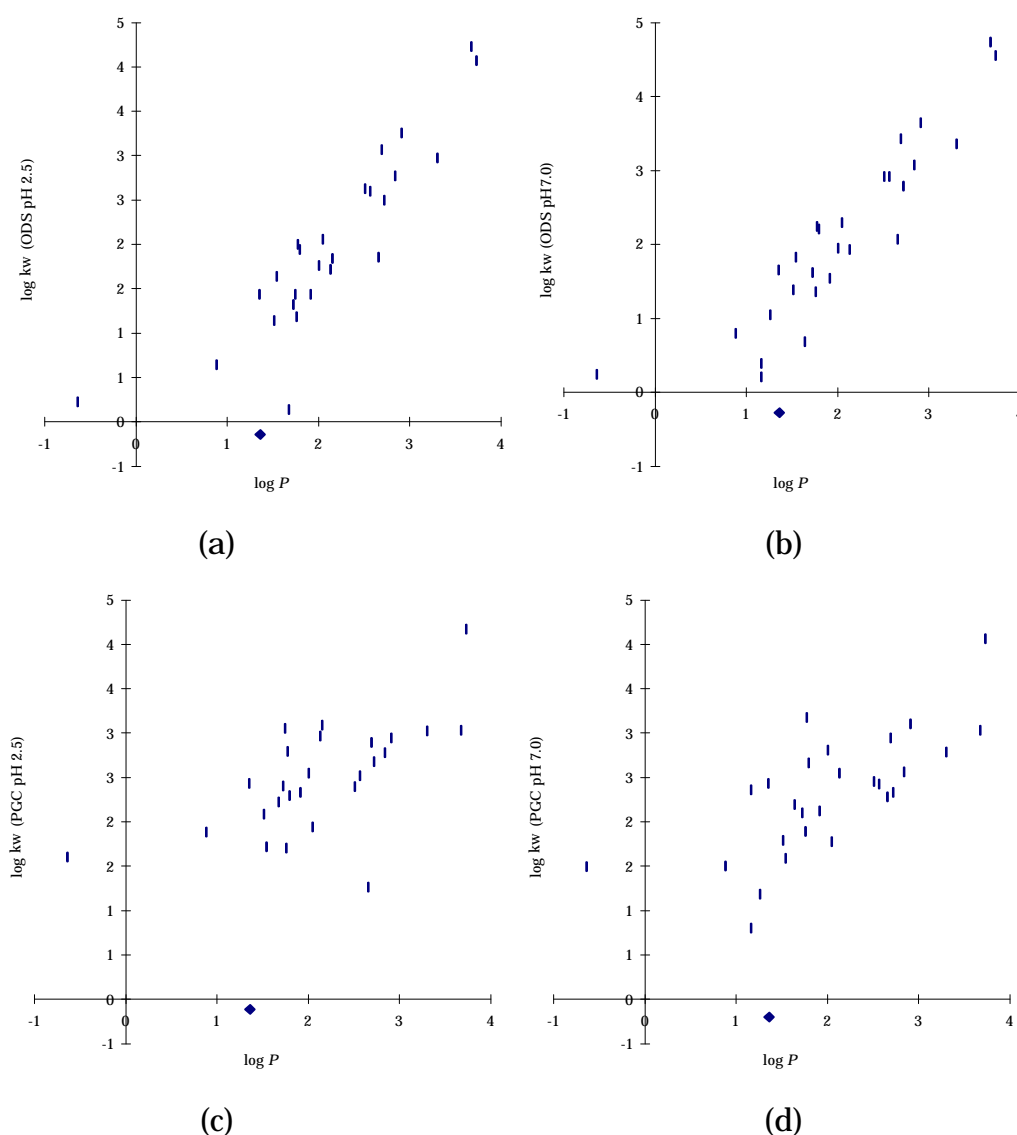


Figure 4. 19 The relationship between $\log k_w$ and $\log P$ on ODS at (a) pH 2.5 and (b) pH 7.0 and on PGC at (c) pH 2.5 and (d) pH 7.0.

The relationship between retention and the Hansch-Fujita

Chapter 4 - The retention mechanisms of benzene derivatives on PGC hydrophobicity constant, π is shown in figure 4.20 for both ODS and PGC stationary phases. On ODS there was a strong linear relationship between π and $\log k_w$ at both pH values. However PTMAC was an outlier from the rest of the analytes and as such reduced the linear correlation. Removing PTMAC from the data-set increased the correlation (r^2 is increased from 0.714 to 0.967 at pH 7.0 and from 0.785 to 0.966 at pH 2.5).

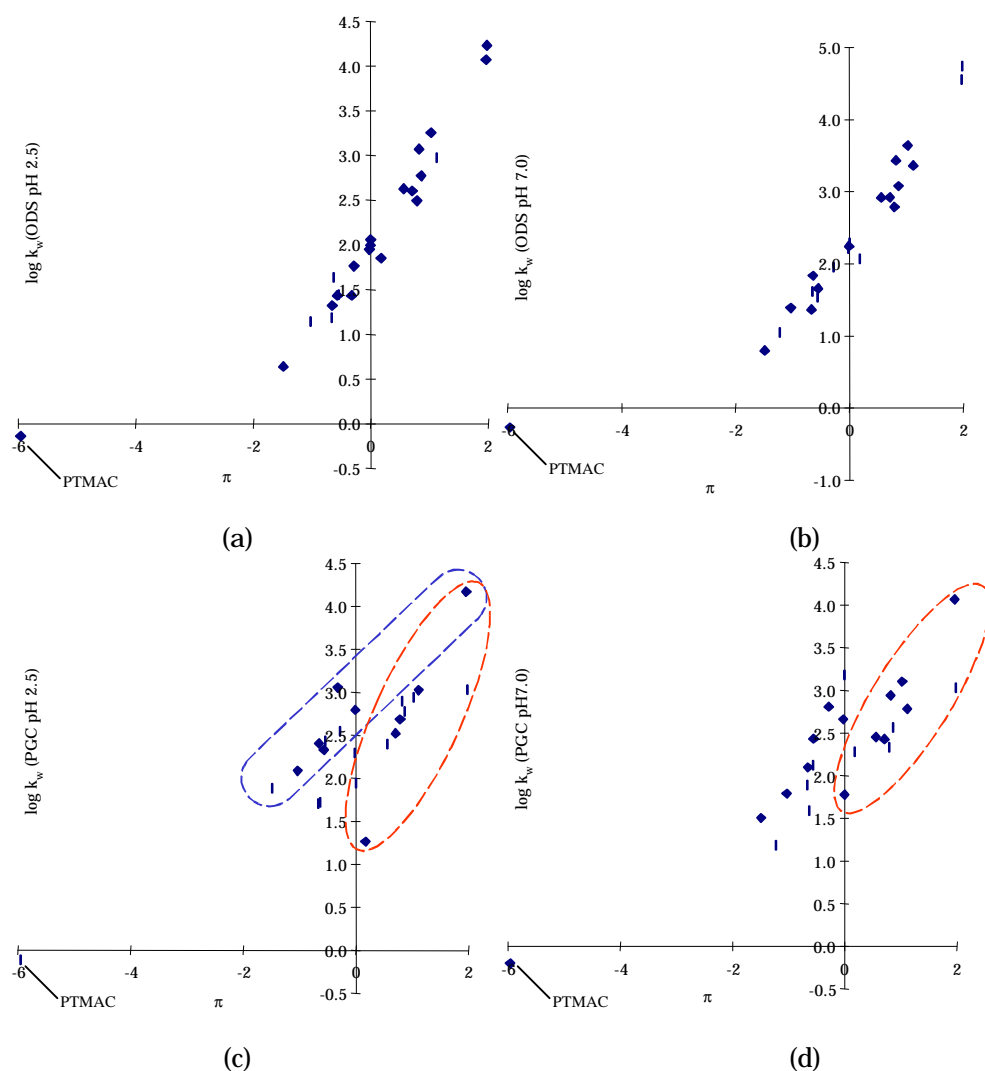


Figure 4.20 The relationship between retention and the Hansch-Fujita hydrophobicity constant on ODS at (a) pH 2.5 and (b) pH 7.0 and on PGC at (c) pH 2.5 and (d) pH 7.0

On PGC (figure 4.20 c & d) there were strong linear trends for subsets of the analytes. In particular, analytes (circled in blue) which have the ability for charge separation by delocalisation of electrons (through

Chapter 4 - The retention mechanisms of benzene derivatives on PGC (different canonical forms) showed the strongest linear relationships. The hydrophobic hydrocarbons and halohydrocarbons are highlighted in red on figure 4.20c & d. This shows that the polar and non-polar analytes showed two separate correlations for π on PGC.

The relationship between retention on PGC at pH 2.5 and pH 7.0 is given in figure 4.21 below. This figure highlights the difference between analytes that have a fixed charge (ringed in the figure) which showed a strong correlation, and the analytes for which charge is a function of pH (which are outside of the ring).

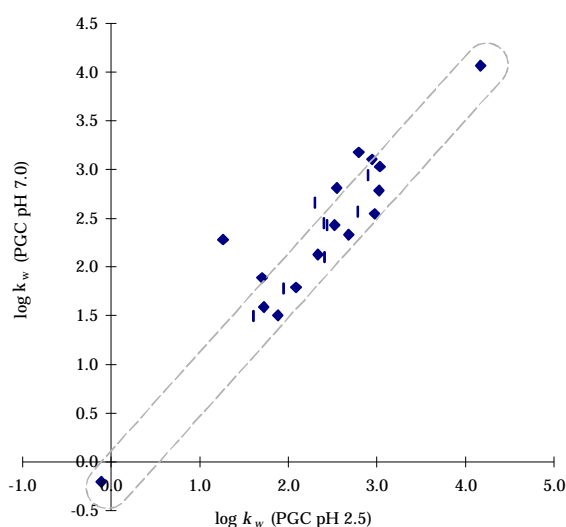


Figure 4.21 The relationship between $\log k_w$ at pH 7.0 on PGC and $\log k_w$ at pH 2.5 on PGC.

The relationship between retention on PGC and mean polarisability is given in figure 4.22 below. The best linear correlation was found for PGC at pH 2.5 ($r^2 = 0.740$). This is because of the 3 outliers (the PTMA cation, the anilinium cation and biphenyl) distorting the correlation. Figure 4.22b seems to show a limited linear correlation (given by the dashed line) for a subset of the analytes, however this appears to be more of an accidental correlation than for any reason, as the analytes involved are not particularly closely related.

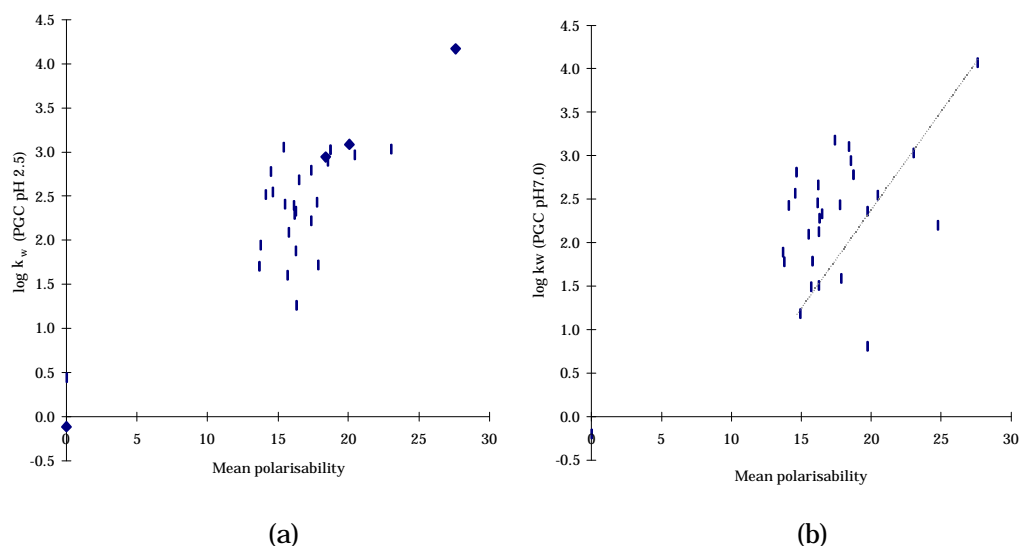


Figure 4.22 The relationship between $\log k_w$ and mean polarisability on PGC (a) at pH 2.5 and (b) at pH 7.0.

4.5.2 Multiple linear regression analysis

Historically, multiple linear regression (MLR) analysis [15] was the first, and foremost, statistical method applied in quantitative structure- activity relationship (QSAR) studies. This method was established by Hansch [16] to relate bioactivity data to measures of lipophilic, electronic and steric properties in a congeneric series of derivatives. At present this is also the statistical method most frequently used in QSRR studies [17, 18].

MLR analysis was performed for each of the 4 chromatographic conditions used within this study. MLR was carried out using the TSAR software package (Oxford Molecular Ltd.) on a Silicon Graphic Indigo² workstation.

PGC pH 2.5

MLR analysis was carried out to find which structural descriptors best correlated with $\log k_w$ at pH 2.5 on PGC. All descriptors used in the section 4.3.1 (and summarised in table 4.15) were used as candidates for MLR analysis. The analysis with the most significance is given below in equation 4.3 and figure 4.23.

$$\log k_w = 0.0692 P_E + 0.432 \pi - 0.359 E_{lumo} + 1.24 \quad (4.3)$$

$$n = 28 \quad r^2 = 0.821 \quad F\text{-value} = 29.0 \quad \text{significance} = 7.88 \times 10^{-8}$$

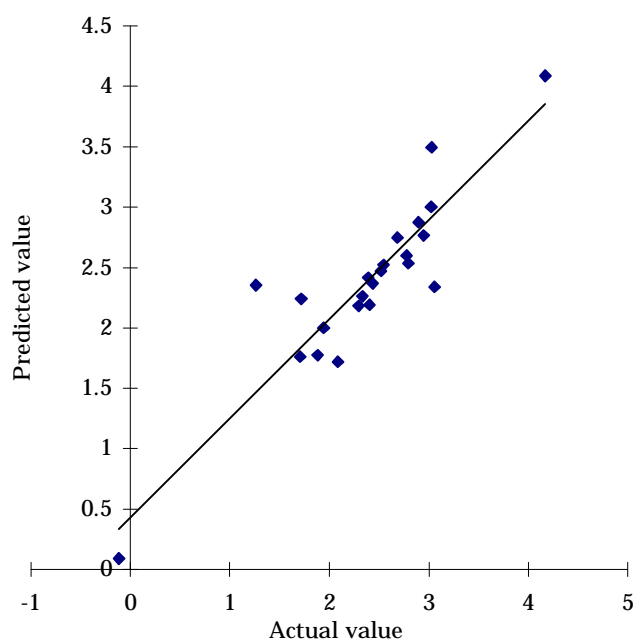


Figure 4. 23 MLR analysis of $\log k_w$ on PGC at pH 7.0. Variables used are π , mean polarisability (P_E) and E_{lumo}

Equation 4.3 describes 82.1 % of the variance within the dataset above a 99.99% significance level (as $1 - 7.88 \times 10^{-8} > 0.9999$). The three descriptors used were mean polarisability, P_E , the Hansch-Fujitsa parameter, π , and the lowest unoccupied molecular orbital (LUMO) energy (E_{lumo}).

This is a very significant, because retention on PGC has been found to depend upon a hydrophobic descriptor (π) and two electrostatic descriptors (P_E and E_{lumo}).

PGC pH 7.0

MLR analysis was carried out to find which structural descriptors best correlated with $\log k_w$ at pH 7.0 on PGC. All descriptors used in the section 4.3.1 (and summarised in table 4.15) were used as candidates for MLR analysis. The analysis with the most significance is given below in equation 4.4 and figure 4.24.

$$\log k_w = 0.636 \pi - 0.358 E_{lumo} + 2.35 \quad (4.4)$$

$$n = 28 \quad r^2 = 0.856 \quad F\text{-value} = 59.2 \quad \text{significance} = 1.39 \times 10^{-9}$$

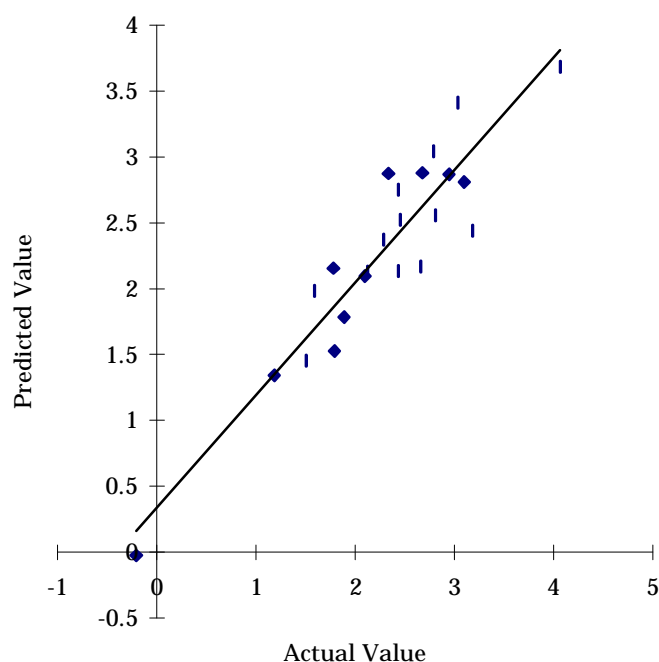


Figure 4.24 MLR analysis of $\log k_w$ on PGC at pH 7.0. Variables used are π and E_{lumo} .

Equation 4.4 describes 85.6 % of the variance within the dataset above a 99.99% significance level (as $1 - 1.39 \times 10^{-9} > 0.9999$). The two descriptors used were the Hansch-Fujitsa parameter, π , and the lowest unoccupied molecular orbital energy (E_{lumo}).

ODS pH 2.5

MLR analysis was carried out to find which structural descriptors best correlated with $\log k_w$ at pH 2.5 on ODS. All descriptors used in the section 4.3.1 (and summarised in table 4.15) were used as candidates for MLR analysis. No MLR results were found which explained retention on ODS at pH 2.5 with more significance than the bivariate analysis method given in section 4.3.1.

ODS pH 7.0

MLR analysis was carried out to find which structural descriptors best correlated with $\log k_w$ at pH 7.0 on ODS. All descriptors used in the section 4.3.1 (and summarised in table 4.15) were used as candidates for MLR analysis. The analysis with the most significance is given below in equation 4.5 and figure 4.25(a).

$$\log k_w = 0.454 \pi - 0.118 \log P + 2.63 \quad (4.5)$$

$$n = 28 \quad r^2 = 0.641 \quad F\text{-value} = 17.9 \quad \text{significance} = 2.48 \times 10^{-5}$$

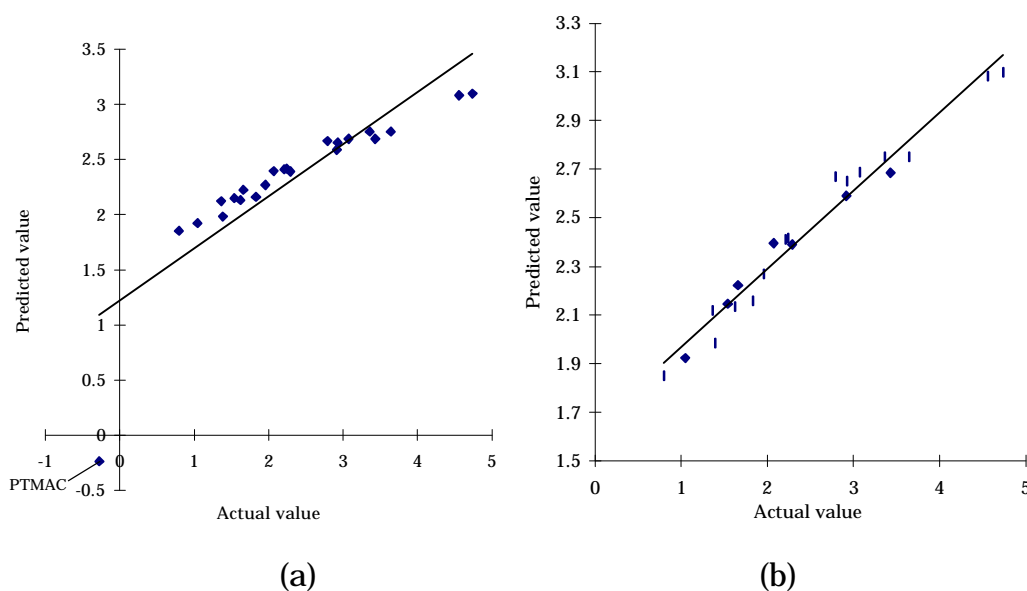


Figure 4.25 MLR analysis of $\log k_w$ on ODS at pH 7.0. Variables used are $\log P$ and π . (a) Complete dataset where $r^2 = 0.641$ (the outlier is PTMAC) and (b) with PTMAC removed (r^2 improves to 0.970)

Equation 4.5 describes 64.1 % of the variance within the dataset above a 99.99% significance level (as $1 - 2.48 \times 10^{-5} > 0.9999$). The two descriptors used were the Hansch-Fujitsa parameter, π , and $\log P$. However if phenyl trimethyl ammonium chloride was removed from the dataset, 97.0 % of the total variance within the dataset can be described by π and $\log P$. This improvement may indicate that the retention of PTMAC on ODS is different to the other analytes. This may be explained by PTMAC being the only positively charged analyte at neutral pH. As there are likely to be ionised silanol groups (SiO⁻) on the surface of the ODS support, it is possible that ionic interactions may be present which cannot be explained by π and $\log P$ and these ionic interaction therefore cannot be described by these parameters.

4.5.3 Principal component analysis

Factor analysis (including principal component analysis) is normally applied in chemistry to determine the “intrinsic dimensionality” of certain experimentally determined chemical properties, that is, the number of “fundamental factors” required to account for the variance [4].

As already discussed in section 1.4.3, the intercorrelation among allegedly “independent” variables affects the reliability of multiple regression results. Principal component analysis side-steps this issue by transforming the original independent variables into a smaller series of orthogonal variables or “principal components”. These principal components can then be used for regression analysis with the retention data.

Principal component analysis was employed for this dataset with the objective of exposing any important relationships between retention ($\log k_w$) and structural descriptors. Using this technique it was possible to reduce the set of descriptor variables from sixteen

Chapter 4 - The retention mechanisms of benzene derivatives on PGC structural descriptors to three orthogonal eigen vectors (principal components) which explained 94.9% of the total variance for the 16 original descriptors at pH 2.5 and 91.1% at pH 7.0 (table 4.16).

Table 4.16 Principal component analysis of the structural descriptors used for statistical analysis of benzene derivatives.

Principal Component	pH 2.5		pH 7.0	
	Variance explained %	Total explained %	Variance explained %	Total explained %
PC1	82.5	82.5	80.2	80.2
PC2	8.7	91.2	7.7	87.9
PC3	3.7	94.9	3.2	91.1

However, these eigen vectors produced poor correlations when regression analysis with the retention data is performed (table 4.17). In this study, the application of principal component analysis was not found to be of any additional benefit to the study. The use of multiple linear regression analysis did not reveal any stronger linear relationships.

Table 4.17 Bivariate analysis of principal components with $\log k_w$.

Principal Component	ODS		PGC	
	pH 2.5	pH 7.0	pH 2.5	pH 7.0
PC1	0.257	0.292	0.423	0.387
PC2	0.120	0.145	0.153	0.110
PC3	0.108	0.131	0.180	0.092

4.6 Conclusions

4.6.1 Chromatographic studies

The PGC stationary phase is very different from alkyl bonded silica supports. PGC is much more selective for the separation of both polar and non-polar geometric isomers and related compounds. Also in contrast to ODS, polar non-hydrogen bonding solutes tend to be more retained on PGC. This means that these supports use not only hydrophobic retention mechanisms, but they also retain solutes through electronic interactions. Retention on PGC is not adequately described by the traditional theories of retention past [6-8] mentioned in Chapter 1.

The main trends shown on PGC are:

1. Similar or reduced retention of hydrophobic analytes such as hydrocarbons, halobenzenes and benzyl halides on PGC when compared with ODS.
2. Increased retention of polar and charged species on PGC when compared with ODS.
3. Particularly strong retention for polarisable and highly conjugated analytes with heteroatoms in their functional groups.
4. Strong retention of conjugated analytes which can become highly planar with many resonance forms. This increased retention is thought to be a result of the planar nature of the analytes, their high polarisability and also their ability to spread charge throughout the molecule.
5. Massive increases in retention (when compared with ODS) for selected polar and charged analytes (see table 4.18).

There was a large drop in retention for *t*-butylbenzene on PGC compared with ODS. This shows that PGC is not a true reversed-phase stationary phase. Retention is also based on analyte shape. The bulky *t*-butyl group prevents the benzene ring from interacting in a

Table 4.18

Analyte	Δk_w	
	pH 2.5	pH 7.0
phenylacetic acid	1445.72	1026.25
benzene sulfonic acid	602.04	513.75
benzamide	194.13	89.25
benzoic acid	113.09	107.70
<i>trans</i> -cinnamic acid	67.81	220.58

Analysis of retention data for benzene derivatives on PGC suggests the presence of weakly acidic groups on the PGC surface. This may be from any residual silica left over from the template process in manufacturing or alternatively from acidic functionality at the edges of the sheets of graphite. This can be seen in the changing retention of hydrophobic analytes, where retention decreases with increased pH. This may also explain the increased retention of positively charged species with increased pH.

4.6.2 QSRR studies

Bivariate (linear regression) analysis showed that retention on ODS is based largely on hydrophobicity whereas for PGC, other additional factors need to be considered. Retention on ODS was seen to be highly correlated with π with PTMAC as an outlier. For PGC there was grouping of analytes into polar and non-polar subsets which both showed a strong correlation with π , however, as an overall dataset, correlation was poorer. Furthermore, linear regression analysis did not reveal a dependence of retention upon any single structural descriptor parameter.

Multi-parameter techniques in gave mixed success. Multiple linear regression analysis produced some excellent correlations for retention

Chapter 4 - The retention mechanisms of benzene derivatives on PGC on PGC. Considering that the analytes studied were a diverse range of hydrophobic molecules, polar molecules, weak and strong acids and bases, MLR correlation analysis produced important results. On PGC at pH 2.5, $\log k_w$ was found to be dependant on hydrophobic (π) and electronic (P_E and E_{lumo}) parameters. This is in accordance to the observed retention behaviour which is clearly based to some degree on reversed-phase or hydrophobic interactions, but also exhibits an additional dependence on polar interactions. On PGC at pH 7.0, $\log k_w$ was also found to be dependant on hydrophobic and electronic parameters, however at pH 7.0, the dependence was based only on π and E_{lumo} .

4.6.3 Molecular modelling studies

The molecular modelling studies undertaken within this chapter were invaluable for showing the geometry of strongest interaction for the analytes studied. Such studies are important because they highlight that retention on PGC is based very much on molecular shape and the ability of analytes to maximise their coverage of the PGC surface.

The reduced retention of *t*-butylbenzene on PGC when compared to ODS was explained by the inability of the benzene ring to interact strongly with the surface, because of the steric effect of the bulky *t*-butyl functional group. This result was mirrored in the calculation. The strong retention of large conjugated analytes such as *trans*-cinnamic acid was explained by the ability of these molecules to interact with the graphite surface in a cofacial geometry.

The molecular modelling studies do not however yield a strong correlation between ΔHf_{min} and $\log k_w$. The main reason for this may be the simplicity of the model used. This suggests that the model used is unable to provide a valid representation of all systems studied. However for subsets of the data-set interesting correlations have emerged. The model does not appear to be valid for all systems under

study, but has reproduced a number of the experimental chromatographic trends.

Overall, these preliminary modelling studies have provided a much deeper insight into the geometries of interaction for the analytes with the PGC stationary phase and have reproduced a number of experimental trends. Our model only considered the analyte and stationary phase in isolation and ignored the presence of solvent yet yielded important new information regarding the geometry of interaction for an analyte with the stationary phase. The modelling results for charged analytes suggest that the lack of solvent in our model is a weakness when considering hydrophilic species, as the value of ΔH_{min} is overestimated.

4.7 References

- [1] J. H. Knox, P. Ross, *Advances In Chromatography* 37 (1997) 73.
- [2] J. Kriz, E. Adamcova, J. H. Knox, J. Hora, *J. Chromatogr. A* 663 (1994) 151.
- [3] J. H. Knox, K. K. Unger, H. Mueller, *J. Liq. Chromatogr.* 6 (1983) 1.
- [4] R. Kaliszan, *Quantitative Structure- Chromatographic Retention Relationships*, John Wiley & Sons, New York 1987.
- [5] A. Streitwieser, C. H. Heathcock, *Introduction to Organic Chemistry*, Macmillan Publishing Company, New York 1985.
- [6] C. Horváth, W. Melander, I. Molnár, *J. Chromatogr.* 125 (1976) 125.
- [7] D. E. Martire, R. E. Boehm, *J. Phys. Chem.* 87 (1983) 1045.
- [8] L. R. Snyder, *Principles of Adsorption Chromatography*, Marcel Dekker Inc., New York 1968.
- [9] V. R. Meyer, *Practical High-Performance liquid Chromatography*, Wiley, New York 1994.
- [10] A. L. Patterson, *Institute of Pharmaceutical Sciences*, University of Nottingham, Nottingham 2000.
- [11] J. J. P. Stewart, *J. Comp-Aided Molecul. Design* 4 (1990) 1.
- [12] O. Bastiansen, S. Samdel, *J. Mol. Structure* 128 (1985) 115.
- [13] K. C. Park, L. R. Dodd, K. Levon, T. K. Kwei, *Macromolecules* 29 (1996) 7149.
- [14] M. C. Hennion, V. Coquart, S. Guenu, C. Sella, *Journal Of Chromatography A* 712 (1995) 287.
- [15] C. Daniel, F. S. Wood, *Fitting Equations to Data*, Wiley, New York 1971.
- [16] C. Hansch, in E. J. Ariens (Ed.): *Drug Design, Vol. 1*, Academic Press, New York 1971, p. 271.
- [17] R. Kaliszan, *Structure and Retention in Chromatography. A Chemometric Approach*, Harwood Academic Publishers, Australia 1997.
- [18] R. Kaliszan, *J. Chromatogr. A* 656 (1993) 417.
- [19] J.H. Knox, P. Ross, *Surface modification of porous graphitic carbon*, HPLC 99, Granada, Spain (1999)

Appendix 4.1

Analyte	ODS						PGC					
	pH 2.5			pH 7.0			pH 2.5			pH 7.0		
	log k_w	r^2	slope									
benzene	2.058	0.998	-0.025	2.289	0.999	-0.027	1.945	0.995	-0.025	1.778	0.996	-0.026
toluene	2.627	0.998	-0.031	2.917	0.999	-0.033	2.396	0.992	-0.030	2.454	0.963	-0.030
ethylbenzene	3.254	0.995	-0.037	3.641	0.997	-0.040	2.946	0.992	-0.036	3.102	0.994	-0.037
<i>t</i> -butylbenzene	4.230	0.996	-0.044	4.739	0.998	-0.047	3.032	0.997	-0.037	3.030	0.980	-0.036
styrene	3.071	0.994	-0.036	3.429	0.995	-0.038	2.896	0.998	-0.031	2.945	0.983	-0.031
biphenyl	4.070	0.997	-0.042	4.557	0.989	-0.046	4.172	0.999	-0.034	4.066	0.995	-0.035
chlorobenzene	2.602	0.998	-0.031	2.924	0.998	-0.033	2.520	0.996	-0.030	2.430	0.991	-0.028
bromobenzene	2.773	0.994	-0.033	3.074	0.996	-0.035	2.777	0.999	-0.032	2.568	0.996	-0.028
iodobenzene	2.975	0.998	-0.034	3.358	0.998	-0.037	3.026	0.999	-0.032	2.786	0.998	-0.028
benzyl chloride	1.853	0.998	-0.024	2.071	0.998	-0.026	1.264	0.922	-0.015	2.284	0.999	-0.028
benzyl bromide	2.495	0.998	-0.031	2.788	0.999	-0.033	2.684	0.998	-0.033	2.336	0.997	-0.028
benzyl alcohol	1.142	0.990	-0.020	1.388	0.989	-0.022	2.087	0.999	-0.028	1.789	0.998	-0.024
benzaldehyde	1.324	0.992	-0.020	1.620	0.987	-0.024	2.406	0.999	-0.028	2.099	0.999	-0.023
benzoic acid	1.435	0.990	-0.021	0.387	0.999	-0.016	3.058	0.982	-0.039	0.803	0.998	
methyl benzoate	1.999	0.996	-0.026	2.241	0.997	-0.028	2.794	0.999	-0.027	3.179	0.992	-0.032
anisole	1.947	0.996	-0.025	2.209	0.996	-0.027	2.295	0.996	-0.027	2.661	0.991	-0.032
nitrobenzene	1.760	0.997	-0.025	1.952	0.998	-0.026	2.545	0.998	-0.027	2.807	0.997	-0.030
cinnamaldehyde	1.720	0.996	-0.025	1.926	0.997	-0.026	2.971	0.991	-0.024	2.548	0.991	-0.033
<i>trans</i> -cinnamic acid	1.841	0.995	-0.026	0.684	0.989	-0.015	3.089	0.990	-0.023	2.193	0.998	-0.017
phenyl acetate	1.637	0.997	-0.024	1.830	0.998	-0.026	1.720	0.988	-0.024	1.588	0.999	-0.022
acetophenone	1.441	0.992	-0.022	1.657	0.994	-0.023	2.434	0.998	-0.026	2.434	0.997	-0.025
benzonitrile	1.435	0.994	-0.023	1.538	0.995	-0.023	2.332	0.999	-0.029	2.124	0.999	-0.025
phenol	1.188	0.993	-0.020	1.364	0.995	-0.022	1.705	0.998	-0.024	1.889	0.998	-0.026
aniline	0.478	0.994	-0.028	1.048	0.991	-0.019	0.443	0.979	-0.005	1.186	0.991	-0.018
benzamide	0.640	0.986	-0.016	0.796	0.988	-0.018	1.881	0.994	-0.023	1.506	0.997	-0.019
benzene sulfonic acid	0.228	0.997	-0.021	0.243	0.998	-0.021	1.604	0.984	-0.024	1.494	0.997	-0.027
phenyl acetic acid	0.144	0.998	-0.009	0.210	0.995	-0.010	2.223	0.997	-0.029	2.360	0.997	-0.028
PTMAC	-0.140	0.998	-0.009	-0.271	0.982	-0.008	-0.114	0.990	-0.011	-0.203	0.989	-0.006

Chapter Five

The retention mechanisms of biphenyl derivatives on PGC

5.1 Introduction

Chapter 4 exposed evidence for increased retention of analytes which can increase their planarity due to different resonance structures. In this chapter, the investigation was extended to biphenyl derivatives, which can be thought of as analogues to those studied in Chapter 4, but with an additional planar “anchor”.

The structure of the biphenyl molecule (and its derivatives) consists of two phenyl rings, joined by a carbon-carbon single bond. Because of the small distance between the central four hydrogen atoms (figure 5.1), there is a strong repulsion between them which twists the molecule towards the most sterically favourable arrangement where the two rings are perpendicular.

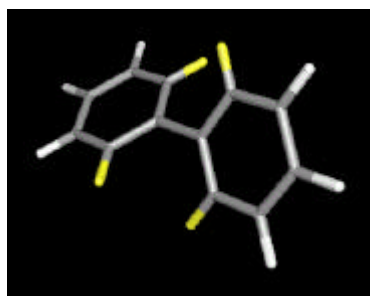


Figure 5.1 The lowest energy conformation of the biphenyl molecule. The four central hydrogen atoms which force the twisted conformation are highlighted in yellow.

The conjugation energy however favours a planar geometry so the final twist must be a compromise between the two effects. This competition results in a torsion angle of $\sim 44^\circ$ as determined from gas phase measurements [1].

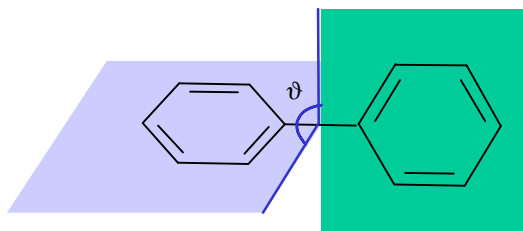


Figure 5.2 Inter-phenyl torsion angle, ϑ

The co-planarity of the two phenyl rings in biphenyl was of interest in this project, because flat molecules have been found to give a greater interaction with the planar graphite surface^[2] than non planar analytes. A measure of flatness of a group of model analytes was therefore desirable. Conformational analysis of the 20 *mono*-substituted biphenyl derivatives was performed using semi-empirical molecular orbital theory methods as given in Chapter 2. The conformational analysis resulted in two descriptors which provide an indication of the planarity of the molecule.

- (i) Inter-phenyl torsion angle, ϑ (see figure 5.2).
- (ii) Rotation barrier to planarity (ΔE_ϑ) defined by equation 5.1

$$\Delta E_\vartheta = E_0 - E_\vartheta \quad (5.1)$$

where E_0 is the heat of formation of the compound for the lowest energy geometry with the two phenyl rings constrained in a coplanar conformation and E_ϑ is the heat of formation of the compound for the lowest energy geometry with no constraints.

The former gives a measure of the lowest energy conformation, “as is”,

Chapter 5 - The retention mechanisms of biphenyl derivatives on PGC
without the influence of the PGC support. The latter gives a measure of the ability of the molecule to attain a planar conformation and thus interact with the planar graphite surface. This barrier may be lower for more conjugated compounds with many canonical forms (e.g. 4-phenylcinnamic acid) than less conjugated molecules (e.g. 4-methylbiphenyl).

Shape selectivity has been found to be important in reversed-phase separations for at least five categories of analyte, including polycyclic aromatic hydrocarbons (PAHs) [3, 4], polychlorinated biphenyls (PCBs) [5], steroids [6], carotenoids [7] and polycyclic aromatic sulfur heterocycles (PASHs) [4]. These groups of molecules all exhibit a fixed conformational structure constrained by steric effects, double bonds or fused rings (or combinations of these).

Sander *et al.* carried out a comprehensive characterisation of commercially available ODS stationary phases where the alkyl chains were bonded to the surface with differing densities of surface coverage [8]. Using two PAHs of different sizes, they were able to calculate the selectivity between these two compounds for each stationary phase. When the selectivity was plotted against the surface coverage (of the silica by the alkyl chains) a linear relationship was found for these planar analytes. Selectivity was found to be greatest for stationary phases which had lower surface coverage of the silica by the bonded alkyl chains. This behaviour was explained by Yan and Martire's "slot model" of analyte retention [9], where the spaces between the alkyl chain were perceived as slots into which analyte molecules may penetrate. The shape of the analyte and the width of the slot (i.e. surface coverage of the silica by the bonded alkyl chains) were of importance for this model. Thus planar molecules may fit into the slots more easily than non-planar analytes. This means that with a higher density of bonded alkyl chains on the surface of the stationary

Chapter 5 - The retention mechanisms of biphenyl derivatives on PGC
phase, there would be fewer or smaller slots for analytes to penetrate and thus selectivity would be decreased.

For PGC this “slot model” is not applicable because the planar surface will not behave in such a manner. In fact rather than slots, it may be suggested that the retention of analytes on PGC is viewed as a table-like surface where planar or flat analytes more strongly adhere to the stationary phase (or the table), whereas more spherical analytes will interact to a lesser degree or “roll off” the stationary phase. This is however a rather simplified model which only accounts for retention based on molecular shape.

For the purpose of this chromatographic study, the analytes were categorised into the five sections given in table 5.1. The structures of these analytes are given in figure 5.3; their chemical names are given in table 5.1.

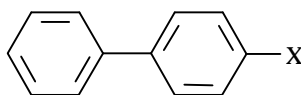


Figure 5.3 General structure of the *para*-substituted biphenyl derivatives

Table 5.1 Analytes studied

Analyte name	X
<i>Hydrocarbons :</i>	
biphenyl	H
4-methylbiphenyl	CH ₃
4-ethylbiphenyl	CH ₂ CH ₃
4-vinylbiphenyl	CH=CH ₂
<i>Halogenated compounds:</i>	
4-bromobiphenyl	Br
4-chloromethylbiphenyl	CH ₂ Cl
<i>Alcohols, aldehydes & ketones :</i>	
4-hydroxybiphenyl	OH
4-methoxybiphenyl	OCH ₃
4-hydroxymethylbiphenyl	CH ₂ OH
(4-biphenyl)ethanol	CH(OH)CH ₃
4-biphenylcarbaldehyde	CHO
4-acetylbiphenyl	COCH ₃
<i>Carboxylic acid derivatives :</i>	
methyl 4-phenylbenzoate	CO ₂ CH ₃
4-acetoxybiphenyl	OCOCH ₃
4-biphenylcarbonitrile	CN
4-biphenylcarbonamide	CONH ₂
<i>Acids :</i>	
4-biphenylcarboxylic acid	CO ₂ H
4-biphenylacetic acid	CH ₂ CO ₂ H
4-phenylcinnamic acid	CH=CHCO ₂ H
4-biphenylsulfonic acid	SO ₃ H

The aim of this chapter was to investigate a series of *mono*-substituted biphenyl derivatives by chromatographic and computational chemistry techniques in order to determine the mechanisms of retention on PGC. The retention characteristics of twenty *mono*-substituted biphenyl derivatives were measured on PGC and ODS using a variety of methanol/water mobile phase compositions. Conformational analysis of the analytes was carried out using semi-empirical molecular orbital methods to determine whether there was a mechanism of retention based on shape-selectivity present. QSRR analysis was performed on the chromatographic and molecular modelling data produced.

5.2 Results and discussion of chromatographic studies on ODS and PGC

Appendix 5.1 gives the values of the logarithm of the chromatographic retention factor extrapolated to 100% water ($\log k_w$) for all the analytes under investigation according to equation 5.1 below.

$$\log k = \log k_w + a C \quad (5.1)$$

where C is the percentage of organic modifier in the mobile phase and a is the slope of the graph produced.

In addition, values of $\log k_w$ and slope (a) have been reproduced throughout section 5.2 for each sub-group of analytes. Each $\log k_w$ value was extrapolated using $\log k$ measurements from 6 different mobile phase compositions. Each $\log k$ value represents the mean of three measurements. Retention times were reproducible to better than 1% from run to run. The experimental methods used in this work are presented in section 2.1.2.

5.2.1 Hydrocarbon substituted biphenyls

The hydrocarbon compounds in this study are non-polar analytes, and as such, the retention of these compounds is expected to be based

Chapter 5 - The retention mechanisms of biphenyl derivatives on PGC largely on hydrophobic interactions in reversed-phase systems. The retention behaviour of these analytes on PGC and ODS over a range of mobile phase compositions at pH 2.5 and pH 7.0 is given in figure 5.4. Values of $\log k_w$ for hydrocarbons can be seen in Table 5.2.

Table 5.2 Retention data for hydrocarbons

Substituent X	ODS				PGC			
	pH 2.5		pH 7.0		pH 2.5		pH 7.0	
	$\log k_w$	a						
H	3.170	-0.030	3.290	-0.031	3.336	-0.026	3.978	-0.032
CH ₃	3.775	-0.035	3.753	-0.035	4.198	-0.029	4.915	-0.036
CH ₂ CH ₃	4.221	-0.039	3.808	-0.035	4.570	-0.034	5.006	-0.038
CH=CH ₂	3.858	-0.036	3.270	-0.030	4.981	-0.033	5.761	-0.037

These analytes exhibited linear relationships between the slope of the graphs in figure 5.4 (C) and $\log k$ over the mobile phase compositions used. The hydrocarbons studied were more strongly retained on PGC than on ODS over the entire range considered.

This retention behaviour may be explained by one of two factors

- (i) Hydrophobicity. The alkylbenzenes in chapter 3 showed increased selectivity on PGC when compared with ODS stationary phase. This means that the retention of compounds may increase more on PGC per unit increase in hydrophobicity than on ODS.
- (ii) Planarity. The increased retention on PGC may be an effect of the increased planarity of these compounds when compared to their benzene analogues in chapter 4.

The smaller *n*-alkylbenzenes in chapter 3 exhibited reduced retention on PGC when compared to ODS, however the selectivity for the addition of a CH₂ group was greater on PGC than ODS and so for *n*-alkylbenzenes larger than phenylhexane retention was greater on PGC than on ODS. This suggests a greater selectivity for retention

Chapter 5 - The retention mechanisms of biphenyl derivatives on PGC based on hydrophobicity for PGC than for ODS. This explanation is in agreement with the retention of the hydrocarbon substituted biphenyl given here.

The *n*-alkylbenzenes in chapter 3 gave a retention order in accordance with their size and hydrophobicity on both PGC and ODS. This was observed for the hydrocarbons in both chapters 4 and 5. All of the analytes in this group exhibited stronger retention at pH 7.0 than at pH 2.5 on PGC.

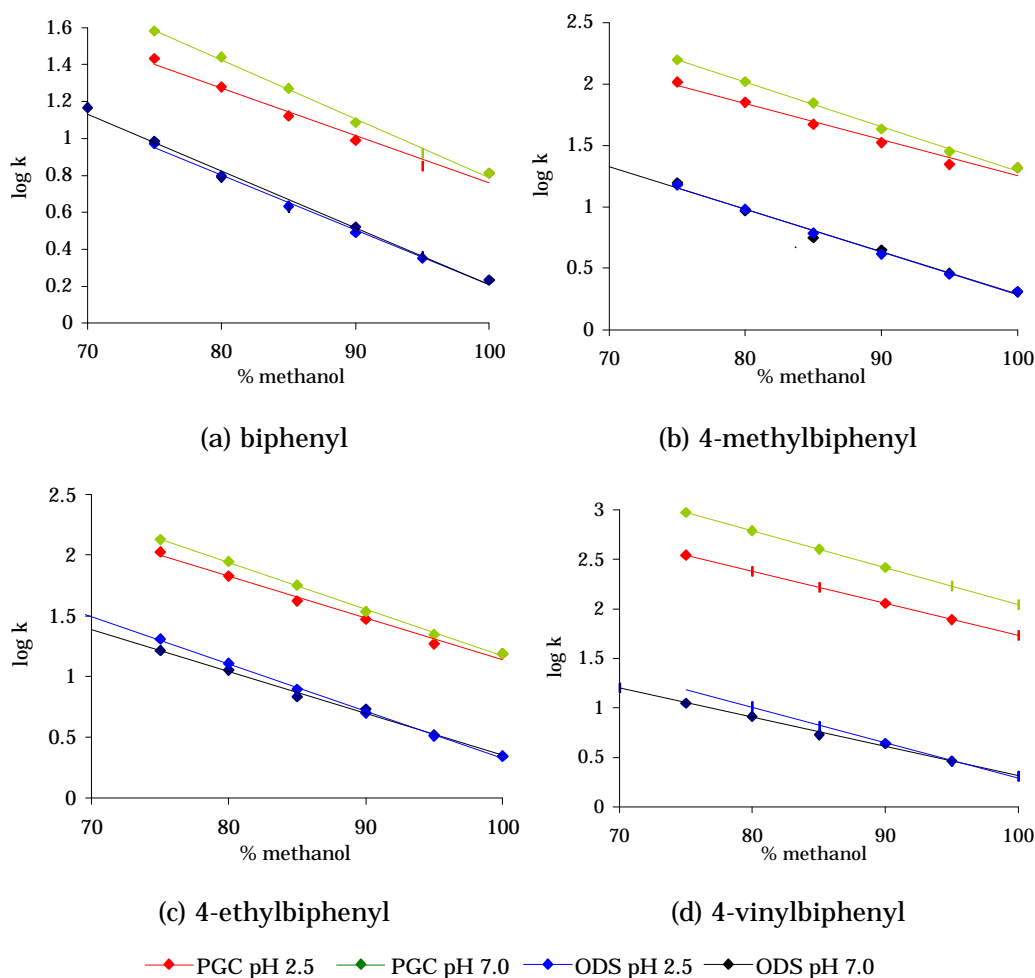


Figure 5.4 The relationship between retention ($\log k$) and mobile phase composition for the hydrocarbons compounds studied.

5.2.2 Halogenated compounds

Retention of the halogenated analytes on PGC and ODS over a range of mobile phase compositions at pH 2.5 and pH 7.0 is given in figure 5.5. Values of $\log k_w$ for the halogenated compounds are listed in table 5.3. Values of a for the halogenated compounds are listed in table 5.3.

Table 5.3 Retention data for halogenated compounds.

Substituent X	ODS				PGC			
	pH 2.5		pH 7.0		pH 2.5		pH 7.0	
	$\log k_w$	a						
Br	3.889	-0.036	3.571	-0.032	4.455	-0.028	5.212	-0.037
CH ₂ Cl	2.947	-0.028	3.107	-0.030	3.912	-0.026	4.273	-0.029

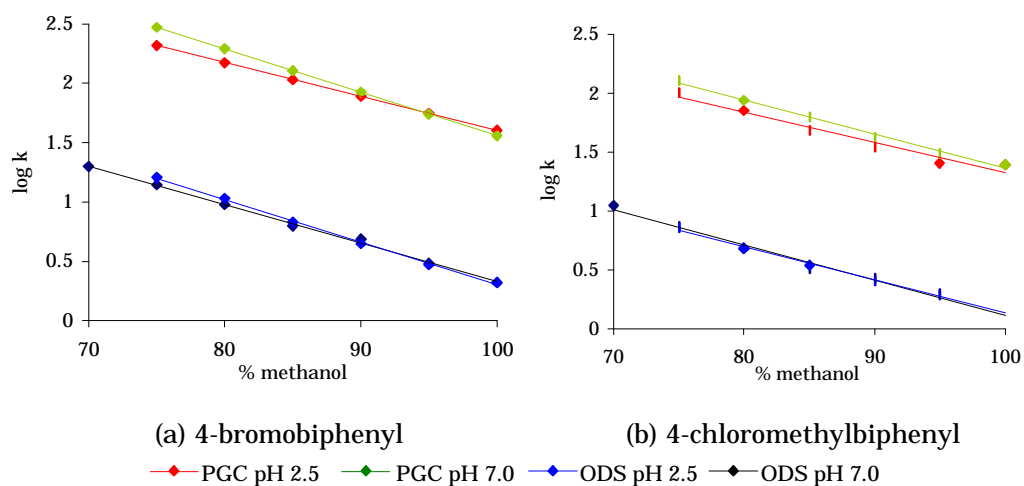


Figure 5.5 The relationship between retention ($\log k$) and mobile phase composition for the halogenated compounds studied.

Retention of the halogenated analytes was stronger on PGC than on ODS. This may be explained by hydrophobic interactions having a stronger effect on PGC than ODS. It may also be explained by the greater affinity of planar molecules with the planar graphite surface. 4-Bromobiphenyl was more strongly retained than 4-chloromethylbiphenyl, on both PGC and ODS. This may be due to the lower polarity of the 4-bromobiphenyl molecule compared with 4-chloromethylbiphenyl. One lone pair of electrons on the bromo atom has the ability to interact with the π -system of the neighbouring

Chapter 5 - The retention mechanisms of biphenyl derivatives on PGC phenyl ring, thus reducing the polarity. This cannot happen in the 4-chloromethylbiphenyl molecule because the chlorine atom is not adjacent to the ring and so, as polarity is increased hydrophobicity, and thus retention, is decreased by reversed-phase mechanisms.

5.2.3 Alcohols, aldehydes & ketones

This group of analytes introduced varying degrees of polarity into the data set under investigation. When the relationship between the mobile phase composition and retention is contrasted for biphenyls (figure 5.6) and their benzene analogues (figure 4.4) it is apparent that the difference in retention between ODS and PGC is greater for the biphenyl group. There is evidence for a polar retention effect on graphite (PREG) for both sets of analytes, however for the biphenyl analytes this may also be a result of the increased hydrophobicity of the analytes or their ability to adopt a more planar conformation.

Table 5.4 Retention data for alcohols, aldehydes & ketones.

Substituent X	ODS				PGC			
	pH 2.5		pH 7.0		pH 2.5		pH 7.0	
	log k_w	a						
OH	1.839	-0.018	1.989	-0.020	3.216	-0.022	3.605	-0.026
OCH ₃	3.071	-0.029	3.213	-0.030	4.156	-0.027	4.530	-0.031
CH ₂ OH	1.803	-0.018	1.969	-0.020	3.381	-0.024	3.703	-0.027
CHO	2.235	-0.022	2.396	-0.023	3.641	-0.026	4.298	-0.033
CH(OH)CH ₃	2.061	-0.021	2.410	-0.024	3.325	-0.026	3.717	-0.030
COCH ₃	2.345	-0.023	2.517	-0.024	3.804	-0.028	4.598	-0.033

This effect was most noticeable when comparing 4-methoxybiphenyl (figure 5.6b) with anisole (figure 4.4b), suggesting that either increased planarity or increased hydrophobicity are responsible for the increased retention of biphenyl analytes.

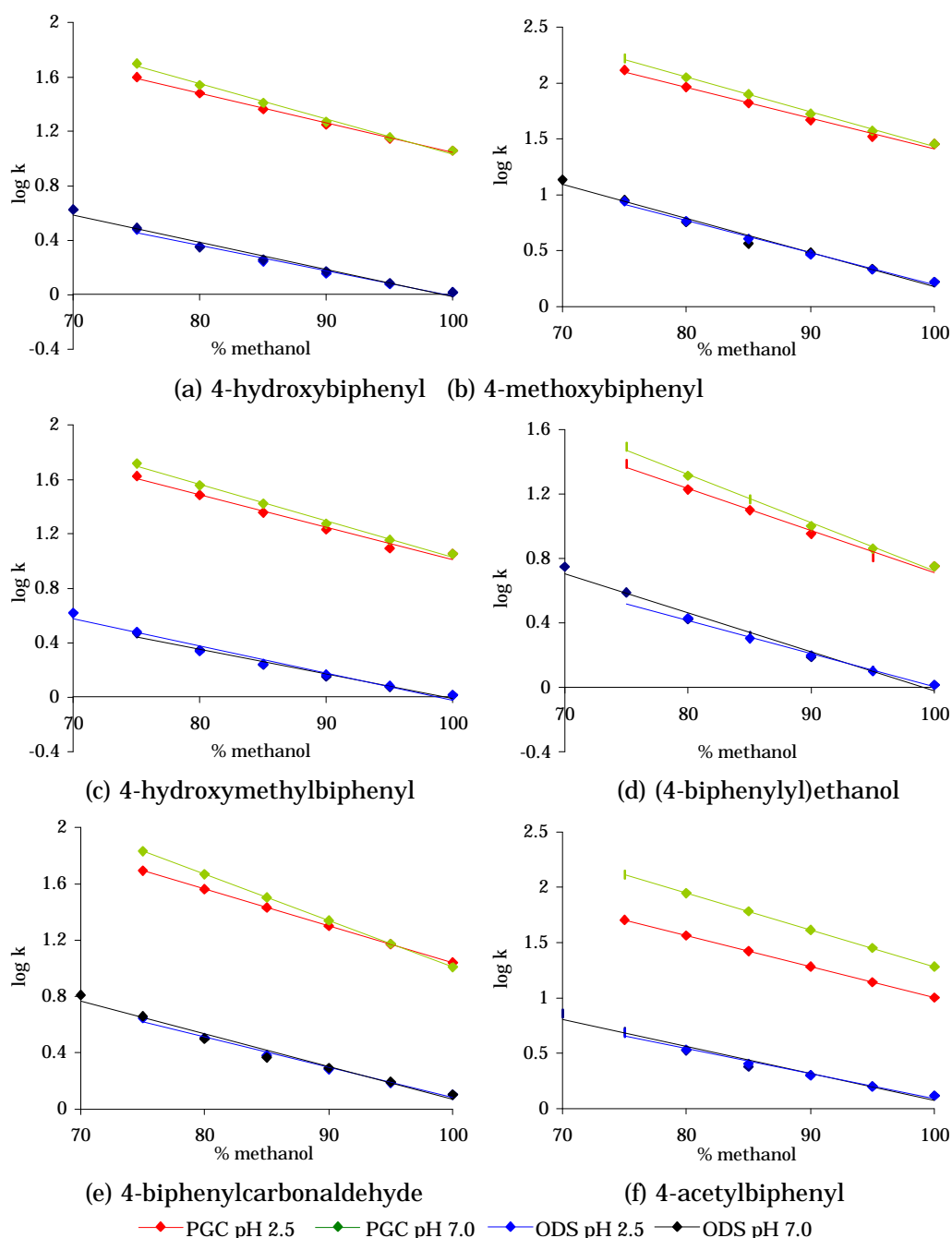


Figure 5. 6 The relationship between retention ($\log k$) and mobile phase composition for the alcohols, aldehydes & ketones studied.

Retention on both ODS and PGC was greater at pH 7.0 than at pH 2.5 for all alcohols, ketones and aldehydes. A possible explanation for this, as stated previously in section 4.2.3, is the polar nature of these analytes. ODS consists of a silica support with hydrophobic alkyl groups chemically bonded onto the silica to create a largely hydrophobic interface with the mobile phase [10]. Any surface silanol

Chapter 5 - The retention mechanisms of biphenyl derivatives on PGC groups, which have not been capped with a C₁₈ hydrocarbon, can also interact with the analyte. In acidic conditions, the effect of this will be minimal. However, at higher pH values, the silanol group will ionise and the effect of their interaction with the analytes will become more apparent. On ODS, at pH 7.0, there are attractive adsorptive secondary interactions between any exposed ionised silanol (SiO⁻) groups on the ODS secondary phase and the polar analyte, resulting in an increase in retention.

Strong retention of 4-biphenylcarboxaldehyde and 4-acetylbiphenyl may be explained by the ability of these compounds to form an interphenyl double bond as seen in figure 5.7. These compounds possess canonical forms that may impart an increased possibility of planarity when these compounds come into close proximity to the planar PGC surface.

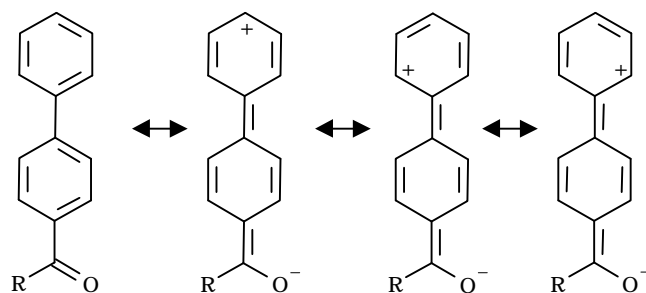


Figure 5.7 Resonance structures of 4-biphenylcarboxaldehyde (where R = H) and 4-acetylbiphenyl (where R = CH₃), showing the interphenyl double bond.

On PGC, the increased retention of this group of polar analytes at pH 7.0 compared with pH 2.5 may be explained by the presence of weakly acidic functionality on the PGC surface. This could be due to the presence of residual silica left over from the template manufacturing process interacting in an associative manner with the polar analytes.

There may also be acidic functionality at the edge of the graphite

Chapter 5 - The retention mechanisms of biphenyl derivatives on PGC sheets which may account for increased retention of polar analytes at pH 7.0 for identical reasons.

5.2.4 Carboxylic acid derivatives

Retention of the carboxylic acid derivatives was substantially stronger on PGC than ODS at both pH values (table 5.5 and figure 5.8).

Table 5.5 Retention data for carboxylic acid derivatives.

Substituent X	ODS				PGC			
	pH 2.5		pH 7.0		pH 2.5		pH 7.0	
	log k_w	a						
CO ₂ CH ₃	2.996	-0.028	3.189	-0.030	4.027	-0.028	4.424	-0.027
OCOCH ₃	2.026	-0.024	2.388	-0.021	2.919	-0.019	3.560	-0.025
CN	2.242	-0.022	2.417	-0.024	3.748	-0.024	4.179	-0.028
CONH ₂	1.192	-0.012	1.368	-0.014	2.800	-0.014	3.259	-0.018

The increase in retention may be explained by three processes:

- (i) The polar retention effect on graphite.
- (ii) The hydrophobic nature of the biphenyl parent molecule.
- (iii) The planar nature of these analytes and their increased ability to interact with the planar graphite surface.

Each of these analytes have the resonance structures where there is a double bond between the phenyl rings. The contribution of these resonance structures to the resonance means that the barrier to coplanarity of the rings is lowered. This may account for the increased retention of these molecules on PGC observed in the chromatographic data (table 5.5 and figure 5.8), however the hydrophobic nature of the biphenyl ring system may also play a strong role in the increased retention of these molecules on PGC when compared with ODS.

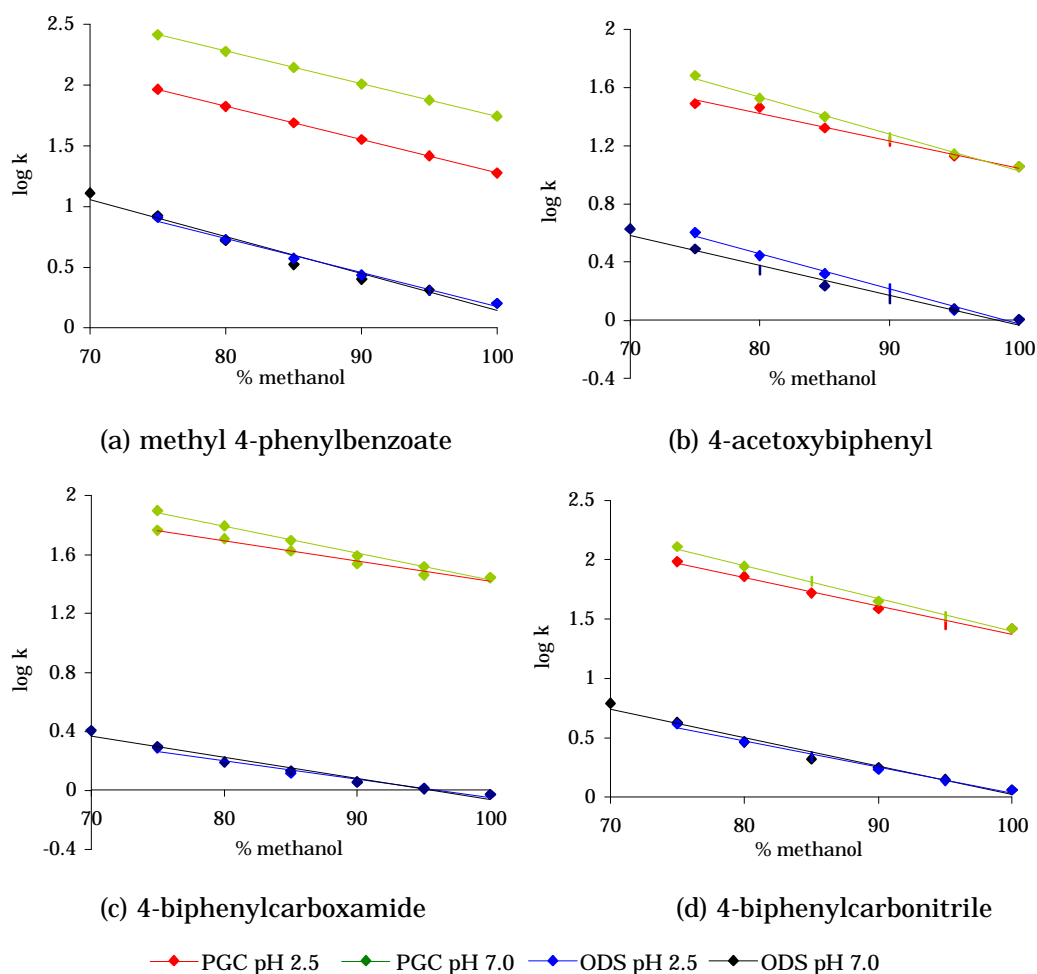


Figure 5. 8 The relationship between retention ($\log k$) and mobile phase composition for the carboxylic acid derivatives studied.

Retention on both PGC and ODS was greater at pH 7.0 than at pH 2.5. On ODS this may be due to the presence of the silanol groups which would be unionised under acidic conditions and ionised at pH 7.0. These silanol groups result in polar secondary interactions with the polar analytes causing an increase in retention, as described earlier in this chapter (section 5.2.3). The increase in retention on PGC from pH 2.5 to pH 7.0 lends increased weight to the hypothesis that there are weakly acidic functionalities on the PGC surface, possibly silanols, left over from the template manufacturing process. This effect was most noticeable for methyl 4-phenylbenzoate (figure 5.8a).

5.2.5 Acids

The retention of the acid analytes on PGC and ODS was studied over a range of mobile phase compositions (figure 5.9). Values of $\log k_w$ and a are given in table 5.6.

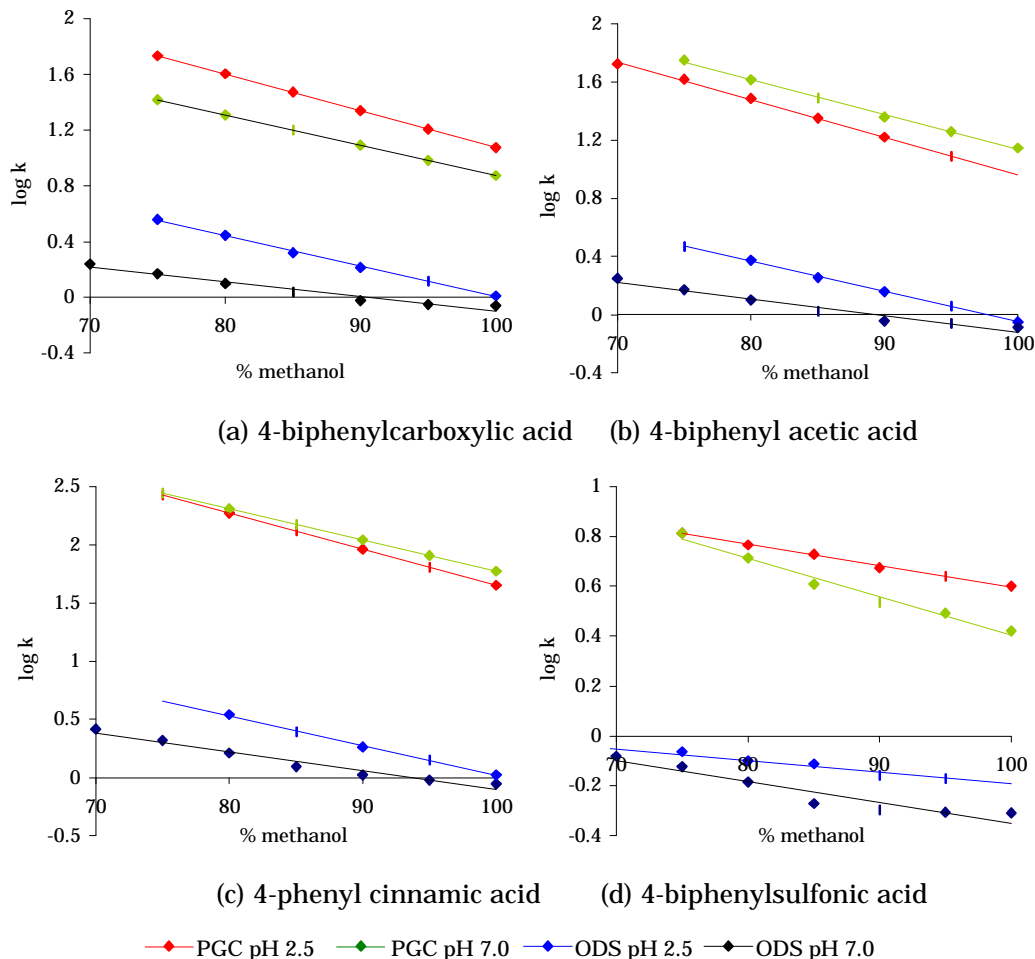


Figure 5.9 The relationship between retention ($\log k$) and mobile phase composition for the acids.

Each of these analytes exhibits stronger retention on PGC than ODS at both pH values. The observed increase in retention from ODS to PGC may be explained by a combination of the polar retention effect on graphite, hydrophobicity and the increased affinity of planar analytes with the planar graphite surface.

Each of the carboxylic acids studied showed stronger retention on both

Chapter 5 - The retention mechanisms of biphenyl derivatives on PGC ODS and PGC at pH 2.5. This may be due to the ionisation of these weakly acidic analytes. At pH 2.5 the carboxylic acids are predominately unionised and so strong reversed phase hydrophobic interactions are present on both ODS and PGC. It is also true that other mechanisms such as planarity based interactions and PREG interactions may be present on PGC.

Table 5.6 Retention data for acids.

Substituent X	ODS				PGC			
	pH 2.5		pH 7.0		pH 2.5		pH 7.0	
	log k_w	a						
CO ₂ H	2.189	-0.022	0.952	-0.011	3.724	-0.027	3.058	-0.022
CH ₂ CO ₂ H	2.028	-0.021	1.035	-0.012	3.608	-0.027	3.549	-0.024
CH=CHCO ₂ H	2.568	-0.025	1.522	-0.016	4.752	-0.031	4.456	-0.027
SO ₃ H	0.362	-0.005	0.480	-0.008	1.470	-0.09	1.947	-0.015

At pH 7.0, the carboxylic acid analytes are predominately ionised and so reversed phase hydrophobic interactions are vastly reduced. This results in a reduction in retention on both ODS and PGC supports for the carboxylic acids. The magnitude of this reduction in retention is larger on ODS (approx. 1.0 log unit) than on PGC (0.05-0.7 log units).

There are two possible explanations for the smaller change in retention on PGC than on ODS:

- (i) The presence of a polar retention effect on graphite compensating for a reduction in the reversed-phase mechanism.
- (ii) The effect that planarity may exert on retention on PGC may also compensate for a reduction in reversed-phase interactions.

These two effects are important because of the reduction in hydrophobicity for these charged acids and also because any acidic functionality on the PGC surface will also be negatively charged at pH 7.0 and so repulsive electrostatic interactions may be present.

On ODS, the retention of the carboxylic acid analytes is reduced by two factors. The main factor that reduces retention is the drop in hydrophobicity for these charged analytes. The other factor will be repulsive electrostatic interactions with any uncapped (and negatively charged ionised) silanol groups on the ODS surface.

The retention of 4-biphenylsulfonic acid on PGC analyte is increased at neutral when compared to pH 2.5. This observation is a reversal of that seen for benzenesulfonic acid in chapter 4 and as such is unexplained. These analytes are charged at both pH values studied so any difference in retention may be explained by a difference in the nature of the stationary phase. However there is evidence for weakly acidic functionality on the PGC surface. At pH 7.0, these acidic functionalities would be negatively charged and so result in repulsive electrostatic interactions which would decrease retention. This logic does not account for the retention of 4-biphenylsulfonic acid.

5.2.6 General results and discussion

It has previously been reported that the retention mechanism on PGC is based on a combination of different types of interactions including reversed-phase interactions, shape and size factors as well as polar interactions [11]. The retention of analytes on ODS is based, for the most part, on reversed-phase interactions [12]. It is possible to identify those analytes whose retention is significantly greater on PGC than on ODS by calculating the Δk_w term shown in equation 5.2.

$$\Delta k_w = 100 \left(\frac{k_w(\text{PGC})}{k_w(\text{ODS})} - 1 \right) \quad (5.2)$$

The values of this change in k_w between ODS and PGC, termed “ Δk_w ” are given in table 5.7 and in figure 5.10.

For the biphenyl analytes, studied in Chapter Five, there are three main trends in Δk_w (figure 5.10):

The value of Δk_w is larger at pH 7.0 than at pH 2.5 as seen for the majority of the analytes studied in chapter 4.

Unlike the benzene derivatives in chapter 4, where Δk_w values were both positive and negative, Δk_w is positive for all the biphenyl analytes studied.

The range and magnitude of Δk_w values are increased substantially in comparison to the benzene derivatives studied in chapter 4.

Benzene derivatives: $-98 < \Delta k_w < 14\ 046$.

Biphenyl derivatives: $47 < \Delta k_w < 85\ 823$

Observation (i) may be explained by the disruption of reversed-phase interactions on ODS at pH 7.0 by the secondary coulombic interactions due to uncapped and ionised silanol groups on the ODS surface. This reduces the retention on ODS and therefore the value of Δk_w should increase as a result.

Observation (ii) may be explained by the planar nature of the biphenyl derivatives and their increased affinity to the planar graphite surface. This effect was seen in the molecular modelling studies in chapter four, where biphenyl was found to have the strongest value of ΔHf_{min} when compared to any of the benzene derivative studied. Observation (ii) may also be explained by the increased hydrophobicity of the biphenyl analytes. The *n*-alkylbenzenes studied in chapter 3 showed a greater selectivity on PGC than on ODS, with stronger retention of *n*-alkylbenzenes larger than phenyl hexane on PGC when compared to ODS.. This effect may be extended to the retention of the biphenyls

Observation (iii) suggests that the combined effect of planarity, hydrophobicity and the so-called polar retention effect on graphite

Chapter 5 - The retention mechanisms of biphenyl derivatives on PGC leads, synergistically, to a far stronger retention on PGC than the sum of these individual effects.

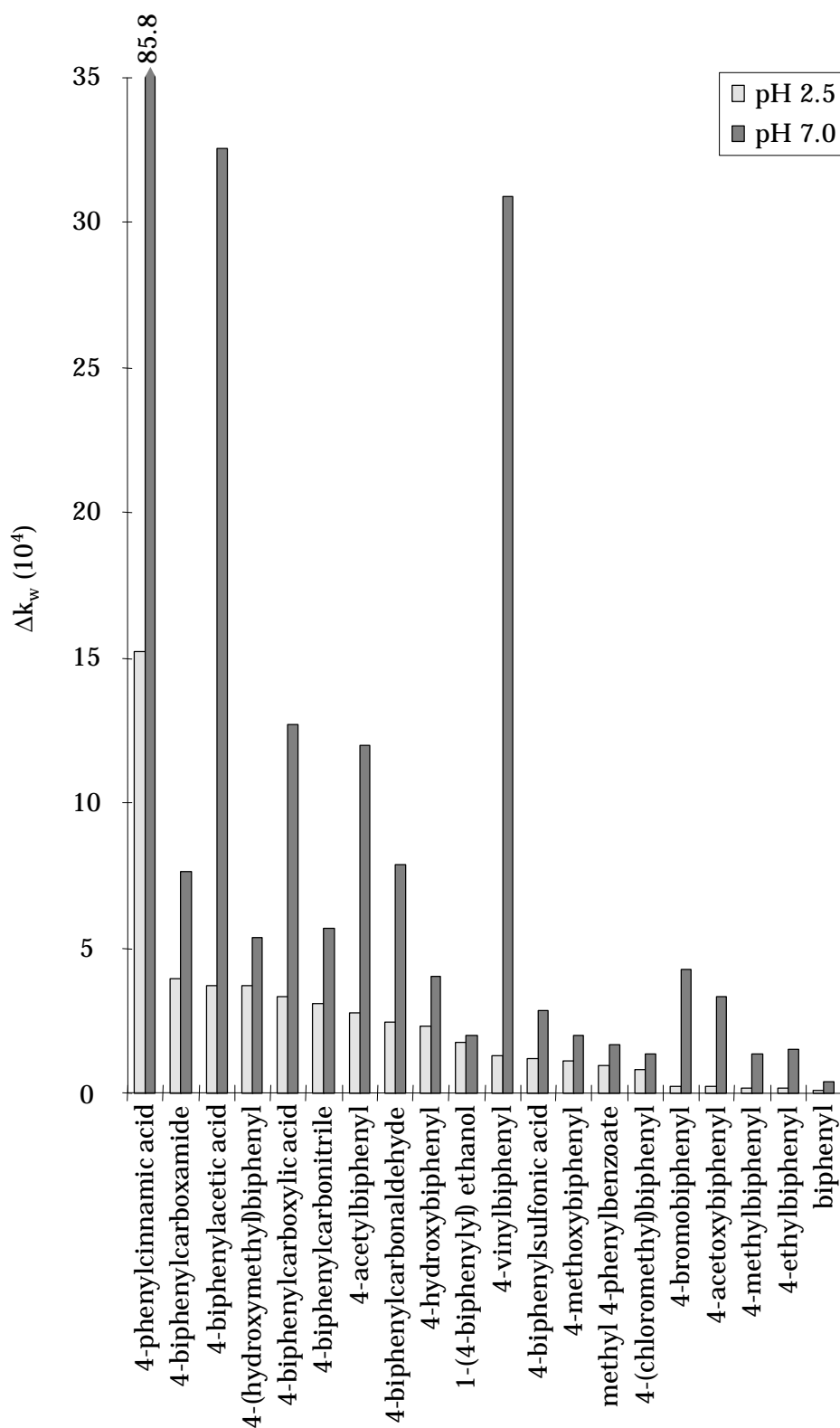


Figure 5.10 Δk_w for *para*-substituted biphenyl derivatives at pH 2.5 and pH 7.0.

Table 5.7 Values of Δk_w for biphenyl derivatives.

Analyte	Δk_w (10^4)	
	pH 2.5	pH 7.0
4-phenylcinnamic acid	15.2	85.8
4-biphenylcarboxamide	3.96	7.67
4-biphenylacetic acid	3.70	32.5
4-(hydroxymethyl)biphenyl	3.69	5.33
4-biphenylcarboxylic acid	3.33	12.7
4-biphenylcarbonitrile	3.11	5.69
4-acetylbiphenyl	2.78	11.9
4-biphenylcarbaldehyde	2.45	7.87
4-hydroxybiphenyl	2.29	4.03
1-(4-biphenyl) ethanol	1.74	1.93
4-vinylbiphenyl	1.23	30.9
4-biphenylsulfonic acid	1.18	2.83
4-methoxybiphenyl	1.12	1.97
methyl 4-phenylbenzoate	0.97	1.62
4-(chloromethyl)biphenyl	0.82	1.36
4-bromobiphenyl	0.27	4.28
4-acetoxybiphenyl	0.24	3.31
4-methylbiphenyl	0.17	1.35
4-ethylbiphenyl	0.12	1.48
biphenyl	0.05	0.39

For benzene derivatives, the values of Δk_w ranged between -98 and 1.4×10^5 , with biphenyl derivative these were extended to between 47 and 8.6×10^5 . Although the range for biphenyls was not much larger than for benzene derivatives, the magnitude of Δk_w was substantially larger for most analytes.

Biphenyl, 4-methylbiphenyl and 4-ethylbiphenyl gave a value of Δk_w of between 47 and 165 at pH 2.5. For 4-vinylbiphenyl, there was a ten fold increase in comparison with a Δk_w value of 1228. This value increased to 3.1×10^6 at pH 7.0 for 4-vinylbiphenyl. For biphenyl,4-

Chapter 5 - The retention mechanisms of biphenyl derivatives on PGC methylbiphenyl and 4-ethylbiphenyl there was approximately a ten fold increase in the value of Δk_w at pH 7.0 when compared with pH 2.5. This was because of a drop in $\log k_w$ at pH 7.0 on ODS and an increase in $\log k_w$ on PGC at pH 7.0, when both are compared with pH 2.5. The magnitude of the increase in $\log k_w$ for PGC at pH 7.0, when compared with pH 2.5 is unexplained. However, in combination with a drop in $\log k_w$ on ODS at pH 7.0 when compared with ODS at pH 2.5 results in the large value of Δk_w (3.1×10^6).

The halogen containing compounds had larger values of Δk_w than the alkyl substituted biphenyls at pH 2.5 with 4-chloromethylbiphenyl having the highest value of Δk_w (821). However, at pH 7.0, the value of Δk_w increased to 1.4×10^4 , a similar Δk_w value was observed for 4-methylbiphenyl. The value of $\log k_w$ for 4-bromobiphenyl was greatly increased at pH 7.0 (4.3×10^4) when compared to pH 2.5 (268). This can be attributed to a reduction of $\log k_w$ (and therefore k_w) at neutral pH when compared with pH 2.5 on ODS. However, the opposite is true for PGC with an increase in $\log k_w$ at neutral pH when compared with pH 2.5.

The alcohols, ketones and aldehydes all exhibited Δk_w values around 10^4 at pH 2.5. This value was increased at pH 7.0. The larger values on Δk_w for these oxygen containing analytes can be seen as further evidence for the polar retention effect on graphite. The difference in Δk_w between pH values is less marked for these analytes. This may be explained by the secondary interactions on ODS at pH 7.0 having a positive effect on retention for these more polar analytes. The presence of uncapped ionised silanol groups on the ODS may contribute to increased retention due to favourable associative interactions with the more polar substituents on the analyte. The increase in Δk_w at neutral pH may also be the result of weakly acidic functionality on the PGC surface. This functionality would not be partially shielded, as is the

Chapter 5 - The retention mechanisms of biphenyl derivatives on PGC

case for the silanol groups on ODS, and so these associative interactions would be stronger and lead to increased retention at pH 7.0.

The 4-biphenylcarboxylic acid derivatives had Δk_w values ranging between 973 (for methyl 4-phenylbenzoate) and 3959 (for 4-biphenylcarboxamide). The value of Δk_w was approximately doubled at pH 7.0 for these compounds. The difference in Δk_w between pH values was less marked for these analytes than for hydrocarbons and halogenated compounds. This may be explained by the secondary interactions on ODS at pH 7.0 having a positive effect on the value of $\log k_w$ for these more polar analytes and a negative effect on $\log k_w$ for the more hydrophobic hydrocarbons and halogenated compounds. The magnitude of Δk_w for these carboxylic acid derivatives may be seen as further evidence for a polar retention effect on graphite.

The other carboxylic acid derivative in this study, 4-acetoxybiphenyl had a Δk_w value of 240 at pH 2.5. This value is lower than those observed for the other carboxylic acid derivatives. However, it is more in line with Δk_w for the hydrocarbon analytes. At neutral pH, Δk_w increased to 3.3×10^4 for 4-acetoxybiphenyl, once more, this is of similar magnitude to the hydrocarbon analytes. If this behaviour is compared to that of its benzene congener, phenyl acetate, it becomes clear that these molecules, though polar, do not appear to behave in the same way as the other polar oxygen containing analytes.

The carboxylic acids in this study had very large values of Δk_w at pH 2.5 ($\Delta k_w > 3300$). These very positive values may be explained, in part, by the planar nature of the analytes, particularly for the planar 4-phenyl cinnamic acid, with its extended conjugated π system (for which $\Delta k_w = 15167$). However, the polar carboxylic group would appear to help increase the value of Δk_w due to the so called polar retention effect

Chapter 5 - The retention mechanisms of biphenyl derivatives on PGC
on graphite. At pH 7.0 Δk_w increased for all carboxylic acids. This may be explained by the vastly reduced value of Δk_w on ODS at pH 7.0 compared with pH 2.5, because of the reduction in hydrophobicity for the negatively charged carboxyl groups. On PGC, the reduction in Δk_w at pH 7.0 (compared with pH 2.5), though substantial (between 0.05 and 0.70 log units) was far less significant than for ODS. These changes are therefore amplified when transformed into Δk_w .

The comparatively small reduction in Δk_w from acidic to neutral conditions on PGC compared with ODS may be attributed to three main factors - (a) hydrophobicity, (b) planarity and (c) PREG.

On ODS, retention is believed to depend mainly on hydrophobicity, so retention will diminish for weak acids as the value of pH is increased. On PGC, retention of these compounds is believed to depend upon a combination of these three factors (a, b and c above). For the carboxylic acids, as pH was increased, the analytes became ionised and so hydrophobicity decreased. However, the polar retention effect on graphite may actually increase as these analytes move from being polar to being negatively charged. Planarity, though an important factor, may not change significantly. As hydrophobicity is only one of three (or more) factors affecting retention on PGC, a change in hydrophobicity on PGC has a far smaller effect on retention than it would for an ODS support.

For 4-biphenylsulfonic acid, retention was stronger on PGC than on ODS. Retention was also stronger at pH 7.0 than pH 2.5. This is reflected with a value for Δk_w of 1183 at pH 2.5 and 2830 at pH 7.0. These high values of Δk_w may be seen as further evidence for a PREG.

5.3 Quantitative structure- retention relationship analysis of *para*-substituted biphenyl derivatives

5.3.1 Bivariate analysis

Linear regression analysis was performed on the experimentally obtained retention data for the benzene derivatives on both PGC and ODS stationary phases. The resulting correlations between structural descriptors and retention are given in table 5.8.

Table 5.8 Linear regression correlation between structural descriptors and $\log k_w$ for *para* substituted biphenyl derivatives, where r is the correlation coefficient.

Parameter	r^2			
	ODS		PGC	
	pH 2.5	pH 7.0	pH 2.5	pH 7.0
Hansch parameter [†]	0.964	0.799	0.767	0.644
σ_p [†]	0.068	0.013	0.010	0.000
Taft E_s [†]	0.246	0.242	0.070	0.097
Coquart's excess charge C_n ^{□□}	0.477	0.508	0.672	0.662
Topolog. electronic index ^{□□}	0.179	0.089	0.113	0.097
Molecular Surface Area [§]	0.057	0.210	0.001	0.030
$\log P$ [§]	0.829	0.776	0.681	0.688
Total Dipole Moment [§]	0.344	0.337	0.267	0.143
Total Energy [*]	0.338	0.502	0.139	0.304
Electronic Energy [*]	0.254	0.376	0.090	0.216
Nuclear Energy [*]	0.235	0.347	0.081	0.197
Surface Area [*]	0.032	0.121	0.001	0.019
Mean Polarizability [*]	0.430	0.419	0.535	0.299
Total Molecular Charge [*]	0.022	0.149	0.076	0.073
Heat of Formation [*]	0.058	0.114	0.051	0.121
Ionizational Potential [*]	0.025	0.325	0.104	0.100
E_{lumo} [*]	0.002	0.049	0.014	0.029
E_{homo} [*]	0.025	0.325	0.104	0.100
Molecular Mass [§]	0.082	0.172	0.029	0.066
Verloop L [§]	0.000	0.002	0.107	0.046
Verloop B_4 [§]	0.026	0.146	0.002	0.019

[†] From reference [13]. These parameters use a reduced dataset due to lack of data for substituents SO₃H, CH₂CO₂H & CH(OH)CH₃

[§] Calculated using TSAR (Oxford Molecular Ltd). ^{*} Calculated using VAMP (Oxford Molecular Ltd).

[□] Calculated using MOPAC (AM1 Hamiltonian) in InsightII (Molecular Simulations Inc.).

^{□□} Calculated by a custom written C++ program from MOPAC (AM1 Hamiltonian) results (see Appendix 5.2 for details).

Figure 5.11 shows the relationship between $\log P$ and $\log k_w$ for the four sets of chromatographic conditions considered. On ODS (figure 4.19 a & b) the linear relationship between $\log P$ and $\log k_w$ gave r^2 values of 0.829 and 0.776 at pH 2.5 and pH 7.0 respectively. Although these were not exceptional linear correlations, they suggest that there is a strong relationship between retention on ODS and hydrophobicity.

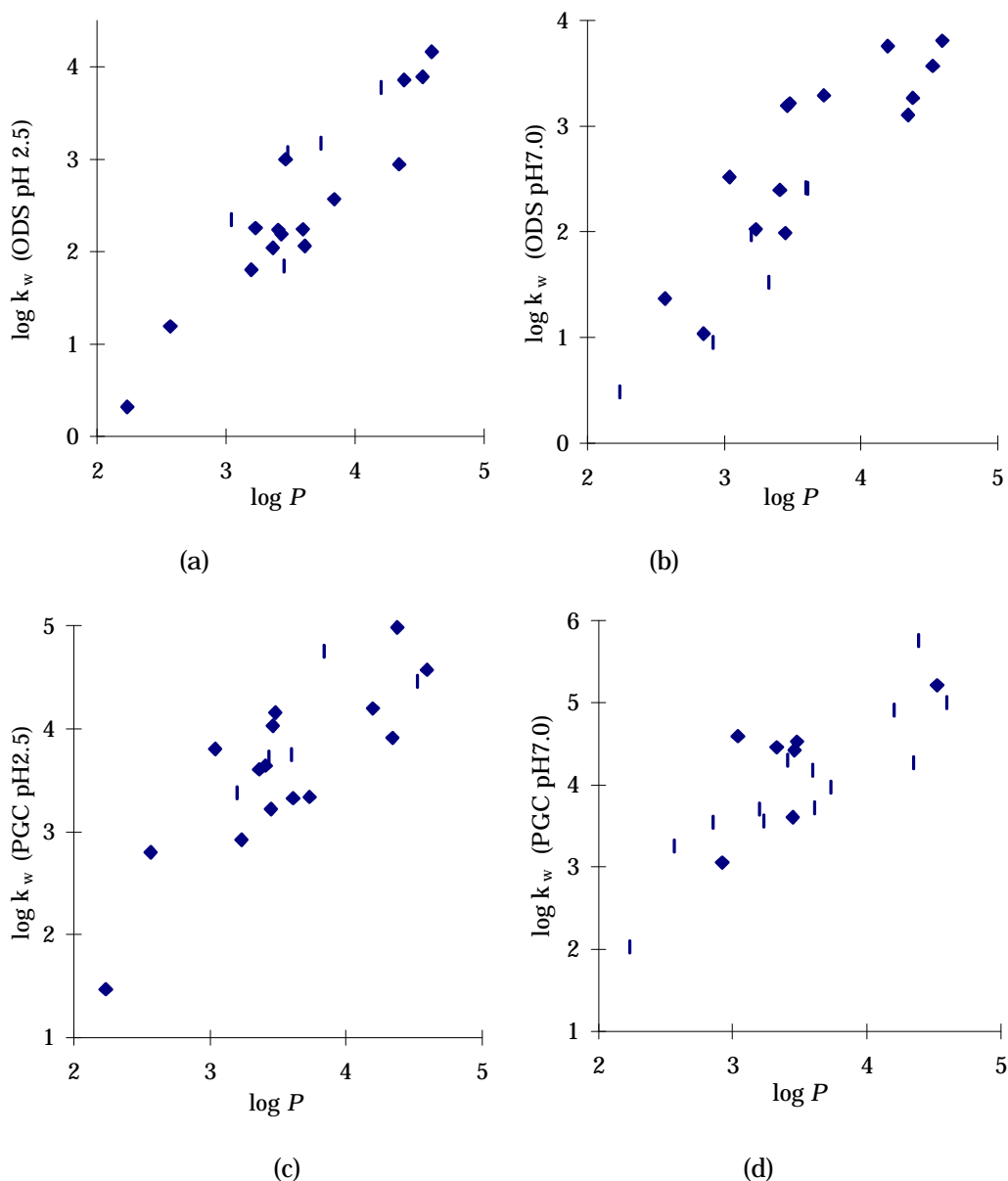


Figure 5.11 The relationship between $\log k_w$ and $\log P$ on ODS at (a) pH 2.5 & (b) pH 7.0, and on PGC at (c) pH 2.5 & (d) pH 7.0.

On PGC, there was a weak correlation between $\log P$ and $\log k_w$ at both

Chapter 5 - The retention mechanisms of biphenyl derivatives on PGC
pH values ($r^2 = 0.688$ at pH 7.0 and 0.681 at pH 2.5). This result shows that hydrophobic interactions, although important for this group of compounds, are not the only interactions governing the retention mechanism on PGC. This observation was mirrored by Hennion [14] for benzene derivatives. She concluded that only if more compounds containing hydrophobic moieties were studied would a trend be obtained. This observation is in agreement with the chromatographic retention of the benzene derivatives studied in chapters 3 and four. The retention of the hydrophobic *n*-alkylbenzene analytes in chapter 3 produced a strong correlation with $\log P$, whereas the more diverse group of benzene derivatives studied in chapter 4 gave a far weaker correlation between $\log k_w$ and $\log P$.

The relationship between the Hansch parameter (π) and $\log k_w$ on ODS and PGC supports is shown in figure 5.12. On ODS at pH 2.5, the linear correlation was stronger than that for $\log P$ under identical conditions. This was also true for ODS at pH 7.0 and PGC at pH 2.5.

One possible explanation for this is that the values for the Hansch parameter were experimentally determined, whereas the TSAR software was used to calculate the $\log P$ values. Whilst calculated values of $\log P$ give good approximations, they do not take into consideration the situation throughout the molecule, only considering atoms and connectivity to their nearest neighbours. The Hansch parameter can thus be considered a more appropriate descriptor of hydrophobicity in this case. At pH 7.0 the correlation of $\log k_w$ on ODS with the Hansch parameter was reduced when compared with pH 2.5. This may be due to increased secondary ionic interactions resulting from any uncapped ionised silanol groups on the surface of the support.

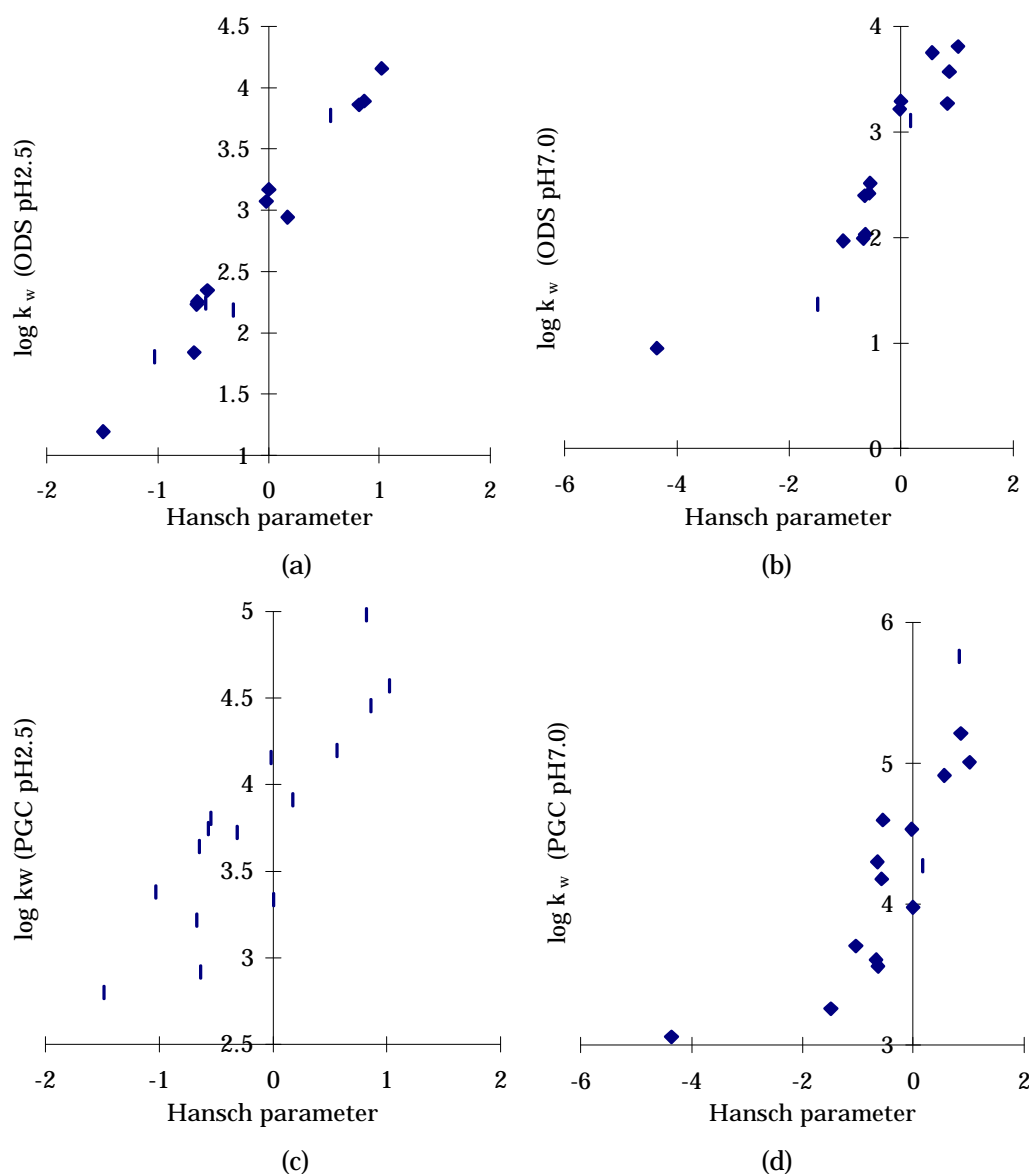


Figure 5. 12 The relationship between $\log k_w$ and the Hansch parameter on ODS at (a) pH 2.5 & (b) pH 7.0, and on PGC at (c) pH 2.5 & (d) pH 7.0.

On PGC, there was a weak relationship between the $\log k_w$ and the Hansch parameter at both pH values. The correlation was stronger at pH 2.5 (where $r^2 = 0.767$) than at pH 7.0 (where $r^2 = 0.644$), suggesting that there may be increased secondary ionic interactions on PGC at pH 7.0. This may be explained by the presence of weakly acidic functionality on the surface of the PGC support which would increase the retention of polar and charged analytes and so reduce the

The topological electronic index (TEI) was introduced into this study as a replacement for the Weiner, Balaban and Randic indices that could not be easily applied to organic compounds containing heteroatoms. Results from Chapter Four exposed a strong relationship between $\log k_w$ and topological indices. Thus, it was thought important to continue studying these relationships for more diverse data sets that included polar moieties. However, the TEI gave a poor relationship with the retention on PGC and also on ODS supports.

The correlation between Coquart's excess charge parameter, C_n and $\log k_w$ on ODS was poor at both pH values. This may be because the dominant factor in retention on ODS is hydrophobicity whereas C_n is primarily a polarity related parameter. The correlation between C_n and $\log k_w$ on ODS increased at neutral pH (compared with pH 2.5). One possible explanation for the poor correlation is the increased secondary electrostatic interactions, due to ionisation of any uncapped silanol functionality on the ODS surface. The relationship between C_n and $\log k_w$ on PGC is given in figure 5.13.

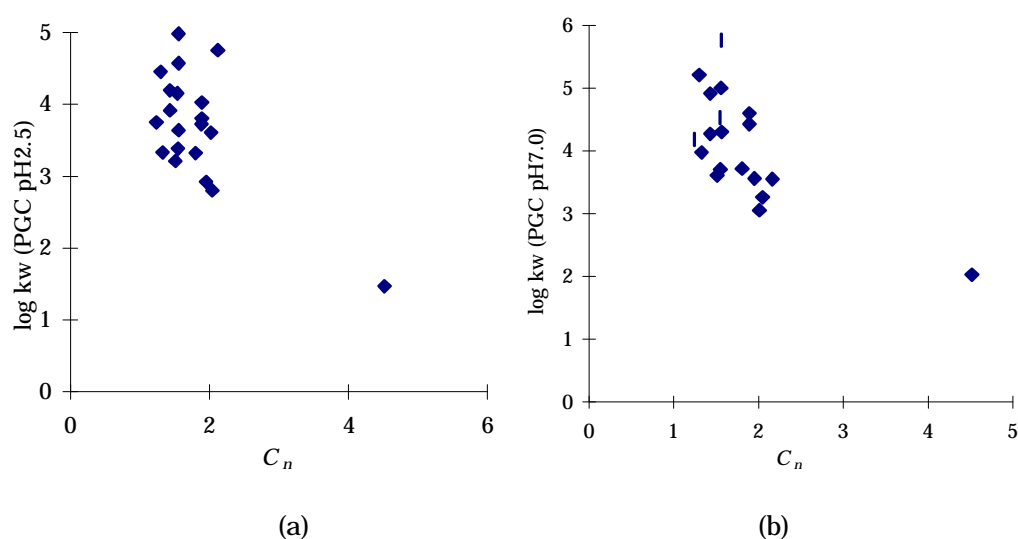


Figure 5.13 The relationship between $\log k_w$ and Coquart's excess charge parameter, C_n on PGC at (a) pH 2.5 and (b) pH 7.0

On PGC, the values of r^2 (0.672 at pH 2.5 and 0.662 at pH 7.0) suggested a weak linear relationship between C_n and $\log k_w$, however these values were artificially high because of the exceptionally high values of C_n for 4-biphenylsulfonic acid ($C_n = 4.52$ for the ionised form). All the other compounds studied had very similar values of C_n (between 1.2 and 2.2) which resulted in grouping of the data and thus low values of r^2 . This observation is significant because previous studies by Coquart *et al.* on benzene derivatives have produced strong linear relationships between C_n and $\log k_w$ [14, 15] for polar molecules.

The relationship between C_n and $\log k_w$ for the polar and ionised analytes studied can be seen in figure 5.14. In this relationship all hydrocarbons have been discarded and also the outlier, 4-biphenylsulfonic acid. This has been done in an attempt to compare the results with those of Coquart *et al.* for polar benzene derivatives. At pH 2.5, the correlation between C_n and $\log k_w$ on PGC is very poor ($r^2 = 0.028$).

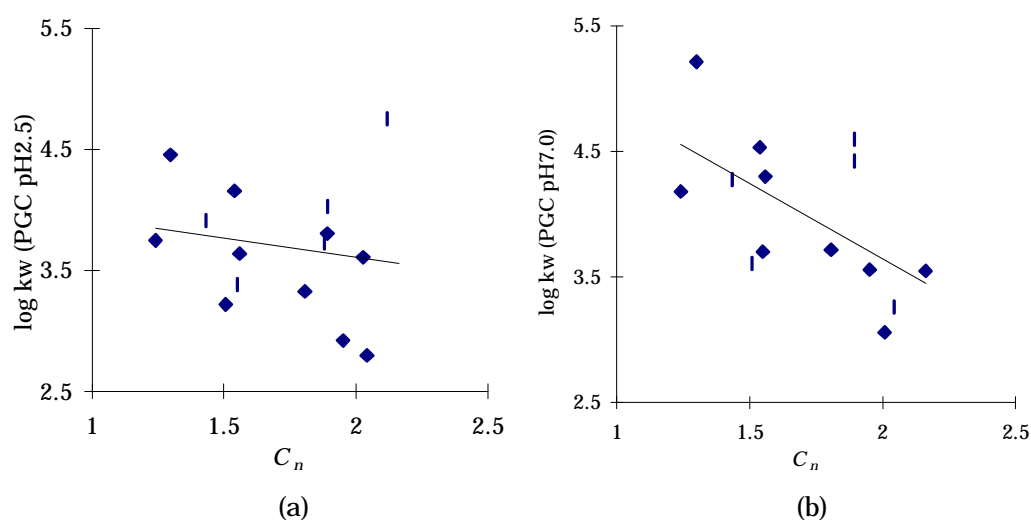


Figure 5.14 The relationship between $\log k_w$ and C_n on PGC for polar analytes at (a) pH 2.5 and (b) pH 7.0.

At pH 2.5, the correlation is improved ($r^2 = 0.347$), however these relationships are poor when compared to those of Coquart *et al.* for polar benzene derivatives. This suggests that for the biphenyl derivatives, there are different factors which influence $\log k_w$ more greatly than C_n . This reduced correlation for the biphenyl data-sets may be a result of the increased ability of the planar biphenyl compounds to interact with the planar PGC surface or may be attributed to the hydrophobicity of these analytes.

Many other structural descriptors were used for bivariate analysis of the retention data ($\log k_w$) including electronic parameters, energies derived from semi-empirical molecular orbital calculations, size descriptors and physicochemical properties as given in table 5.9, however for these analytes it was not possible to obtain strong relationships between the structural descriptors used and $\log k_w$ on PGC.

5.3.2 Conformational analysis studies by semi-empirical molecular modelling methods.

Conformational analysis of the biphenyl derivatives studied was performed according to the methods detailed in section 2.2 of this thesis. Geometries were optimised in isolation in a vacuum using semi-empirical molecular-orbital calculations (AM1 Hamiltonian). Rotation barriers were obtained by calculating the difference in energy between the minimum energy conformation and the molecule constrained in a geometry with coplanar phenyl rings. Results of these calculations are given in table 5.9.

Table 5.9 Rotation barrier and torsion angles for the biphenyl compounds studied.

Substituent X	Rotation barrier (kcal mol ⁻¹)	Torsion angle (°)
H	1.34	37.6
CH ₃	1.30	35.3
CH ₂ CH ₃	1.28	35.3
CHCH ₂	1.14	38.5
Br	1.15	43.3
CH ₂ Cl	1.29	35.5
OH	1.33	35.2
OCH ₃	1.28	35.1
CH ₂ OH	1.29	35.5
CH(OH)CH ₃	1.26	35.1
CHO	1.30	39.3
COCH ₃	1.25	39.2
CO ₂ CH ₃	1.29	40.2
OCOCH ₃	1.32	35.0
CN	1.34	37.6
CONH ₂	1.39	37.5
CO ₂ H	1.20	39.5
CO ₂ ⁻	1.33	37.4
CH=CHCO ₂ H	1.02	37.5
CH=CHCO ₂ ⁻	1.28	36.4
CH ₂ CO ₂ H	1.22	35.0
CH ₂ CO ₂ ⁻	1.28	35.4
SO ₂ OH	1.38	36.6
SO ₂ O ⁻	1.44	37.5

Biphenyl was the most stable when the torsion angle between the phenyl rings was 37.6°. This torsion angle is of similar size to those calculated by Park *et al.* (42°) from molecular mechanics simulations [16] and those measured by Bastiansen and Samdal [17] by electron diffraction studies (44.3°). All compounds studied had torsion angle within a narrow range (35.1° – 44.3°). These results agreed with observations made by Bastiansen and Samdal, who found that the average torsional angle for non-*ortho*-substituted biphenyl derivatives

Chapter 5 - The retention mechanisms of biphenyl derivatives on PGC seemed to be little influenced by substitution in the *meta* or *para* position [17].

Table 5.10 Linear regression correlation between structural descriptors and $\log k_w$ for *para* substituted biphenyl derivatives, where r is the correlation coefficient.

Parameter	r^2			
	ODS		PGC	
	pH 2.5	pH 7.0	pH 2.5	pH 7.0
Rotation barrier	0.251	0.331	0.587	0.683
Torsion angle	0.034	0.031	0.042	0.082

The relationship between torsion angle and chromatographic retention ($\log k_w$) on PGC is given in figure 5.9. No linear relationship was found between $\log k_w$ and torsion angle because of the small range in torsion angle and thus the lack of influence that substitution at the *para* position gave.

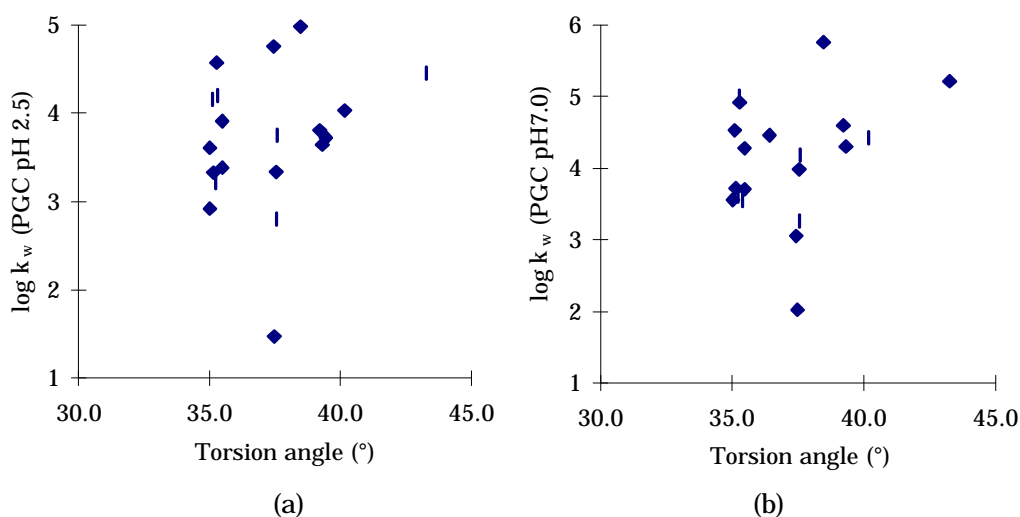


Figure 5. 15 The relationship between $\log k_w$ and the torsion angle on the inter-phenyl bond on PGC at (a) pH 2.5 and (b) pH 7.0.

Rotation barriers were found to be in the range 1.02 – 1.44 kcal mol⁻¹ for the compounds studied. The rotation barrier to planarity for

Chapter 5 - The retention mechanisms of biphenyl derivatives on PGC
biphenyl was $1.34 \text{ kcal mol}^{-1}$. This value is of similar magnitude to that calculated by *ab initio* molecular orbital methods by Almlöf [18] which gave rotation barriers of $1.21 \text{ kcal mol}^{-1}$ and $4.5 \text{ kcal mol}^{-1}$ at the planar and the perpendicular form respectively.

The retention of the compounds could depend on the ability of the compounds to attain a planar geometry, therefore a measure of this ability to become planar may correlate with chromatographic retention ($\log k_w$). The relationship between rotation barrier and chromatographic retention ($\log k_w$) on PGC is given in figure 5.16. The rotation barrier was found to give a weak correlation with $\log k_w$ on PGC. At pH 2.5, the linear relationship was described by an r^2 value of 0.587, at pH 7.0, this value increased to 0.683.

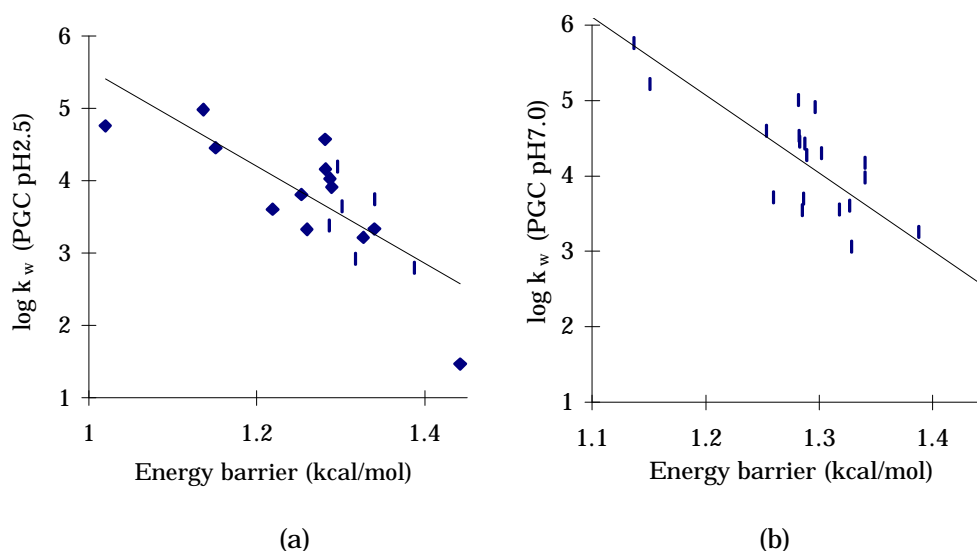


Figure 5. 16 The relationship $\log k_w$ and between the energy barrier to coplanarity of the biphenyl rings on PGC at (a) pH 2.5 and (b) pH 7.0.

These results show that retention of *para*-substituted biphenyls on PGC gave a weak, but significant correlation with the rotation barrier. This correlation when coupled with the molecular modelling of the interaction between biphenyl and a model PGC surface discussed in chapter 4 suggest that the optimum geometry of interaction between biphenyl derivatives and the PGC surface is a cofacial geometry. The work of Echols *et al.* [19] on polychlorinated biphenyl compounds

Chapter 5 - The retention mechanisms of biphenyl derivatives on PGC (PCBs) mirrors this conclusion. For PCBs, the strength of the interaction was found to be dependant upon the ease with which a planar conformation could be achieved. This was found to be dependant upon *ortho* substitution and the total number of chlorines on the biphenyl ring. PCBs with no *ortho* chlorines were found to be most strongly retained and PCBs with four *ortho* chlorines were found to be the most weakly retained.

One explanation of why this correlation was not as strong as expected may lie in the kinetic energy of these molecules. The kinetic energy of one mole of molecules, E , is given by equation 5.4

$$E = \frac{1}{2} M v_{rms}^2 = \frac{3}{2} RT \quad (5.4)$$

for an ideal gas, where M is the molar mass of the molecule, v_{rms} is the root mean squared velocity of the molecules, R is the gas constant and T is the temperature [20].

At 40°C (the temperature of the chromatographic system), the kinetic energy was approximately 0.25 kcal mol⁻¹. This represents a significant contribution towards overcoming the energy barrier to planarity and therefore may result in a weaker relationship between rotation barrier and log k_w . This also shows that the theoretical energy calculations underpinning this work have given a rotation barrier which agreed, not only with the chromatographic studies and previously published experimental studies [18] but was also of the same order of magnitude to the kinetic energy of the system, giving further weight to the accuracy of the calculations. The theoretical model used gave accurate estimates of the physical properties that were being examined.

Another possible explanation of the weakness of the correlation between the rotation barrier and log k_w may be that hydrophobicity is also an important factor in retention and as hydrophobicity cannot be

explained by rotation about a carbon-carbon single bond, the correlation between rotation barrier and retention will not be strong. This explanation may also be applied to the polar mechanisms of retention on PGC.

The mechanism by which analytes are retained on PGC is not trivial and so cannot be described by a single parameter. For this reason, a multi-parameter technique was applied to the data-set.

5.3.3 Multi-variate analysis

Multiple linear regression

Stepwise multiple linear regression analysis was examined as a possible method for determining linear dependancies of $\log k_w$ upon two or more structural descriptor variables. The structural descriptors used were identical to those used in section 5.5.1.

On ODS, the strong relationship between the Hansch parameter and $\log k_w$ at pH 2.5 and the weak relationship at pH 7.0 could not be improved upon by the addition of further descriptors. This may be because retention on ODS is based mainly on hydrophobicity and so additional factors are of little importance. The weaker relationship between the Hansch parameter and $\log k_w$ at pH 7.0 may be attributed to the ionisation of the weak acids in this data-set. $\log D$ (as defined in section 1.3.2) may be better descriptor of hydrophobicity for this situation as it is better at the evaluation of hydrophobicity for ionisable compounds.

On PGC, MLR analysis again failed to provide further insight into the data-set. This may be because the structural descriptors used to describe polar effects gave poor correlations with $\log k_w$. The dataset in chapter 4 gave good MLR correlations with mean polarisability and E_{lumo} . This was not the case for the biphenyl derivatives.

Principal component analysis

In addition to MLR, principal component analysis was examined as a possible method for determining linear dependancies of $\log k_w$ upon two or more structural descriptor variables. The structural descriptors used were identical to those used in section 5.5.1.

Using this technique it was possible to reduce the set of descriptor variables from 21 structural descriptors to 4 orthogonal eigen vectors (principal components) which explained 96.3 % of the total variance for the 21 original descriptors at pH 2.5 and 95.7 % of the total variance at pH 7.0 (table 5.11).

Table 5.11 The variance explained by principal component analysis of the structural descriptors used for statistical analysis of biphenyl derivatives.

Principal Component	pH 2.5		pH 7.0	
	Variance explained %	Total explained %	Variance explained %	Total explained %
PC1	75.8	75.8	74.3	74.3
PC2	14.3	90.1	16.0	90.6
PC3	4.6	94.7	3.9	94.5
PC4	1.6	96.3	1.2	95.7

However, these eigen vectors produced poor correlations when regression analysis with the retention data was performed (table 5.12). In this study, the application of principal component analysis was not found to be of any additional benefit to the study. The use of multiple linear regression analysis did not produce any stronger linear relationships.

Table 5.12 Bivariate analysis of principal components with $\log k_w$.

Principal Component	r^2			
	ODS		PGC	
	pH 2.5	pH 7.0	pH 2.5	pH 7.0
PC1	0.301	0.290	0.243	0.211
PC2	0.344	0.362	0.185	0.270
PC3	0.185	0.103	0.207	0.089
PC4	0.100	0.152	0.111	0.075

5.3.4 Summary of QSRR analysis

Weak dependencies were found on the Hansch parameter and the rotation barrier of the inter-phenyl bond for $\log k_w$ on PGC. These findings suggest that for this group of analytes, two of the main factors affecting retention were hydrophobicity and the ability of the two phenyl rings in the biphenyl derivatives to achieve planarity. The results of this section fail to account for the strong retention of the more polar and charged analytes. However it may be argued that the planarity of the molecules was a more important factor in the retention on PGC than any polar or charge effects.

5.4 Conclusions

5.4.1 Chromatographic studies

The chromatographic data outlined in this study demonstrates that the retention of the biphenyl derivatives on PGC is far stronger than that observed on ODS for all analytes at both pH values examined. These observations suggest that the presence of a planar moiety (or an increased hydrophobicity) in a molecule will have a positive effect on chromatographic retention when using PGC as the stationary phase.

The chromatographic retention data show that there exists a pH effect on the retention of the biphenyl derivatives (except carboxylic acids).

This is manifested by an increased retention (increased $\log k_w$) at pH 7.0 when compared to data obtained at pH 2.5. Since this effect is observed even for non-ionisable (and non polar) analytes, it suggests that the pH effect is influencing the planar or hydrophobic retention properties of the PGC phase. This effect is absent for the carboxylic acids studied. This implies that, at higher pH values where the analytes are ionised a repulsive interaction between the analyte and the stationary phase is present. At pH 2.5, when the degree of ionisation of the analytes is considerably reduced, this repulsive interaction is consequently diminished resulting in an increased retention.

5.4.2 Conformational analysis studies

The results of the conformational analysis studies showed that the average torsional angle for *para*-substituted biphenyl derivatives seemed to be little influenced by substitution in the *para* position. These results were in agreement with published experimental data [17]. Rotation barriers were found to be in the range 1.02 – 1.44 kcal mol⁻¹ for the compounds studied. The rotation barrier was found to correlate with $\log k_w$ on PGC. At pH 2.5, the linear relationship was described by an r^2 value of 0.587, at pH 7.0, this value increased to 0.683. These correlations when coupled with the molecular modelling of the interaction between biphenyl and a model PGC surface discussed in chapter 4 suggest that the optimum geometry of interaction between biphenyl derivatives and the PGC surface is a cofacial geometry. These findings are in agreement with the qualitative results of Echols *et al.* on retention of PCBs, where retention was attributed to the ease with which the PCB molecule can achieve a planar conformation [19].

One explanation of why this correlation is not as strong as may be

expected may lie in the kinetic energy of these molecules, which at 40°C is approximately 0.25 kcal mol⁻¹. This represents a significant contribution towards overcoming the energy barrier to planarity and therefore may result in a weaker relationship between rotation barrier and log k_w . Another explanation could be that other factors such as hydrophobicity are important as seen from the strong correlations between log k_w on PGC and hydrophobic parameters.

5.4.3 QSRR studies

Bivariate analysis results suggested that the main factor influencing retention on ODS was hydrophobicity, as log k_w on ODS was found to correlate strongly with hydrophobic parameters such as the Hansch parameter and log P .

Bivariate analysis for correlation of retention data (log k_w) on PGC with structural descriptors produced weaker correlations than for ODS. However weak correlations were obtained for log k_w with the Hansch parameter, log P and also with the inter-phenyl bond rotation barrier at both pH 2.5 and pH 7.0 as previously stated in section 5.6.2.

Multivariate analysis was unsuccessful in describing retention on ODS or PGC. However a combination of molecular planarity and hydrophobicity as well as polar effects appear to be the main factors influencing log k_w on PGC for the biphenyl derivatives. Better parameters to describe molecular planarity and the ability of a molecule to achieve a planar geometry are required for a fuller explanation of the retention of biphenyls on PGC.

5.5 References

- [1] A. Almenningen, O. Bastiansen, L. Fernholt, B. N. Cyvin, S. J. Cyvin, S. Samdal, *J. Mol. Structure* 128 (1985) 59.
- [2] J. H. Knox, P. Ross, *HPLC 99* (Granada, Spain), Surface modification of porous graphitic carbon (Hypercarb) (1999).
- [3] S. A. Wise, L. C. Sander, W. E. May, *J. Chromatogr. A* 642 (1993) 329.
- [4] J. C. Fetzer, W. R. Biggs, *Chromatographia* 27 (1989) 118.
- [5] L. C. Sander, R. M. Parris, S. A. Wise, P. Garrigues, *Anal. Chem.* 63 (1991) 2589.
- [6] M. Olsson, L. C. Sander, S. A. Wise, *J. Chromatogr.* 537 (1991) 73.
- [7] M. Dachtler, K. Kohler, K. J. Albert, *J. Chromatogr. B* 720 (1998) 211.
- [8] L. C. Sanders, M. Pursch, S. A. Wise, *Anal. Chem.* 71 (1999) 4821.
- [9] C. Yan, D. E. Martire, *J. Chem. Phys.* 96 (1992) 7510.
- [10] R. E. Majors, *LC-GC* 9 (1991) .
- [11] J. H. Knox, P. Ross, *Adv. Chromatogr.* 37 (1997) 73.
- [12] V. R. Meyer, *Practical High-Performance liquid Chromatography*, Wiley, New York 1994.
- [13] C. Hansch, Leo, *Substituent constants for correlation analysis in chemistry and biology*, John Wiley & Son, New York 1979.
- [14] M. C. Hennion, V. Coquart, S. Guenu, C. Sella, *J. Chromatogr. A* 712 (1995) 287.
- [15] V. Coquart, *PhD Thesis*, University of Paris, Paris 1993.
- [16] K. C. Park, L. R. Dodd, K. Levon, T. K. Kwei, *Macromolecules* 29 (1996) 7149.
- [17] O. Bastiansen, S. Samdel, *J. Mol. Structure* 128 (1985) 115.
- [18] J. Almlöf, *Chem. Phys.* 6 (1974) 135.

- [19] K. R. Echols, R. W. Gale, K. Feltz, J. O'Laughlin, D. E. Tillitt, T. R. Schwartz, *J. Chromatogr. A.* **811** (2000) 135.
- [20] P. W. Atkins, *Physical Chemistry*, Oxford University Press, Oxford 1995.

Appendix 5.1

Retention data for *para*-substituted biphenyl analytes on PGC and ODS at pH 2.5 and pH 7.0

Analyte	ODS						PGC					
	pH 2.5			pH 7.0			pH 2.5			pH 7.0		
	log k_w	r^2	slope									
biphenyl	3.170	0.995	-0.030	3.290	0.992	-0.031	3.336	0.978	-0.026	3.978	0.995	-0.032
4-methylbiphenyl	3.775	0.996	-0.035	3.753	0.988	-0.035	4.198	0.977	-0.029	4.915	0.997	-0.036
4-ethylbiphenyl	4.221	0.999	-0.039	3.808	0.995	-0.035	4.570	0.988	-0.034	5.006	0.998	-0.038
4-vinylbiphenyl	3.858	0.997	-0.036	3.270	0.997	-0.030	4.981	0.999	-0.033	5.761	0.996	-0.037
4-bromobiphenyl	3.889	0.998	-0.036	3.571	0.998	-0.032	4.455	0.999	-0.028	5.212	0.994	-0.037
4-methoxybiphenyl	3.071	0.994	-0.029	3.213	0.985	-0.030	4.156	0.990	-0.027	4.530	0.997	-0.031
4-hydroxybiphenyl	1.839	0.985	-0.018	1.989	0.982	-0.020	3.216	0.998	-0.022	3.605	0.994	-0.026
4-(hydroxymethyl)biphenyl	1.803	0.983	-0.018	1.969	0.979	-0.020	3.381	0.985	-0.024	3.703	0.994	-0.027
4-biphenylcarboxaldehyde	2.235	0.991	-0.022	2.396	0.981	-0.023	3.641	0.998	-0.026	4.298	0.999	-0.033
4-biphenylcarboxylic acid	2.189	0.998	-0.022	0.952	0.956	-0.011	3.724	0.991	-0.027	3.058	0.999	-0.022
methyl 4-phenylbenzoate	2.996	0.992	-0.028	3.189	0.975	-0.030	4.027	0.989	-0.028	4.424	0.995	-0.027
4-acetoxybiphenyl	2.388	0.990	-0.024	2.026	0.978	-0.021	2.919	0.982	-0.019	3.560	0.993	-0.025
4-acetylbiphenyl	2.345	0.988	-0.023	2.517	0.977	-0.024	3.804	0.991	-0.028	4.598	0.994	-0.033
4-biphenylcarboxamide	1.192	0.970	-0.012	1.368	0.967	-0.014	2.800	0.978	-0.014	3.259	0.994	-0.018
4-biphenylcarbonyl chloride	2.999	0.992	-0.028	3.173	0.980	-0.030	4.021	0.994	-0.028	4.273	0.990	-0.029
4-(chloromethyl)biphenyl	2.947	0.995	-0.028	3.107	0.984	-0.030	3.912	0.966	-0.026	4.273	0.994	-0.029
4-phenylcinnamic acid	2.568	0.998	-0.025	1.522	0.962	-0.016	4.752	0.992	-0.031	4.456	0.993	-0.027
4-biphenylcarbonitrile	2.242	0.988	-0.022	2.417	0.978	-0.024	3.748	0.981	-0.024	4.179	0.995	-0.028
1-(4-biphenyl)ethanol	2.061	0.995	-0.021	2.410	0.985	-0.024	3.325	0.988	-0.026	3.717	0.995	-0.030
4-biphenylacetic acid	2.028	0.999	-0.021	1.035	0.962	-0.012	3.608	0.990	-0.027	3.549	0.997	-0.024
4-biphenylsulfonic acid	0.362	0.979	-0.005	0.480	0.899	-0.008	1.470	0.996	-0.009	1.947	0.980	-0.015

Appendix 5.2 - The charge program

This C++ program was written to read the Cartesian co-ordinates, x, y, z and the charge (q) on an atom in a MOPAC archive file and transform them into three electronic descriptors, which are defined in section 1.3.2:

- Topological electronic index
- Coquart's excess charge
- Sum of the squares of charge on atoms

The program prompts for the number of atoms in the molecule and reads the items highlighted in bold from the sample archive file below:

```
4-biphenylcarboxaldehyde:
      x           y           z           q
C   0.0000000 0   0.0000000 0   0.0000000 0 0 0 0  -0.1309
H   1.1000111 1   0.0000000 0   0.0000000 0 1 0 0  0.1340
C   1.3933089 1   119.799932 1   0.0000000 0 1 2 0  -0.1143
H   1.1004921 1   119.955125 1   -0.292110 1 3 1 2  0.1353
C   1.4023433 1   120.290338 1   -179.745362 1 3 1 2  -0.0501
C   1.4023519 1   119.202793 1   -0.092499 1 5 3 1  -0.1135
H   1.1005427 1   119.744196 1   -179.607526 1 6 5 3  0.1364
C   1.3933084 1   120.286481 1   -0.107784 1 6 5 3  -0.1306
H   1.1000142 1   119.797055 1   -179.772303 1 8 6 5  0.1344
C   1.3947676 1   120.006337 1   -179.944752 1 1 2 3  -0.1219
H   1.0997729 1   120.095091 1   -0.147592 1 10 1 2  0.1337
C   3.7629923 1   105.540740 1   -167.582223 1 5 3 1  -0.0869
H   1.1010622 1   138.526850 1   35.693447 1 12 5 3  0.1346
C   1.4005695 1   101.523651 1   -144.536226 1 12 5 3  -0.1776
C   1.4002015 1   119.464222 1   0.041217 1 14 12 5  -0.0689
H   1.1025063 1   119.105494 1   179.888428 1 15 14 12  0.1551
C   1.3919480 1   120.310006 1   -0.077797 1 15 14 12  -0.1370
H   1.1006766 1   119.886246 1   179.634157 1 17 15 14  0.1419
C   1.4024861 1   120.366933 1   0.092093 1 17 15 14  -0.0012
C   1.3912134 1   18.743383 1   35.354159 1 12 5 3  -0.1370
H   1.1005867 1   119.920200 1   179.432024 1 20 12 5  0.1401
C   1.4708635 1   119.882723 1   -179.890572 1 14 12 5  0.2235
H   1.1144440 1   115.034951 1   -0.391604 1 22 14 12  0.0901
O   1.2331811 1   123.753954 1   179.556426 1 22 14 12  -0.2894
```

Source code:

```
#include<fstream.h>
#include<iostream.h>
#include<math.h>

class atom
{
float x;
float y;
float z;
float q;

public:
atom();
```

Chapter 5 - The retention mechanisms of biphenyl derivatives on PGC

```
~atom();
atom(float ,float ,float,float );
friend float rsqu(const atom& a,const atom& b);
friend float charge(const atom& a,const atom& b);
atom squ();
atom sqt();
friend ostream& operator<<(ostream& stream,const atom& a);
const atom& operator=(const atom& a);
friend atom operator-(const atom& a,const atom& b);
friend atom operator+(const atom& a,const atom& b);
friend float operator*(const atom& a,const atom& b);
friend atom operator/(const atom& a,const float& k);

};

int main()
{
    cout<<"© 1999 Simpson & Harris.  Written by S. Harris."<<endl;
    cout<<"Hello Dave you sexy bugger....."<<endl;
    cout<<"Make sure that your data is in the file sarah.arc."<<endl;
    cout<<"Remember to remove all the written portions from the top of
this file. Good luck!."<<endl;
    ifstream results("sarah.arc");

    int N=0;

    cout<<"Please enter the number of atoms in your molecule"<<endl;
    cin>>N;

    atom in_molecule[N];
    char a_char;
    float x_entry,y_entry,z_entry,a_number;
    float the_charge,squ_charge,total_charge,total_sqcharge;
    float diff_r,diff_charge,index,total_index;
    total_charge=0;
    total_sqcharge=0;

    for(int i=0;i<N;i++)
    {
        results>>a_char>>x_entry>>a_number>>y_entry>>a_number>>z_entry>>a_num
ber>>a_number>>
        a_number>>a_number>>the_charge;
        in_molecule[i]=atom(x_entry,y_entry,z_entry,the_charge);
        squ_charge=(the_charge*the_charge);
        total_charge+=sqrt(squ_charge);
        total_sqcharge+=squ_charge;
    }

    cout<<"Sum of squares of charges:"<<total_sqcharge<<endl;
    cout<<"Coquart excess charge:"<<(total_charge/2)<<endl;

    total_index=0;
    for(int r=0;r<N;r++)
    {
        for(int s=0;s<N;s++)
        {
            if(s!=r)
            {
                diff_charge=fabs(charge(in_molecule[r],in_molecule[s]));
                //cout<<"diff_charge:"<<diff_charge<<endl;
                diff_r=rsqu(in_molecule[r], in_molecule[s]);

                index=diff_charge/diff_r;
                total_index+=index;
                //cout<<"total_index:"<<total_index<<endl;
            }
        }
    }
    cout<<"Topological Electronic Index:"<<(total_index/2)<<endl;
}
```

Chapter 5 - The retention mechanisms of biphenyl derivatives on PGC

```
//Functions used in the program!

atom::atom()
{
  x=0;
  y=0;
  z=0;
  q=0;
}

atom::~atom()
{}

atom::atom(float i,float j,float k,float l)
{
  x=i;
  y=j;
  z=k;
  q=l;
}

ostream& operator<<(ostream& stream,const atom& a)
{
  stream<<" "<<a.x<<" "<<a.y<<" "<<a.z<<" ";
  return stream;
}

const atom& atom::operator=(const atom& a)
{
  x=a.x;
  y=a.y;
  z=a.z;
  q=a.q;
  return a;
}

atom operator-(const atom& a,const atom& b)
{
  atom c;
  c.x=a.x-b.x;
  c.y=a.y-b.y;
  c.z=a.z-b.z;
  c.q=a.q-b.q;
  return c;
}

float rsqu(const atom& a,const atom& b)
{
  float c=0;
  c=((a.x-b.x)*(a.x-b.x)+(a.y-b.y)*(a.y-b.y)+(a.z-b.z)*(a.z-b.z));
  return c;
}

float charge(const atom& a,const atom& b)
{
  float c=0;
  c=a.q-b.q;
  return c;
}

atom atom::squ()
{
  atom b;
  b.x=x*x;
  b.y=y*y;
  b.z=z*z;
  return b;
}

atom atom::sqt()
{
```

```
    atom b;
    b.x=sqrt(x);
    b.y=sqrt(y);
    b.z=sqrt(z);
    return b;
}

atom operator+(const atom& a,const atom& b)
{
    atom c;
    c.x=a.x+b.x;
    c.y=a.y+b.y;
    c.z=a.z+b.z;
    return c;
}

float operator*(const atom& a,const atom& b)
{
    float c;
    c=((a.x*b.x)+(a.y*b.y)+(a.z*b.z));
    return c;
}

atom operator/(const atom& a,const float& k)
{
    atom b;
    b.x=a.x/k;
    b.y=a.y/k;
    b.z=a.z/k;
    return b;
}
```

Chapter Six

Concluding remarks

Systematic exploration of the separation mechanisms of benzene and biphenyl derivatives on porous graphitic carbon stationary phase by an integrated approach incorporating chromatography, molecular modelling and QSRR analysis has revealed complex and subtle retention behaviour of these analytes which has not previously been documented. This combined approach allowed a more thorough appreciation of analyte behaviour which was more powerful than each method individually. Whilst the use of chromatography coupled with QSRR techniques is far from unique, the additional use of molecular modelling for a deeper understanding of the interaction between an analyte and the stationary phase can be seen as a novel approach.

The mechanism of retention on porous graphitic carbon is dependant on many factors. The basis of the retention mechanism has been found to be strongly influenced by the type of compounds under consideration. If only hydrocarbons are used, as is the case for the *n*-alkylbenzenes studied, retention strongly correlates with hydrophobic interactions. If only structural isomers, such as amylbenzenes, are considered, retention can be related to topological indices. If only polar analytes are examined, retention is strongly influenced by electronic parameters such as Coquart's excess charge

parameter [1]. For polychlorinated biphenyls, retention has been found to relate to the ability of the analyte to achieve a planar conformation [2, 3].

The retention behaviour on porous graphitic carbon has been demonstrated to be very different to that of silica-based stationary phases such as octadecyl-silica. The study of alkylbenzenes in chapter 3 suggested a retention mechanism mainly based upon hydrophobic effects, however the use of molecular modelling suggested that the orientation of the strongest interaction between the analyte and the graphite surface significantly affected the retention. Small *n*-alkylbenzenes (such as toluene and ethylbenzene) as well as benzene were found to have the strongest interaction with the model surface in a cofacial geometry. The short alkyl chain for these analytes was found to aid adsorption in a cofacial geometry. For larger *n*-alkylbenzenes, the flexible nature of the alkyl chain was found to aid retention based on a perpendicular face-edge geometry. QSRR methods showed that retention of amylbenzene structural isomers was strongly correlated to topological indices such as those defined by Wiener [4] and Balaban [5]. The reasoning for this relationship was confirmed by molecular modelling studies of these analytes and their interaction with the PGC stationary phase. The flexible alkyl chain on the *n*-amylbenzene molecule may easily change conformation to maximise its coverage of the planar graphite surface, leading to a face-edge geometry. For the more branched amylbenzene isomers, this ability to adsorb onto the planar surface is diminished with increased branching of the alkyl chain. These findings strongly support the integrated approach used herein, where each method is complementary.

Molecular modelling of the analytes interactions with a model graphite surface provided a unique insight into the geometries of interaction between analyte and stationary phase. For the alkylbenzene analytes,

this work was exemplary in combination with the statistical analysis performed for elucidating the mechanisms underpinning retention. For the more diverse selection of analytes studied in chapter 4, this approach was weaker when viewing all analytes without discrimination. However, when studying groups of related compounds, clear trends that affect the retention of the analytes were observed. This approach is surprisingly versatile when the simplicity of the model is considered. The model system neglected to account for the influence of solvent in the chromatographic system and therefore any solvation effects that exist. This model proved to be robust for hydrophobic analytes, where solvation effects could be neglected, however the weakness of the model was highlighted for charged analytes by the repulsive interactions produced. A more thorough model is therefore required to accurately determine the geometries and strengths of interaction between the analytes and the surface of the PGC stationary phase.

Multivariate QSRR analysis of the benzene derivatives studied in chapter 4 revealed a strong dependency of retention on PGC upon hydrophobic factors (the Hansch parameter) and also electronic parameters (E_{lumo} and mean polarisability), whilst the retention of these analytes on ODS was found to be strongly dependant on hydrophobicity. The inclusion of a dependency of the retention on PGC upon electronic factors such as mean polarisability suggests that the polar retention effect on graphite may be related in some way to charge separation within analyte molecules, this possibly involves polarisation of the electronic structure of the graphite surface. This conclusion is in agreement with the work of others [1, 6-8].

Retention of *para*-substituted biphenyls on PGC was found to be correlated with both hydrophobic factors (the Hansch parameter) and also with the ability of the analyte to achieve a planar conformation

(the energetic rotation barrier to planarity for the inter-phenyl bond).

These observations suggest that:

- (i) Hydrophobicity is an increasingly important factor affecting retention for larger molecules.
- (ii) Co-planarity of the phenyl rings in biphenyl is an important factor influencing retention.

The strong selectivity found for *n*-alkylbenzenes together with the strong retention of all the biphenyl derivatives studied suggests that PGC is highly selective towards hydrophobic effects, however there is evidence to suggest that polar effects are equally important.

Observation (ii) agrees with recent work by Echols *et al.* [2, 3] who studied the retention of *ortho* and non-*ortho* substituted PCBs, however the work presented in this study concentrated on only *para*-substituted biphenyls and so the differences in ability to achieve a planar conformation were far subtler. As this rotation barrier occurs due to the balance between the steric repulsion of the *ortho* hydrogen atoms and the conjugation energy, this means that the electronic structure of these compounds strongly influences retention on PGC.

The retention mechanism on PGC has been found to be based on a number of different factors. These factors include:

- Hydrophobicity
- The polar retention effect on graphite
- Topological indices
- Shape selectivity/planarity
- Ion exchange
- Hydrophilic adsorption

With so many factors to consider, when compared to retention on ODS (which is based mainly on hydrophobicity) we are clearly some way from producing a definitive unifying theory of retention for this complex and unique chromatographic material. There is clearly much

further work to be undertaken for a complete understanding of the complex retention mechanisms on porous graphitic carbon. A detailed analysis of the surface functionality of the PGC stationary phase should be undertaken in order to determine the nature of the weakly acidic functionality observed. This surface functionality may be attributed to one of two possible explanations. The explanation favoured by Patterson [9] suggests the presence of carboxylic acid functionality at the edges of the graphite sheets. One other possible explanation is the presence of residual silica from the template manufacturing process which have surface silanol functionalities. An explanation of this weakly acidic phenomenon may be incorporated into a revised molecular model of the chromatographic system.

References to chapter 6

- [1] M. C. Hennion, V. Coquart, S. Guenu, C. Sella, *J. Chromatogr. A.* 712 (1995) 287.
- [2] K. R. Echols, R. W. Gale, K. Feltz, J. O'Laughlin, D. E. Tillitt, T. R. Schwartz, *J. Chromatogr. A.* 811 (1998) 135.
- [3] K. Echols, R. Gale, D. Tillitt, T. Schwartz, J. O'Laughlin, *Environmental Toxicology and Chemistry* 16 (1997) 1590.
- [4] H. Wiener, *J. Amer. Chem. So.* 69 (1947) 2636.
- [5] A. T. Balaban, *Chem. Phys. Lett.* 89 (1982) 399.
- [6] J. H. Knox, P. Ross, *Advances In Chromatography* 37 (1997) 73.
- [7] B. J. Bassler, R. Kaliszan, R. A. Hartwick, *J. Chromatog.* 461 (1989) 139.
- [8] M. C. Hennion, *J. Chromatogr. A.* 885 (2000) 73.
- [9] A. L. Patterson, PhD thesis, *Institute of Pharmaceutical Sciences*, University of Nottingham, Nottingham 2000.